Crvena Stijena in Cultural and Ecological Context

Multidisciplinary Archaeological Research in Montenegro

edited by

Robert Whallon

National Museum of Montenegro
Montenegrin Academy of Sciences and Arts
2017

Table of Contents

Continued on next page…

List of Contributors

Mile Baković	Centar za konzervaciju i arheologiju Crne Gore Bajova 150 81250 Cetinje, Montenegro
Vera Biberdžić	Prirodnjački muzej Crne Gore Trg Bećir-bega Osmanagića 16 81000 Podgorica, Montenegro
Nikola Borovinić	Centar za konzervaciju i arheologiju Crne Gore Bajova 150 81250 Cetinje, Montenegro
Nada Bubanja	Prirodnjački muzej Crne Gore Trg Bećir-bega Osmanagića 16 81000 Podgorica, Montenegro
Katarina Burzanović	Prirodnjački muzej Crne Gore Trg Bećir-bega Osmanagića 16 81000 Podgorica, Montenegro
Natalija Čađenović	Prirodnjački muzej Crne Gore Trg Bećir-bega Osmanagića 16 81000 Podgorica, Montenegro
Ilinka Ćetković	Prirodnjački muzej Crne Gore Trg Bećir-bega Osmanagića 16 81000 Podgorica, Montenegro
Goran Ćulafić	Prirodnjački muzej Crne Gore Trg Bećir-bega Osmanagića 16 81000 Podgorica, Montenegro
Vesna Dimitrijević	Laboratory for Bioarchaeology Faculty of Philosophy Čika Ljubina 18-20 11000 Belgrade, Serbia
Snežana Dragićević	Prirodnjački muzej Crne Gore Trg Bećir-bega Osmanagića 16 81000 Podgorica, Montenegro
Marko Karaman	Prirodnjački muzej Crne Gore Trg Bećir-bega Osmanagića 16 81000 Podgorica, Montenegro
Suzana Malidžan	Prirodnjački muzej Crne Gore Trg Bećir-bega Osmanagića 16 81000 Podgorica, Montenegro

Ramiro. J March	CReAAH. UMR6566 Université de Rennes 1 Bâtiment 24-25 Campus de Beaulieu 263, Avenue du général Leclerc Campus de Beaulieu CS 74205 F-35042 Rennes Cedex, France
Norbert Mercier	IRAMAT-CRP2A, UMR 5060 CNRS Université Bordeaux Montaigne Esplanade des Antilles 33600, Pessac Cedex, France.
Bojana Mihailović	Narodni muzej u Beogradu Trg Republike 1a 11000 Beograd, Serbia
Dušan Mihailović	Department of Archaeology Faculty of Philosophy Belgrade University 18-20 Čika Ljubina 11000 Belgrade, Serbia
Eugène Morin	Trent University Department of Anthropology DNA Bldg Block C 2140 East Bank Drive Peterborough, Ontario, Canada K9J 7B8
Mike W. Morley	Centre for Archaeological Science University of Wollongong, Northfields Avenue, Wollongong, NSW, 2522, Australia
Lidija Polović	Prirodnjački muzej Crne Gore Trg Bećir-bega Osmanagića 16 81000 Podgorica, Montenegro
William J. Rink	School of Geography and Earth Sciences McMaster University Hamilton, Ontario, Canada
Kathleen Rodrigues	Division of Earth and Ecosystem Sciences Desert Research Institute 2215 Raggio Parkway Reno, NV 89512 USA
Jennie Deo Shaw	Salix Archaeological Services LLC P.O. Box 31911 Seattle, WA 98103, USA

Marie-Cécile Soulier	CNRS UMR 5608 TRACES Université de Toulouse-Jean Jaurès Maison de la Recherche 5 allées A. Machado 31058 Toulouse Cedex 9, France
Marc Vander Linden	UCL Institute of Archaeology 31-34 Gordon Square London WC1H 0PY, UK
Andrej Vizi	Prirodnjački muzej Crne Gore Trg Bećir-bega Osmanagića 16 81000 Podgorica, Montenegro
Snežana Vuksanović	Prirodnjački muzej Crne Gore Trg Bećir-bega Osmanagića 16 81000 Podgorica, Montenegro
Zvezdana Vušović-Lučić	Zavičajni muzej (retired) Nikšić, Montenegro
Robert Whallon	University of Michigan Museum of Anthropological Archaeology Ann Arbor, MI 48109-1079, USA

Chapter 18

Studying Neanderthal Fire Structures from Crvena Stijena

Ramiro J. March, Robert Whallon, Mike W. Morley

Introduction

The site of Crvena Stijena offers an extraordinary opportunity to study a very long sequence of Neanderthal occupations where the traces of fire are well preserved. In this sense, Crvena Stijena could be included in the short list of Lower and Middle Paleolithic sites with features containing abundant ash and charcoal and exhibiting a substrate of reddened sediment (Schiegl et al. 1996; Mallol et al. 2013) in the Mediterranean area such as Kebara, Hayonim, L'Abric Romani, and El Salt (Meignen et al. 1989; Mercier et al. 1995; Stiner et al. 1995; Meignen et al. 2001; Albert et al. 2003; March et al. 2008; Sistiaga et al. 2011; Courty et al. 2012; March et al. 2014).

The analysis of ancient fire structures is closely related to the analysis of the history of human social behavior. The use of fire radically changed human adaptive strategies and provoked changes in social organization that may be reflected in archaeological contexts (Hough 1926; Perlès 1977; Clark and Harris 1985; Goudsblom 1992; Bar Yosef et al. 1996; Pine 2001; March, 2002; Wrangham, 2009). The analysis of ancient fire structures could thus contribute to a better understanding of Paleolithic history (Bellomo 1994; Weiner et al. 1998; James 1989, 1996; March, 2001; March et al. 2006; Roebroeks and Villa 2011) and particularly Neanderthal social behavior.

As hunter-gatherers, Neanderthal groups generated different kinds of archaeological contexts including the frequent occupation of rock shelters and caves. These kinds of contexts seem to preserve many different occupations where the use of fire is attested, which can contribute to an improved understanding of Neanderthal camps and their organization. As fire played a central place in hunter-gatherer camps and activities, its localization could aid in inferring the organization of activity areas and in establishing relations and connections with other debris, such as that related to artifact production, cooking, and food-processing activities, or different kinds of waste management (Leroi-Gourhan and Brezillon 1972; Yellen 1977; Binford 1978, 1983, 1996; Otte, 2012). The analysis of different occupations requires that we be able to differentiate the different kinds of fire structures, to understand the stratigraphic sequence, and to separate and define the spatial organization of different occupation levels (Vaquero and Pastó 2001; Henry et al. 2004; Speth 2006; Sandgathe et al. 2001; Henry 2012; Sorensen 2017). This is crucial if we want to discuss with solid arguments whether the spatial organization of Neanderthal groups and behavior reflects their social organization and allows us to understand their degree of complexity.

Fire-related activities can be inferred from the presence of ashes, charcoal, burnt bones, stones, and soils, and even from organic matter. The multiple combinations and structures of these elements can be indicative of different kinds of fire structures, from fireplaces themselves to areas of evacuation of combustion debris (Courty et al. 2012; Goldberg et al. 2012; James 1989; March et al. 2006, March, Dumarçay and Lucquin 2006; March et al. 2014; March, 2014; Stiner et al. 1995; Schiegl et al.1996; Théry-Parisot 2001, 2002; Shahack-Gross et al. 2014; Vidal-Matutano, 2016).

At Crvena Stijena, fire structures are recurrent in different layers, showing changes of size, position, and internal sequences, which indicate changes in the form and intensity of use of each fire structure and of the shelter habitat. The activity related to fire is so intense in some cases that the remains of these activities are one of the most important components of the anthropic layers of sediments deposited at the site (Morley, Chapter 7, this volume). At the same time, Crvena Stijena

like many Neanderthal sites shows a dominance of flat fire structures, that were lit directly on the soil without any arrangement, except the position of wood at the moment when these fires were in use. This uniformity in form is a challenge for the understanding of their different functions, but a detailed description and analysis of their forms and their constituents can help us to understand their nature, their mode of functioning, and their role in Neanderthal social life. For these data it is necessary to identify the nature of these different kinds of fire structures, which can vary from hearths to fire residue deposits, which also can change in their characteristics, from very well preserved ash accumulations to layers that contain mostly combustion residues or thermally altered debris. The degree of resolution that we can reach is closely related to our capacity to disentangle the palimpsest of occupations that was created by the formation processes of the anthropic layers in Crvena Stijena.

As with other aspects of Neanderthal behavior, the study of Neanderthal fire structures at Crvena Stijena involves many challenges. First at all, the study is conditioned by the real conditions of the site today where the fire structures from the Middle Paleolithic are only accessible from the profiles that earlier excavations left in place in the rear portion of the shelter. But at the same time these profiles show many interesting superpositions that change in form and distribution within a single layer, and also between different layers, and can give us a possible indication of the formation processes, (natural or anthropic) that contributed to their archaeological state.

We here apply a descriptive, analytical and experimental approach that combines different analytical techniques to reveal the nature and the possible functions of different kinds of fire structures found here. This approach combines the analytical characterization of the elemental constituents of each layer by X-ray fluorescence and X-ray diffraction (XRD), an organic chemistry characterization that combines the micromorphological and geological analyses developed by Morley and an experimental approach that can lead us to better interpret the different kinds of fire structures found at Crvena Stijena. Finally, this overall approach was combined with an analytical study of the stratigraphic sequences of fire structures to try to understand some of the characteristics of the Crvena Stijena sequence and of Neanderthal spatial organization as well as possible, given the limitations of working entirely from archaeological profiles.

The Crvena Stijena profiles presented many different layers, from we have chosen to study two as good examples of intensive Neanderthal occupation: layer XX (classified by Basler as "Mousterian with Triangular Points") and layer XXIV (identified by Basler as simply Mousterian), and a third one, layer XXIII, considered as sterile in terms of Neanderthal hearths (Morley, Chapter 7, this volume) which is studied here for comparative purposes.

Fire structures: From a Descriptive Analysis to a Dynamic View of Neanderthal Social Space Behavior

Layer XX (Mousterian with Triangular Points)

As described by Morley (Chapter 7, this volume), layer XX is made up of a sequence of anthropic layers that contain predominately fine-grained material with occasional medium gravel and whose color is mainly 10 YR 3/2 to 2/2, brownish black. Moderate quantities of bone were observed throughout most of the layer, and moderate to abundant amounts of charcoal were detected. Carbonates are also present, showing values with a distinctive up-profile increase from 16.1 % at the base to 57.4 % about two-thirds of the way up, before dropping back to 40.5 %. Quantities of organic matter vary from 15.6 % at the base of the layer to a low of 3.2% at the point of maximum carbonate content. All these values indicate a high anthropization of the entire layer (see also Morley, Chapter 7, this volume).

For our work, we cleaned a 3 m (width) by 0.75 m (height) surface on the E-W profile, between 4.5 m and 5 m in depth (Figs. 18.1-18.3). The photograph of the profile was put in real scale and the profile was designed with an architectural/data base software that allowed us to obtain dimensions of the different kinds of layers that were recognized at the site. Following geological (texture, composition, color) and anthropic (presence or absence of anthropic debris such as burnt bones, charcoal, lithic industry) description criteria and Morley's earlier study, we could identify six kinds of layers: ash layers, black layers, grey layers, reddish layers, burnt bone layers, and grey soils.

Layer XX presents sixteen fire structure "ash" layers, which have different dimensions (Fig. 18.2, see also Appendix). The minimum width of these layers is 8.1 cm and the maximum is 183.5 cm. Their maximum thickness varies between 0.7 and 6.4 cm and their area between 5.96 and 534.13 sq cm (Table 18.1).

These ash layers are accompanied by a suc-

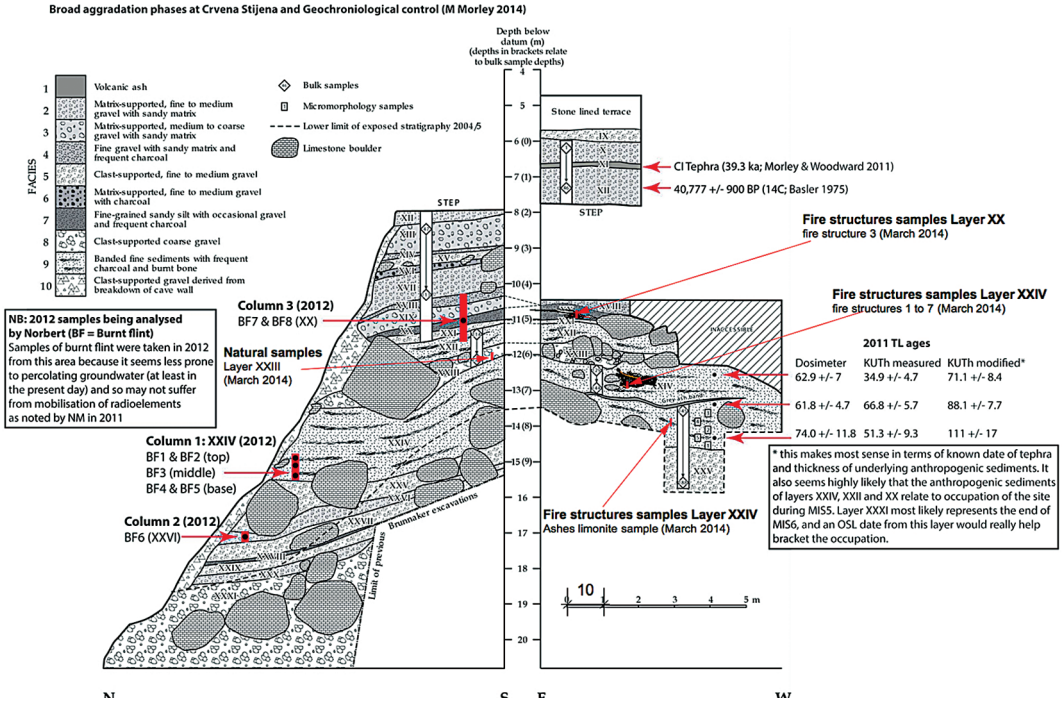

Fig. 18.1. General plan of profiles of Crvena Stijena and situation of the fire structures sampled for this work (modified from original by M. Morley).

Fig. 18.2. Layer XX studied profile.

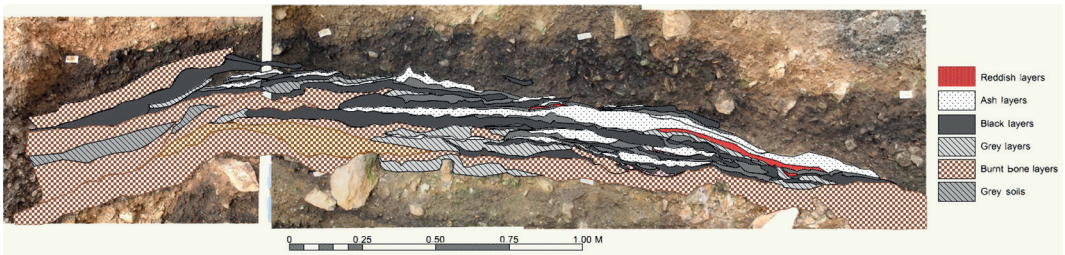

Fig. 18.3. Layer XX studied profile with reconstructed layers.

cession of 22 black layers that are intercalated between or contain the ash layers. The minimum width of these layers is 7.45 cm and the maximum is 143.5 cm. Their thickness varies between 0.7 and 8.1 cm. Their height ranges between 1.55 and 16.5 cm (Table 18.1).

We can observe also 22 grey layers of minor dimensions. The minimum width of these layers is 6.4 cm and the maximum is 64.2 cm. Their thickness varies between 0.5 and 4.2 cm and their height between 1.39 and 9.09 cm (Table 18.2).

We also observed a limited number of reddish layers that also have small dimensions. The minimum width of these layers is 4.2 cm and the maximum is 57.9 cm. Their maximum thickness varies between 0.8 and 1.9 cm and their height between 1.62 and 14.65 cm (Table 18.2).

At a macro observational level, burnt bones in these layers are sometimes *in situ* and some of them seem to be burned by heat transfer from above and have multiple or single colors (white, white-grey, grey, black, brown, and light brown) consistent with the changes observed in the coloration of the surrounding sediment layers and with burning processes. These colors and their distribution on bones are related to temperature and conditions of exposure of bones to fire as has been shown in many previous works (Nicholson 1993; Stiner et al. 1995; Joly and March 2003; Costamagno et al.2005; March et al.2012).

Finally we observed two other different kinds of layers: 15 grey soil layers and 12 burnt bone layers. The grey soils, are in general larger than the other layers presented above. Their maximum thickness is between 0.60 to 5.10 cm with a mean of 3.21 cm, their height is between 2.55 and 15.10 cm, and their width falls between 11 and 56 cm. These layers are mostly composed of fine grey sediments and fragments of calcareous stones. Another characteristic is that they do not contain bones of great size, or burned or carbonized bones.

These latter, layers of burnt bones, are the major layers within layer XX, their maximum width reaches 311.4 cm, their maximum height 34.25 cm, and their maximum thickness 28.7 cm. These layers contain large quantities of partially burnt bones, burned at lower temperatures, as seen in their characteristic dark brown or partially black coloration, and are not necessarily related to the *in situ* fire structures. These layers seem to be the product of anthropic debris that makes up the soil surfaces where human occupations were installed (Table 18.3).

The vertical surface of the profile zone where we identified these layers has an area of 8803.62 sq cm. Inside this area, ash layers occupied 977 sq cm (11%), black layers 1410.30 sq cm (16%) grey layers 542.21 sq cm (6.15%) reddish layers 99.02 sq cm (1.12%), burnt bone layers 4787 sq cm (54%) and finally grey soils 988.08 sq cm (11.22%).

Table 18.1. Summary statistics for ash layers and black layers from layer XX of Crvena Stijena.

	Layer XX ash layers				Layer XX black layers			
	THICKNESS	HEIGHT	WIDTH	AREA sq.cm	THICKNESS	HEIGHT	WIDTH	AREA sq.cm
N	16	16	16	16.00	22	22	22	22
Min (cm)	0.70	1.00	8.10	5.96	0.70	1.55	7.45	2.95
Max (cm)	6.40	24.75	183.55	534.13	8.10	16.60	143.75	492.24
Sum	37.20	87.69	529.28	977.32	50.90	125.77	803.21	1410.30
Mean	2.33	5.48	33.08	61.08	2.31	5.72	36.51	64.10
Std. error	0.39	1.50	10.25	32.02	0.34	0.74	6.68	22.76
Variance	2.47	36.08	1682.35	16401.83	2.57	11.93	980.35	11394.75
Stand. dev	1.57	6.01	41.02	128.07	1.60	3.45	31.31	106.75
Median	1.65	3.14	20.96	21.13	1.80	4.93	27.91	26.34
25 percentile	1.33	2.33	17.35	11.71	1.48	3.13	16.74	12.73
75 percentile	2.98	5.29	31.70	61.97	2.93	7.38	45.88	65.37
Skewness	1.43	2.60	3.71	3.80	2.58	1.59	2.22	3.42
Kurtosis	1.68	7.24	14.37	14.85	7.94	3.56	5.90	13.10
Geom. mean	1.93	3.85	24.47	27.15	1.98	4.88	27.85	30.15
Coeff. var	67.60	109.60	123.99	209.67	69.29	60.43	85.76	166.52

In layer XX, ash layers lie generally on top of black layers (45%) or grey layers (36%) and more rarely on other ash layers or reddish ones (both 9%). In some cases (n = 6) ashes cover different kinds of underlying layers, such as black/grey layers, or grey ashes (Fig. 18.4).

We must note that in layer XX the black layers are generally thicker than the layers of ashes that only partially cover them. This seems to indicate that these blackened sediments and their contents are not only the result of the action of the heat of fire structures but may have a more complex origin. They may, for example, be an accumulation and mixture of anthropic burned debris produced by the human occupation of the shelter—disturbed sediment and debris of ancient occupation floors. These black layers lie mostly on top of burnt bone layers or grey layers (33%), but they also cover ash

Table 18.2. Summary statistics for grey layers and reddish layers from layer XX of Crvena Stijena.

	Layer XX grey layers				Layer XX reddish layers			
	THICKNESS	HEIGHT	WIDTH	AREA sq.cm	THICKNESS	HEIGHT	WIDTH	AREA sq.cm
N	22	22	22	22	4	4	4	4
Min (cm)	0.50	1.39	6.40	3.33	0.80	1.62	4.20	2.91
Max (cm)	4.20	9.09	64.20	70.08	1.90	14.65	57.98	80.82
Sum	40.00	92.21	555.22	542.21	4.50	21.22	90.70	99.03
Mean	1.82	4.19	25.24	24.65	1.13	5.31	22.67	24.76
Std. error	0.21	0.51	2.90	4.12	0.26	3.13	12.01	18.72
Variance	0.99	5.69	184.95	373.51	0.28	39.10	576.58	1401.87
Stand. dev	0.99	2.39	13.60	19.33	0.53	6.25	24.01	37.44
Median	1.45	3.65	24.30	19.96	0.90	2.48	14.26	7.65
25 percentile	1.08	1.79	15.10	7.09	0.80	1.73	6.57	4.04
75 percentile	2.53	6.65	33.51	32.89	1.68	11.71	47.19	62.59
Skewness	0.87	0.52	1.05	1.15	1.82	1.96	1.76	1.98
Kurtosis	0.04	-1.01	1.89	0.73	3.29	3.85	3.34	3.93
Geom. mean	1.58	3.54	21.74	17.74	1.05	3.45	14.91	10.83
Coeff. var	54.60	56.94	53.89	78.42	46.68	117.86	105.90	151.23

Table 18.3. Summary statistics for burnt bone layers and grey soils from layer XX of Crvena Stijena.

	Layer XX burnt bone layers				Layer XX grey soils			
	THICKNESS	HEIGHT	WIDTH	AREA sq.cm	THICKNESS	HEIGHT	WIDTH	AREA sq.cm
N	12	12	12	12	15	15	15	15
Min (cm)	2.50	4.44	11.55	18.08	0.60	2.55	11.00	8.08
Max (cm)	28.70	34.25	311.45	2056.97	5.10	15.10	56.10	219.50
Sum	102.90	200.94	908.23	4787.58	48.10	103.65	438.05	988.09
Mean	8.58	16.75	75.69	398.97	3.21	6.91	29.20	65.87
Std. error	2.12	3.02	22.74	159.75	0.31	0.92	3.91	15.65
Variance	53.70	109.20	6206.74	306249.20	1.46	12.74	229.52	3673.91
Stand. dev	7.33	10.45	78.78	553.40	1.21	3.57	15.15	60.61
Median	6.20	14.30	65.10	273.00	3.00	6.40	22.05	38.11
25 percentile	3.35	7.86	26.56	66.35	2.30	3.80	16.15	24.74
75 percentile	11.70	27.10	79.06	419.03	4.20	9.70	44.40	86.40
Skewness	2.06	0.36	2.78	2.82	-0.37	0.95	0.46	1.52
Kurtosis	5.19	-1.44	8.76	8.78	-0.11	0.54	-1.31	1.86
Geom. mean	6.54	13.51	53.49	194.02	2.91	6.11	25.56	45.05
Coeff. var	85.46	62.41	104.09	138.71	37.63	51.66	51.88	92.02

Fig. 18.4. Percentage distribution of kind of underlying layers for ash, black , grey, reddish layers, burnt bone layers, and grey soils.

layers (17%) or grey soils (10%). In a few cases they cover other black layers (7%), but they do not cover any reddish ones. Here, also, in some cases (n = 6) black layers cover different kinds of underlying layers.

Grey layers lie generally on top of black layers (51%) or ash layers (31%) and, in fewer cases, grey (10%) or reddish layers (7%). These grey layers seem to be closely related to black layers and ash layers. Grey layers situated between ash and black layers could indicate vertical migration of ashes, representing the formation of transitional layers between the black and ash layers, or the thermal alteration of underlying black layers at high temperatures.

Reddish layers, which, as we said before, can be the result of the direct oxidation of soils beneath fireplaces, lie on top of black (40%) or grey layers (40%), and in one case an ash layer (20%).

Burnt bone layers overlie mostly other burnt bone layers (48%), black layers (29%), and grey soils (24%), rarely ash layers (5%), and they never overlie reddish layers or grey layers. In many cases (n = 8) burnt bone layers lie on different kinds of layers.

Grey soils overlie many different kinds of layers, principally black layers (30%) or burnt bone layers (30%). After these two kinds of layers are grey layers (23%) and ash layers (15%). Reddish layers are never overlain by grey soils.

These burnt bone layers and grey soils are the only layers on layer XXI.

As was demonstrated by Morley (Chapter 7, this volume), the superposition of ash layers and reddish layers indicates the *in situ* position of

ancient fires, while the superposition of ash layers could indicate palimpsests of combustible residues in an area with no interruption of function. As we can see, the superposition of ash layers and reddish layers is not a regular phenomenon. Different situations could explain these stratigraphic patterns. For example, we could suppose that in some cases the temperatures of fire structures in Crvena Stijena did not reach the temperature needed to rubify (oxidize) underlying soils. In this case, the underlying sediments would only be blackened. If the temperature needed to rubify sediments at Crvena Stijena was higher than 500°C, ashes could also indicate *in situ* fire structures with temperatures below 500°C, but still sufficient to burn sediments and carbonize their organic content, leading to blackened sediments. However, considering that in layer XX ashes lie mostly on top of black layers, it is possible to imagine that fires were ignited directly on black layers that constituted soils where heat transfer provoked thermal changes. Given that these black layers were composed essentially of organic debris, it is clear that their transformation by fire action will be different from rubification and similar to the reaction of isolated organic matter such as bones or charcoal, involving the thermal alteration and combustion of carbon. In this case, the coloration of organic layers will evolve from the natural color to brown, dark brown, black, dark grey, grey, and, finally, white with increasing degrees of thermal transformation of organic components.

To evaluate both hypotheses, we made an experiment in which sediments from layer XXIII and a black layer of layer XX were exposed to controlled temperatures (between 100°C to 1000°C) in an electric oven for one hour in an oxidizing atmosphere (Fig. 18.5). For this experiment, the sediments from layer XXIII are considered as natural soils of Crvena Stijena. Morley (2007) characterized this layer as a coarse gravel layer that has low levels of organic matter, high concentrations of carbonates, and low magnetic values. The color of the samples from layer XXIII taken for this study is very pale brown (10 YR 7/3) or brown (7.5 YR 5/3), and our samples contained no traces of bone or charcoal. Their elemental composition is characterized by CaO, (41.33%), SiO_2 (22.43%), and Al_2O_3 (5.60%), P_2O_5 (1.36%). XRD shows that the sediments contain calcite, dolomite, and quartz, but hydroxyl apatite is totally absent. The granulometry of our samples corresponds to coarse sand. The essential difference in mineralogical and elemental composition of the black layer is thus the presence of hydroxyl apatite. The black layer presents a similar concentration of CaO (41.73%) but lower concentrations of SiO_2 (16.50%) and Al_2O_3 (2.64%). We can also mention the absence of MgO, and higher levels of P_2O_5 (9.97%) and S and Cl (in ppm) even if in both layers these last two elements are present in low concentrations. The concentration of organic matter is greater in the black layer (1.12 μg/g) than in the sterile one (0.59 μg/g).

Our experimental results show that these two layers change in radically different ways under heat exposure. The black layer exhibited light oxidation at 500°C but was transformed progressively into a lighter grey, and became ash between 500°-600°C. The natural soil of Crvena Stijena (layer XXIII samples) turned to red above 500°C, its coloration darkening between 300° and 500°C and turning definitively to a red color at more than 600°C (Table 18.4, Fig. 18.5).

These data are very interesting because they indicate that if fire structures were lit above black layers, the transformation of these layers under heat could lead to the formation of grey or ash layers. The ashes are produced by the combustion of organic matter present in the black layers, like bones, charcoal, and possibly other materials with carbon content that have not yet been identified. On the other hand, this experiment also confirms that reddish soils at Crvena Stijena could appear only if fire structures achieve high temperatures.

Further related to fire action on soils, Morley (Chapter 7, this volume) has found that the magnetic susceptibility (χ_{lf}) of the layer XX sediments does not co-vary with charcoal count, and the same is true for other parameters which might be associated with anthropogenic activity, with χ_{lf} showing no significant correlation with the loss-on-ignition index LOI ($r = 0.30$), or with his Laboratory Anthropogenic Index (LAI) that combines all the data generated from the parameters LOI, the Munsell Value Index (MVI), and laboratory charcoal counts ($r = 0.17$). nor, finally, with his Field Anthropogenic Index (FAI) that uses the data from the bone and charcoal frequency recording scheme used in the field, ($r = -0.30$). This is unusual given that for the entire sequence values of LOI, for example, have a very good level of correlation with magnetic susceptibility ($r = 0.75$). It seems that even if we can detect

Table 18.4. Munsell colors in function to temperature for black sediments of layers XX and XXIII.

	Black layer, layer XX			Sterile layer, layer XXIII		
natural	10YR	2/2	very black brown	7.5YR	5/3	brown
100°C	10YR	2/2	very black brown	7.5YR	5/3	brown
200°C	10YR	2/2 to 3/1	very black brown	7.5YR	6/3	light brown
300°C	10YR	2/2 to 3/1	very black brown	7.5YR	6/4	light brown
400°C	10YR	4/2	dark grayish brown	7.5YR	5/4	brown
500°C	10YR	6/3	pale brown	7.5YR	5/4	brown
600°C	10YR	7/3	very pale brown	7.5YR	5/4 to 5/6	brown/ strong brown
700°C	10YR	7/3	very pale brown	7.5YR	6/4 to 6/6	light brown/reddish yellow
800°C	10YR	7/2	light gray	5.4R	6/4	light reddish brown
900°C	10YR	7/2	light gray	2.5YR	6/6	ligth red
1000°C	7.5Y	8/2	Light grey	2.5YR	6/6 to 6/4	light red/light reddish brown

Fig. 18.5. Color and texture changes as a function of temperature for sediments of black layers in layers XX and XXIII.

charcoal and burnt bones in these layers, the action of fire did not modify the magnetic susceptibility. That is consistent with a view of these layers as soils made up of anthropic debris that includes a mixture of elements coming from fire structures but all exposed to low temperatures. Another possible explanation for these results is that the sedimentary component of these layers contains low quantities of quartz, aluminum, and iron constituents of the natural clays, in which case magnetic susceptibility would be minimally affected.

Overall, looking at the layer XX fire structures, we see that they have stratigraphic sequences which can be summarized as follows: ash layers above reddish layers, ash layers over black layers, ash layers above grey layers, and finally ash layers over other ash layers.

The first sequence can be explained simple as fire structures *in situ*, which burn the underlying sediments at high temperatures, as Morley (Chapter 7, this volume) saw in his micromorphological analyses. The second sequence can be now interpreted in three different ways: 1) if ashes came from combustible residues, we can interpret them in the first place as evacuation areas of combustible (wood or bone) debris, 2) still considering that the ash layers come from combustible debris, they might be interpreted as fire structures that burned at lower temperatures (less than 400-500°C), which did not oxidize or transform the underlying layers, and finally 3) we could interpret them as burned soils created by fires at high temperatures of more than 500°C which transformed the soil beneath them to ashes. In this last case, ash layers indicate the intensity of the fire structure and could be also related to the length of time of burning of each soil (March and Ferreri 1989, 1991; Ferreri and March 1996; March et al.2010; Muhieddine et al. 2011). The same processes could explain the superposition of ash and grey layers, with the difference in color being explained by the temperatures reached, depending on the depth of the soil that was affected by heat.

Finally, the superposition of ash layers over ash layers can be interpreted as the superposition of combustible debris over altered soils, or by the superposition of fire structures *in situ*, or even by the superposition of evacuation areas situated

outside the fire. In any case, we can consider that both ash layers and reddish layers are related to the direct action of fire.

The dynamics of fire in layer XX

If we can consider that ash layers and reddish layers are a direct consequence of the action of fire, we can analyze the dynamics of fire that are still observable in the exposed profile of layer XX. This analysis of the stratigraphic sequence may thus give us a preliminary idea of the Neanderthal use of the space related to fire. To measure the relative intensity of the use of space for fire structures in each section of the profile analyzed, we propose to use the proportion occupied by ash or reddish layers within the vertical surface (defined by the boundaries of Basler's layers) that contains the studied layers. This index, I, is simply the proportion of the surface of the profile occupied by the layers or structures in question. In the section of layer XX studied here, I = 0.11 for ash layers and I = 0.01 for reddish layers. The mean (E-W, N-S) surface of these layers is 61.06 sq cm for ash layers, with a minimum of 5.96 sq cm and a maximum of 534.13 sq cm, and for reddish layers 24.76, 2.91 and 80.92 sq cm, respectively. The grey layers, which could be also related to the use of fire as discussed above, have an index of I = 0.06, and the black layers, which could represent the accumulation of combustion debris coming from other episodes of fire and presenting higher concentrations of charcoal and carbonized bones, have an index of I = 0.16. The highest index, however, is I = 0.54 for burnt bone layers.

To construct a 3D model that allows us to explore the dynamics of the use of fire in Crvena Stijena, we use the stratigraphical data and dimensions obtained from the profile. The center of the width of the exposed surface of each layer will be used here as the reference for their central position (see Appendix). Layer width will be used as the hypothetical diameter occupied by the fire horizontally. The maximum thickness of each layer will be used as the thickness of each structure. Following this procedure, we can make a first schematic 3D model to represent the positions of fire structures and their arrangement in layer XX (Figs. 18.6-18.7).

As we can see from the vertical view of the ash layers (Fig. 18.7), most ash concentrations have relatively small dimensions, between 13 and 40 cm in width (diameter), and only two are particularly different, one small layer of 8 cm and a very large one that is 183 cm in diameter. The horizontal E-W distance between the extremes of these layers is 230 cm.

Within the studied profile, ash layers frequently occur in pairs associated at the same stratigraphic position (Figs. 18.8-18.9). Twelve of the 16 structures exhibit this organization, forming six pairs of structures east and west of each other. We can observe that in these pairs of associated structures, there is frequently an asymmetry where one structure has larger dimensions than the other. The larger structure is situated indifferently either on the west or the east in each pair. In four cases the structures are separated by different distances and in two cases the structures are in contact. This organization in pairs could be the consequence of different functions of each structure. For exam-

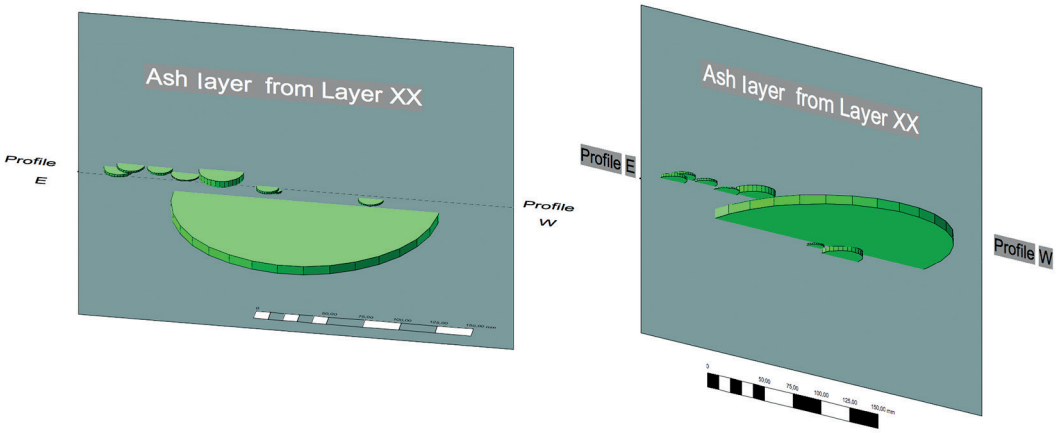

Fig. 18.6. 3D schematic model of ash layers from layer XX, right rear and lower right rear position.

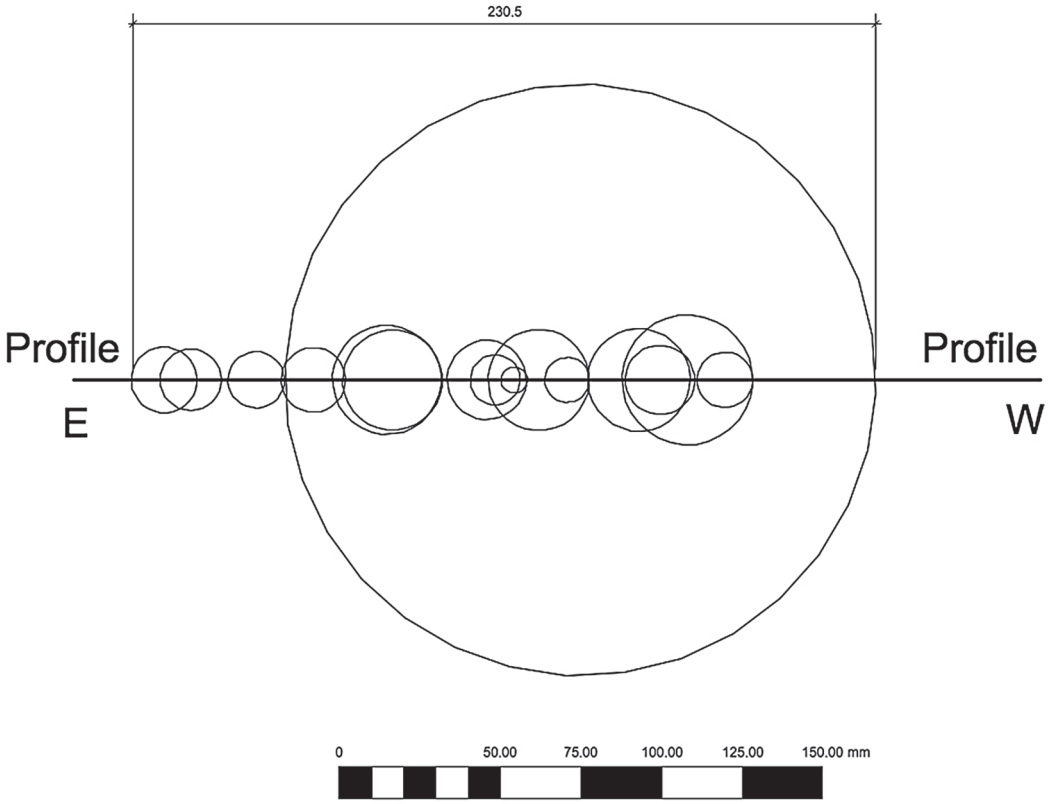

Fig. 18.7. Top view of the position of fire structures in the profile of layer XX; the diameter of the circles represents the width of each fire structure in the profile.

ple, we could have a small structure to prepare the fire and burn wood to get embers and, very close to this structure, another one with a larger surface intended for cooking. In fact, if we take into account these associations, the dimensions used for fire activities in this space could be interpreted as more important, and would have larger dimensions, ranging from 39 cm to 65 cm in diameter as a function of the size of each pair of structures and their horizontal separation.

Their displacements over time (X = horizontal and Y = vertical) following the axis of the profile, show that, if we take into account all the ash layers as isolated structures, the majority of the horizontal displacements are between 2.8 and 50 cm, with a mean of 31.28 cm. If we consider the pairing of some structures, the displacement between the central point of each combustion area (that can contain one or two structures depending on the case) runs from 3.8 cm to 59 cm, with a mean of 32.2 cm. In layer XX, their stratigraphical vertical separation runs from 1 to 5.7 cm, with a mean of 2.36 cm. The vertical position of groups of fire structures can not be considered accurately because the slope of the layers creates measurement errors.

Following their sequence of deposition (Figs. 18.8-18.11), we distinguish a first series of displacements oriented to the east at the base of the sequence, showing the superposition of six fire structures that form three combustion areas. This series begins with a pair of ash layers (in yellow in Figs. 18.8-18.9) of very different dimensions, one of 32 cm diameter and the other of only 14 cm to the east of the larger one (layers 20-11 and 20-11b, see table of values in Appendix). These ash layers are in contact and constitute a combustion area with a total diameter of 46 cm and an E-W inclination of −10.6°. The thickness of these two structures also shows great variation; the larger one is 3 cm thick and the smaller one only 1 cm. A second combustion area (clear blue in Figs. 18.8-18.9) that is also constituted of two ash layers was located 58.5 cm to the east of the first one, in the same stratigraphic position. Therefore, we can assume that these first two areas were part of the same installation. The second area is made up of two ash layers (ash layers 20-10 and 20-9, see

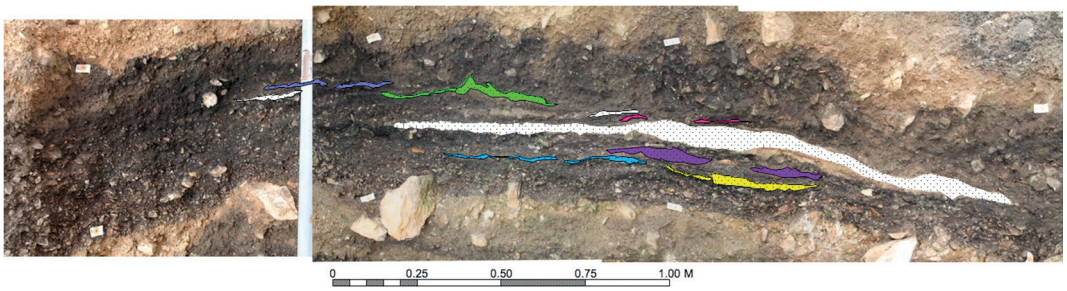

Fig. 18.8. Association of fire structures (ash layers) as a function of their stratigraphic position for layer XX; similar colors indicate stratigraphic association.

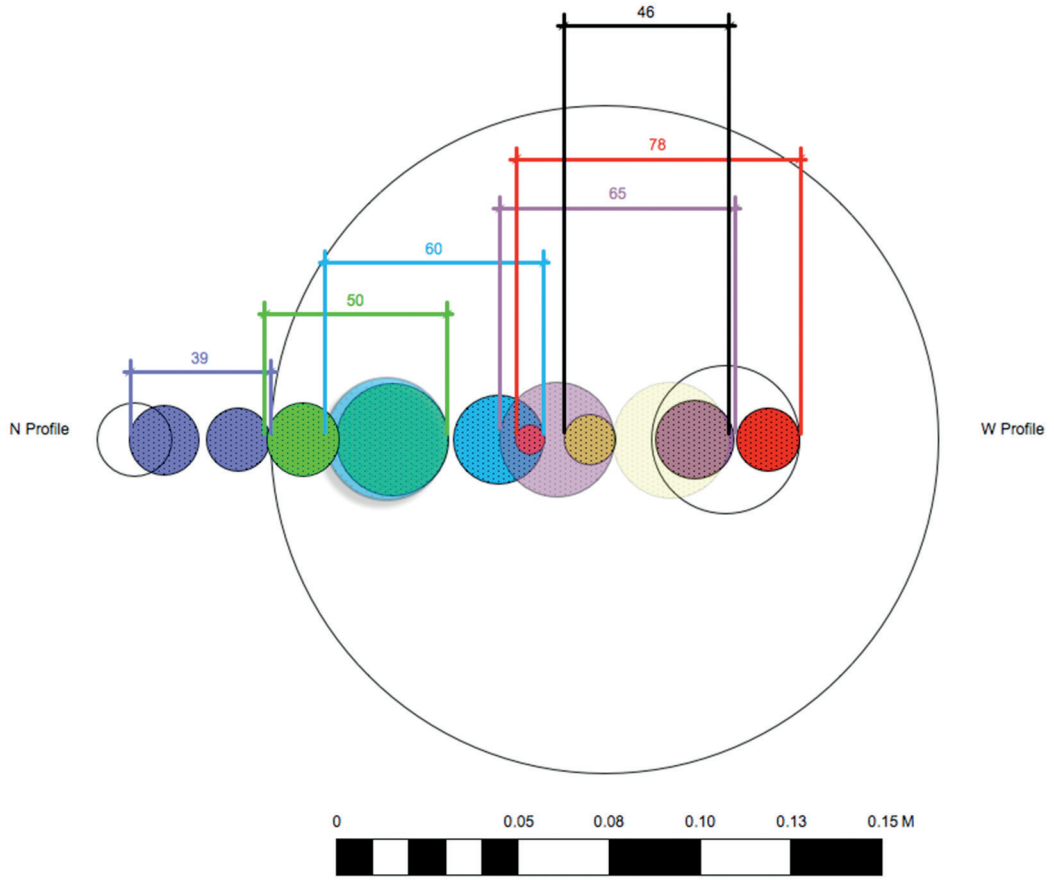

Fig. 18.9. Model top view of the associations of fire structures in layer XX.

table of values in Appendix) 24.5 and 33.7 cm in diameter that are separated by 1.8 cm, forming together a total area of 60 cm in diameter. This combustion area presents a gentler slope than the first one, −2.8°. These two ash layers are 1.4 and 1.9 cm thick respectively. It is interesting to note that the two combustion areas are organized such that the smaller ash concentrations of each area are near to each other, forming a mirror distribution where the smaller ash layers are in the interior and the larger ones on the exterior along an E-W axis.

This first installation, with four ash layers and two combustion areas of different dimensions, was covered by a new series of two ash layers (ashes 20-7 and 20-8, see Appendix; purple in Figs. 18.8-18.9) that form a combustion area of 65 cm in diameter and are displaced 50.4 cm

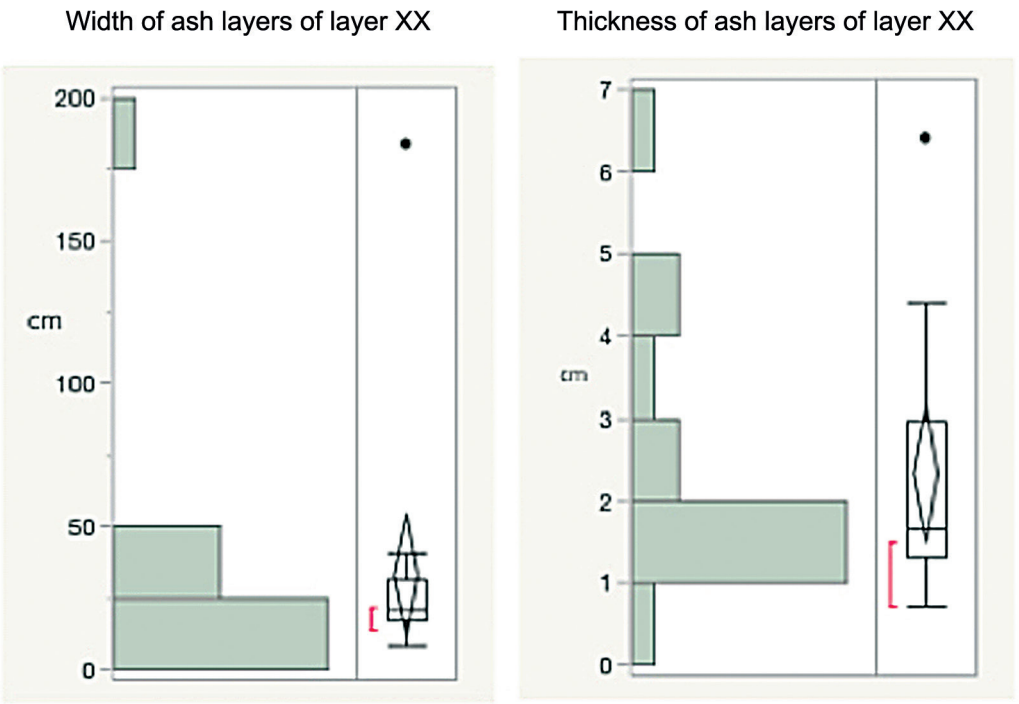

Fig. 18.10. Histograms of displacement on x (horizontal) and y (vertical) axes; width and whickness of the profiles of the ash layers of layer XX.

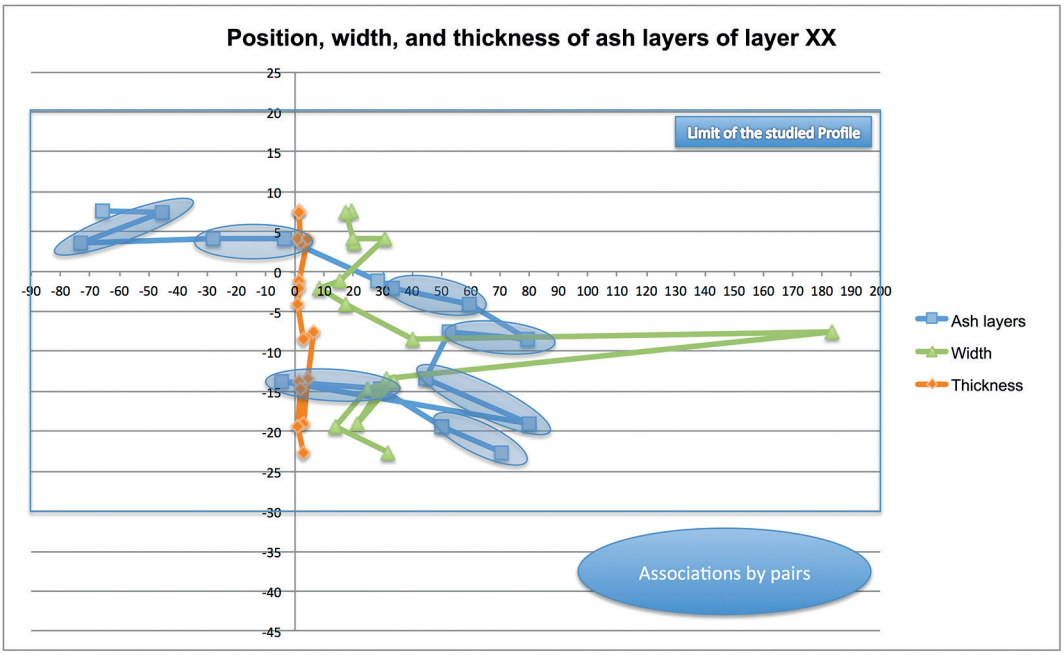

Fig. 18.11. X center position, width, and thickness in time relative to the profile studied for layer XX.

to the west. The vertical separation of this third combustion area from the first one (yellow) is between 1.6 and 3 cm and from the second one (clear blue) is 1 to 1.6 cm. These two layers are also arranged on an E-W axis, with dimensions similar to those of the second combustion area described above. The larger ash layer is 31.4 cm long in the profile. and the smaller one 21.51 cm.

The two structures are arranged like the second combustion area, with the larger one on the east, but here both layers are well separated (11.5 cm). This area shows an inclination of −7.18° on the E-W axis.

This third series was followed by the most important stratigraphic interruption in the sequence of ash layers, an interruption that includes the oxidation of a layer of soil by the following fire structure. This vertical separation is between 2.6–4.6 cm and consists of black layers, grey layers, and grey soils.

Above these layers we find the largest structure of the sequence, which extends over all the previous ash layers (white in Figs. 18.8-18.9). This structure is 183 cm in width with a thickness of 6.4 cm, with a center that is displaced 5 cm to the east in relation to the preceding area. The dimensions of this structure show that use of space related to fire at this moment of human occupation changes radically in comparison with the structures that we have previously described. The size of this structure implies the use of a large zone in the shelter only for activities related to fire. This size represents nearly six times the mean space occupied by fires in all the other structures (of the entire sequence). This structure (Appendix: Structure 3, Upper part of white grey ashes; Structure 3, White transition ashes; Structure 3, reddish soil) exhibits a complex internal stratigraphy and exhibits another difference from the other structures in its superposition of ash layers, showing the reutilization of the space for the same purposes but with a change in fire structure dimensions. This layer follows the slope of layer XX with an inclination of −7.87°. Here the presence of the reddish soil brings to the fore a question as to its nature because, if it is the result of some natural soil formation, this could indicate an interval in the formation of layer XX that links the big structure to two different natural processes that lead to the introduction and deposition of some natural sediment in the shelter.

Above this big structure, we observe a fifth sequence characterized by a combustion area containing two ash layers (Appendix: Ashes 20-5 and Ashes 20-6) at the same stratigraphic level (red in Figs. 18.8-18.9) and positioned partially over a grey layer, a black layer, and a small reddish layer that cover the big structure. This combustion area, which is 39 cm in diameter, contains two small ash layers 17.3 and 8.3 cm in diameter and 1 and 1.3 cm thick that are separated by 13 cm and present a slope of −3.8°. This area shows very little displacement to the east, only 3.8 cm in relation to the center of the big structure. The vertical separation of this combustion area from the big structure is 0.7–1.4 cm. The smaller structure is located to the east of the larger structure. This combustion area is one of the two smallest areas of the sequence.

This area of combustion was followed by a new isolated structure (Ashes 20-4) of relatively small dimensions, 15.5 cm in diameter and 0.6 cm thick, that is displaced 20.6 cm to the east of the preceding one. This structure is separated from the preceding structure by a black layer. The presence of this small structure not paired with a second one could indicate a change in the axial orientation of fire structures (for example to a N-S direction) which could create the absence of a second structure in the profile. Another explanation could be a difference in the function of this isolated structure, related to a reduction of the surface occupied by fire in this part of the sequence in this part of the shelter.

Above this isolated layer we observe a new displacement to the east of 43.2 cm, where a new combustion area 50 cm in width was created. This combustion area contains two juxtaposed ash layers (Ashes 20-3 and Ashes 20-3b) of relative large dimensions (20 cm and 30 cm in width), separated from the preceding area by more than 6 cm and inclined in an angle of −1.7° (in green in Figs. 18.8-18.9). Contrary to the last two series, the stratigraphic sequence here shows the presence of black or grey layers, and not reddish ones, forming the sediment that separates this area from the preceding, isolated fire structure. Here again the smaller structure is positioned to the east of the larger one. As in the first sequence where the structures are also juxtaposed, the larger structure is thicker than the smaller one (4.4 cm vs. 0.7 cm).

Following this pair of structures, we observe a new combustion area, 48 cm in diameter, formed by a new pair of ash layers (Ashes 20-2 and Ashes 20-2b) with widths of 17.5 cm and 20.4 cm respectively, which are separated by 9.8 cm (in violet in Figs. 18.8-18.9) and displaced 46.5 to the east. These two areas are 1.4 and 1.8 cm thick, and show an inclination of 6.8°. As we can see, the slope of this combustion area is reversed here, and the layer exhibits a noticeable inclination to the

east. In this area, the larger ash layer is situated on the east.

Finally this sequence is finished by a new isolated ash layer (Ashes 20-1) that overlaps the area of combustion just described. This ash layer is 19.6 cm wide and 1.4 cm thick, and is displaced 4.7 cm to the west. These ashes are separated from the preceding area by a black layer and a grey layer that underlie the ash concentration.

It is evident that the human occupation of the shelter was not interrupted while the hiatuses within this series of fire structures were formed. Other layers that are also made up of anthropic debris separate the sequences of fire structures. Thus the interruptions observed indicate that fire activities were displaced within the site. It is interesting to note the thinness of the layers of anthropic debris that separate fire structures within each sequence. That contrasts with the thickness observed in the natural hiatuses that precede and follow the installation of the large fire structure. If we could interpret this in terms of rhythms of anthropic sedimentation and if we think that fire is always present in Neanderthal habitat, this implies a greater mobility in the occupation space in the shelter that results in the creation of fire structures alternating with other human debris in this part of the site. The possibility remains that this dynamic was displaced to other parts of the occupied space when formation of fire structures was not ongoing here.

The organization of fire structures by pairs and also their consistent E-W orientation shows a recurrent behavior. As we can see, we can summarize their organization as two ash layers juxtaposed or separated by small distances. In all cases we observe an asymmetry between the two structures present in each area. This asymmetry is greater in the case of the juxtaposed layers. Occurrences of fire structures in the same layer can also be seen in other Neanderthal sites as Kebara (Speth et al. 2012; Goldberg 2012), or Tor Faraj (Henry 2012) or Mujina Pećina (Karavanić 2007). Some isolated structures of similar dimensions are also present and may indicate a rotation of the axis of activities to a north-south orientation. Finally we have the very big structure for the space in this part of the site. Except for this large structure, the paired or isolated fire layers have small dimensions compared to other ash concentrations or fire structures identified previously in other Neanderthal sites as Kebara (Speth et al. 2012), Tor Faraj (Henry, 2012), l'Abric Romani (Carrancho et al. 2016), Mujina Pećina (Karavanić 2007), or Roc de Marsal (Aldeias et al. 2012).

As we have determined experimentally, the reddish layers present in layer XX seem to indicate processes that cause the oxidation of the underlying soil at more than 500°C. The reddish layers of layer XX (Appendix: Reddish layer 1, 2 and 3 and Structure 3 reddish soil) follow the displacement of ashes in the profile but do not reach the N-S part of the profile. They tend to occupy smaller surfaces than the ash layers or grey layers that cover them (Fig. 18.12). Three of them have widths that are les than 20 cm (Reddish layers 1, 2, 3). Their presence indicates that heat had penetrated into the substrate, and their position reveals where the action of heat was greater in intensity or over time. In this sense it is interesting to note that the larger reddish layer (Structure 3 reddish soil) is directly related to the larger fire structure ash layer (Structure 3 in the Appendix). In this particular case the reddish zone is shifted under the west part of the ash layer and does not cover exactly the same surface (Fig. 18.13).

This might suggest that the ancient hearth did not have a homogenous distribution of temperatures, but had a higher heat in the center that covered a smaller surface than the present ash layer, or that the ash layer could be also the result of the dispersion of ashes beyond the original surface of the heat center of the fire structure. In another case the ash layer is also larger than the reddish zone, but the reddish zone is shifted to the east. In a third case the ash layer is smaller than the reddish one, but between the reddish and the ash zones we can observe a larger grey layer that covers the oxidized soil. In this last case, the ash layer is the smallest of all the ash layers preserved in layer XX and could indicate a very high temperature over a very limited surface of the fire structure. Finally, a last example shows a reddish layer covered by a grey layer, that could confirm that the grey layers are soils burned at high temperatures but not so high as to reach a white color (Fig. 18.14). The presence of ash layers over black layers that do not generate a reddish zone could be explained by two different possibilities: 1) that the black layers that underlie ash layers did not develop a clearly reddish color due to their content, or 2) that these ash layers are combustion debris that has been displaced from its *in situ* position, i.e., evacuation areas.

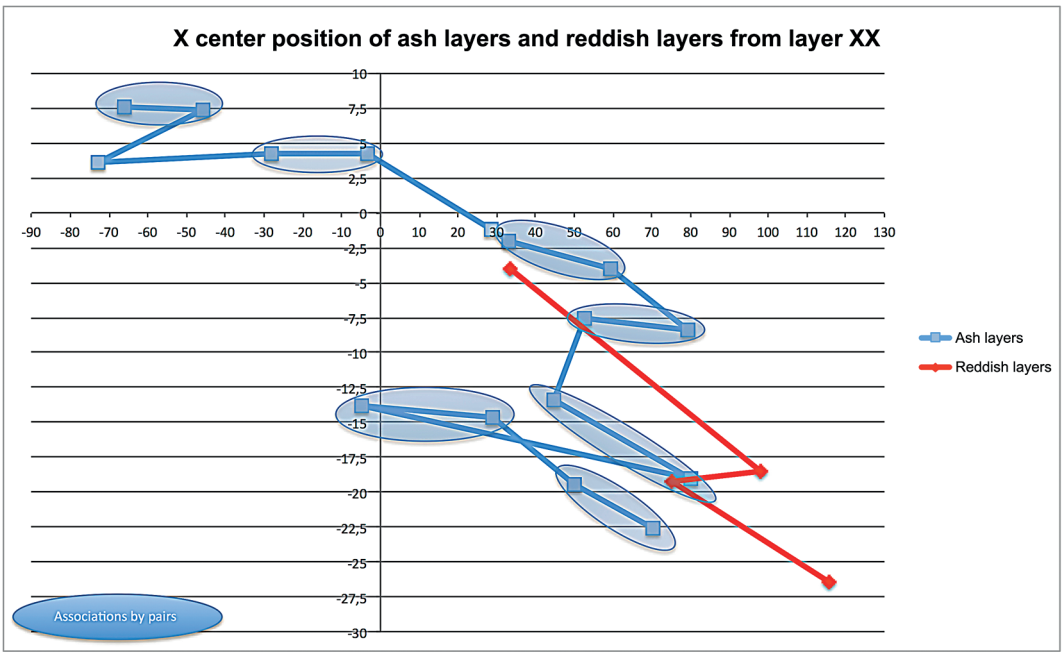

Fig. 18.12. X center position of ash layers and reddish layers from layer XX.

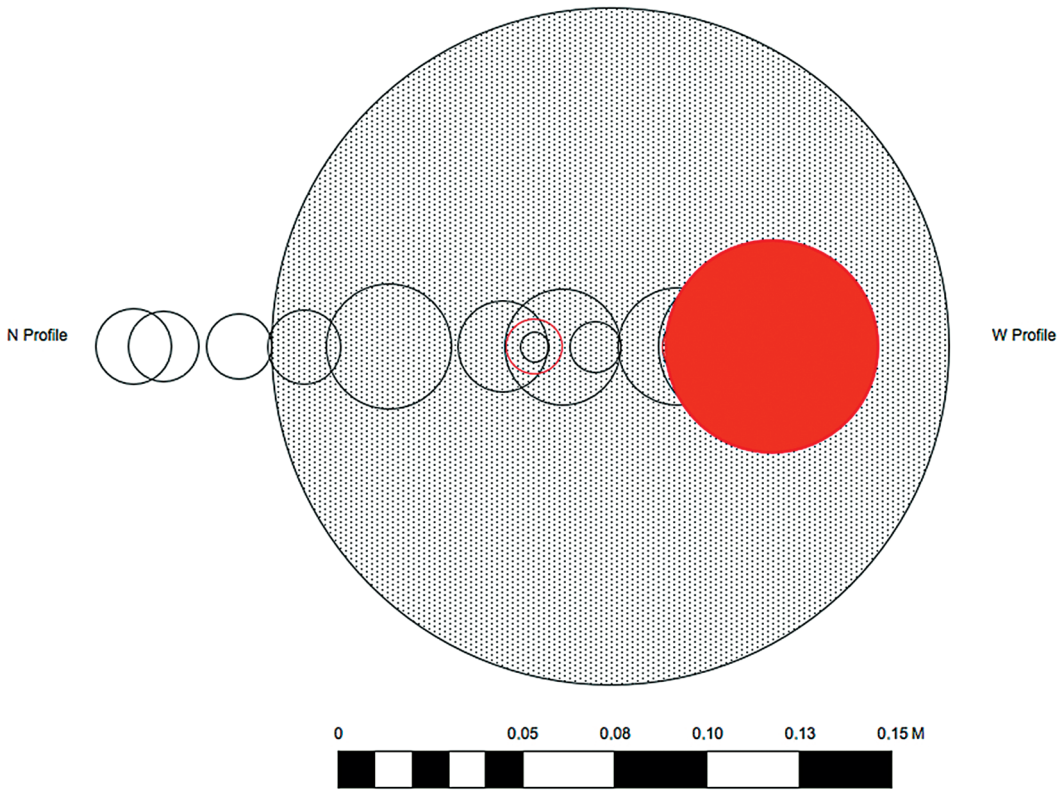

Fig. 18.13. Modeled top view of ash and reddish layers from layer XX with emphasis on the dimensions of the reddish layer and the big ash layer (red and black white pattern); the diameter of the circles represents the width of each fire structure in the profile.

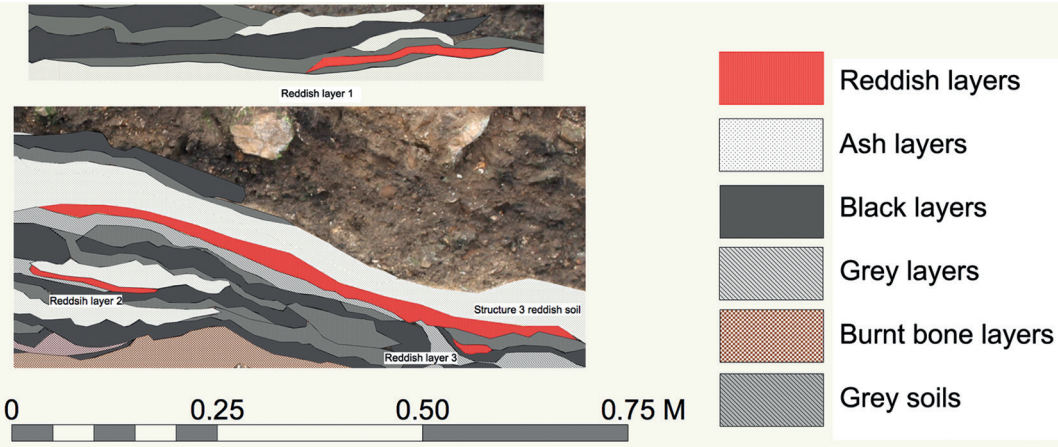

Fig. 18.14. Detail of reddish layers relative position in the stratigraphy of layer XX.

It is interesting to note then that reddish layers are always connected to ash layers or grey layers, in no cases did we observe paired associations of reddish layers as we do with ash layers. This could imply that when two associated ash layers exist they reached different temperatures which could be related to different functions and that they can be the result of high temperatures that burned black layers and not the deposition of combustion residues.

The function of the large structure detected in the first sequence may be different from the others found in the sequence. This structure also presents an internal stratigraphic sequence that could be studied in detail. Therefore we have chosen it for further analytical study (by X-ray fluorescence, XRD, and gas chromatography (GC), gas chromatography–mass spectrometry (GC-MS), and gas chromatography combustion isotope ratio mass spectrometry (CG-C-IRMS). These analyses may help to evaluate some of the various possibilities set out above. For this study, this structure was named "structure 3 big" (Fig. 18.15). It has a length of 1.83 m, and presents a complex stratigraphy that shows many internal layers of more than 3 cm thickness, which are not homogenously represented throughout its length and are contained between two black layers (anthropic soils) in the following stratigraphic sequence:

1) Upper black layer (soil)
2) Grey black layer that overlies the ash layer of the structure
3) White ash layer
4) Reddish soil
5) White transition (between red and black soil)
6) Grey soil
7) Lower Black layer (soil)

The analyses of this large structure are presented below in the section on "The Analytical Study of Sampled Fire Structures in Crvena Stijena."

Layer XXIV (Mousterian)

Layer XXIV has a maximum thickness of 2.3 m and contains many different sequences of fire structures that were accessible from the profile (Figs. 18.1, 18.16). Two of these sequences, situated at the middle and lower part of the layer, were selected for study. Here we will present the results of the fire structure sequence situated in the middle part of the layer. Samples of the lower part were taken for anthracological analysis by J. D. Shaw (see Shaw, Chapter 17, this volume).

As mentioned above, this whole layer is dominated by a matrix with high proportions of charcoal, ash, burnt and unburnt bones, and occasional lithics that seem to be thermally altered *in situ*; it also contains some interbedded fine sandy gravels and coarse sand units (Morley 2007; Baković et al. 2009; see also Morley, Chapter 7, this volume). Between the black layers we observed some fine-grained black layers that contain clays which can be related to the presence of very finely comminuted charcoal and high proportions of organic matter (Morley 2007).

As in layer XX, black layers are accompanied by ash layers (which can present different colors—gray, blue-gray, white, or red) and reddish layers. It is interesting to note that many bones seem to agree in their colors with the layer in which they were found and with the temperature

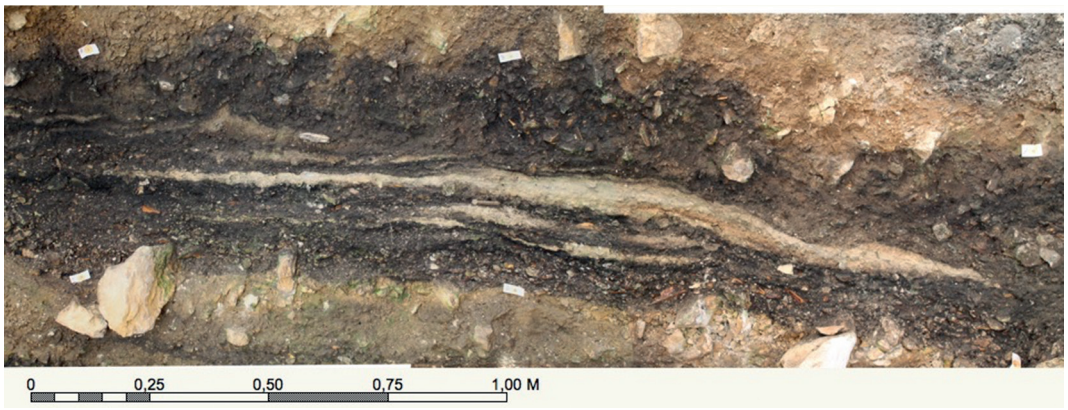

Fig. 18.15. Detail of structure 3 from layer XX.

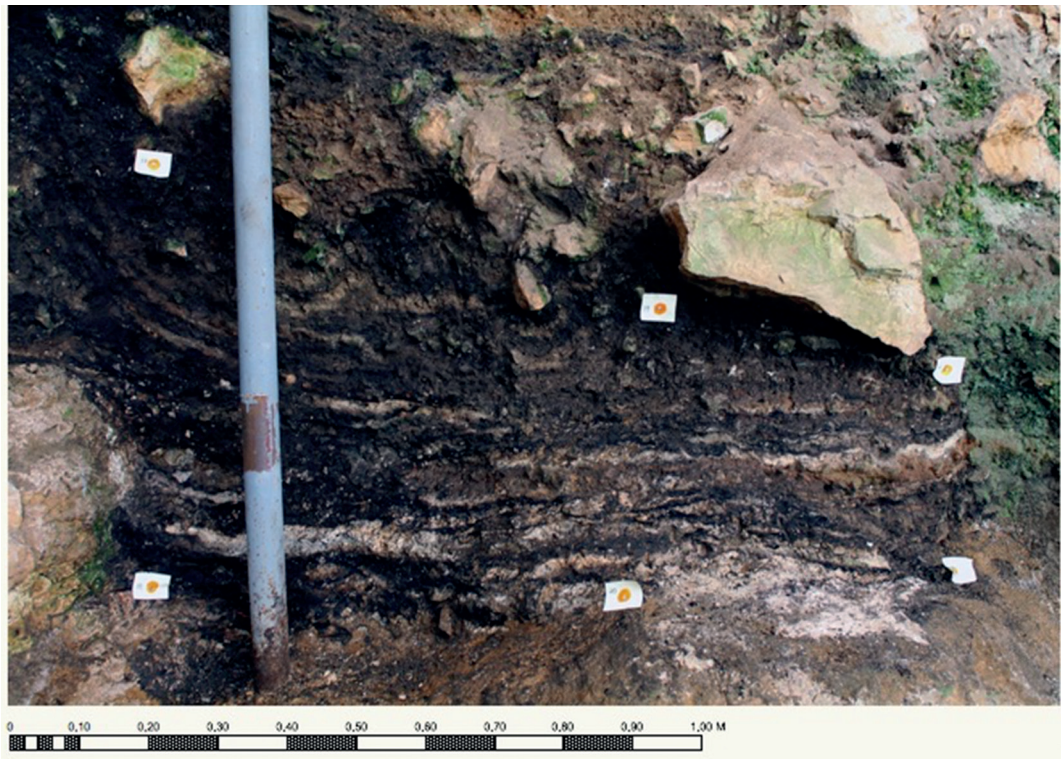

Fig. 18.16. Layer XXIV studied profile.

reached by these layers as could be inferred from our experimental results (Fig. 18.17). As we saw in our fieldwork, it is easy to find blackened and brownish bones in blackened layers, while we find white-grey bones, blue-gray bones, or blue-white bones in the ash. The same thing can occur with calcareous burnt stones that can be grey or white as a function of the temperature reached by the layer. Burnt stones became more friable in ash layers where we suppose them to have been exposed to higher temperatures. In consequence, these layers seem to have a specific composition that indicates differences both in their constituents and in their formation processes, including the temperatures of hearths in the past.

The analysis of magnetic parameters performed by Morley indicates a high quantity of magnetic minerals but a variable degree of correlation with charcoal contained in these layers. His results show non-significant correlation with lab measures of charcoal ($r = 0.09$) and only a slightly better correlation with field measures

Fig. 18.17. Detail of carbonized bone and burnt calcareous stones in black layers, and yellow-brown bones in burnt bone layers from layer XXIV.

of charcoal (r = 0.53). (Morley, Chapter 7, this volume). This led Morley to conclude that "it is not just the charcoal rich layers which have a high magnetic signal, but the substrate on which the fires have been lit may have been subject to heating/burning which would also increase the magnetic signal" and that magnetic susceptibility (associated with burning) may be "a coarse proxy indicator for in-situ burning, as it would be expected that if the ash and charcoal layers were the remains of either raked out fires, or constituted redeposited anthropogenic remains, then the χlf signal would tally more closely to the presence of charcoal and burnt material in the sediments" (Morley 2007:279-280).

For our study we selected a group of fire structures present in the E-W profile at a depth of 12-13 m. The second section sampled is situated at a lower position in the same profile, between 13-14 m (Figs. 18.1, 18.16). We cleaned a window in the profile 1.42 m wide by 1 m high (Fig. 18.16). In this section, layer XXIV presents 127 distinguishable layers related to fire structures that are covered by a large blackened layer or dark brown layer that is not investigated in this analysis. Forty-two of these layers are ash layers, 44 are black layers, 30 are grey layers, 5 are reddish layers, 6 are burnt bone layers, and, finally, there are 2 grey soils (Fig. 18.18). At the bottom-east part of the profile we observed an ash layer emerging from the profile that was very disturbed. Although it would have been interesting to see the form of these ash layers in a horizontal perspective, the high degree of disturbance of the layer did not encourage us to proceed with its specific study.

The studied zone has two particularities. The first one is the presence of large rocks at the base and west of the profile that had evidently limited the surface that could be occupied by Neanderthals in the past. The other one is the presence of two major disturbances coming from above that had cut into the underlying layers and could indicate the presence of a superstructure that was installed over the hearths or the presence of ancient rocks removed from their position and which limited the extension of fire structures in the past (Fig. 18.19). This disturbance disappeared slowly as we cleaned the profile for analysis.

Within this portion of the profile (that covers 10,224 sq cm), layer XXIV presents 42 ash layers. The minimum width of these layers is 2.24 cm and the maximum is 68.31 cm. Their thickness varies between 0.3 and 4.20 cm, their height ranges from 0.86 to 9.31 cm, and their area between 0.58 and 111.44 sq cm (Table 18.5 and Appendix). These ash layers have smaller dimensions than the ash layers of layer XX.

As in layer XX, the ash layers are accompanied by a series of black layers. Here the 45 black layers detected have a minimum width of 4.10 cm and a maximum width of 68.50 cm. Their thickness runs between 0.6 and 6 cm, their height from

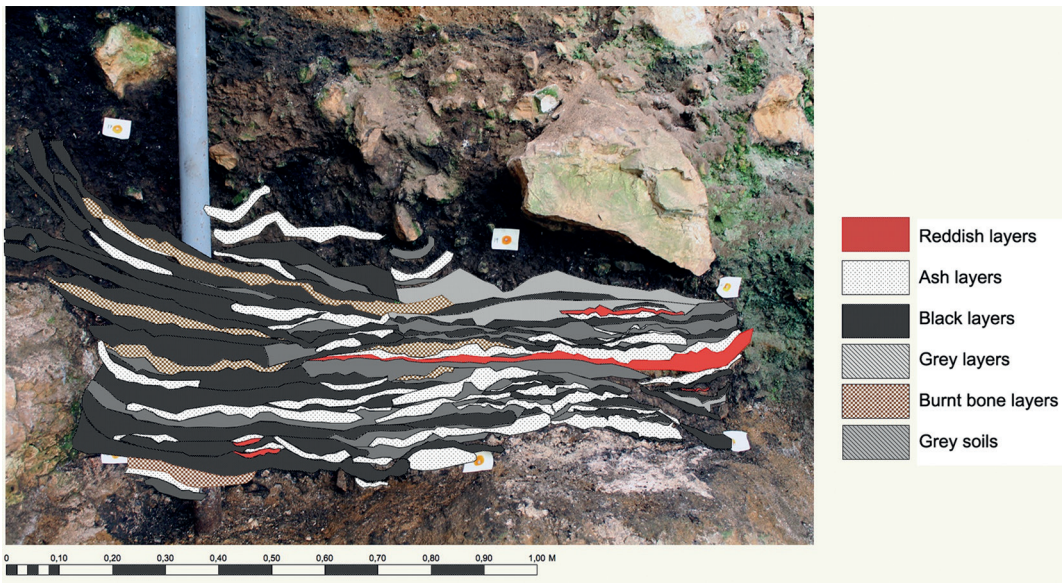

Fig. 18.18. Layer XXIV studied profile with reconstructed layers.

Fig. 18.19. Detail of the disturbed zone coming from above into layer XXIV.

Table 18.5. Summary statistics for ash layers and black layers from layer XXIV of Crvena Stijena.

	Layer XXIV Ash Layers				Layer XXIV Black layers			
	THICKNESS	HEIGHT	WIDTH	AREA sq cm.	THICKNESS	HEIGHT	WIDTH	AREA sq cm.
N	42.00	42.00	42.00	42.00	45.00	45.00	45.00	44.00
Min	0.30	0.86	2.24	0.58	0.60	1.40	4.10	3.14
Max	4.20	9.31	68.31	111.44	6.00	30.60	68.50	203.53
Sum	75.60	164.33	726.81	997.86	101.60	312.12	1278.75	2218.49
Mean	1.80	3.91	17.30	23.76	2.26	6.94	28.42	50.42
Std. error	0.14	0.35	1.83	3.63	0.19	1.00	2.93	8.07
Variance	0.81	5.05	141.14	553.82	1.61	45.29	385.14	2866.13
Stand. dev	0.90	2.25	11.88	23.53	1.27	6.73	19.63	53.54
Median	1.80	3.26	14.37	17.26	2.10	4.20	18.80	22.39
25 prcntil	1.28	1.98	9.55	5.84	1.25	2.50	13.30	11.93
75 prcntil	2.40	5.65	20.35	31.33	2.65	9.15	47.13	95.51
Skewness	0.55	0.68	2.27	1.83	1.34	1.81	0.80	1.31
Kurtosis	0.35	-0.53	7.45	3.83	1.64	3.03	-0.79	0.68
Geom. mean	1.55	3.30	14.33	14.56	1.96	4.82	22.30	28.44
Coeff. var	49.96	57.45	68.65	99.05	56.13	97.03	69.06	106.18

1.4 to 30.6 cm, and their area between 3.14 and 203.53 sq cm (Table 18.5).

Associated with these layers, we can observe 30 grey layers that have widths between 5.45 and 66.10 cm, while their thickness varies between 0.6 and 4.4 cm. Their height falls within 0.9 and 10.40 cm, and their area between 2.53 and 142.19 sq cm (Table 18.6).

The 5 reddish layers found have widths between 5.48 and 65.60 cm, and thicknesses that range from 0.3 to 3.5 cm. Their height runs from 0.72 to 8.10 cm, and their areas have a minimum

Table 18.6. Summary statistics for grey layers and reddish layers from layer XXIV of Crvena Stijena.

	Layer XXIV Grey layers				Layer XXIV Reddish layers			
	THICKNESS	HEIGHT	WIDTH	AREA sq cm	THICKNESS	HEIGHT	WIDTH	AREA sq cm
N	30.00	30.00	30.00	30.00	5.00	5.00	5.00	5.00
Min	0.60	0.90	5.45	2.53	0.30	0.72	5.48	1.61
Max	4.40	10.40	66.10	142.19	3.50	8.10	65.60	109.67
Sum	60.20	112.64	609.89	719.06	7.90	14.42	109.43	141.32
Mean	2.01	3.75	20.33	23.97	1.58	2.88	21.89	28.26
Std. error	0.19	0.41	2.91	5.54	0.57	1.33	11.41	20.59
Variance	1.14	5.04	254.27	921.32	1.63	8.79	651.45	2119.17
Stand. dev	1.07	2.24	15.95	30.35	1.28	2.97	25.52	46.03
Median	2.30	3.81	14.74	15.63	1.00	1.90	9.25	7.09
25 prcntil	1.08	1.69	9.66	6.62	0.60	1.14	5.57	2.56
75 prcntil	2.63	4.83	27.71	28.08	2.85	5.13	44.53	64.55
Skewness	0.46	1.29	1.75	2.78	0.95	2.05	1.82	2.12
Kurtosis	-0.67	2.40	2.55	8.40	-0.09	4.39	3.25	4.53
Geom. mean	1.72	3.16	16.03	14.07	1.16	2.06	13.45	9.69
Coeff. var	53.19	59.79	78.44	126.64	80.73	102.83	116.62	162.87

dimension of 1.61 and a maximum of 109.67 sq cm (Table 18.6).

Finally, we observed 6 burnt bone layers and only 2 grey soils that were situated in the upper part of the profile. The burnt bone layers have a width between 6.95 and 11.30 cm and a thickness that varies from 1.80 to 3.30 cm. Their height is a minimum of 2.75 cm and reaches a maximum of 22.05 cm while their surface areas are between 10.06 and 107.75 sq cm. The limited number of grey soils show widths between 58.65 and 62 cm, and a thickness from 4 to 6.8 cm. Their height is comprised between 5 and 7 cm and their surface areas run between 107.4 and 166.88 sq cm (Table 18.7).

Here the vertical surface of the profile analyzed has an area of 4685 sq cm. Within this area, ash layers occupied 997 sq cm (22.6%), black layers 2218.50 sq cm (50.42%) grey layers 719.58 sq cm (16.31%), reddish layers 141.32 sq cm (3.20%), the burnt bone layers 334.30 sq cm (7.6 %), and, finally, the grey soil layers occupied a surface of 274.29 sq cm (5.85 %) (Fig. 18.20).

The reduction of the area occupied by burnt bone layers and the reduction of the surface occupied by grey soils explains the increase in the proportion of area occupied by the other layers in layer XXIV. If the same processes discussed above explain the formation of these layers, the accumulation of large burnt bone layers that could imply the accumulation of various anthropic debris in the same space, did not occur in this part of the shelter. This does not imply that such large accumulations did not occur in the period of formation of layer XXIV but indicates that the dimensions of these accumulations were less important in this part of the site at that time, which implies a certain hiatus in activities related. Always in this sense it is interesting to note that the total surface covered here by the grey soils is more important and represents 82% of the surface of burnt bone layers, much more than in layer XX where they represent only 20% of the area occupied by burnt bone layers. The other kinds of layers are also proportionally less important in comparison to grey soils. The grey soils here thus occupy some of the area that was occupied by the burnt bone layers in layer XX. This could imply a difference in the rhythm of deposition of these two kinds of layers and an increment of the natural calcareous sediments that composed the grey soils. These grey soils are thicker than in layer XX.

Another point to note about the layers of layer XXIV is that the mean areas of the ash layers,

Table 18.7. Summary statistics for burnt bone layers and grey soils from layer XXIV of Crvena Stijena.

	Layer XXIV Burnt bone layers				Layer XXIV Grey soils			
	THICKNESS	HEIGHT	WIDTH	AREA sq m	THICKNESS	HEIGHT	WIDTH	AREA sq.cm
N	6.00	6.00	6.00	6.00	2.00	2.00	2.00	2.00
Min	1.80	2.75	11.30	10.06	4.00	5.00	58.65	107.40
Max	3.30	22.05	69.95	107.75	6.80	7.00	62.00	166.88
Sum	15.80	52.79	219.68	334.30	10.80	12.00	120.65	274.29
Mean	2.63	8.80	36.61	55.72	5.40	6.00	60.33	137.14
Std. error	0.20	2.98	8.17	13.40	1.40	1.00	1.68	29.74
Variance	0.25	53.13	400.60	1076.58	3.92	2.00	5.61	1769.00
Stand. dev	0.50	7.29	20.01	32.81	1.98	1.41	2.37	42.06
Median	2.65	6.10	34.27	52.25	5.40	6.00	60.33	137.14
25 prcntil	2.33	3.39	20.98	32.01	3.00	3.75	43.99	80.55
75 prcntil	3.00	14.66	51.76	81.44	5.10	5.25	46.50	125.16
Skewness	-0.65	1.52	0.73	0.39	0.00	0.00	0.00	0.00
Kurtosis	1.63	1.97	1.06	0.90	-2.75	-2.75	-2.75	-2.75
Geom. mean	2.59	6.80	31.75	45.12	5.22	5.92	60.30	133.88
Coeff. var	18.86	82.84	54.67	58.89	36.66	23.57	3.93	30.67

black layers, grey layers, and burnt bone layers are smaller than for layer XX. The most important reductions are observed for ash layers and for the burnt bone layers. Only the reddish layers and the grey soils have larger mean areas in layer XXIV than in layer XX. The reason for the difference for the grey soils was explained above. For the reddish layers this could be easily explained by the dimensions of a red layer observed in only one structure that clearly surpass the dimensions of reddish layers observed for layer XX. This could imply a longer duration of this fire episode, seeing that the dimensions of the ash layer that covers it in this structure are smaller than the ash layer that covers the reddish layer in layer XX.

In fact, seeing the deformation of some of these layers in the upper part of the profile, we could also think that these differences could have been created by a compaction of the layers in layer XXIV coming from the very large stones that cover the section of the profile chosen for this study. But when we analyze the thickness and the width of these layers we see that for all the layers except the grey soils the widths are smaller in layer XXIV, while thickness is relatively more stable. Thickness is greater for the grey soils, the grey layers, and the reddish layers and less for the ash layers, black layers and burnt bone layers. This implies that the reduction affects the diameters of the ash layers, black layers, grey layers, and burnt bone layers more than the volumes of their accumulated sediments (Table 18.8). The only kind of layer that shows an increment in volume is the grey soils, which seems to confirm their more important accumulation in the upper part of layer XXIV.

In layer XXIV ash layers mostly overlie black layers (56%) or grey layers (23%). They less frequently cover other ash layers (12%), in only 2 cases do they lie directly on reddish layers (4%), and in 3 cases burnt bone layers (6%). In 24% of cases ash layers cover more than one layer, primarily ash layers and black layers or grey layers and black layers (Fig. 18.21).

Black layers that underlie ash layers are larger than in layer XX. These layers as described by Morley are extremely rich in bone, charcoal, and ash, as well as reddened materials (limestone clasts and fine sediments) which would suggest that these materials have been burnt. In some cases analysis of these layers shows significant clay content and relatively high levels of total organic matter. The clay peak could be related to the presence of very finely comminuted charcoal

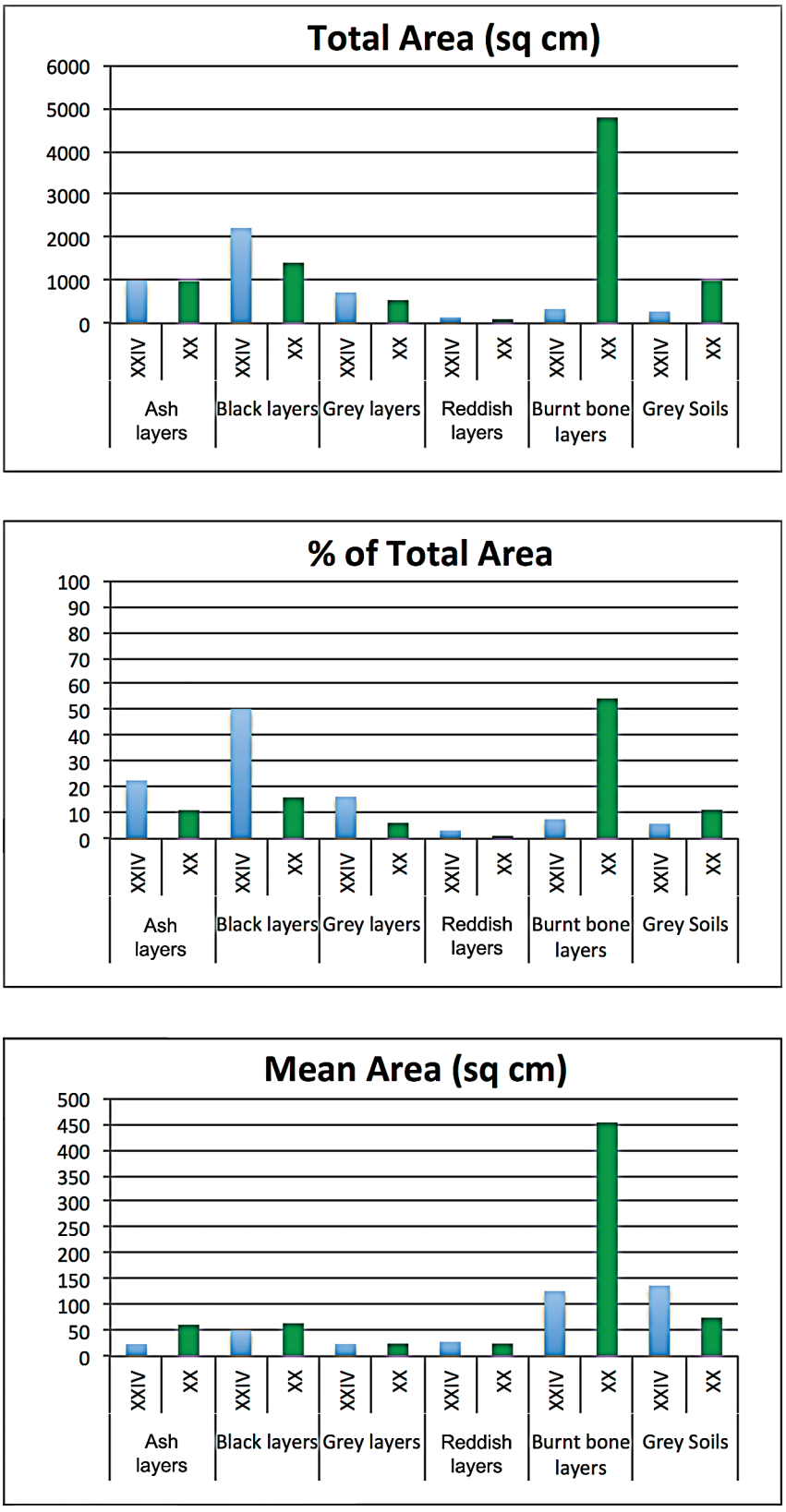

Fig. 18.20. Relative dimensions of different kinds of layers found in layer XX and layer XXIV.

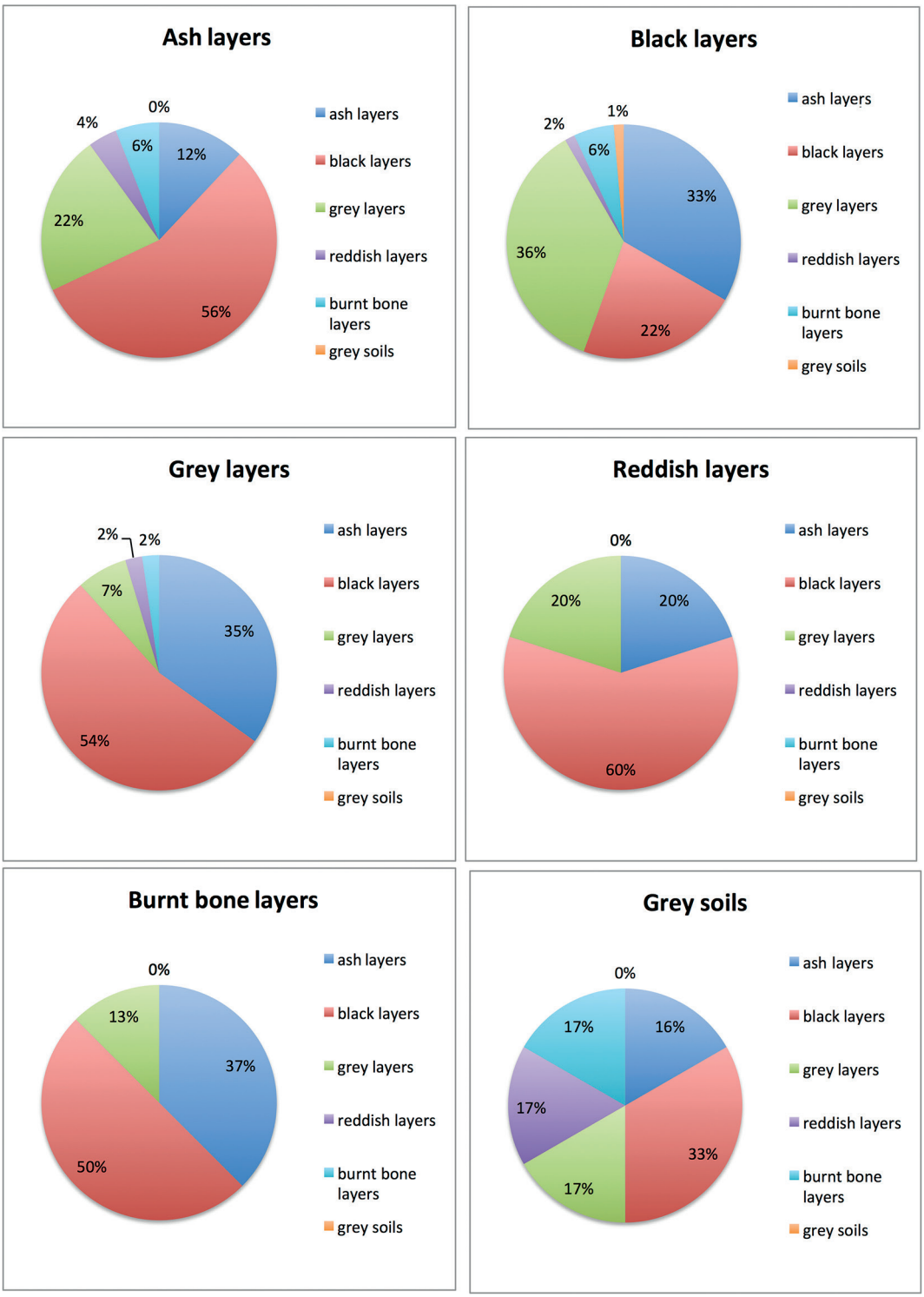

Fig. 18.21. Percentage distribution of the kinds of underlying layers for ash, black , grey, reddish, and burnt bone layers.

dispersed in the matrix of this layer. (Morley 2007, see also Morley, Chapter 7, this volume). Here black layers lie mostly on grey layers (37%) or ash layers (34%), contrary to layer XX where they lie mostly under burnt bone layers. Here these layers also lie on other black layers (21%). This

Table 18.8. Relation of mean dimensions of ash, black, grey, reddish and burnt bone layers between layer XX and layer XXIV.

	Relation of mean dimensions of ash layers between layer XX and layer XXIV		
	THICKNESS	WIDTH	AREA sq.cm
Index	1,29	1,91	2,57
	Relation of mean dimensions of black layers between layer XX and layer XXIV		
	THICKNESS	WIDTH	AREA sq.cm
Index	1,02	1,28	1,27
	Relation of mean dimensions of grey layers between layer XX and layer XXIV		
	THICKNESS	WIDTH	AREA sq.cm
Index	0,91	1,24	1,03
	Relation of mean dimensions of reddish layers between layer XX and layer XXIV		
	THICKNESS	WIDTH	AREA sq.cm
Index	0,71	1,04	0,88
	Relation of mean dimensions of burnt Bone layers between layer XX and layer XXIV		
	THICKNESS	WIDTH	AREA sq.cm
Index	3,26	2,07	7,16

	Relation of mean dimensions of grey soils between layer XX and layer XXIV		
	THICKNESS	WIDTH	AREA sq.cm
Index	0,59	0,48	0,48

seems to confirm that black layers are frequently the soil that characterized the shelter in this part of the site during layer XXIV formation. Black layers cover burnt bone layers in only four cases (5.5 %) and reddish layers in only one (1.35%).

Like ash layers, grey layers are underlain frequently by black layers (53%) or ash layers (34%). These proportions are very similar to those observed for layer XX. This seems to confirm their relation to fire action and also the relative positions of these grey layers with respect to ash and black layers.

Reddish layers (n = 5) cover black layers 60% of the time and one ash layer and one grey layer (both = 20%). As we saw previously, the reddish layers here have larger dimensions compared to those from layer XX.

Burnt bone layers are underlain mostly by black layers (50%) and ash layers (37.5%), and in one case by a grey layer (12.5 %). These data show a different formation process for this part of layer XXIV compared to layer XX, where burnt bone layers basically cover other burnt bone layers and occupy important surfaces.

Finally, the only two grey soils observed cover mostly black layers (33%) and all the other layers in equal proportions. This obviously represents only two cases, where one case covers a complex structure formed by a black layer, an ash layer, and a reddish layer, and in the other case only a more homogenous black layer and a small part of an emerging grey layer underlying a grey soil formation.

In conclusion we can observe that in layer XXIV we find the same tendencies for superpositioning of layers, except for burnt bone layers. Fire structures seem to have the same trends: ash and grey layers are positioned mostly over black layers and in some cases over red ones. This seems in conformity with heat transfer phenomena and the thermal transformations observed in our experiments. Reddish soils are more easily detected in this part of the site and seem to have a different nature here. The two largest ones may be the remains of a soil formation that might have interrupted anthropic deposition in layer XXIV and that became thermal oxidates under the action of the first fires ignited on it. Except for this

particular case, the dimensions of fire structures in this layer seem to be smaller than those of fire structures in layer XX.

The Dynamic of Fire in Layer XXIV in Comparison to Layer XX

The analysis of the stratigraphic sequence of layer XXIV shows that the intensity of the use of fire is not exactly the same in this section of layer XXIV as that observed in layer XX. This can be seen easily from the analysis of the surfaces occupied in the vertical area of the profile studied (Fig. 18.22). Here the intensity "I" index for ash layers is I = 0.22 and for the reddish layers is I = 0.03. Even the grey layers and black layers show an increase in their I indexes; here the grey layer index is equal to I = 0.16 while in layer XX it has a value of I = 0.06, and the index for black layers goes from I = 0.16 in layer XX to I = 0.5 for layer XXIV. This progression is accompanied by a reduction in the mean surface area of individual layers but an increment in the number of ash layers, reddish layers, grey layers, and black layers in layer XXIV. Thus, in terms of relative surface areas, we have more ash layer fire structures in layer XXIV than in layer XX, but these fire structures have smaller dimensions. This it is not the case for the reddish layers that are a little bit larger than the reddish layers from layer XX. Along with this, the I index is significantly reduced for the burnt bone layers, decreasing here to 0.07, compared to a value of 0.54 in layer XX. As we just saw, these changes are accompanied by a reduction in the mean area occupied by individual ash layers, indicating that the frequency of the use of fire was greater here, although this is accompanied by a reduction of the dimensions of each fire structure. As we see, the larger total area of ash layers could be explained by fire intensity (constant duration at the same temperature) in one specific place. Black layers and grey layers have also small mean dimensions of their surfaces. This greater intensity of the use of space for fire is easily seen by applying the same methodology used to analyze the use of fire in layer XX, both in 3D and top view of the model representation (Figs. 18.23-18.24).

In this part of the profile of layer XXIV, we could observe different kinds of groupings of ash layers in the stratigraphic sequence. A majority of these groupings are of two ash layers at the same level, but we can see also two combustion areas with associations of three or four ash layers. As in layer XX, many pairs of ash concentrations show different patterns of organization. In some cases, these fire structures are in contact, and in other cases they are separated to a varying degree. Finally, there is also one case of juxtaposition of fire structures. Thirteen combustion areas of different dimensions, constituted by 31 ash layers, are superposed or intercalated, with nine isolated fire structures.

As we can clearly see in Fig. 18.24, all these fire structures extended over a relatively smaller extent of the profile in the E-W axis. The distance between the most separated structures at this level in the profile is here 123.2 cm, while it was 300 cm in layer XX. This corroborates our interpretation of a greater intensity of the use of space for fire and agrees with the larger values observed for the vertical surfaces (I Index) in the layer XX profile that we presented above. As just discussed, the ash layers in layer XXIV have smaller dimensions than those of layer XX. The mean area of individual ash layers is 23.75 sq cm while their mean thickness is 1.8 cm. The minimum area observed was only 0.57 sq cm and the largest one 111.44 sq cm. Their width ranges between 2.23 and 78.3 cm, but in most of layer their width is between 10 and 30 cm. If we take into account their groupings, the width of the combustion areas that incorporate more than one ash layer rises from 21.7 cm to 87 cm. This range in width is greater compared to layer XX, where it was between 39 and 65 cm. The mean width for these combustion areas in layer XXIV is a little larger (54.3 cm) than that observed in layer XX (51.33 cm).

One interesting fact is that the internal separation between the fire structures in a combustion area is clearly larger for layer XXIV (mean distance of separation 18.4 cm) than for layer XX (mean distance of separation 9.25 cm). The greater separations in layer XXIV reach 53 cm, while in layer XX the maximum distance is 14 cm. Seven groups of structures are separated in layer XXIV by more than 25 cm (Figs. 18.25-18.27), and these internal distances increase over time from the bottom to the upper part of the studied sequence. This increment in internal separation in the upper part of the sequence could be related to being above and unconstrained by the large stone that limited the space available for occupation in the bottom part of the sequence. Thus, more space

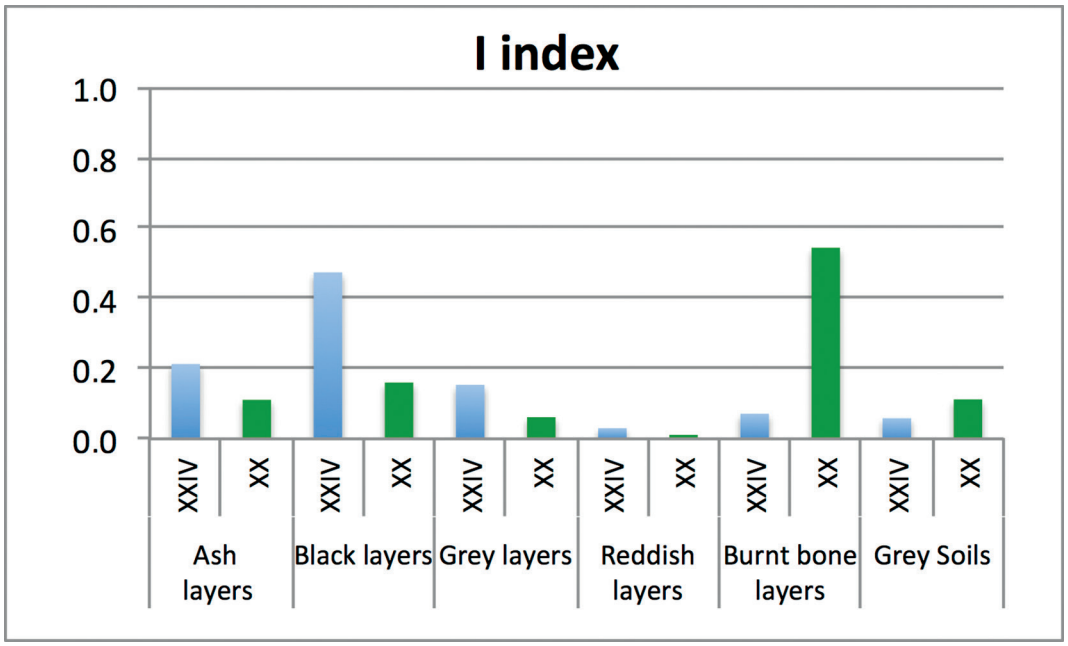

Fig. 18.22. I index changes between layer XX and layer XXIV studied profiles.

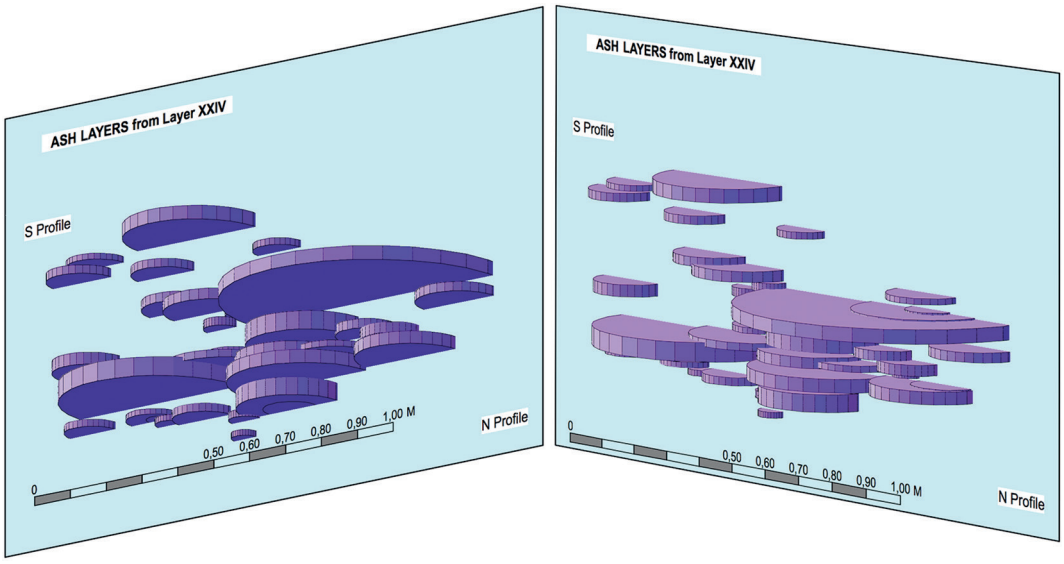

Fig. 18.23. 3D schematic model of ash layers from layer XXIV, right rear and lower right rear position.

was available for the installation of Neanderthal activities related to fire in the same part of the site.

But this data is also relevant for interpretation because we observe here a great intensity in the use of space for fire, but nonetheless a difference in the arrangement of the structures, which are grouped by pairs that are more widely separated in layer XXIV even though the space was larger and less constrained in layer XX, given the absence of large rocks that limited space use. This difference could imply a different function for these groupings, or a different mode of functioning, which led to the introduction of a small difference in the arrangement of pairs over time as a function of the availability of space. If we take into account the different observed arrangements in combustion areas containing paired structures, we can note

the following different kinds of organization: a juxtaposition of structures, two layers in contact position, and two kinds of separations between pairs, a smaller and a larger one (Figs. 18.25-18.28). These different kinds of organization might imply different kinds of activities related to the use of fire that we will have to explore by other methods.

The E-W horizontal displacement of individual ash layers in layer XXIV runs from 0.2 to 102.9 cm, with a mean displacement of 32.4 cm. This mean is similar to that in layer XX (32.2 cm), but has a higher standard deviation. Their stratigraphical vertical separation ranges from 0.11 cm to 7.06 cm, with a mean of 2.85 cm (see Appendix).

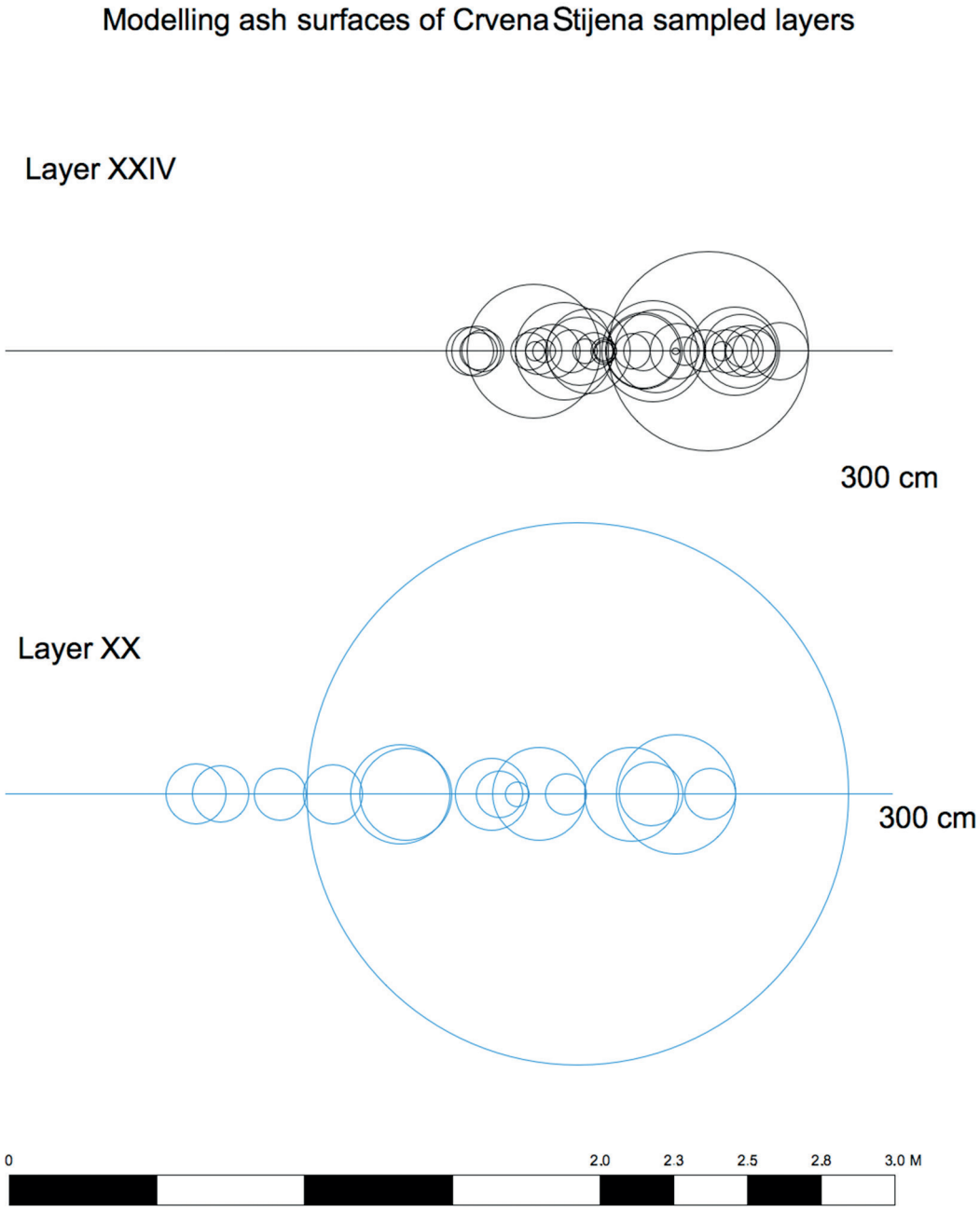

Fig. 18.24. Top View of the position of fire structures in the profiles of layer XX and layer XXIV; the diameter of the circles represents the width of each fire structure in the profile.

The sequence in this part of layer XXIV is more difficult to establish because of the great superpositioning of small anthropic layers of different kinds observed in the profile. It begins with the presence of two isolated fire structures (Fig. 18.25). The first one (Ashes 24-41, see Appendix), which has a diameter of 14.25 cm and a thickness of 1.8 cm, is situated near a large stone over a black layer and shows an inclination of −18.31°. The second one (Ashes 24-34) is a very little structure only 6.24 cm in diameter and 1.3 cm in thickness positioned 39.47 cm to the W with an inclination of −14.50°.

This first structure is covered by a black layer over which lies a first combustion area made up of four ash layers: Ashes 24-35, Ashes 24-33, Ashes 24-25, Ashes 24-24 (see Appendix). This combustion area (in blue in Figs. 18.25-18.26) has a diameter of 43.9 cm and consists of four layers with widths of 13.12 cm, 7.69 cm, 14.48 cm and 7.78 cm from W to E. These four layers show a minimal inclination of −1.86°. Similar to what we observed in layer XX, the first of these layers Ashes 24-35, is very different in thickness from the other three ash layers. It reaches 3.9 cm in thickness, while the other three structures are 1.6, 1.8, and 1.3 cm thick, respectively. The first of the four structures is separated by a space of 2.5 cm from the second one, Ashes 24-33, while the second and the third structures are in contact, and the third structure, Ashes 24-25, overlaps the fourth one, Ashes 24-24 at the east end of the area (Figs. 18.25-18.26). It is interesting to note here that the two smaller structures show underlying thermally altered soils, a reddish layer for the structure situated at the east and a grey layer for the structure situated at the west of the area, while the larger ones do not present these characteristics. This could imply the existence of small heat centers that reached elevated temperatures (more than 500°C) which have larger structures where fire was kept at lower temperatures. The superpositioning of ash layers that integrate this combustion area could indicate the reuse of the space within a very short period, which did not let the formation of new anthropic layers take place. The small areas are here situated to the east of the larger ones.

This combustion area was covered by a black layer that separates it (1.8 cm) from a new

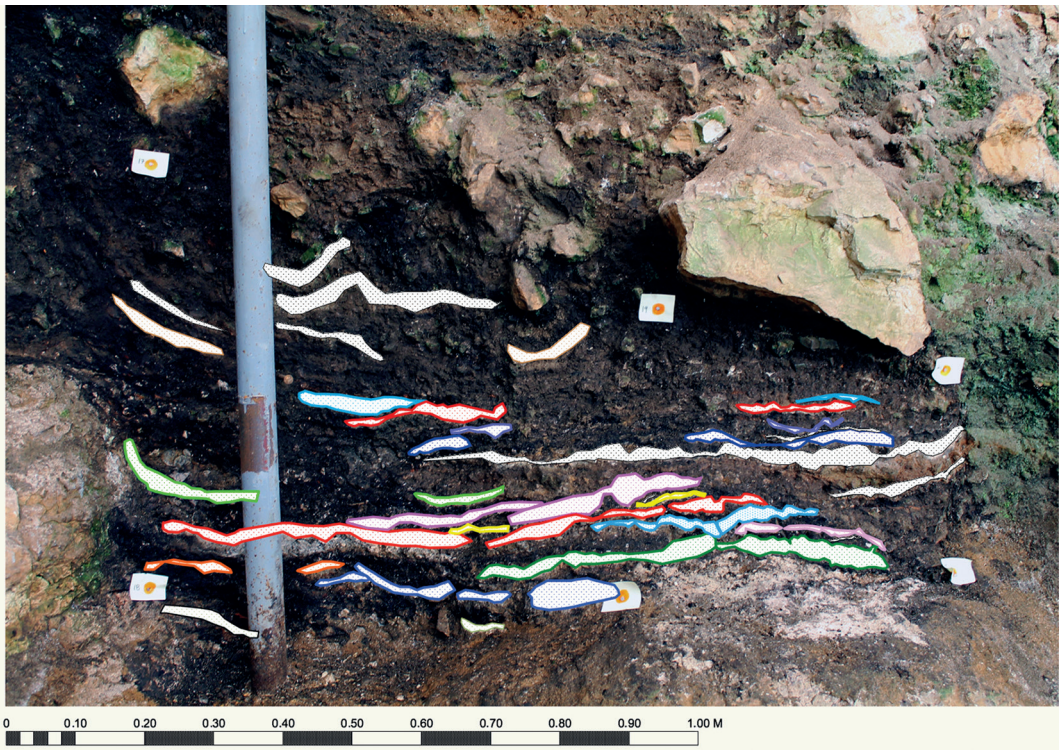

Fig. 18.25. Association of fire structures (ash layers) as a function of their stratigraphic position for layer XXIV; similar colors indicate stratigraphic association.

combustion area (in orange in Figs. 18.25-18.26) made by of two ash layers (Ashes 24-23 and Ashes 24-22) of different dimensions that are situated to the east of the first association of ashes and has no inclination. This combustion area, which is displaced 37 cm to the east, has minor dimensions, only 28.8 cm in width, and contains two ash structures, one on the west of 12.6 cm diameter and the other situated 9.5 cm to the east that is only 6.7 cm in diameter. Their thickness is 1.2 cm for the smaller structure and 1.6 for the larger one. The relevance and signification of this little structure (Ashes 24-23) with a diameter of only 6.7 cm, which could be interpreted as the remains of an excavated structure, lies in the fact that, here again, the little structure shows a thermally altered soil underlying the ash layer. Here this soil is characterized by a reddish oxidation, as was the case for one of the two little structures observed in the preceding area.

After these first two fire structures, we observe a new combustion area (in green in Figs. 18.25-18.26) made up of two ash layers (Ashes 24-32 and Ashes 24-38) of larger dimensions, situated on the west side of the profile. This combustion area is 59.3 cm in diameter and was displaced 63.4 cm to the west. Inside this area, the west structure (Ashes 24-38) is 24.95 cm wide and the east one 34.48 cm. Their thickness is also greater, the larger structure situated on the east having 3 cm and the smaller one 2.8 cm. Both structures are in contact at the same level and follow the curvature formed by an underlying stone, showing an inclination of 1.28°. It is important to note that this combustion area was still visible beyond the profile where a zone of disturbed ashes was horizontally dispersed. This area overlay a grey and a black layer and was covered by two different grey layers, one associated with each ash structure.

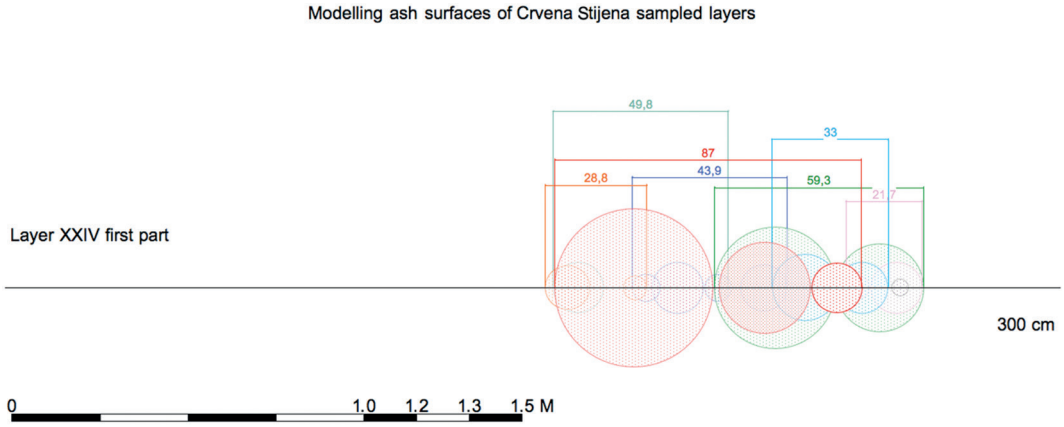

Fig. 18.26. Model top view of the association of the first fire structure group in layer XXIV.

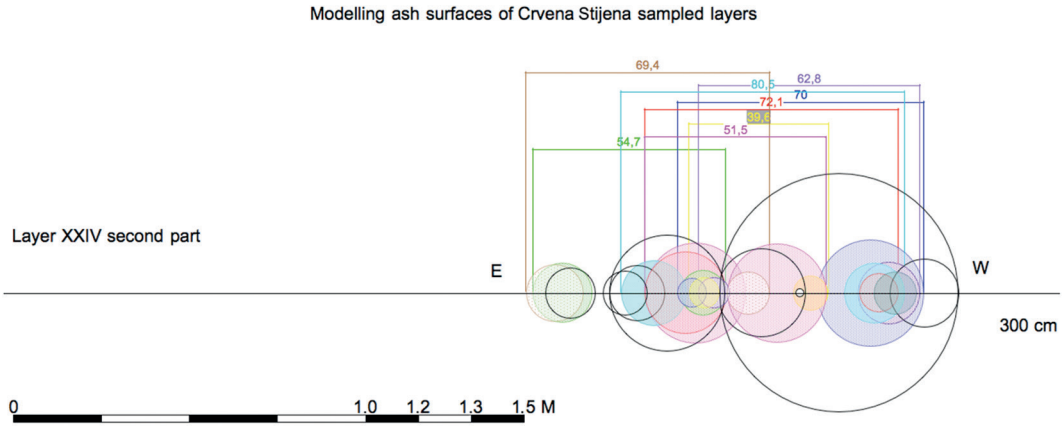

Fig. 18.27. Model top view of the association of the second fire structure group in layer XXIV.

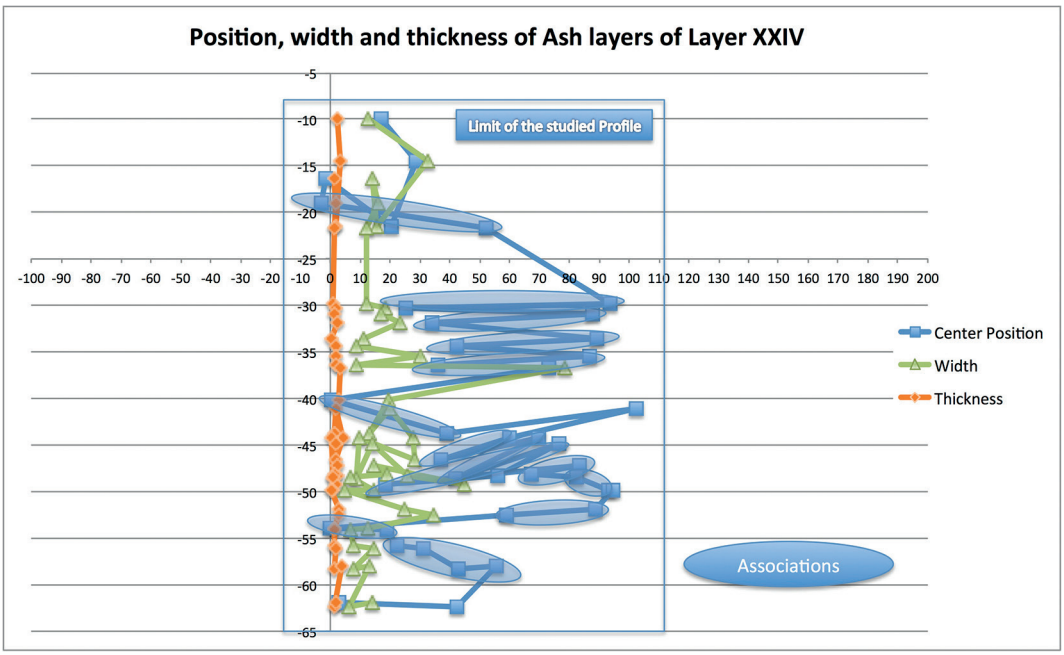

Fig. 18.28. X center position, width, and thickness in time relative to the profile studied for layer XXIV.

A small, isolated structure (Ashes 24-40) is situated over the ash layer located on the west and interrupts the sequence of combustion areas. This little structure, which is only 4.4 cm in diameter and 0.4 cm thick, is 2.59 cm above the grey layer and in a black layer that separates both structures and covers the west structure of the combustion area just described as well as this little structure. This ash layer is displaced 23.32 cm to the west of the center of the preceding area but is situated only 1.42 cm to the west of the western ash layer of the preceding area. The nature of this ash layer remains uncertain, positioned near a vertical disturbance that was found in the profile, it may be only the remains of a destroyed structure, or a small accumulation of combustion ashes left on this part of the site, or, finally, the emergence of an ash layer that is still inside the profile. To complicate our analysis, this ash layer does not respect the general form of the black layer that contains it, and is positioned horizontally, bringing to the fore a break in the sequence of deposition of the combustion debris that constitutes the black layer. Unfortunately, its small volume does not allow us to include it in our analytical procedure.

Continuing the sequence, a new pair of small ash layers (Ashes 24-37 and Ashes 24-36) cover this last area, forming a new combustion area (in pink in Figs. 18.25-18.26), and mark the beginning of a new sequence of five combustion areas that are displaced to the east. This area occupies a zone of 21.7 cm width in which there are two structures 6.60 and 14.56 cm in diameter. These two ash layers are nearly in contact and are separated by only 0.4 cm. They are relatively thin, with thicknesses of 1.1 and 0.9 cm. Here, contrary to the other cases observed, the thinner structure is the larger one (Ashes 24-37). The smaller structure is situated to the east, and the area is more inclined (−9.95°) than the preceding one.

This last area is covered by a new one consisting of two ash layers (Ashes 24-31 and Ashes 24-31b), 14.55 cm and 18.75 cm in diameter that form a combustion area 33 cm wide in the profile (in light blue in Figs. 18.25-18.26). These two layers are significantly different in their constitution. The west one (Ashes 24-31b) is characterized by a mixture of white ashes, charcoal, and carbonized bones, and the east one is composed of ashes of different grain sizes but with smaller amounts of charcoal and carbonized bones. Both structures converge at a central depression, forming a concavity that was covered by grey and black layers. This form, which seems to accompany a depression in the anthropic layers, is an atypical form for the ash layers observed both in layer XX and layer XXIV.

Overlying the black and grey layers that cover this combustion area we find a new area that contains three ash layers (Ashes 24-21, Ashes 24-27, and Ashes 24-30, in red in Figs. 18.25-18.26) that occupies a zone of 87 cm width, always in the E-W axis, and whose center was displaced 35 cm to the east. The dimensions of this area are the largest observed in the whole profile. As we can see, the use of fire occupied nearly all the area available in this part of the site for fire activities. These three structures become larger from west to east. The western one (Ashes 24-30) is 14.16 cm, the center one (Ashes 24-27) 25.88 cm, and the eastern one (Ashes 24-21) 44.68 cm in diameter. The three structures are separated by very small distances, 0.7 and 1.8 cm, and have thicknesses of 2.1, 2.4, and 2.1 cm, which raises the question of their original continuity. This area shows an inclination of 2.63°. The two larger structures situated on the east cover a big and uniform grey layer of thermo-altered sediment underlying the structure that reaches 2.8 cm in thickness, while the western one covers a succession of grey and black layers where the thickness of the grey layer is less. The ash concentration situated on the east also shows an internal stratification where the ashes change in color from grey to white and from white to light brown, that shows similarities to the big structure in layer XX already mentioned. Other activities could not take place to the east of the structure because of the presence of a large stone there; thus, in this case activities here could not have followed the classical model of a circular disposition around fire but must be have been displaced to one side of the fire structure, to the west, north, or south.

On the west side of the profile, this large combustion area was covered by a succession of structures of small or medium size. Therefore, after the construction of this large structure, fire-related activities continue to take place in the same zone but occupying smaller surfaces. First, two little ash structures (Ashes 24-20 and Ashes 24-29) having diameters of less than 10 cm (9.83 and 8.6 cm) came to replace the large structure in this part of the site (in yellow in Figs. 18.25, 18.27), forming a combustion area of 39 cm that has an inclination of 9.58°. The center of this area is displaced 16.4 cm to the east. The thickness of these two ash structures is very similar and are among the thinnest of the entire sequence, 0.6 and 0.7 cm. These structures are installed over a grey and a black layer of thin dimensions, that vertically separates both structures by 1.5 cm from the large structure. However, the east extremity of the eastern ash layer is in contact with the ashes of the underlying large structure, showing that these two structures may be the result of a contemporary re-utilization of the space for combustion practices above the earlier structure.

These two small structures were covered by a black and a grey layer having a variable thickness. Over this black layer, a new combustion area 51.5 cm in diameter was detected, composed of two large, juxtaposed ash layers (Ashes 24-19 and Ashes 24 26) (in purple in Figs. 18.25, 18.27) that have different dimensions and forms. This new area was displaced 44.7 cm to the east and is still centered over the large structure described above. It has an inclination of 6.73°. The two structures are 27.91 (Ashes 24-19) and 28.36 cm (Ashes 24-26) wide, with thicknesses of 4.2 and 1.7 cm, respectively. The eastern structure is partially superimposed on the western one. This latter is formed of two parts with its thickness strangled in the middle, forming a bi-lobal structure. This deformation was present in other ash layers, but not so marked as in this example. This deformation of some layers could be the result of taphonomic processes but is a deformation originating from the lower part of the layer and not from the upper part. This repeated characteristic leads us think that this phenomenon could be related to heat penetration of the soil. If, as we suppose, these ash layers could be the result of thermal alteration of soil, these forms could be explained by a differential penetration of heat coming from a displacement of the heat center in the fire structure during its utilization, thus creating the existence of more than one center of heat during the functioning of the structure. Contrary to this hypothesis we could argue that some of these ash layers have a convex aspect to their upper surface. These convex forms are consistent with ash accumulations coming from combustible debris in fire structures. As we can see, the eastern ash layer that partially overlies this structure is a flat layer and does not present this kind of deformation.

This combustion area was covered again by a grey layer and by a black layer, and over the black layer we find a new combustion area having a diameter of 54.7 cm (in green in Figs. 18.25, 18.27). This new area is displaced to the east of the last described area and it is partially superposed

above it. Two ash layers (Ashes 24-17 and Ashes 24-18) that are 19.40 and 12.88 cm in width, 2.7 and 1.3 cm in thickness, and separated by 25.4 cm constitute the combustion area. This area is the first one having a large separation and initiates a change in the organization of combustion areas in the profile, which continues in the upper layers above the big reddish soil layer and the big and continuous ash layer that mark an interruption in this sequence and are described below. These two ash layers continue the displacement to the east, and here the eastern structure is in contact with the rock that limits the space which seems to be deformed in an arc, following the form of the rock. It is important to note that the rock under this layer shows traces consistent with thermal alteration: fractures and fissures, and also a white discoloration in relation of the rest of the rock. This indicates the effect of fire on the rock under the ash layer and heat transfer from above. No reddish zone was detected here.

We must mention here that at the west of the profile an isolated structure was detected (Ashes 24-16), having a width of 19.90 cm and a thickness of 2.1 cm. This structure is positioned directly under a reddish layer of large dimensions and covers a thin black layer and a very thin reddish layer, but cannot be connected stratigraphically to the last combustion area due the presence of a vertical disturbance in the profile.

Covering this last structure and also a great part of the profile we observe a new large and unique ash structure (Ashes 24-11, in black and white in Figs. 18.25, 18.27) overlying a reddish layer having similar dimensions. This reddish layer, formed on the west of the profile, signals the formation of a different kind of soil that indicates a partial interruption in the process of deposition of anthropic layers in this part of layer XXIV. This ash layer occupied an area that is 78.3 cm wide and has a thickness of 3.1 cm. This structure has a resemblance to the combustion area containing three ash layers observed before, both in its diameter and thickness. Its greatest thickness is clearly related to the zone where the reddish layer also reaches its greatest thickness. This phenomenon could be related to the intensity of fire and the temperatures reached in this part of the fire structure. This structure does not continue to the east, and a black layer and a burnt bone layer continue the ash layer. Finally, we can mention that very different layers cover this structure, showing that other debris accumulations often have dimensions similar and perhaps related to fire structures in this part of the site.

This large layer was partially covered by the formation of a burnt bone layer that indicates another change in the organization of the management of the debris in layer XXIV.

Here again the question is raised of the possible functions of this kind of large structure, comparing them to the dimensions of the other structures observed in the profile. Structures of this diameter are frequently observed both as central fires for cooking within the space of a habitat or as external ones that are for specialized activities. The important oxidation of the underlying sediment could imply a more prolonged and regular utilization of this structure. This is the case also for the grey layer that was observed underlying the other larger area described above and having three ash layers at the same level and in a very orderly position. The difference in color here may be due to the constitution of the underlying sediment which could respond differently to thermal alteration (reddish vs. grey). Otherwise, it seems that these two areas had different uses.

Above this large structure, we observe a change in the distribution of ash layers. We can see four combustion areas having similar organizational characteristics. These combustion areas are characterized by an arrangement in pairs, where the fire structures are separated by more than 30 cm, forming two vertical accumulations of fire structures that show a very little displacement in their horizontal position (Fig. 18.25). The width of these areas is between 62.8 and 80.5 cm, showing larger dimensions in comparison to the paired structures in the lower part of the studied profile. Even if these arrangements have similar dimensions to the combustion areas made of pairs of ash layers that were observed in layer XX, the difference is the distances between the paired structures in each area. We must remember that in layer XX the pairs of ash layers varied in their positions, being in contact, juxtaposed, or separated, while in this part of the sequence of paired combustion areas all the structures are horizontally separated. The arrangement of the thinner layers that vertically separate these different structures shows a regular dynamic in the use of space that could suggest that they were deposited over a short time. Again, these layers have an organization where a bigger

structure is accompanied by a smaller one that in this case is situated systematically on the east in the profile.

These paired combustion areas are represented in blue, violet, dark red, and light blue in Figs. 18.25, 18.27. Their diameters are, from the lowest to the top, 70, 62.8, 72.1, and 80.5 cm. Two ash layers (Ashes 24-9 and Ashes 24-15) of 8.8 and 30.05 cm diameter with thicknesses of 2.1 and 1.9 cm respectively and a separation of 31.5 cm constitute the first area. The second area is displaced only 1.8 cm to the west and is made up of two ash layers (Ashes 24-8 and Ashes 24-14) that have diameters of 8.6 and 17.34 cm, thicknesses of 1.9 and 0.5 cm, and are separated by 37.8 cm. The third area is displaced 10.2 cm to the east and consists of a pair of ash layers (Ashes 24-7 and Ashes 24-13) having diameters of 23.21 and 10.92 cm, thicknesses of 2.4, and 0.5 cm, and are separated by 37.8 cm. Finally, the fourth area is composed of two layers (Ashes 24-6 and Ashes 24-12) that are relatively more equal in their dimensions, being 18.41 and 16.96 cm in diameter, 2.1 and 1.3 cm thick, and are separated by 33.9 cm. Throughout this sequence there is very little inclination of each pair, namely 0.82° 0.19°, −0.69°, and −0.79°.

Various possibilities could explain this particular and recurring organization of ash layers. One of them is that one of each pair of accumulations corresponds to the fireplace and the other with the evacuation of combustion debris. Alternatively, in the case of these accumulations coming from flat fire structures, these structures could be representative of combustion events that involved the use of two fires at some smaller or larger distance from each other.

Similar examples of small paired fire structures, exhibiting two or more rounded areas and showing asymmetry, were observed in layer D2 of the Mousterian site of Mujina Pećina in Croatia (Karavanić 2007). The fire structures have similar dimensions and are situated at 2 or 4 meters from the entry to the shelter. The different dimensions of these fire structures could be explained by a different arrangement of wood for the fire. A radial disposition of wood can occupy a larger spatial surface than the traces that this structure will create in the underlying soil. On the contrary, a parallel and transversal organization of wood branches transforms the soil surfaces in proportional relation to the length of the branches used (March et al. 2014). Another possibility is that we have two kinds of structures, one for the fire itself where flames can be used for different functions and the other for embers, as we just mentioned. In this case, the heat produced by each structure could be different. At Crvena Stijena, however, most pairs of ash layers are situated over black layers and only one pair over a gray layer, showing that the temperatures reached by these structures individually and in pairs are similar. A second possibility is an alternating use of the structures in each pair, moving fire to the east or the west at the same level, pivoting the activity following this axis. The cooking hypothesis for one or both structures could be also an explanation for this recurrent use of the space and could be explored by the analytical procedures proposed below.

Last but not least, we can bring up the possibility that these paired structures were related to the internal organization of the occupation. The fire structures studied are situated in the lower part of the shelter and are distributed along an E-W axis, parallel to the back wall of the shelter (Figs. 18.29-18.30). Thus, these fire structures could enclose a restricted space in the part of the shelter between the wall and the entrance. Then the possibility exists that these fire structures were related to a delimitation of the internal space of the shelter for living or sleeping. For example, there are other cases in caves/rockshelters where fires were thought to be near a place reserved for sleeping, such as the Perigordian and the early Aurignacian 1 levels at the Abri Pataud (Movius 1975, 1977; Binford 1983). In Crvena Stijena the beds could be disposed along the same axis but behind the fires, or, in some cases, between the fire structures. Further investigation and analysis of the documentation from the first excavations at Crvena Stijena are needed to test these hypotheses, which could serve as a basis also for future excavations and research programs.

Following this sequence of paired structure accumulations, the use of fire shows a different pattern. We now find a series of individual structures that are dispersed in space. This change coincides with the moment when the large stone situated on the east side of the profile became covered by sediments. At this moment, available space was thus enlarged and structures could be displaced to the east.

The first individual structure (Ashes 24-39, in dark green in Figs. 18.25, 18.27) is positioned

in the west of the profile and is situated over a reddish layer that covers an ash layer that is part of the last pair described for the last sequence. It is interesting to note that here the individual ash layer has smaller dimensions (width 11.9 and thickness 0.9 cm) than the underlying reddish one (width 23.45 cm and thickness 2.2 cm). This ash layer is covered by a black layer that has the same dimensions, and the whole sequence is then covered by a grey soil that occupies an extended surface in the profile. This structure is thus positioned at a first interruption, marked by the presence of the reddish, oxidized layer, of the anthropic sedimentary processes that character-

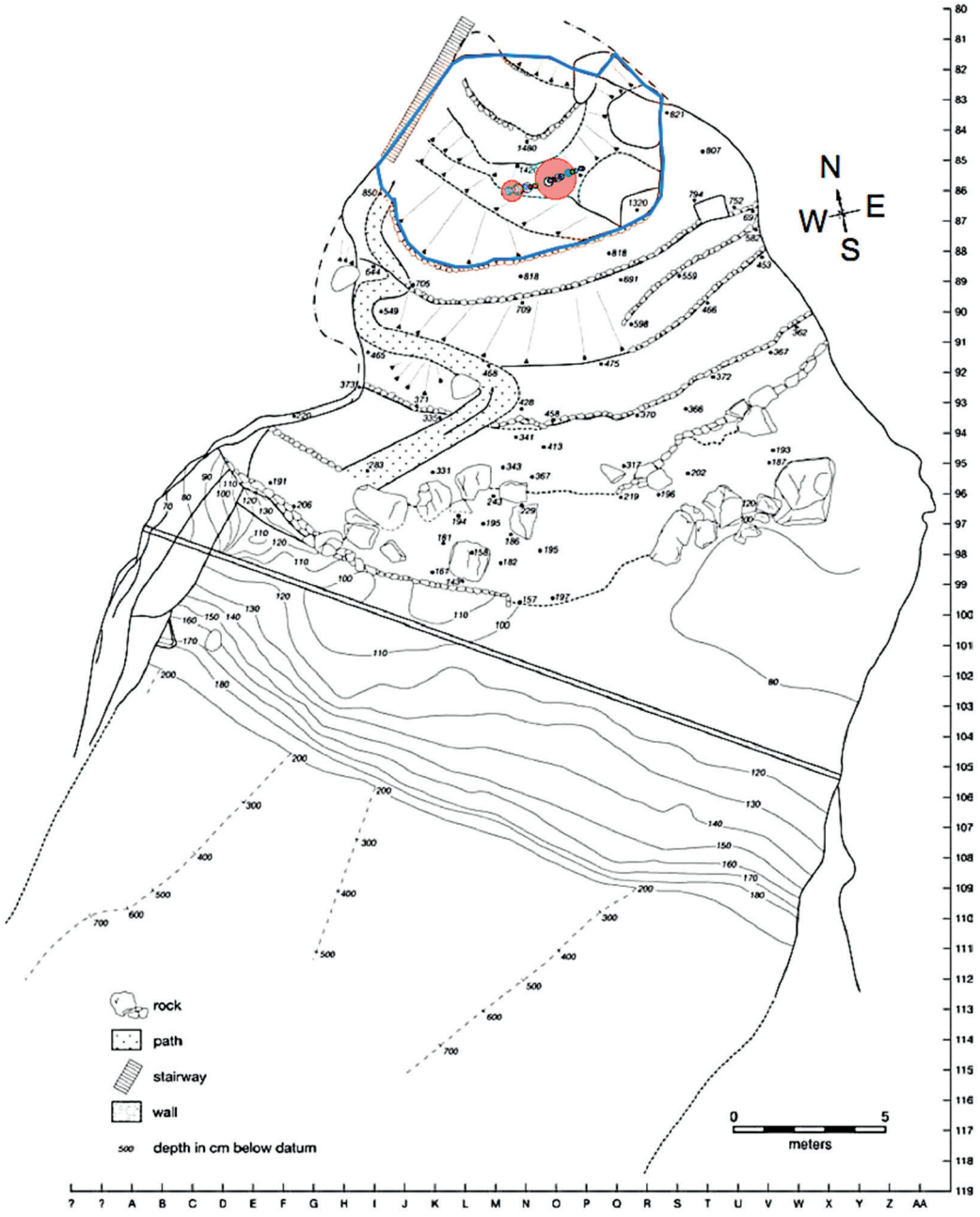

Fig. 18.29. Position and orientation of the fire structures analyzed in this chapter (layer XX and layer XXIV) in the interior space of Crvena Stijena.

Fig. 18.30. Detail of the position of fire structures analyzed (layer XX and layer XXIV) in this study in the lower part of the site.

ized the series of ash layers that we described above.

After this sequence we see a break in the presence of ash layers in the profile that is characterized by a hiatus of 8.125 cm in the sequence of sediment formation. This hiatus is characterized by a grey soil, a black layer, and a grey layer. After this interruption, we find a succession of 6 isolated ash layers that are situated at the east of the profile (Figs. 18.25, 18.28). The first three layers of this sequence of isolated fire structures (Ashes 24-10, Ashes 24-2, and Ashes 24-1) are interspersed by black or burnt bone layers. These three structures have similar dimensions. Their widths are 11.9, 16.04, and 14.18 cm, and their thicknesses are 1.5, 1.9, and 1.3 cm. These three layers also have important inclinations, following the deformation of the layers observed in this part of the profile: −27.44°, −29.45°, and −18.55°.

The other three layers (Ashes 24-5, Ashes 24-4, and Ashes 24-3) present in the upper part of this sequence show important deformations that could be related to the pressure exerted by a series of rocks that fell from the roof of the shelter. These three layers are characterized by a massive dark sediment that envelopes them, but they are situated in a zone of compression where the stratigraphy is unclear.

In this last portion of the sequence, we can observe that when space is more open the organization of fire in this part of the shelter is modified. If we compare these observations to those from the layer XX, we can see that in layer XX, where a larger space was available, the fire structures were distributed in pairs. Therefore, the presence of a larger space was not necessarily linked to the occurrence of individual and isolated structures. Evidently the human groups that were living in layers XX and XXIV were not the same and did not necessarily have exactly the same behavior in relation to space. However, as we have seen, there are some similar trends, even if they are not exactly the same. Taking this observation into account, it may be possible that the function of fire structures and the use of space could have changed in the last part of the sequence of the layer XXIV occupation period.

Five reddish layers were observed in layer XXIV. As we have said previously, this kind of layer is directly related to the action of heat on the soil, given the presence of a kind of sediment that can be oxidized (Figs. 18.31-18.32). As we can see in Figs. 18.27 and 18.28, the reddish layers are associated with the position of ash layers in four of the five cases. The only case where this association is absent is related to a zone where we observed a disturbance in the profile and where the reddish layer seems to be a remnant of a layer conserved in the disturbed zone.

The dimensions of these five layers are greatly variable. Three of them have very small dimensions and are present in the lower part of the sequence. Two of them, Reddish layer 24-23 and Reddish layer 24-3, are situated on the east of the profile under two small ash layers and were less than 10 cm wide (5.65 and 9.25 cm), with

similar thicknesses of 0.9 and 1 cm respectively. These two structures are situated under two small ash layers that form parts of two combustion areas, one characterized by the presence of four ash layers and the other by two ash layers in the lower part of the profile (Figs. 18.31-18.33), and demonstrate that these small ash layers are in some cases linked to the *in situ* action of fire.

The third reddish layer is situated on the west of the profile (Reddish layer 24-5) in the disturbed zone and also has small dimensions, 5.48 cm wide and only 0.3 cm thick. This layer, which is situated between two grey layers, is not in contact with ashes or a black layer and could be considered as a remnant of disturbed oxidized soil that is situated under a grey layer, a phenomenon that was observed previously in layer XX.

The two other reddish layers are *in situ* and well preserved. They are also significantly different (Figs. 18.31-18.33). One of them is the largest red layer of the entire sequence (Reddish layer 24-1) with a width of 84.08 cm and a thickness of 4 cm. This layer marks a break in the sequence of anthropic deposits in layer XXIV, covering a big black layer and being covered by the biggest ash layer recorded in layer XXIV (comparable to Structure 3, reddish soil of layer XX). This reddish layer has a larger surface than all the ash layers observed in this part of the profile. As we mentioned in presenting the ash layers, it is interesting to note that the ash layers covering these reddish layers have smaller dimensions than the oxidized underlying zone, contrary to the situation in layer XX. But in this case these differences are less, and the two layers have more similar dimensions. Therefore, the ashes in this case seem to not be so dispersed over the oxidized surface. These ashes seem to be more important near the position where the reddish layer is also thicker; at this spot the reddish zone has a profile that could reflect the transmission of heat to the underlying soil, completely altering it to this greater thickness. Although the difference observed in the thickness of this layer could have been caused by a displacement of the heat center in the ancient fire, it could also reflect a differential distribution of temperatures within the fire structure, which must have been higher in the thicker area.

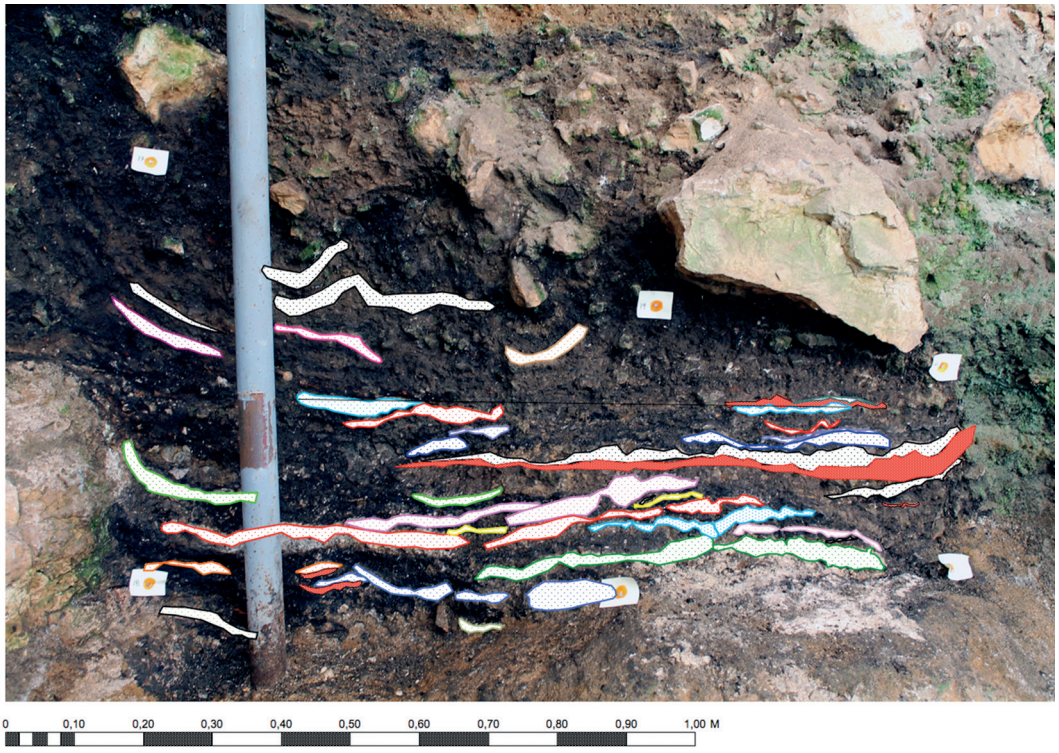

Fig. 18.31. Association of fire structures (ash layers) and reddish layers (red massive pattern) as a function of their stratigraphic position for layer XXIV; similar colors indicate stratigraphic association for ash layers.

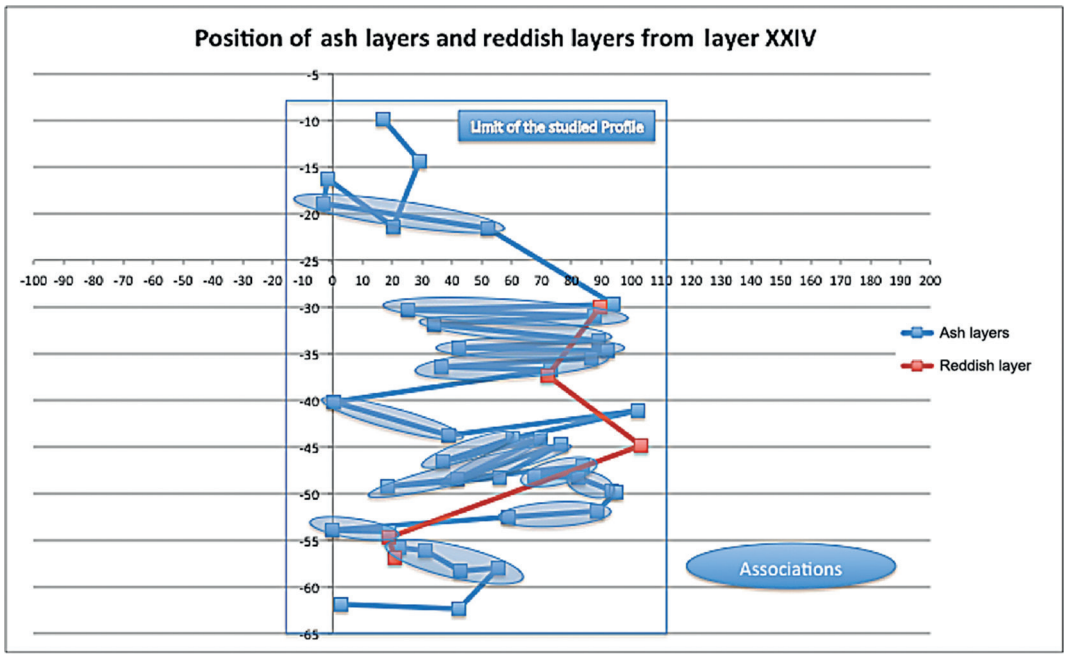

Fig. 18.32. X center position of ash layers and reddish layers from layer XXIV.

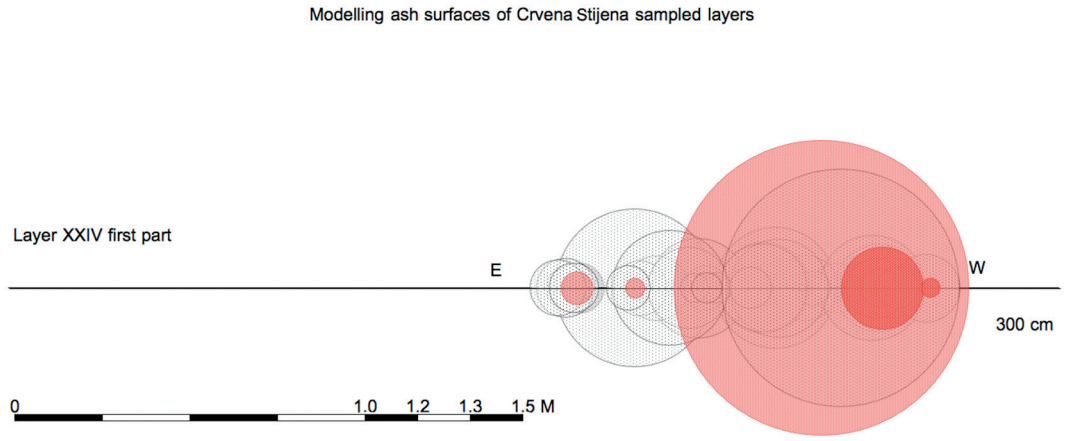

Fig. 18.33. Modeled top view of ash and reddish layers from layer XXIV, with emphasis on the dimensions of the layers (black-white and red patterns, respectively); the diameter of the circles represent the width of each fire structure.

The last reddish layer is 23.45 cm wide and 2.2 cm thick (Reddish layer 24-4), and is situated in the west part of the profile, covering an ash layer, which is in turn covered by a second ash layer of small dimensions. In this case again the ash layer only partially covers the reddish one.

Once again we have not detected any pair of reddish layers in the sequence. This ascertainment, again raises the question of the related formation processes that lead to this result. In first place, we must remember that we did not observe any natural soil which had two ash layers on it, one with oxidation and other one without it. This pattern is present when the paired structures occur over black layers in layer XXIV or over grey layers in layer XX. In the case of black layers in layer XXIV, this could bring us to think that we have here two kinds of fire structures, one that represents an *in situ* fire and the other an evacuation of ashes into an area near the fire. Following our

experiments discussed earlier, when oxidation is present under a grey layer, we can associate it with heat penetration into a black layer that was altered by fire.

Another possibility to explain the presence of reddish layers between ash layers and black layers is that small variations exist in the compositions of the black layers which provoke these different colorations. Finally, another possibility is related to the duration of functioning of these fires, the longer the duration the easier it will be to find zones of coloration in the underlying layer. Even if the combustion area is small, a more prolonged use could allow us to better detect the different transformations because a zone changing from a dark grayish brown color to a pale brown could emerge more clearly and, infused with humidity at the site, with a reddish coloration. This layer could be imperceptible with fires of short duration without a micromorphological approach. We therefore chose to sample some of these zones for elemental analysis in an attempt to verify or discard some of these possible explanations.

Moreover, it is evident that if we discard the possibility of *in situ* fires where the kind of reddish layers that emerged in our experiments are not observed, we would observe only a very small number of *in situ* fires (four for layer XX and five for layer XXIV) and a great number of deposits of ashes coming from fires that must have been ignited in another part of the site. This would completely change the meaning and analysis of the intensity and the rhythm of the use of fire determined from the study of these profiles.

Therefore, as for layer XX, we will proceed by sampling seven fire structures from layer XXIV (Fig. 18.34) to better explain the nature of these different layers using a series of techniques (X-ray fluorescence, XRD, GC, GC-MS, and CG-C-IRMS).

Preliminary Conclusions about the Dynamics of Fire in Layers XX and XXIV, prior to Analytical Results

After the preliminary analysis of these sequences we can observe some trends and differences in both layers XX and XXIV in this part of the shelter. First, all the combustion structures must be classified as flat fire structures. Only one flat structure seems to lie in a natural depression in layer XXIV, but none show any signs of hav-

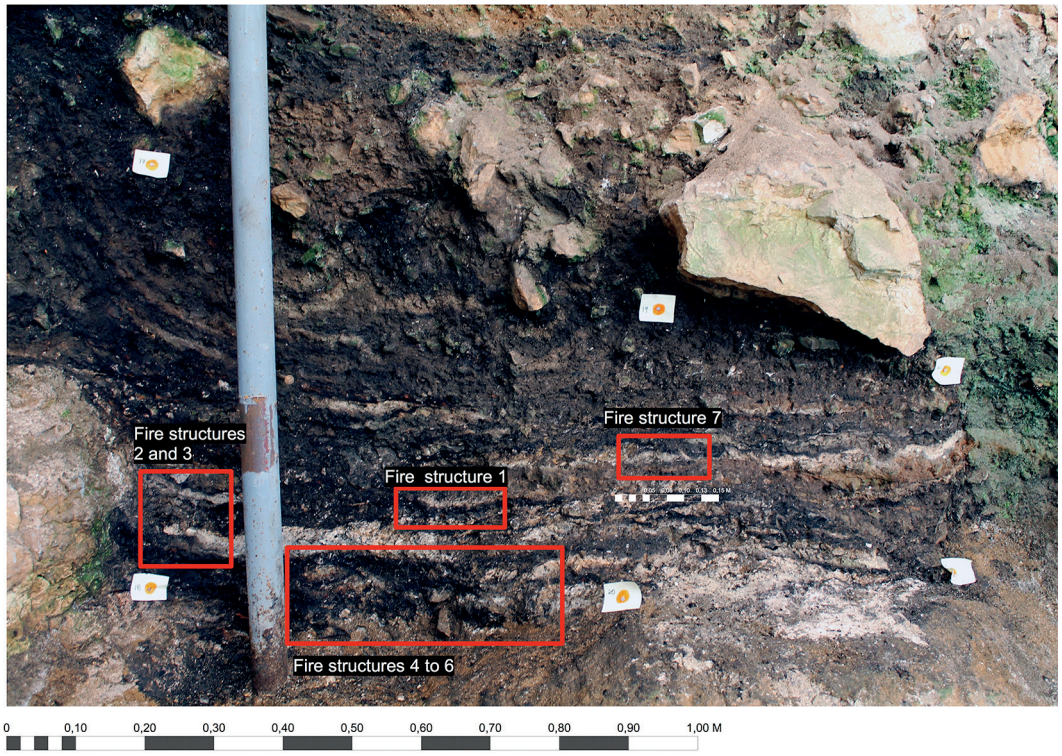

Fig. 18.34. Sampled zones for the analytical study of layer XXIV.

ing been excavated. These flat fire structures are spaced in time, showing alternation at any given place between fire activities and the accumulation of debris coming from other activities but mixed with combustion debris that came from fire activities at other places in the shelter.

So, although the entire layer presents traces of fire activities, different formation processes are represented. As we see from our experimental results, the interpretation of the ash layers at Crvena Stijena must take into account the possibility that some are not the result of the accumulation of combustion debris but may be burnt soils formed by the action of fire. In the same sense some grey layers could be also the result of heat action.

The ash layers in both sequences occur more frequently as pairs of two (or more) structures than isolated singly in space. These paired structures are aligned along an E-W axis, but we can not conclude with certainty that there were not other orientations, given that our work follows the excavated profile. This leaves open the possibility that the isolated structures in some cases represent paired structures that have a different orientation, for example N-S, and that the paired structure was not detected. In layer XX we observed a sequence of paired structures with an intercalated large and unique structure that occupied a large part of the space. In layer XXIV we have a similar process but in a more limited space and showing some variations in the arrangement of paired structures. But here, contrary to layer XX, we can observe a sequence of isolated structures in the upper part of the profile.

In some cases many structures are aligned along the same axis, forming areas of three or four combustion structures, which could be interpreted as the result of the modification of a larger layer that occupied the space and was divided into different concentrations by taphonomic processes that altered the ash concentrations.

In the sequences of pairs we can observe four different modes of spatial organization: contact between the pairs, separation of two degrees: pairs less than 16 cm and pairs more than 24 cm of apart, and, finally, juxtaposition. This last indicates a reutilization of the space and a superposition of fire structures within short periods. Beyond their spatial arrangement, we can see different kinds of paired structures considering their size, combustion areas with both structures of similar dimensions, and others ones showing a great dissimilarity.

As we see, these paired structures can be interpreted as two *in situ* contemporary or immediately successive fire structures, or an *in situ* fire structure accompanied by an area of combustion debris. We could also see that the size of the structures in this case is not necessarily an indication that the larger ash layer was a *in situ* fire structure, observing that smaller ones sometimes show clear stratigraphic associations with oxidized soils that allow us to identify them as *in situ* fire structures.

Beyond these general conclusions, we see also in layer XXIV that space limitations could change the dimensions and the distribution of fire structures in space, with greater dispersion noted when the space is unlimited, as we see in layer XX. Looking at the dimensions and organizations of all kinds of layers, we can also conclude that the intensity of the use of space was different between layers XX and XXIV, being more intense and presenting a greater dynamic in layer XXIV.

It is evident that this analysis made from the observation of the exposed profiles cannot take into account all the richness of information that could be obtained from these structures following an extensive excavation. We are also perfectly aware that the dimensions measured can be affected by the position of these structures relative to the profile. However, taking these limitations into account, the analysis presented above seems to be the only way that we have to get a first anthropic reading on these structures while waiting for their future excavation and analysis. Our experience analyzing other sites shows that the dimensions observed in the profile can be used effectively to obtain a first analysis of such series of fire structures, and we think that the results of this first modeling of the dynamic of fire in this extensive sequence has given a series of hypothesis that can be used in the future to interpret the Neanderthal behavior related to fire at Crvena Stijena. At the same time, this first approach gives us a necessary archaeological framework to interpret our further analytical work and allows us to refine our questions while trying to elucidate the different hypotheses evoked here.

The Analytical Study of Sampled Fire Structures in Crvena Stijena

The objective of this part of our work is to better understand the nature, composition, mode

of functioning, and use of the fire structures of Crvena Stijena through scientific analysis of their sampled sediments. To do this we proceed as follows: elemental analysis by X-ray fluorescence to determine the chemical nature and possible contents of each sample, XRD analysis to analyze their crystallographic and mineralogical composition, and finally GC, GC-MS, and GC-C-IRMS to determine their organic matter composition.

As we said above, we have chosen to study three different layers, two as examples of Neanderthal occupation—layers XX (Mousterian with triangular points) and layer XXIV (Mousterian)—and a third one, layer XXIII, considered as sterile in terms of Neanderthal hearths and which is studied here as a "control" for comparative purposes. Layers XX and XXIV have been briefly described above, in the first part of this chapter. Layer XXIII is described by Morley (Chapter 7, this volume) as a layer marking a rupture in the lithology of the site, which has a matrix characterized by sub-angular to sub-rounded, coarse sediments. In this layer the clay component decreases, here giving place to a larger proportion of sand. It has low levels of organic matter and shows low magnetic values. The color ranges between 7.5 YR 6/4 and 6/6, dull orange to orange. In this layer, bones and charcoal decline to very low levels or are completely absent. These changes are related to a deterioration of climate that changed the habitability of the site. Its carbonate composition is between 51.5 and 66.4 % which is considered here as the natural carbonate values for Crvena Stijena layers in this analysis.

From layers XX and XXIV, we have chosen to study several different fire structures to elucidate some of the questions we developed about the different kinds of layers, fire structures, and combustion areas that we have described above.

For layer XX we chose to study the largest structure, which gives us the opportunity by it is dimensions and thickness to establish a sequence of samples following the internal stratigraphy of the structure in a vertical column. We took 7 samples from structure 3 as follows (Figs. 18.1, 18.35):

Sample 1 - the upper black layer
Sample 2 - the grey-black transition layer (grey layer) over ashes
Sample 3 - the upper part of the white grey ashes
Sample 4 - the reddish soil
Sample 5 – white transition between reddish layer and black layer
Sample 6 - grey layer
Sample 7 - the black layer 2, lower black layer of structure 3

For layer XXIV we took samples from 7 different fire structures (Figs. 18.1, 18.36). First we wanted to study paired and multiple structures

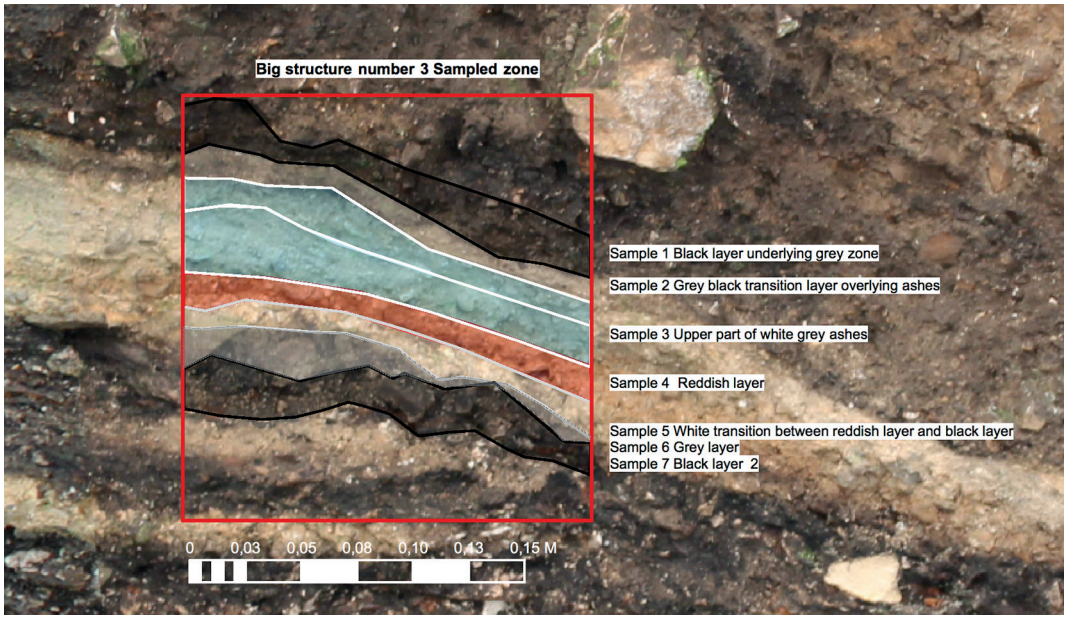

Fig. 18.35. Detailed sampled zones for the big structure 3 and upper layers in layer XX.

that presented a separated disposition and that lay over a black layer. From fire structure 1 (Ashes 24-18) we took two samples, one from the ash layer and another one from the underlying black layer (24-5), and from fire structure 2 (Ashes 24-27) we took three samples, one from the ash layer, a second one from a rodent hole that disturbed the structure, and a third one from the same black layer 24-5 underlying both structures. Fire structure 3 (Ashes 24-21) was also sampled in a column of three samples, one from the ash layer, a second one from the transition zone that corresponds to the underlying grey layer 24-4, and finally a third one from the black layer 24-5 situated under the grey layer. We also chose to sample a combustion area with four ash layers, choosing from them ash layer 24-25 (fire structure 4) and taking samples from the ash layer itself, from an anthropic hole that had disturbed the structure creating an artificial division in the ash layers, and finally one sample from the underlying black layer 24-9. Fire structure 5 (Ashes 24-23) is the small member of a pair. This sample was accompanied by a second sample coming from the underlying black layer 24-8. In the same part of the profile we completed our sampling of paired and multiple ash concentrations with a combustion area in which two ash layers are in contact, choosing ash layer 24-32 and the underlying black layer 24-27 (fire structure 6).

We also sampled the large ash layer in the middle of the profile (fire structure 7; Ashes 24-11). Here we took one sample from the ash layer, a second one from the reddish layer 24-1, and a third one from the black layer 24-3 that covered the structure (Fig. 18.36). Finally, we took two samples from an ash layer from layer XXIV that presents different characteristics of texture and color (fire structure 8, identified variously as 'limonite white yellow' or 'ashes limonite' below). This layer is not included in the profile presented and was taken from a deeper part of layer XXIV. Its texture was more "greasy" than the other layers, and its color was yellow-orange. Here we studied two samples from the same layer to compare the results at different places in the same layer.

All these archeological samples were accompanied by the study of two samples coming from layer XXIII and which are considered here as representing the natural sediments and their organic composition that existed at the site when human occupation declined or ceased (Figs. 18.1, 18.37).

Table 18.9 gives the complete list of the 29 samples studied.

Elemental Analysis by X-ray Fluorescence

The elemental analysis of samples was done using a handheld XRF energy dispersive X-ray fluorescence spectrometer Niton™ XL3t 950 Goldd+ in the laboratory. The samples were analyzed after organic matter was extracted following the procedures described below. Before analysis,

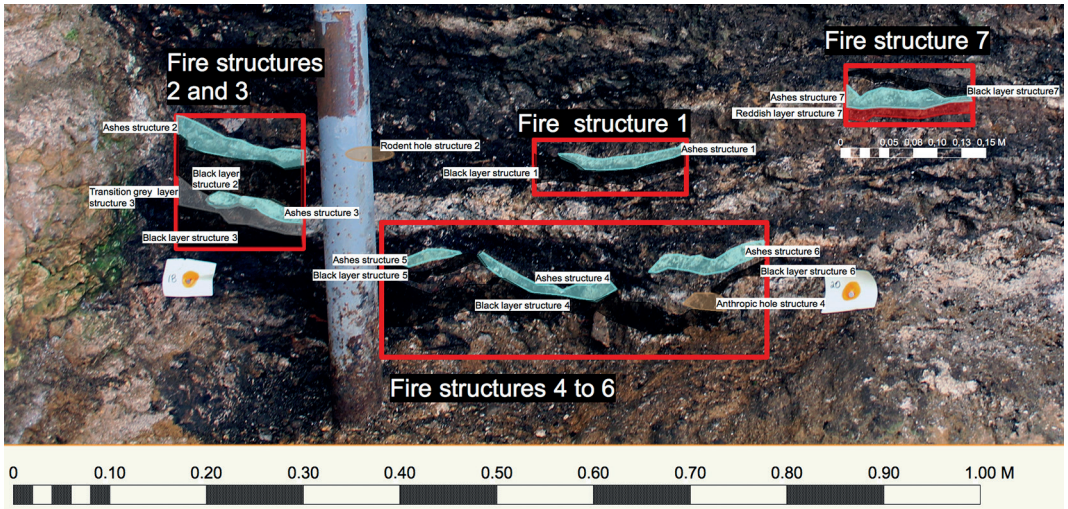

Fig. 18.36. Detailed sampled zones for structures 1 to 7 in layer XXIV.

samples were ground with a Fritsch™ planetary mill pulverisette 5 at 300 rpm three times (10 min each) in an agate recipient to homogenize their composition. Analysis was performed three times at equal times of exposure (3 min) to obtain a mean elemental composition. The results are expressed in percentage of oxides for the principal components and in ppm for the minor ones.

DRX analysis of Mineralogical Composition

The characterization of the mineralogical composition of different layers was performed in an Inel Equinox 1000 Benchtop X-Ray Diffractometer. The samples studied are the same samples studied by X-ray fluoresence. The powder sample was exposed to X-rays with a time lapse of 10 minutes. Diffractograms were analyzed using the DRX library. (The X-ray fluorescence and DRX analyses were carried out at the analytic facilities of the UMR 6566 CREAAH with the technical support of Mikaël Guivarch.)

Organic Chemical Analysis and Molecular Isotopic Study

Extraction and Separation

Sediments of all samples were collected at the site with sterile spoons and put in aluminum foil before being stored in plastic bags to avoid contamination with plasticizers. However, some samples in this study contain plasticizer contamination from previous contamination at the site. Laboratory blanks were regularly analyzed in order to test for the absence of recent contamination of the analysis extracts.

The samples were extracted twice with 60 mL to 300 mL (as a function of volume) of chloroform/methanol solution (2:1) by ultrasonication for 90 min at 40°C. The obtained solution (38% and 43%, dry weight of extract, of total sample weight) was then separated according to the method of McCarthy and Duthie (1962) by column chromatography on potassium hydroxide impregnated silica gel (10 g). The neutral compounds were eluted first with ethyl ether (100 mL).

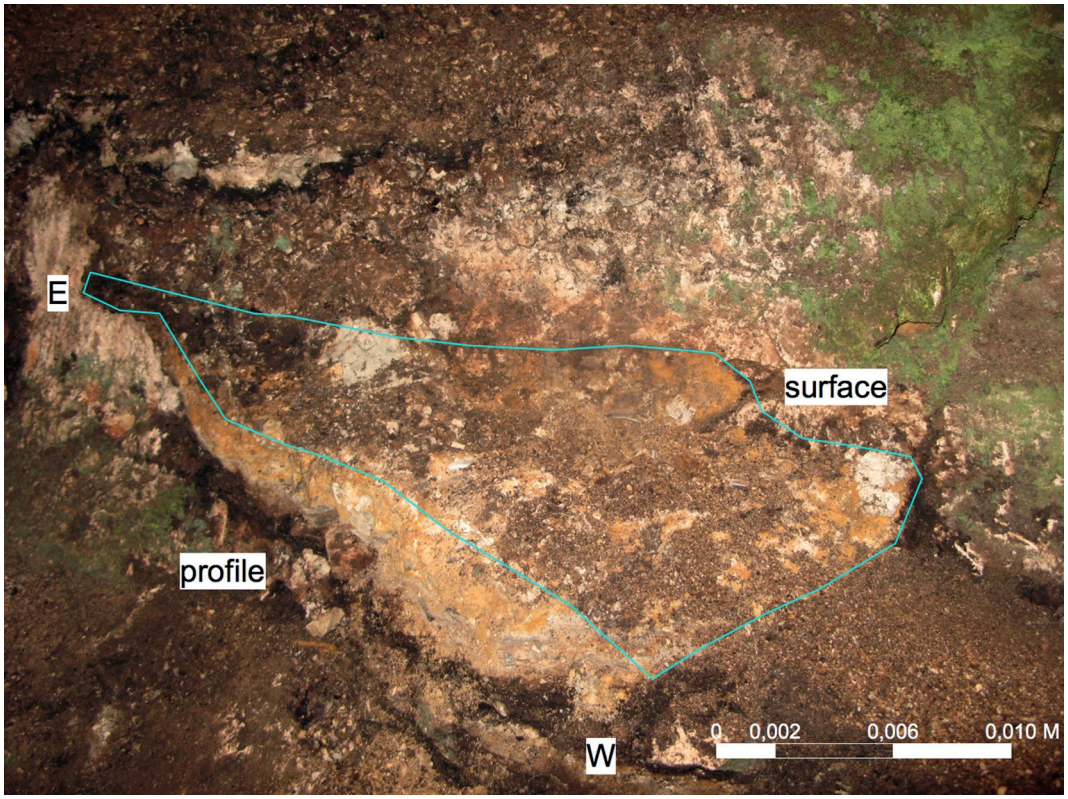

Fig. 18.37. Detailed sampled zones for the limonite ash layer from layer XXIV.

Table 18.9. List of samples from fire structures from Crvena Stijena.

N°	Layer	Fire Structure Number	Description	Mass (g)
1	XX	Str 3	Blackened soil	120.12
2	XX	Str 3	Gray black superior layer that covers the ash layer of the structure 3	109.00
3	XX	Str 3	Upper part of white grey ashes	70.00
4	XX	Str 3	Reddish soil	29.30
5	XX	Str 3	White transition (Between red and black)	48.50
6	XX	Str 3	Grey soil	120.02
7	XX	Str 3	Blackened soil bis	76.56
8	XXIII	Sterile 1	Natural soil light brown	120.00
9	XXIII	Sterile 2	Natural soil light brown	120.08
10	XXIV	Str 1	Ashes (white sediment sample)	54.64
11	XXIV	Str 1	Blackened soil	45.50
12	XXIV	Str 2	Ashes	82.32
13	XXIV	Str 2	Blackened soil	49.64
14	XXIV	Str 2	Rodent hole	50.43
15	XXIV	Str 3	Ashes	66.45
16	XXIV	Str 3	Intermediate layer	27.93
17	XXIV	Str 3	Blackened soil	58.35
18	XXIV	Str 4	Hole (anthropic)	120.00
19	XXIV	Str 4	Ashes	84.63
20	XXIV	Str 4	Blackened soil	37.08
21	XXIV	Str 5	Ashes	30.41
22	XXIV	Str 5	Blackened soil	49.77
23	XXIV	Str 6	Ashes	99.00
24	XXIV	Str 6	Blackened soil	23.40
25	XXIV	Str 7	Grey soil (Ashes)	65.60
26	XXIV	Str 7	Blackened soil	47.32
27	XXIV	Str 7	Reddish soil	120.00
28	XXIV	Str 8	Limonite white yellow layer	120.01
29	XXIV	Str 8	Limonite white yellow layer bis	104.80

The acidic compounds, eluted with 2% formic acid in ether (100 mL) were derived in their methyl ester by treatment with acetyl chloride in methanol solution for 20 min at 80°C. The neutral fraction was further separated according to functional group by column chromatography (5 g of silica) in four sub-fractions by elution with 50 mL of heptane/ether mixtures of increasing polarity (1:0, 3:1, 1:1, 0:1). Each sub-fraction contains, respectively, hydrocarbons, ketones, alcohols, and finally nothing in the samples from Crvena Stijena in the most polar sub-fraction. The separation of the neutral fraction allowed better identification of minor components.

The three obtained sub-fractions and the acidic fraction were then analyzed by gas chromatography (GC) and gas chromatography coupled with mass spectrometry (GC/MS).

Compounds were identified by their retention time within the GC, their fragmentation pattern within the MS, and by matching their mass spectra to reference spectra from the literature or from libraries (NBS75K and Wiley).

GC Analysis

The GC analyses were carried out with a Hewlett Packard (HP 6890 series) apparatus equipped with an FID detector at a temperature

of 250°C and with an HP-5 capillary column ((5%-Phenyl)-methylpolysiloxane, 0.25 mm internal diameter, 30 m length, 0.25 mm phase thickness). Helium was used as carrier gas (1 mL/min flow rate). The injection was made splitless at a temperature of 250°C. The oven temperature was ramped from 40°C to 300°C at 4°Cmin^{-1} and held for 30min at 300°C.

GC-MS analysis:

The GC/MS analyses were carried out with a Hewlett Packard apparatus (HP 6890 coupled to an HP 5973 quadrupole mass selective detector) equipped with a DB5-ms non-polar capillary column ((5%-Phenyl)-methylpolysiloxane, 0.25 mm internal diameter, 30 m length, 0.25 mm phase thickness). The chromatography was carried out under the same conditions as the GC analysis. The MS was operated in the electron impact mode at 70 eV, source temperature of 250°C, emission current of 1 mA and multiple-ion detection with a mass range from 40 to 800 amu. (I would like here to thank my collaborators who aided me in the preparation of this work as part of their professional formation: M. Garcia, R. Samson, E. C. Avalos-Perez, A. G. Fernandez-Lopez, and C. Guillou.)

CG -C-IRMS Analysis

Carbon-13 content of palmitic (C16:0) and stearic (C18:0) acids in their fatty acid methyl ester form (FAME) was determined by gas-chromatography-combustion-isotope ratio mass spectrometry (GC-C-IRMS) on an HP6890N (Agilent technologies, Hewlett Packard) interfaced with an Isoprime mass spectrometer (GV Instruments, Manchester, UK). Briefly, the effluent stream from the capillary GC column enters a combustion furnace where compounds are quantitatively combusted to CO_2 and water. Water is then removed from the carrier stream using a cryogenic trap and the sample-derived CO_2 is then analyzed in the high precision IRMS for its carbon-13 content. In both systems, temperatures in the interface and combustion oven were regulated to 350°C and 850°C respectively and carrier gas (He) was set at a constant flow rate of 1.2 mL/min.

Separation of fatty acids methyl esters was performed on a DB-5MS capillary column (J&W Scientific, Courtaboeuf, France) with the following characteristics: 30 m, 0.25 mm i.d., and 0.25 μm film thickness. Depending on concentrations of FAMEs, samples were injected either in split or in splitless mode and analyzed at least in duplicate.

In this study, the best chromatographic conditions were as follows: injector temperature was 240°C, the column was held isothermal at 45°C for 2 min after injection and then temperature was increased to 180°C at 8°C/min, further elevated to 205°C at 3°C/min, and finally at 20°C/min to 300°C where it was held for 2 min.

The stable isotopic composition of carbon is reported in the conventional delta per mil notation ($\delta^{13}C$), expressed relative to the international Vienna Pee Dee Belemnite standard (V-PDB) via the following equation:

$$\delta^{13}C\ ‰ = \left[\left(\frac{^{13}C}{^{12}C} \right)_{sample} / \left(\frac{^{13}C}{^{12}C} \right)_{PDB} - 1 \right] \times 10^3$$

This calibration occurs via a bottle of reference CO_2 connected to the IRMS system for introducing directly in the source 3 pulses at the beginning and end of every isotopic GC determination and 5 pulses during the chromatogram in order to take into account a potential background change during the run. Analyses were all performed using IonVantage software for Isoprime (build 1.3.6.0). Accuracy and precision on reference gas pulses in each run were better than 0.3‰ specification of the system. The carbon-13 content of the reference CO_2 was previously calculated via an inter-laboratory comparison study using 6 different standards analyzed in 20 laboratories either with EA-IRMS or GC-C-IRMS systems.

$\delta^{13}C$ values of FAME were corrected to take account of the dilution of fatty acid carbons by the methylating reagent. This isotopic shift was calculated by a mass balance equation:

$$\delta^{13}C_{FAME} = f_{FA}\,\delta^{13}C_{FA} + f_{MeOH}\,\delta^{13}C_{MeOH}$$

where $\delta^{13}C_{FAME}$, $\delta^{13}C_{FA}$, and $\delta^{13}C_{MeOH}$ are the carbon isotope compositions of the fatty acid methyl ester, the fatty acid, and the methanol used for methylation of the fatty acid, respectively, and f_{FA} and f_{MeOH} are the carbon fractions in the fatty acid methyl ester due to the alkanoic chain and methanol, respectively. In this case, the values for f_{FA} is 16/17 for C16:0 and 18/19 for C18:0. The carbon 13 content of methanol was analyzed by EA-IRMS (CA1500 NC Elemental Analyzer, Carlo Erba, Milano, Italy / Isoprime isotope ratio mass spectrometer, GV Instruments, Manchester, UK) :

$\delta^{13}C_{MeOH} = -40.5$ ‰ (n = 5, SD = 0.3 0).

Finally, the day-to-day and long term analyt-

ical accuracy of the 2 GC-C-IRMS systems were checked by the injection of an in-house mixture of FAMEs (sigma Aldrich Standards) in each batch of analysis: the $\delta^{13}C$ values for C16:0 and C18:0 are respectively −29.9 ‰ (sd = 0.25 0) and −24.2 ‰ (sd = 0.25 0) for 80 analyses within one year. (The GC-C –IRMS analysis was done with the collaboration of Jean-Noel Thibault at the UMR 1348 Pegase INRA–CNRS.)

Analytical Results and Discussion.

Determination of the Elemental Composition of Crvena Stijena Samples by X-Ray Fluorescence

The analysis of the elemental composition of the different samples studied at Crvena Stijena lets us better understand the characteristics and origin of these different layers. The major elements present in the Crvena Stijena samples are calcium (CaO), followed by silica (SiO_2), phosphorus (P_2O_5), and magnesium (Mg0) when present. If magnesium is not present, the following element is aluminum (Al_20_3) (Fig. 18.38, Table 18.10)

This distribution it is not surprising if we take into account the results presented for the site by Morley (2007, Chapter 7, this volume). Calcium could be related here to both natural composition of the sediments of the shelter and the presence of ashes because of the presence of calcite or dallite or even the oxalates of calcium coming from plant residues. The silica and aluminum are related to the clay and sands present in the natural composition of the different layers. The phosphorus is introduced here from the organic components of the layers in the form of bones, which contribute hydroxyl apatite. This element can be also associated with other biological sources that come from the process of decomposition of organic matter, or even from fecal matter. The coprolites of *Crocuta* (hyenas) have been found in final Pleistocene habitats in the region (Ivanova et al. 2016), and hyena remains, gnawed bones,

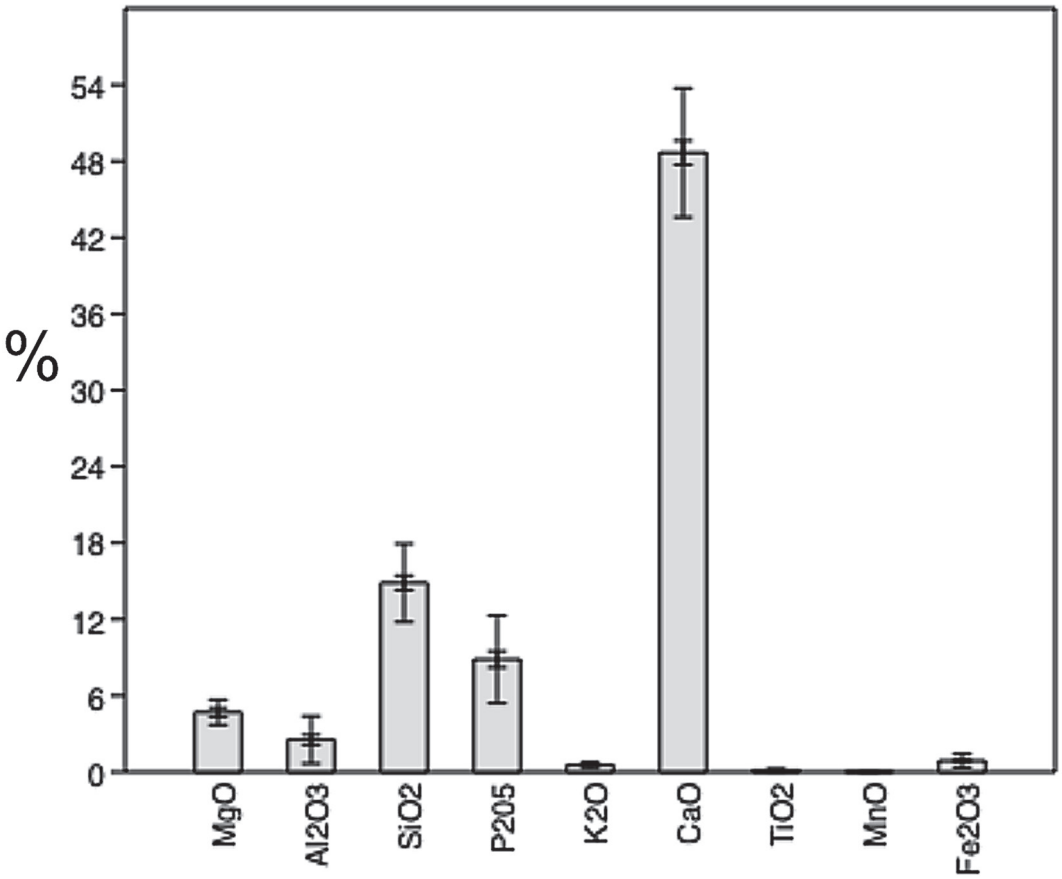

Fig. 18.38. Percentage distribution of major elements present in Crvena Stijena Samples.

Table 18.10. XRF results (oxide percentages) from the major elements of Cvena Stijena samples.

	Sample	MgO	Al_2O_3	SiO_2	P_2O_5	K_2O	CaO	TiO_2	MnO	Fe_2O3
Big Structure 3 Layer XX	Blackened soil S1	<LOD	2.64	16.5	9.97	0.79	41.73	0.17	<LOD	1.06
	Grey black layer	<LOD	3.18	15.58	10.24	0.5	48.79	0.14	<LOD	0.88
	White gray ashes	5.32	1.25	14.81	7.55	0.45	51.41	0.14	<LOD	0.84
	Reddish soil	5.32	1.08	12.62	14.33	0.32	52.33	0.1	<LOD	0.53
	White transition	<LOD	<LOD	12.21	11.11	0.21	55.39	0.07	<LOD	0.45
	Grey soil	5.19	3.59	17.87	3.65	0.77	50.19	0.2	<LOD	1.34
	Blackened soil	<LOD	<LOD	12.98	11.73	0.36	48.45	0.05	<LOD	0.49
Structure 1 Layer XXIV	Blackened soil	<LOD	0.92	13.17	8	0.4	50.06	0.13	<LOD	0.64
	Ashes	<LOD	<LOD	11.69	7.62	0.21	58.93	0.12	<LOD	0.4
Structure 2 Layer XXIV	Blackened soil	< LOD	0.649	12.18	11.62	0.34	48.52	0.05	<LOD	0.456
	Ashes	<LOD	0.82	12.16	11.22	0.26	48.9	0.07	<LOD	0.43
	Rodent hole	<LOD	4.36	21.01	5.56	1.08	39.36	0.26	<LOD	1.87
Structure 3 Layer XXIV	Blackened soil	<LOD	1.55	12.93	11.79	0.41	46.69	0.08	<LOD	0.56
	Ashes	<LOD	1.63	12.69	7.89	0.41	52.85	0.07	<LOD	0.54
	Intermediate layer	<LOD	1.44	13.73	8.67	0.49	49.55	0.08	< LOD	0.599
Structure 4 Layer XXIV	Blackened soil	<LOD	0.99	13.76	11.75	0.57	44.27	0.1	<LOD	0.75
	Ashes	<LOD	1.1	13.21	11.11	0.34	52.07	0.13	<LOD	0.68
	Hole (anthropic)	<LOD	2.57	14.67	9.86	0.56	46.44	0.12	<LOD	0.77
Structure 5 Layer XXIV	Blackened soil	6.1	2.09	13.76	15	0.48	48.61	0.15	<LOD	0.72
	Ashes	<LOD	<LOD	11.55	8.45	0.26	56.69	0.11	<LOD	0.39
Structure 6 Layer XXIV	Blackened soil	<LOD	<LOD	12.91	12.24	0.32	50.98	0.1	<LOD	0.5
	Ashes	4.6	1.67	13.6	8.14	0.5	53.07	0.16	<LOD	0.83
Structure 7 Layer XXIV	Blackened soil	4.33	1.74	14.79	11.5	0.6	43.72	0.11	<LOD	0.84
	Grey soil (ashes)	<LOD	1.46	13.32	6.97	0.48	52.33	0.13	<LOD	0.66
	Reddish soil	<LOD	2.64	15.03	8.26	0.66	53.2	0.19	<LOD	1.01
Structure 8 layer XXIV	Ashes limonite	< LOD	7.042	21.04	4.703	0.918	40.016	0.309	< LOD	2.396
	Ashes limonite	< LOD	7.181	20.245	5.289	0.861	41.441	0.286	0.017	2.237
Steril Layer XXIII	Sterile 1	3.28	5.6	22.43	1.36	1.17	41.33	0.25	<LOD	1.67
	Sterile 2	3.39	3.37	18.51	1.06	0.76	43.96	0.16	<LOD	1.02

and hyena coprolites were identified by Malez (1975:153-154) from layers XXI and XXIV in Crvena Stijena). Finally, magnesium (MgO) could also be related to the presence dolomite degradation, or to its dilution by water that penetrates by infiltration into the shelter. Manganese (MnO) and Iron (Fe_20_3) could have the same origin, but iron and titanium TiO_2 could be also related to the processes of deposition of natural sediments in the shelter. Finally Iron can also be overrepresented in some layers that were exposed to heat action.

The statistical analysis of these results shows that aluminum has strong correlations, $r > 0.9$, with silica, iron, and titanium and a somewhat weaker correlation with potassium, $r = 0.87$. These elements could be associated in the clays of the soils of the layers studied here. At the same time, phosphorus has a negative correlation $r = -0.72$ with silica while calcium has also negative correlations with both silica, $r = -0.77$, and iron, $r = -0.72$.

The analysis of the distribution of these elements by kind of layer shows that CaO, which is the principal component, is more concentrated in the reddish soils, followed by the ashes, the blackened soils, and the natural soils. Silica and aluminum are more concentrated in the natural soils, and phosphorus has its lowest concentration in these natural layers (Fig. 18.39).

Among the minor elements present in these samples, estimated in ppm, the most important are sulfur (S) and chlorine (Cl) (Fig. 18.40). Sulfur is relatively important for our work because it could be from pyrite which can be used for lighting fire. Nevertheless, even if its distribution is more concentrated in the ash layers, its concentrations in reddish layers and blackened soils are also important, and therefore its origin must be related to other causes. As we know, sulfur (S) is

present in organic matter contained in sediments. Evidently the identification of the exact nature or state of this sulfur requires more studies and other analytical techniques (Schroth et al. 2007), but we know that such sulfur has its origin in the incorporation of sulfides produced by bacterial reduction of sulfate during deposition and early diagenesis (Sinninghe Damste and de Leeuw 1989; Vandenbroucke and Largeau 2007). But, as we also know, sulfur is present in significant amounts in animal bodies (Emsley 1998; Frausto Da Silva and Williams 2001; Bergada 2015) and could be related also to the decomposition of the remains of animal carcasses at the site. Chlorine

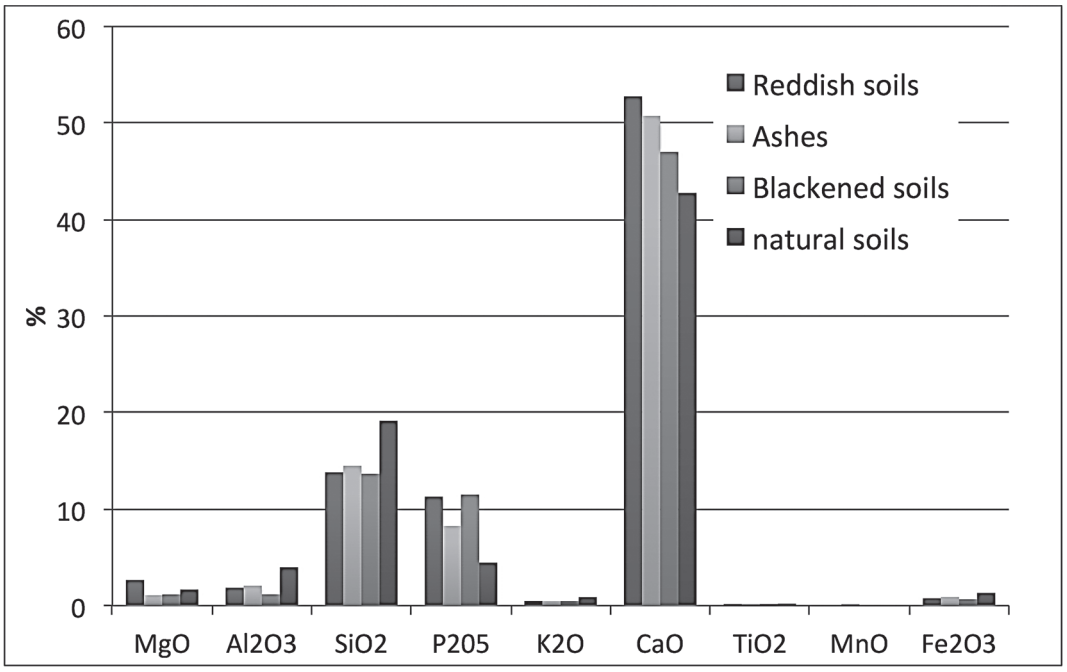

Fig. 18.39. Percentage distribution of major elements by kind of layer at Crvena Stijena.

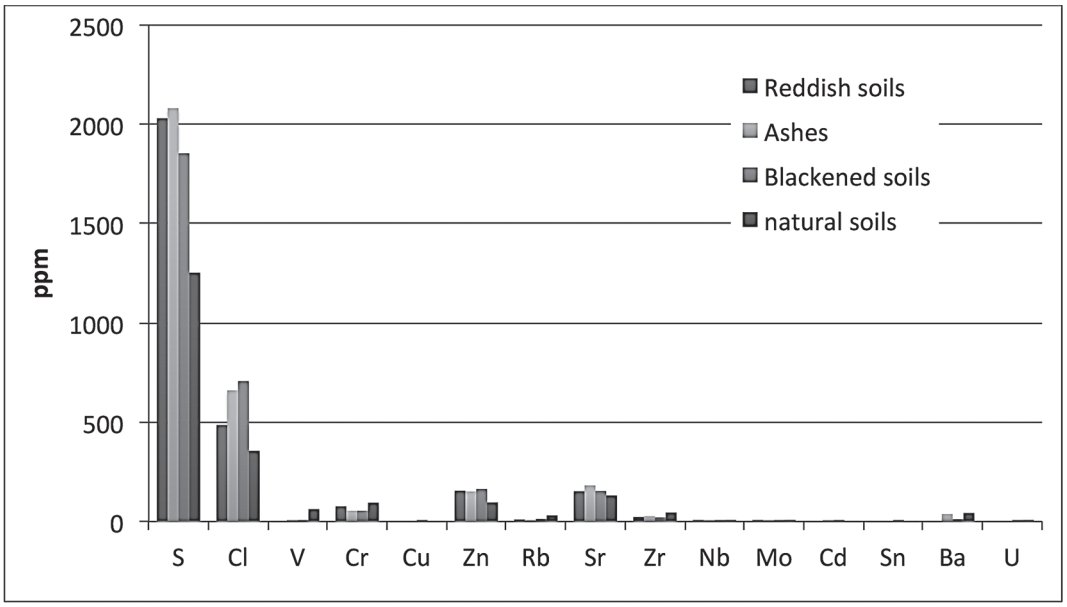

Fig. 18.40. Ppm distribution of minor elements by kind of layer at Crvena Stijena.

could be related to some clays as chlorite, but also with natural salts.

The distributions of these elements in each structure follow the general distribution presented by kind of layer and show clearly the differences between the natural soils from layer XIII and the rest of the samples. But ashes are not always the samples in each layer that present a high concentration of CaO. Sometimes the blackened layers show a larger concentration of CaO than the ash layers. These data are a little surprising given the color and texture differences between these layers. It may be that the black layers are composed of the same elements as the ashes but in a different state. The same may also be the said for the distribution of phosphorus that is quasi-systematically less in ash layers than in blackened ones. (Fig. 18.41).

These observations are complemented by a factorial correspondence – principal components analysis (FCA-PCA) of the distribution of the major elements present in the samples (Fig. 18.42), where we see on Component 2 an opposition between the proportions of phosphorus and calcium and a weaker opposition on Component 1 between these two elements together and silica, aluminum, potassium, iron, and titanium. This analysis also lets us generally distinguish two groups of samples, the blackened layers and the

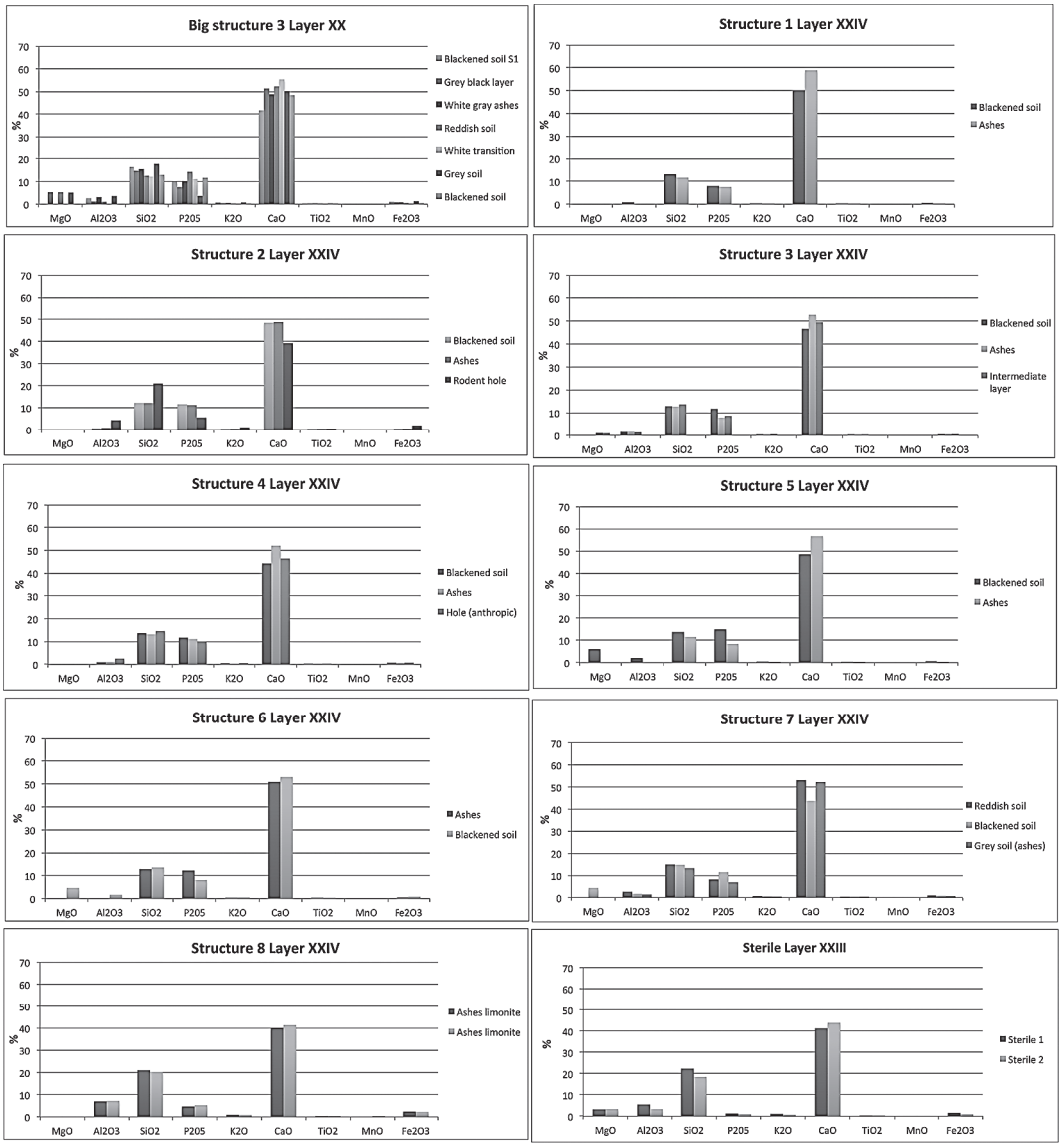

Fig. 18.41. Percentage distribution of major elements by kind of layer and structure at Crvena Stijena.

ash layers, against the natural soils. It is interesting to see that in this analysis the layer named ashes limonite is placed near the natural soils by its content of silica, aluminum, and potassium. This elemental composition could explain the different textures noted in the field between this particular ash layer and the other ash layers sampled. Another separation in the group of ash layers and black layers is established by following their content of phosphate and calcium. As we saw before, all the layers contain both elements, but some changes in their proportion can be observed.

As we see in Fig. 18.42 some layers contain more calcium and others more phosphorus. It is interesting to see that we found more ash layers associated with phosphorus than with calcium, while the blackened layers are equally distributed between these two elements. This could imply, if we relate the phosphorus to hydroxyl apatite ($Ca_5(PO_4)_3(OH)$), that in some cases a more important quantity of burned bones was in the ash layers than in black ones. This could have significance concerning the function of these structures or the utilization of bones as fuel for certain fire structures. Another explanation could be a concentration of phosphorus in burned black layers from the destruction of the organic matter present in them. In any case, the generally similar composition of ash layers and black layers reinforces our hypothesis that the ashes could be the result of the action of heat above the black layers and are not simply or always residues of combustibles. Another interesting result is the differentiation between the reddish soil of layer XX and the reddish soil of fire structure 7 in layer XXIV by the differences observed in their concentrations of phosphorus and calcium. This could imply different formation processes for these two layers before they were thermally altered, with structure 3 of layer XX showing in its reddish soil a more important concentration of bones.

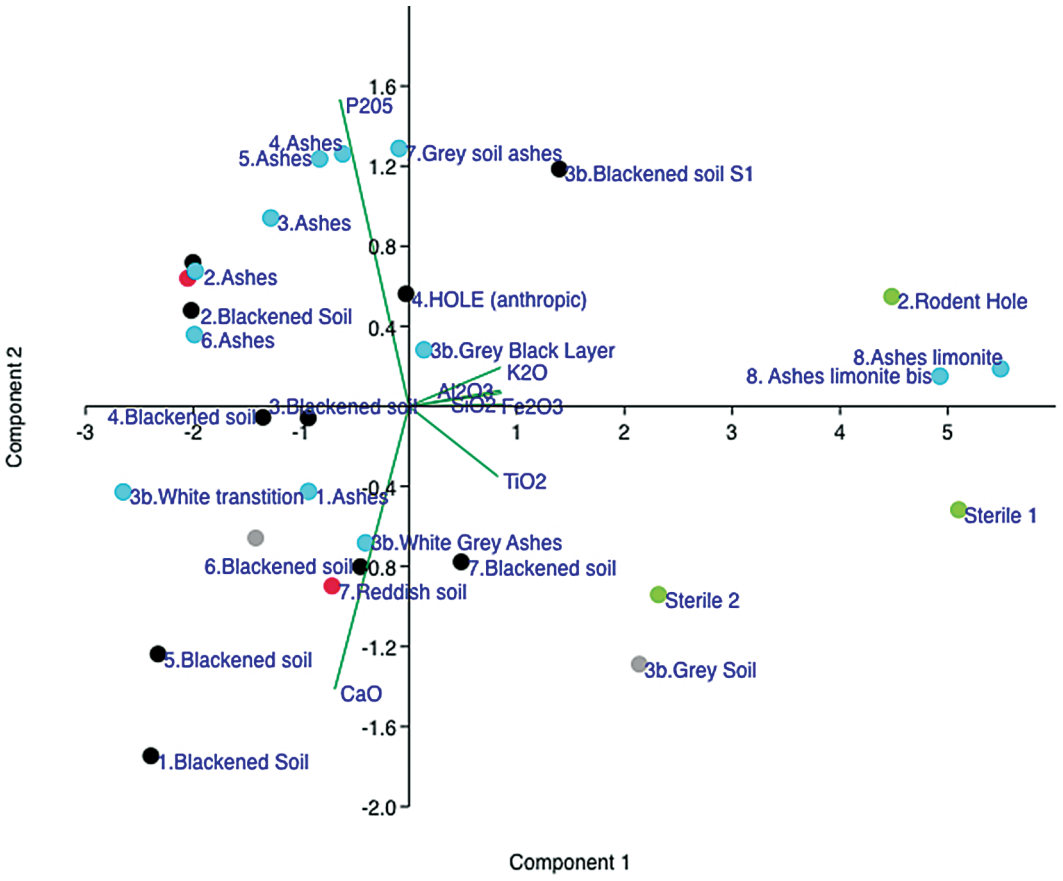

Fig. 18.42. FCA-PCA analysis of the percentage concentrations of major elements of Crvena Stijena samples (without MnO and MgO).

Mineralogical characterization by XRD

The mineralogical characterization by XRD of the different layers of Crvena Stijena shows similar trends. All the samples contain calcite ($CaCO_3$) as the principal component which is accompanied by hydroxyl apatite ($Ca_5(PO_4)_3(OH)$) and sometimes by quartz (SiO_2) and/or dolomite $CaMg(Co_3)_2$ (Fig. 18.43, Table 18.11). The peaks of hydroxyl apatite are very small and are masked by the characteristics of the sample and their high content of calcite but are well present. Dolomite is frequently associated with the natural soils and the rodent hole, being present in only one

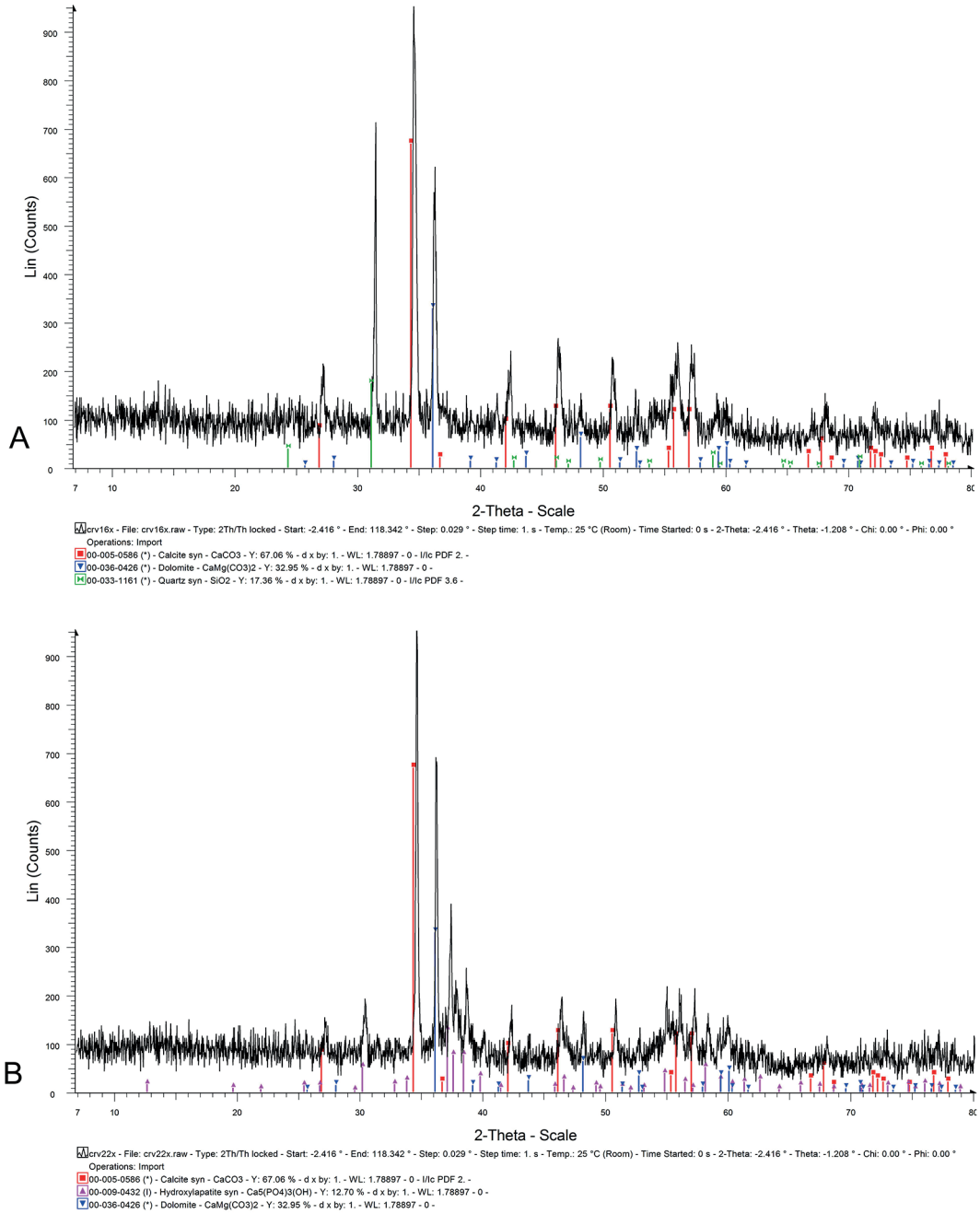

Fig. 18.43. Typical diffractograms obtained from Crvena Stijena samples: A - sterile layer containing calcite , dolomite and quartz, B - samples of the ashes of structure 2 in layer XXIV, showing calcite hydroxyl apatite and dolomite.

Table 18.11. Results of the DRX analysis of samples from Crvena Stijena.

	Sample	n°drx	Calcite CaCO3	Hydroxylapatite (Ca5(PO4)3(OH))	Dolomite $CaMg(CO_3)_2$	Quartz SiO2	Heigth of hydroxilapatite peaks
Big Structure 3 layer XX	Blackened soil S1	crv10	x	x		X	great
	Grey black layer	crv12	x	x		?	middle
	White gray ashes	crv11	x	x		?	little
	Reddish soil	crv13	x	x		?	great
	White transition	crv18	x	x		?	very little but well defined
	Grey soil	crv9	x	x		?	little
	Blackened soil	crv10	x	x		X	great
Structure 1 layer XXIV	Blackened soil	crv4	x	x		?	little
	Ashes	crv6	x	x		?	little
Structure 2 layer XXIV	Blackened soil	crv21	x	x		?	little
	Ashes	crv22	x	x	x	?	great and well defined
	Rodent hole	crv23	x	?	x	?	little
Structure 3 layer XXIV	Blackened soil	crv15	x	x		?	little
	Ashes	crv20	x	x			very little
	Intermediate layer	crv27	x	x		?	very little
Structure 4 layer XXIV	Blackened soil	crv24	x	x		?	little
	Ashes	crv25	x	x		?	very little but well defined
	Hole (anthropic)	crv26	x	x		?	little
Structure 5 layer XXIV	Blackened soil	crv7	x	x		?	great
	Ashes	crv8	x	x		?	little
Structure 6 layer XXIV	Blackened soil	crv3	x	x			little
	Ashes	crv5	x	x			little
Structure 7 layer XXIV	Blackened soil	crv17	x	x		?	little
	Grey soil (ashes)	crv1	x	x			little
	Reddish soil	crv2	x	x		?	little
Structure 8 layer XXIV	Ashes limonite	crv28	x	x		?	little
	Ashes limonite	crv28	x	x		?	little
Sterile layer XXIII	Sterile 1	crv14	x		x	x	absent
	Sterile 2	crv16	x		x	x	absent

ash sample situated near the rodent hole in layer XXIV, fire structure 2. As we said before, the presence of dolomite could explain the presence of magnesium in our analysis which could have been deposited by dissolution of its carbonates. Some differences could be observed in the width of the peaks of calcite that are larger in some samples of grey soils and natural soils, but the regular presence of thin spectra in the ashes and black layers do not let us conclude that there is a relation between these differences and the thermal alteration of the samples. Separating the hydroxyl apatite to analyze its state, which also changes with temperature, is left for a future work due to recurring difficulties with our equipment. No clay fraction was clearly identified in this first series of analyses. These results thus confirm the homogeneous composition of our samples of black layers and ash layers, along with the variations observed by the X-ray fluorescence analysis of the distribution of major elements.

The Organic Matter Approach

Concentrations of Organic Matter: Saturated Fatty Acids (FAMEs - SFA), Unsaturated Fatty Acids (UnSFA), Branched Fatty Acids (Branched FA), Alkanes, and Sterols

The total concentration of organic matter, taking into account the saturated fatty acids (FAMEs - SFA), unsaturated fatty acids (UnSFA),

branched fatty acids (Branched FA), alkanes, and sterols, showed that the highest concentration of organic matter was found in fire structures 2 and 3 from layer XXIV, followed by fire structure 7 of layer XXIV and fire structure 3 of layer XX. The lowest concentrations were found in fire structures 1 and 8 from layer XXIV. The natural soils contain low amounts of organic matter that are similar to the minor contents observed in the fire structures. Finally, we see only one structure with small dimensions, the structure 5 of layer XXIV, that has greater amounts of organic matter than larger structures from the same layer, like structures 1, 4, and 6 (Fig. 18.44).

The black layers contribute largely to this distribution in all the structures sampled. Two cases, structure 2 and structure 3 of layer XXIV, are significantly different. In the first case, it is the rodent hole that shows the largest concentration of organic matter, while for structure 3 it is the intermediate grey layer underlying the ashes and covering the black layer that shows the greatest concentration (Fig. 18.45). Thus, the large concentration of organic matter observed for structure 2 is related to the rodent hole and not to the fire structure itself and its underlying soil.

As we could expect, black layers have greater concentrations of organic matter, followed by the ash layers, and finally by the red soil layers. The natural soil layers and the rodent holes have more organic matter than ashes and red soil layers, but less quantities compared to black layers, which have an anthropic origin (Fig. 18.46). These results are consistent with the thermal alteration hypothesis, where natural soils lost their natural content by heat action, and where ashes that also were affected by heat could conserve certain quantities of organic matter related to the use of fire for cooking. These results could be also consistent with the hypothesis that ashes are the result of heat action on black layers; here the ash layers would be considered to be black layers more or less altered and having more or less concentrations of organic matter as a function of temperatures reached and their time of exposure. Moreover, in this case ashes would also be the layer where the mixture of organic matter coming from fire related activities would be deposited. We must take into account that ashes have a greater porosity than natural soils, which could favor the penetration of organic matter and its encapsulation in carbonates.

If we analyze the distribution of organic matter in the ash layers (Fig. 18.47), we can observe that the greatest concentrations come from structures 5 and 2 in layer XXIV, and the least ones come from structures 3 and 1 in layer XXIV, while the big structure 3 from layer XX and structures 4, 7, and 8 in layer XXIV have intermediate concentrations of organic matter. These different concentrations show that small structures can have higher concentrations of fat residues than

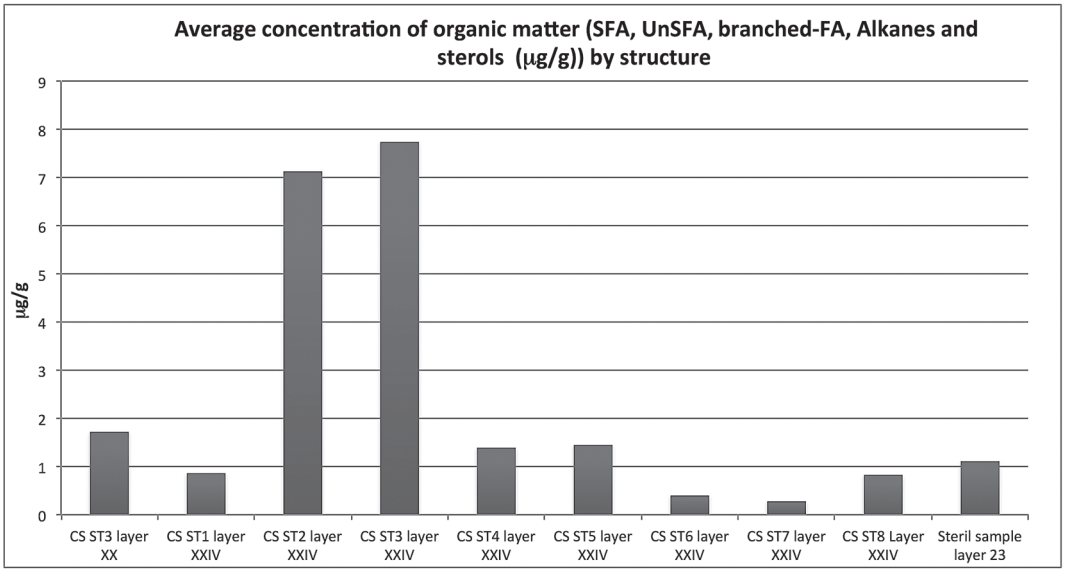

Fig. 18.44. Average concentrations of organic matter - concentrations (mg/g) of SFA, unSFA, branched FA alkanes. and sterols by structure at Crvena Stijena.

larger ones and pose some questions about the different processes that could create this situation. In fact, nothing indicates that cooking cannot be done over small structures, where the zone of fire action is reduced and could thus concentrate organic matter in comparison to larger structures that could have had a different function and, in any case, have a larger surface for cooking which could make for a greater dispersion of organic matter.

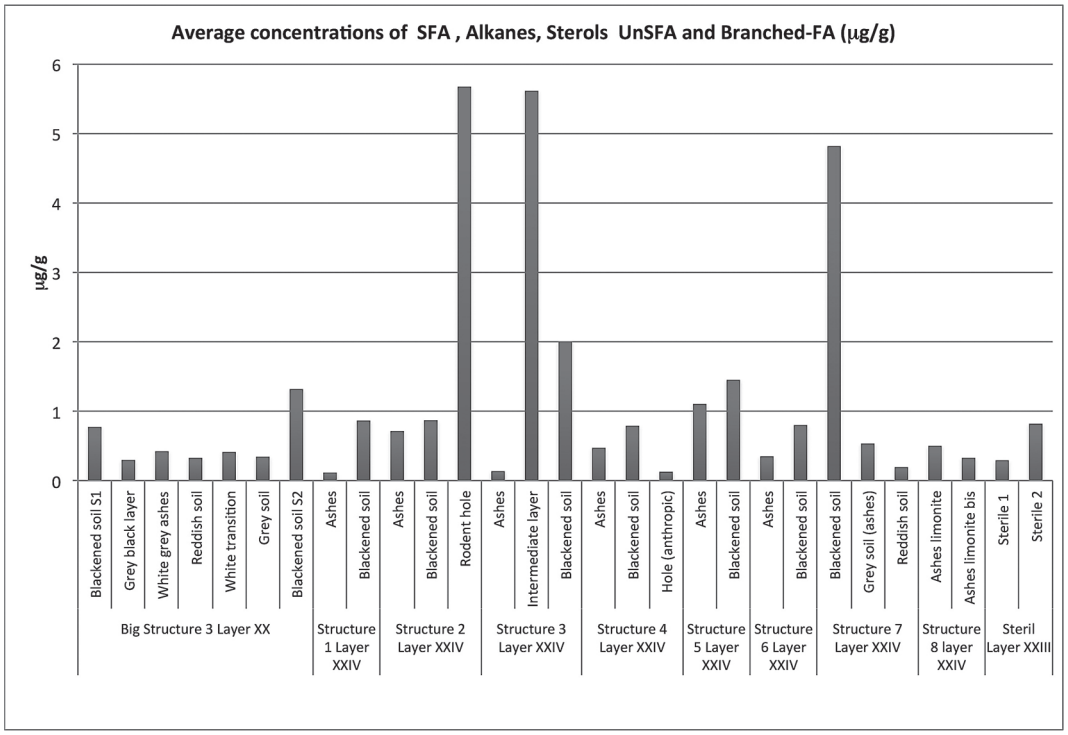

Fig. 18.45. Average concentrations of organic matter - concentrations (mg/g) of SFA, unSFA, branched FA alkanes, and sterols by kind of layer and structure at Crvena Stijena.

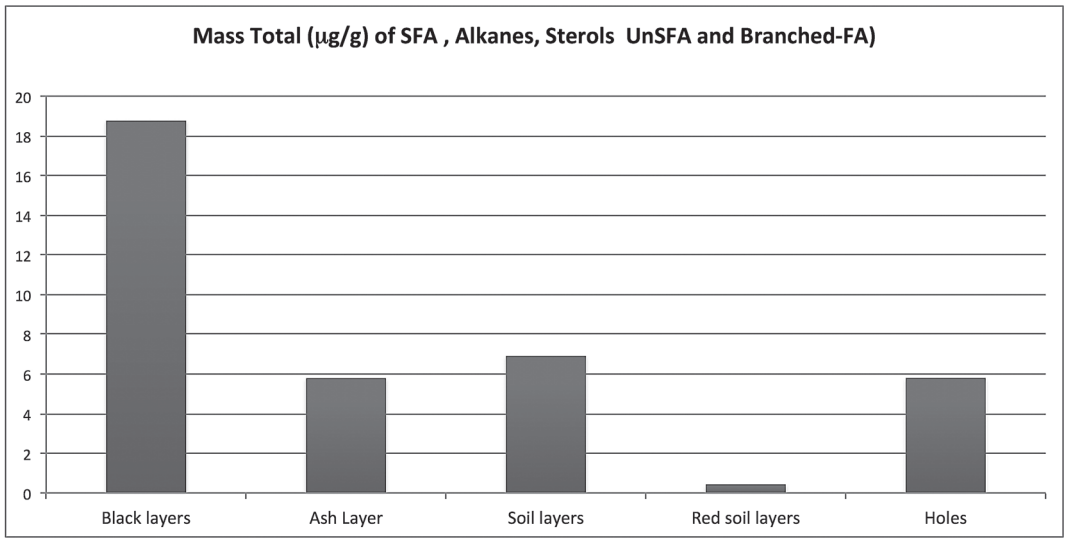

Fig. 18.46. Average concentrations of organic matter - concentrations (mg/g) of SFA, unSFA, branched FA alkanes, and sterols by kind of layer and structure at Crvena Stijena.

If we analyze the contribution of each family of molecules studied in these concentrations, we observe that the saturated fatty acids (SFA) constitute the most important contribution of organic matter (Fig. 18.48). The SFA are followed by sterols and, in lower proportions, by the alkanes, the branched fatty acids, and finally by unsaturated fatty acids. The greater part of the sterols (96%) came from the sample taken at the rodent hole and from the samples of the sterile soil. Only structure 5 and structure 8 have sterols preserved among the fire structures. From a quantitative point of view, the SFA and alkanes are present in larger amounts in the black layers, while they are present in minor quantities in the ashes, the reddish layers, and the grey layers. At the same time the branched and unsaturated fatty acids are higher also in the black layers. But it is interesting to note that in the black layers there is a group that contains more fatty acids, branched and unsaturated, than the others. These results could be related to differences in heat action among the samples. If our hypothesis is correct, some samples of black layers could indicate that the disappearance or the diminution of unsaturated fatty acid methyl esters (UnSFAMEs) and branched fatty acid methyl esters (BFAMEs) could be related also to thermal processes. These inferences seem to be confirmed by the FCA-PCA analysis (Fig. 18.49) where the thermally altered samples are located along the negative values of Component 1 with most of the black layers opposed to them along positive

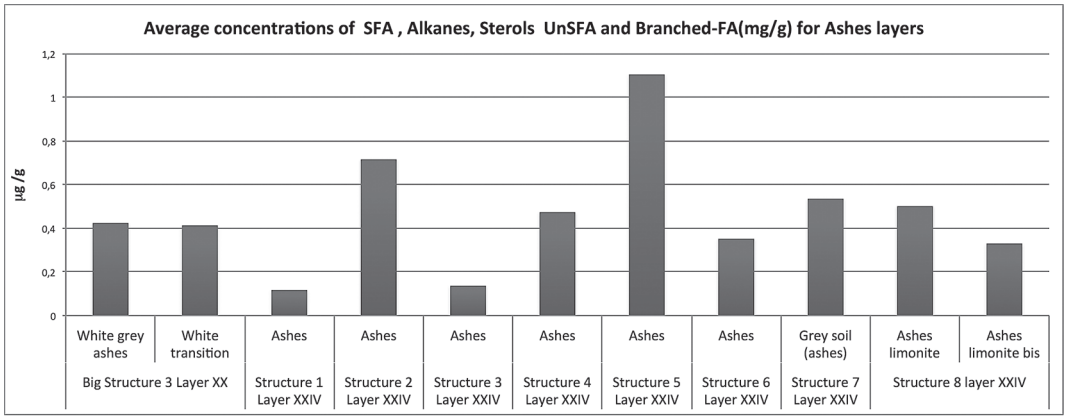

Fig. 18.47. Average concentrations of organic matter - concentrations (mg/g) of SFA, unSFA, branched FA alkanes, and sterols for ash layers at Crvena Stijena.

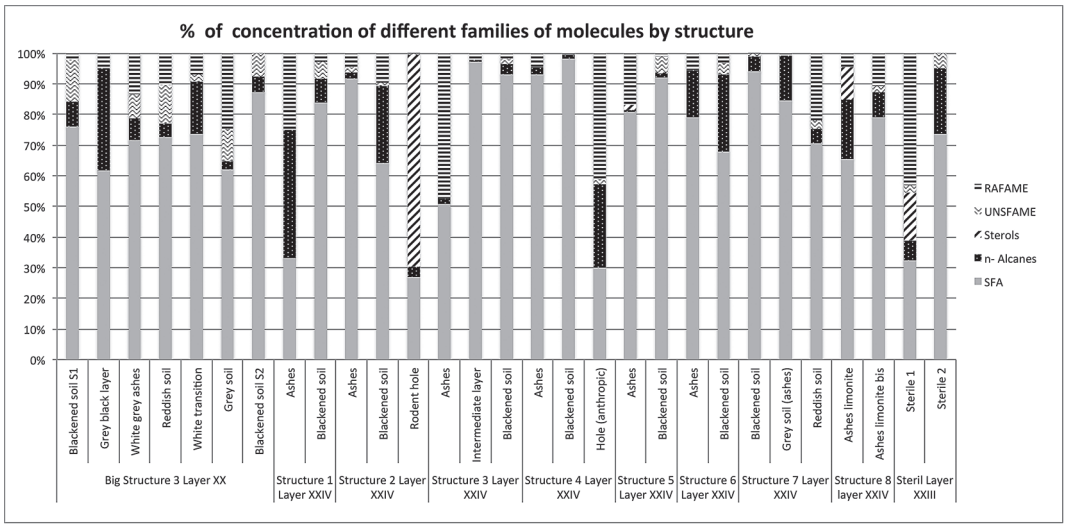

Fig. 18.48. Proportions of concentrations (mg/g) of SFA, unSFA, branched FA alkanes, and sterols of Crvena Stijena samples.

values. These last samples are differentiated on Component 2, reflecting the concentrations of SFA and n-alkanes as a function of the unsaturated and branched content of the samples. A positive correlation between the concentration of n-alkanes and the branched fatty acids was also observed, which could relate these two families of molecules to the process of maturation of the organic matter in the site.

When we analyze the proportional distribution of these different families of molecules in each sample by FCA-PCA, we see also that they are separated by their saturated fatty acids and the n-alkanes in terms of their internal proportions (Fig. 18.50). This analysis groups the samples that contain more n-alkanes, more fatty acids, more unsaturated fatty acids, and branched fatty acids. This groups together different kinds of samples, for example, we see the ashes of structure 1, the anthropic hole of structure 4, and the grey black layer of layer XX structure 3 near the blackened soils of structures 6 and 2. This ensemble of samples is characterized by an important presence of n-alkanes. Opposite these, characterized by important amounts of SFA, we find the intermediate layer and the ashes of structure 3, structure 5, the black layers of structures 3, 4, and 7, and the reddish layer of structure 7. Finally, some samples contain high concentrations of unsaturated fatty acids and branched fatty acids, such as the samples of the white transition, the grey soil, the black layers, and reddish soils of structure 3 in layer XX, the blackened soil of structure 5, the sterile soils of layer XXIII, and the ashes of structure 8 (Figs. 18.49-18.50). These groups could be related to differences in the maturation process of organic matter in the different samples and not related to the action of heat.

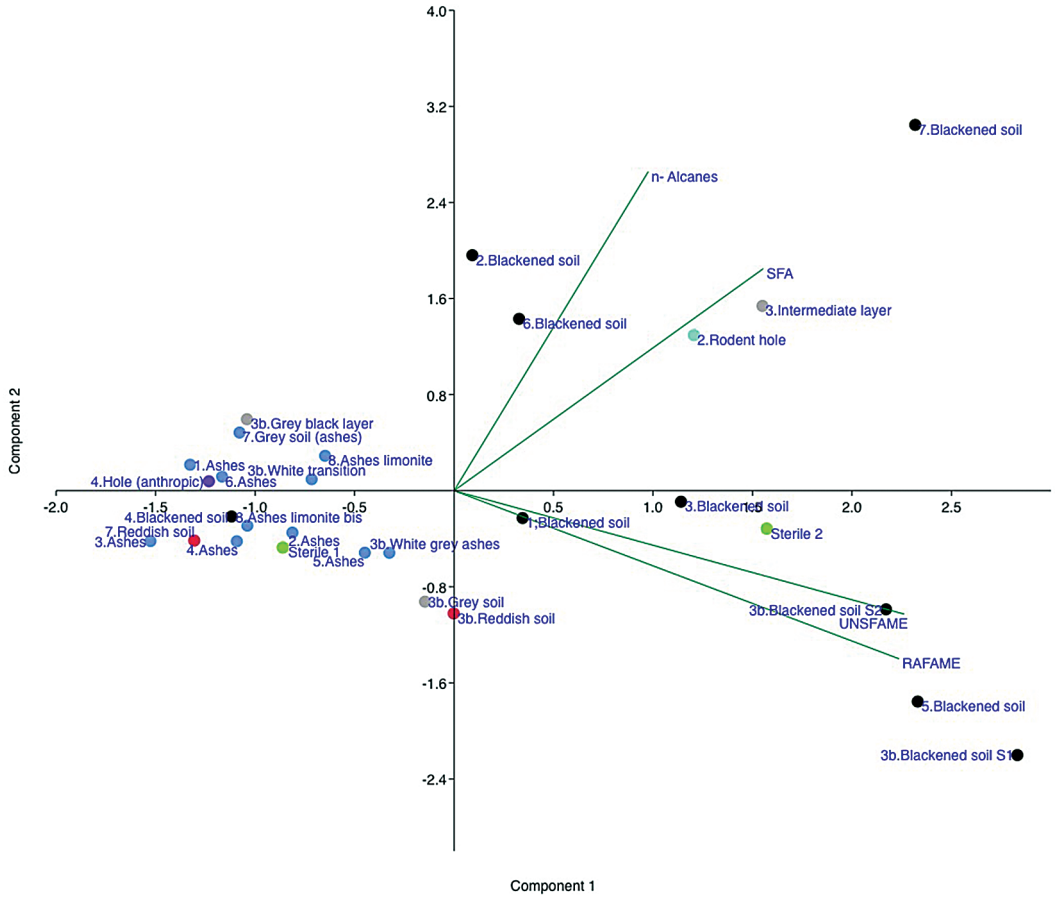

Fig. 18.49. FCA-PCA analysis of the concentrations (mg/g) of SFA, unSFA, branched FA alkanes, and sterols of Crvena Stijena samples.

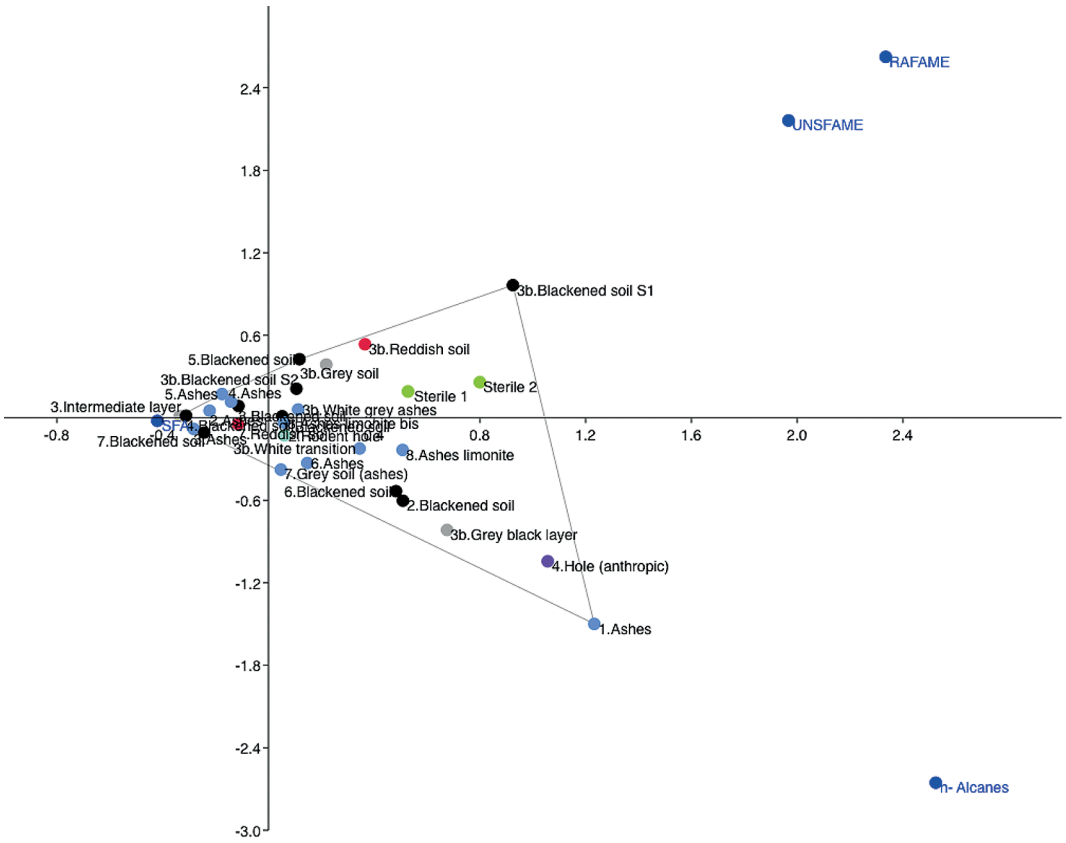

Fig. 18.50. FCA analysis of the concentrations (mg/g) of SFA, unSFA, branched FA alkanes, and sterols of Crvena Stijena samples.

Organic Matter Degradation

The CPI (Carbon Preference Index, from Cooper and Bray 1963) is a better way to establish the degradation of organic matter (SFA and n-alkanes) in samples (Pepe and Dizabo 1990; March 1999; March and Soler Mayor 1999; March et al. 2003; March 2014). The CPI is calculated according to a formula that takes into account the different proportions between odd and even molecules (Fig. 18.51). The closer the value of CPI is to 1, the more the sample is degraded. First at all, we can note that at Crvena Stijena the samples have relative good preservation but also great variation in the CPI values. The mean value for CPI SFA is 4.94, the median is 3.91, and the variance is 18. For the CPI alkanes the mean value is 3.26, the median 1.73, and the variance 10. The highest value for CPI SFA is 22.94 and the lowest 0.94, while the maximum value for alkanes is 11.45 and the minimum 0.19 (Fig. 18.52). Thus, the Crvena Stijena samples show important variations among the different kinds of samples and structures analyzed. As in all other sites, values

$$\mathrm{CPI\ (alkanes)} = \frac{1}{2}\left[\frac{\sum_{21}^{n}\mathrm{odd}}{\sum_{20}^{n-1}\mathrm{even}} + \frac{\sum_{21}^{n}\mathrm{odd}}{\sum_{22}^{n+1}\mathrm{even}}\right]$$

$$\mathrm{CPI\ (acids)} = \frac{1}{2}\left[\frac{\sum_{22}^{n}\mathrm{even}}{\sum_{21}^{n-1}\mathrm{odd}} + \frac{\sum_{22}^{n}\mathrm{even}}{\sum_{23}^{n+1}\mathrm{odd}}\right]$$

Fig. 18.51. CPI formulas for saturated fatty acids and alkanes fraction (n+1=maximum number of carbons found).

of CPI SFA are larger than the CPI alkanes. The CPI alkanes have 20 samples with values under 2 and four samples with values above 9, showing extraordinary preservation. For the CPI SFA, 22 samples have values under 5 and two samples above 14.

The analysis of CPI values for each sample within individual structures lets us observe these variations better (Fig. 18.53). Within the big

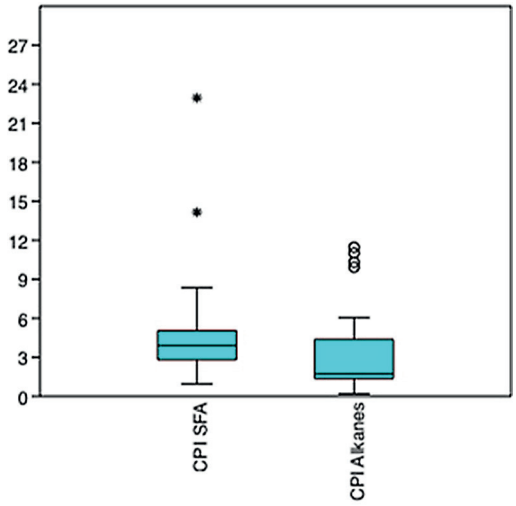

Fig. 18.52. Box plot graphic for CPI –SFA and CPI alkanes values at Crvena Stijena.

structure 3 in layer XX the two samples from the black layers that cover and underlie the structure have the highest values of CPI alkanes. We should note here that the grey black layer in the upper part of the stratigraphic sequence of ashes within this structure presents the most degraded alkanes sample, followed by the white grey ashes and the reddish soil. Under the reddish soil the white transition layer and the lower grey soil also show degraded and low values, but the CPI alkanes of these two layers are a little larger than the values observed in the upper part of the sequence below the top black layer. This could indicate that the white transition observed here is the remains of an ancient ash layer underlying a grey soil over the bottom black layer of the sequence. Any sample of the ashes sequence, including the reddish soil, shows traces of contamination from the upper or the bottom black layer. The CPI SFA of this structure shows much better values of preservation underneath the reddish soil, confirming the existence of two different moments of formation of this structure. The mean values of this bottom part of the big structure 3, including the white transition, the grey soil, and the blackened soil 2 are the highest values registered in the whole site and show that the fatty acids contained in the bottom part of the structure have a different origin from those of the upper part. The CPI SFA values in the bottom part, under the reddish soil, show a pattern similar to the CPI alkanes, decreasing from the white transition to the grey soil, and becoming more important in the blackened soil 2.

The black layer of structure 1 of layer XXIV presents a higher value of CPA SFA than the ash layer. Here, contrary to the general trend observed, the ash layer shows larger values for the CPI alkanes than the black layer, indicating better conservation of this family in the ash sample. For structure 2 the blackened soil shows the most preserved sample for the alkanes, but the ash layer shows the most preserved saturated fatty acids. In this structure, the ashes show the lowest values of the three samples. It is interesting to note the similar values observed between the black layer and the rodent hole that could indicate possible contamination. In structure 3 the intermediate layer and the black layer show better conservation of the fatty acids than the ashes. For the alkanes the black layer shows the best values and the intermediate layer and the ash layer show degraded ones. In structure 4 the better values were found in the anthropic hole, while the ashes and the blackened soil show similar values for the fatty acids, with the ashes being very slightly better for the alkanes than the black layer, and the inverse for the saturated fatty acids. In structure 5 the black layer shows a slightly better value for the CPI SFA and a clearly better one for the CPI alkanes. Structure 6 shows better preservation of the saturated fatty acids in the ash layer and a very slightly better preservation of alkanes in the blackened one. Structure 7 follows the same trend for SFA as in structure 6, but here the preservation of the alkanes in the ashes is better than in all the other ash layers of layer XXIV. The alkanes of the black layer have also excellent preservation, only overshadowed by the values for the black layer of structure 2. The reddish layer shows only low preservation of the alkanes but still better preservation than the fatty acids show in the black layer. Finally, structure 8 shows similar values for the two samples, more degraded for the alkanes than for the saturated fatty acids, and both values are similar to other ash layers present in layer XXIV.

If we consider the mean values of CPI acids and alkanes by kind of layer, we observe that the value of CPI alkanes decreases from the black layers to the ash layers to the reddish layers, while the CPI SFA does not follow the same trend (Fig. 18.54). This is very interesting because as we have previously published (March 2014; March et al. 2014), the value of the CPI decreases under heat action, and these results are consistent with

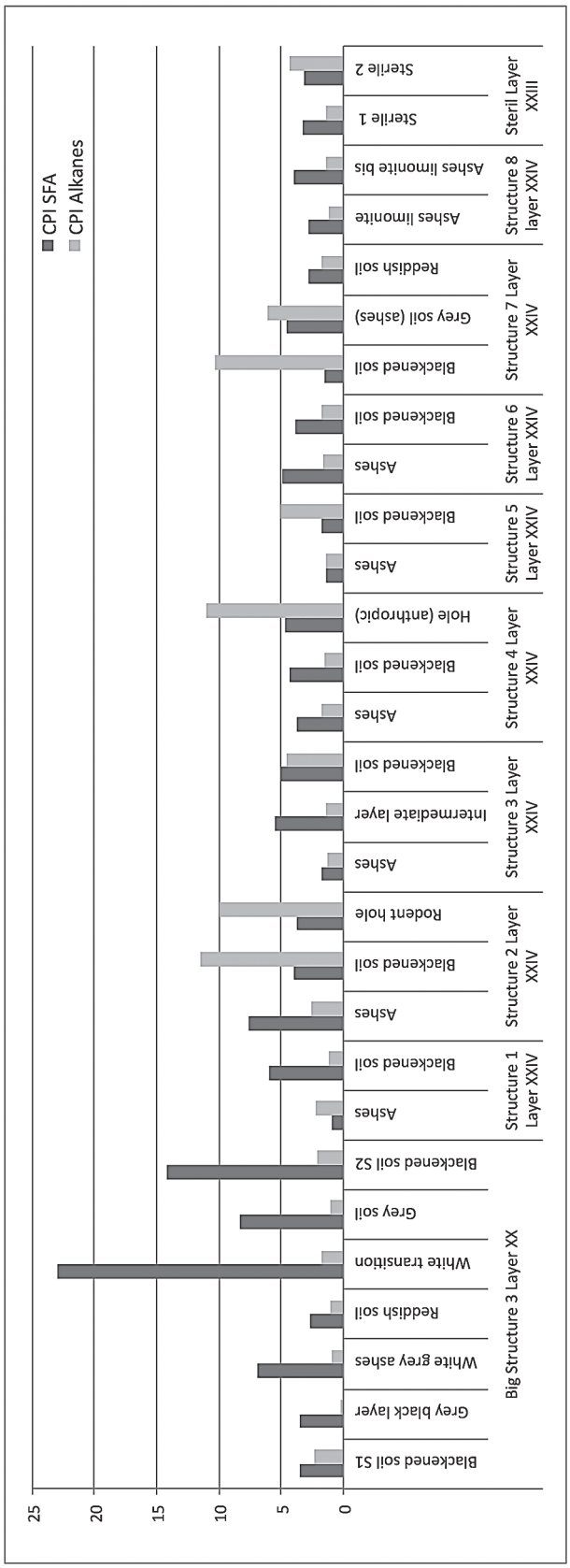

Fig. 18.53. CPI values for alkanes and saturated fatty acids fractions from Crvena Stijena samples.

the thermal hypothesis put forward to explain the differences observed between these layers. The holes sampled present the highest mean values for the CPI alkanes, and the natural soils for the CPI acids. These results show that the saturated fatty acids and the alkanes could have different origins or be affected by different formation processes. As we have suggested before (March 2014), a different degree of preservation for alkanes and SFA in the same sample could indicate a different origin for each fraction.

These results complete the data that indicate the possibilities of thermal alteration of the alkanes and their CPI values by kind of layer. A mass concentration (weight) hypothesis may explain these data, considering the possibility of different origins for alkanes and SFA. The concentrations of SFA are most important in animal cooking residues, while the alkanes are minor and degraded in animal fat, but large concentrations of well preserved alkanes have been observed in degraded vegetal cuticles. Thinking of this, some fluctuation in the lower values of the CPI fatty acids could be related to the preservation of long chain fatty acids of vegetal origin even in low quantities. In the same way, we note here a relation between the concentration of alkanes and the values of CPI that it is indicated by a positive correlation of $r = 0.642$ while the fatty acids are completely independent $r = -0.005$. This could indicate that at Crvena Stijena when alkanes are present in larger amounts we could have in some cases better preservation. Thus, it may be possible that some samples have a complex and historically different origin which we must try to explain. The low values of CPI acids are principally due to the presence of odd longer SFA but also due to a low amount of even longer SFA mostly of vegetal origin. This last point can allow us to infer a mostly animal origin for short SFA in our samples, while the alkanes better reflect the vegetal component of each sample.

n-alkanes

The distribution of alkanes in Crvena Stijena could help us to understand the differences seen in CPI values and to analyze the formation processes of these different structures. As mentioned, values of CPI reflect different preservation states of the studied samples. Looking at the mean values for each kind of layer, it seems that some differences observed in these values could be explained by heat action.

If we analyze the distribution of alkanes we can see that 28 of the 29 (96.55%) samples coming from this site exhibit more than 80% of $>C_{20}$

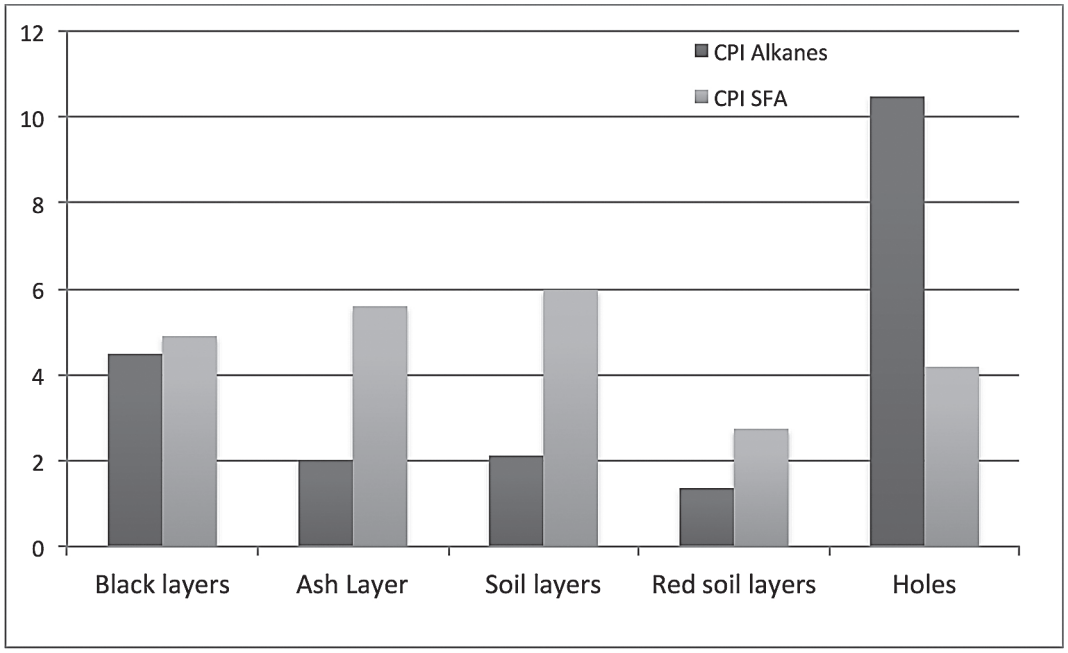

Fig. 18.54. CPI mean values by kind of layer for alkanes and saturated fatty acids fractions from Crvena Stijena samples.

n-alkanes. The mean value for the $>C_{20}$ n-alkanes is 94.55 %. Only one sample, coming from the blackened layer of structure 4, has a lower value of 73.84% (Fig. 18.55). These long chain n-alkanes are biomarkers of higher plants, come from leaf cuticle waxes, and are often considered as having a continental origin (Eglilnn and Hamilton 1963; Eglinn and Pancost 2004; Eglinn and Eglinn 2008).

As biomarkers, the presence of short chain alkanes $\leq C_{20}$ could be related to different processes such as thermal alteration (wood ash or charcoal) or bacterial action (March 1995, 1996, 1999, 2014; March and Soler 1999). Here the short alkanes are present in very low quantities, between 0% and 26.15%. The mean percentage value for $\leq C_{20}$ n-alkanes is 4.15%. They are present in such low quantities in nearly in all samples, but they are absent only in the white grey ashes and the reddish soil layer of structure 3 of layer XX (Fig. 18.56).

If we analyze the mean concentration by kind of layer we observe that the concentration of $>C_{20}$ n-alkanes is highest in the hole samples, next highest in the blackened layers, and then decreases through the soil layers, the ash layers and the reddish soils (Fig. 18.56). But the quantities of $>C_{20}$ and $\leq C_{20}$ n-alkanes have a positive correlation of $r = 0.83$, so an increase of $\leq C_{20}$ n-alkanes is not related to a decrease of $>C_{20}$ n-alkanes.

If we analyze the histograms of distribution of the n-alkanes we can observe that their distribution varies for each layer and in each fire structure. Some samples present a bimodal distribution characterized by the presence two groups, one of short chain alkanes and the other of long chain alkanes.

The distribution of short alkanes changes frequently, being centered variously on C_{18}, C_{19}, C_{20}, or C_{21}, while the distribution of long chain alkanes is mostly centered on C_{31} or C_{29} for layer XXIV, but this is not the case for samples from layer XX, where the distribution of long alkanes is variously centered on C_{27}, C_{29}, C_{31}, or even on C_{28}. The changes in n-alkane distribution show that, in general, there is no contamination between samples. These changes could be related to the degradation process, but also to changes in the vegetal origin of the samples.

For example, in the big structure 3 of layer XX, the distribution of n-alkanes begins in the upper black layer with a bimodal distribution, with a dominance of C_{31} for long chain alkanes, a dominance of C_{21} for the short ones (Fig. 18.57), and a value for the CPI alkanes of 2.37. This layer is followed by very degraded CPI alkanes of 0.19 and a unimodal distribution centered on C_{29} for the grey black layer. The underlying white grey ashes also show a unimodal distribution centered on C_{29} with a degraded CPI alkanes of 0.92 and very low quantities of short alkanes whose distribution begins at C_{22}. The underlying reddish soil has a unimodal distribution centered on C_{28} followed by C_{27} and C_{29} for the long alkanes and a degraded CPI of 0.99. The white transition underlying the reddish soil shows better preservation with a CPI alkanes of 1.72 and a bimodal distribution with low quantities of short alkanes and a distribution centered at C_{21}, while the distribution of long chain alkanes is centered on C_{27}. The grey soil covered by this last ash layer again shows degradation, with a CPI alkanes of 1.09 and a bimodal distribution centered also on C_{21} for the short chain alkanes but displaced to C_{29} for the long chain alkanes. Finally, the lower black layer shows the same bimodal distribution as the upper black layer and a similar CPI alkanes of 2.19 indicating that the same organic matter composes both black layers. These layers also have more short chain alkanes than all the other layers that constitute this structure. Thus we can observe here many changes in this sequence that differentiate each layer from the others and show a coherent degradation of the CPI with thermal alteration but no important concentrations of short alkanes in the thermally degraded samples, while these alkanes are present in the black layers.

In structure 1 of layer, XXIV the ash layer presents a nearly unimodal distribution centered on C_{29} with low quantities of short alkanes that show a distribution centered on C_{18} with a CPI alkanes of 2.19. The underlying black layer shows a unimodal distribution centered on C_{31} but more degraded, with CPI alkanes of 1.20. Thus, the vegetal part of these samples is better preserved here in the ashes, and it is different than the vegetal lipids present in the underlying black layer.

Structure 2 of layer XXIV has a similar unimodal distribution centered primarily on C_{31} for the ash layer and the blackened soil, with a low concentration of short chain alkanes centered on C_{20} in both the ashes and the blackened soil. The difference lies here in the values of the CPI alkanes for the two samples. The ash layer has a very much degraded index in comparison to

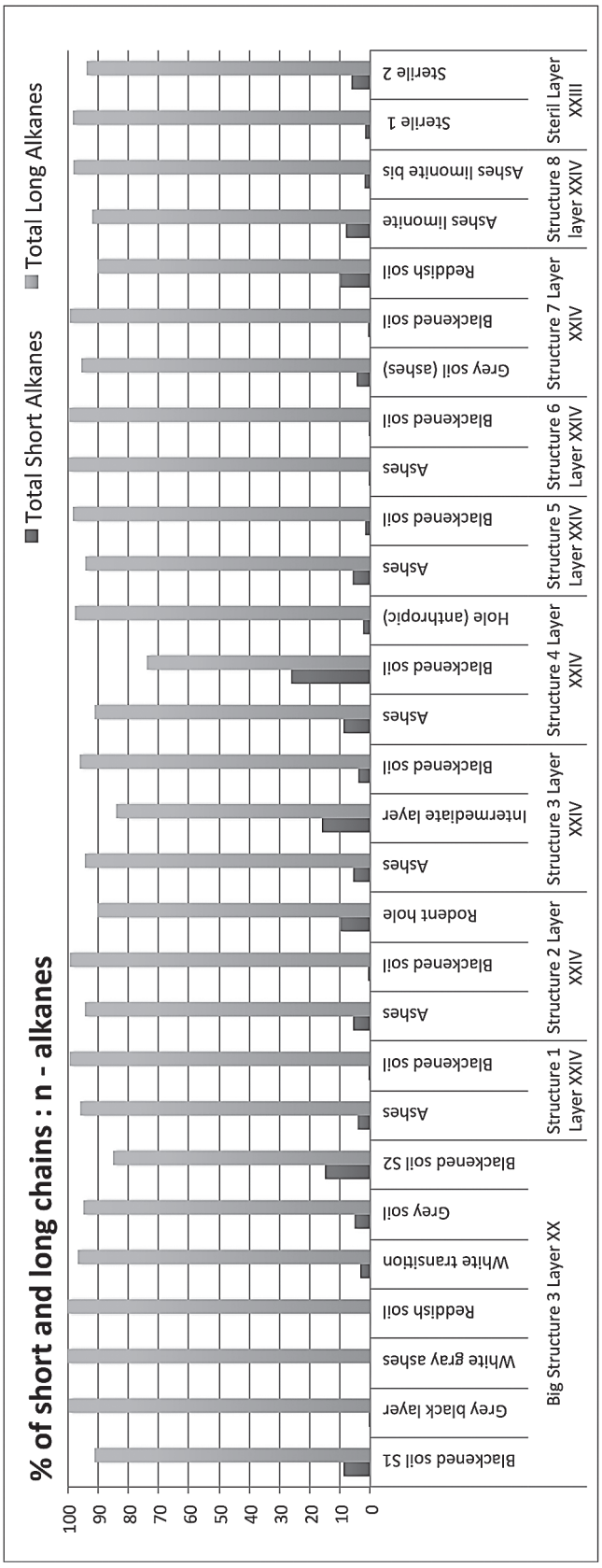

Fig. 18.55. Percentage distributions of short and long chain n-alkanes of the 21 samples (long chain: $>C_{20}$ and short chain: $\leq C_{20}$).

the blackened layer, 2.58 vs. 11.54 respectively. Thus, the ash layer here seems to have the same composition as the black layer, but more degraded, while in structure 1 the ashes seem to show a different composition from the black layer and thus a possibly different origin. The rodent hole, which has a bimodal distribution, shows nearly the same distribution as the two anthropic layers for the long chain alkanes, but it has an increment in the presence of short alkanes that are centered on C_{18}, which shows that taphonomical processes perhaps did not change the signature of alkanes for this sample very much. As the hole was excavated in the black layer, the walls of the hole could represent also the black layer. Thus, the short alkanes may be present at this position and absent where we took the sample under the ashes.

In structure 3 of layer XXIV the ashes and the intermediate grey layer show a very similar composition, with a bimodal distribution having relatively small amounts of short alkanes centered on C_{19} and C_{20}, and long chain alkanes centered on C_{31} but in nearly equal proportions with C_{29}, and weak values for the CPI alkanes of 1.26 for the ashes and 1.40 for the intermediate grey layer. The blackened soil has a unimodal distribution clearly centered on C_{31} and is better preserved (CPI alkanes = 4.56). Here again, the ashes and their underlying soil layer show the same composition and could even be thermally degraded samples of the underlying black layer which is better preserved.

Structure 4 shows a long chain alkanes distribution centered on C_{31} for the three samples: the ashes, the blackened layer, and the anthropic hole, but exhibiting different degrees of maturation, the black layer being the more degraded (CPI alkanes = 1.49), followed by the ashes with 1.76, and finally by the anthropic hole that shows much better preservation with a CPI alkanes of 11.01. The blackened layer shows a difference in the short chain part of the samples, where it is largely dominated by C_{19}. If we ignore the high amounts of C_{19}, which may be a randomly deviate observation for this sample considering that the three layers would otherwise all show a mode at C_{22}, then here again the ashes and the underlying blackened soil would have a similar chemical composition and with small differences in their degradation, but here the ashes contain alkanes that are well preserved. As in the case of the rodent hole of structure 2, here the walls of the anthropic hole have a similar composition in alkanes to the ashes in which it was dug (Fig. 18.48).

Structure 5 shows a unimodal distribution of n-alkanes that are centered on C_{31} for the ashes and the blackened underlying layer, and present a distribution of C_{31} that is equilibrated with C_{29} as we saw before for the ashes and the intermediate layer of structure 3. This phenomenon could be explained by the degradation of the ashes, which show a CPI alkanes of 1.37, compared to the CPI alkanes of the blackened layer that reaches 5.07. The short alkanes component is here very low for

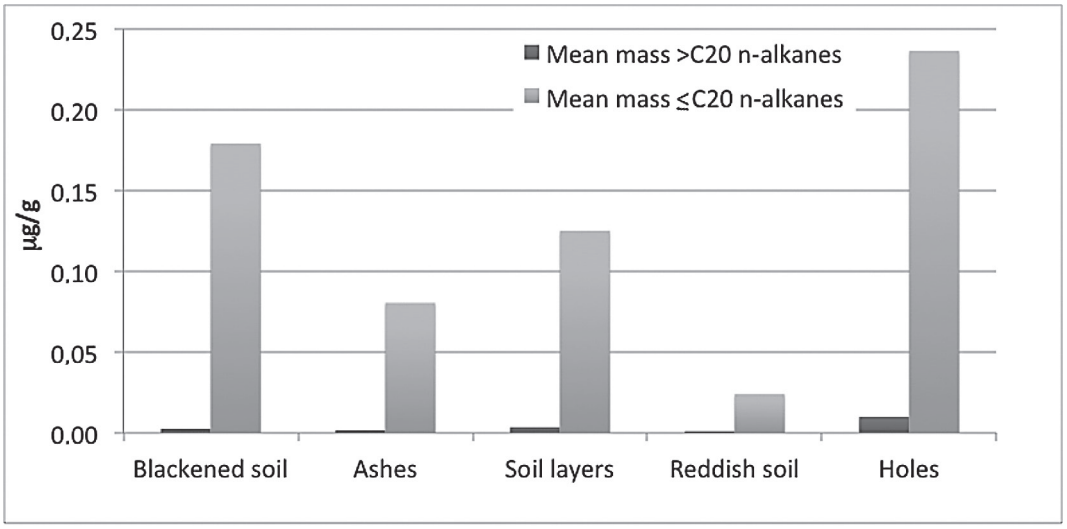

Fig. 18.56. Concentration of short and long chain n-alkanes of the 29 samples (long chain: $>C_{20}$ and short chain: $\leq C_{20}$) in mg/m by kind of layer.

both samples in comparison with the samples of structure 3 (Fig. 18.57).

Structure 6 shows a similar unimodal degraded distribution for both samples, which are centered on C_{29}. The ashes (CPI alkanes = 1.67) are only a little more degraded than the black layer (1.78). The vegetal composition of this sample could differ from the other structures studied from layer XXIV, but at the same time it also could have been transformed by a process of degradation (Fig. 18.57).

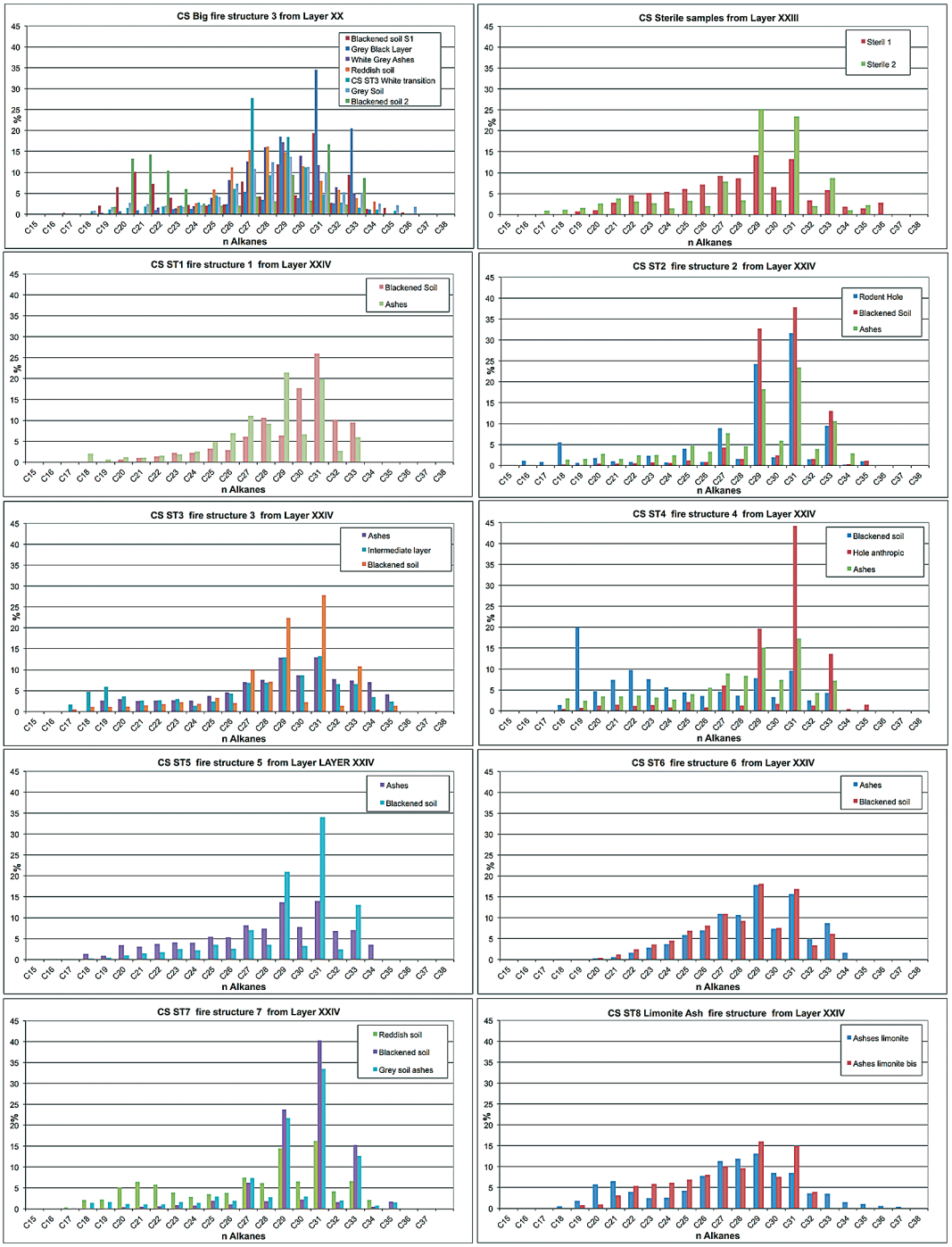

Fig. 18.57. N-alkanes distribution (mass concentration mg/g) for different structures and site unit samples studied at Crvena Stijena.

Structure 7 again shows a unimodal composition centered on C_{31} for the ashes and the blackened layer that in this case covers the structure, but here the reddish soil underlying the ashes shows a bimodal distribution that is centered on C_{21} and C_{31} and where the values of the short n-alkanes are less at C_{21}. Again, the lipids of the ashes (CPI alkanes = 6.02) are more degraded than lipids of the black layer (CPI alkanes = 10.30), but these lipids are well preserved in comparison to other ash layers described above. The reddish soil is the most degraded of the three samples, having a CPI alkanes of 1.73. Its profile is dominated by C_{31}, but C_{29} is close to the value of C_{31} here. Considering these results, it is possible that the ash layers of this structure have been contaminated by lipids coming from the superior black layer (Fig. 18.57).

Finally, both samples of the ashes limonite from structure 8 have the same composition centered again on C_{29} as we saw for structure 6. These two samples, taken from the same layer, have some difference in their CPI values (1.18 and 1.37) and there are more alkanes between C_{18} and C_{22} for the first sample. These results demonstrate that we can find small fluctuations in composition and degradation in the same layer (Fig. 18.57).

The natural soils of Crvena Stijena coming from layer XXIII show some differences in their degradation process. The sterile sample 2 is better conserved, with a CPI alkanes of 4.33, while the first one is degraded and has a lower CPI alkanes value of 1.41. This demonstrates that at some points the natural soils of Crvena Stijena could be degraded in a well preserved matrix. In fact, this confirms the impression that motivated us to take a second sample at the site. When we took it, the first sterile sample had a "greasy" texture that did not reflect the characteristics of the whole matrix, which contains more sand. These characteristics are linked to the presence of humidity and some mycelium formation in the sample. Both samples are characterized by the slight dominance of C_{29}. As we note, the natural samples have a lipid composition similar to some ashes or blackened layers coming from fire structures. At the same time, the well preserved sample has a bimodal distribution where the short part of the spectrum is centered on C_{21}, while this bimodal distribution tends to disappear in the degraded natural sample. This could imply evidently that some samples from fire structures taken from exposed profiles could be naturally degraded.

As we have published before, the presence of short alkanes in majority proportions could reflect the thermal degradation of lipids, indicating the presence of ashes or wood charcoal (March 1995, 1996, 1999, 2014; March et Soler 1999; March et al. 2014). As we can see, the samples of Crvena Stijena do not have a predominance of short chain alkanes in any sample. Nevertheless short chain alkanes are present at Crvena Stijena in many layers of reddish soils, ashes, and even in black layers.

This phenomenon it is not new. We obtained the same kind of signatures from other ashes or black layers from Neanderthal fire structures from sites in a travertine context as in the case of the site of El Salt (March et al. 2008; Sistiaga et al. 2010), where the bimodal distribution with a majority of short chains is absent, but some samples have low quantities of $\leq C_{20}$ n-alkanes.

The first explanation that we can put forward is contamination of the ashes by the chemically unaltered composition of their superior layers, as we hypothesized for the chemical composition of the ash layer of structure 7. But even if this contamination could explain the case of fire structure 7, this cannot necessarily be extrapolated to the other samples.

As we presented in the section above on modeling Crvena Stijena, the soils can by characterized primarily as anthropic soils that contain important concentrations of organic matter, which in some cases could have an origin as combustion debris. The black layers presented here are good examples of this situation. As we have just seen, many of them contain in their composition short alkanes associated with long chain alkanes. Then, a good many of the soils where fire structures were lit, or the blackened soils that are going to be covered after their use, contain also chemical signatures of short alkanes. Here it is important to remember that none of these layers shows an ash signature with a majority of short chain alkanes although many of them have short chain alkanes in their composition.

As must be expected, our experimental laboratory results show that when we exposed natural soils to heat the changes observed were related to the original content of these soils. For example, when we burned anthropized soils that contain bimodal signatures similar to those observed at Crvena Stijena at 200°C we obtained a bimodal degraded signature where the centers of

the distribution are displaced to more short chain alkanes because of thermal cracking of the lipid molecules. But these short chain alkanes continue to diminish as a function of temperature and end up absent at more than 600°C (Fig. 18.58). Thus, it is very likely that if black layers are altered at a temperature between 400°C to 600°C we could obtain both ashes and an alkane degraded signature without short chain alkanes and low values of CPI. This phenomenon could explain also the changes observed in the preservation of long alkanes where this preservation could indicate lower temperatures.

It is evident that the signatures of layer XXIII can not be interpreted in this sense. Their lack of combustion products indicates that the natural composition of soils of the shelter is very close to the data observed in the anthropic layers, with a unimodal distribution dominated by C_{29} and C_{31} and showing also variation in their degradation signatures, with CPI alkanes values fluctuating between 1.41 an 4.36. Thus we can assume that the anthropized layers contain also organic matter coming from this local environment.

These long alkanes indicate the preservation of some vegetal markers in Crvena Stijena black layers. These vegetal biomarkers could come from some remnants of charcoal (due to incomplete combustion) or could came from decomposed vegetal items transported to the site by the Neanderthals. The relation between the three more important long alkanes is frequently used to identify the nature of the ancient vegetal ecosystem. At Crvena Stijena we can discard the presence of submerged or floating aquatic plants given the lack of dominance of C_{23} and C_{25} alkanes (Ficken et al. 2000).

Following the work of Zech (Zech et al. 2009), the distribution of alkanes in natural soils can be informative of vegetation history and give us information about the landscape that existed around the shelter in the past. In fact, the alternation between C_{27} and C_{31} could indicate whether we are in the presence of lipids coming from grasses and herbs or deciduous or coniferous trees (Fig. 18.59). These different landscapes are recognized by the changes in the predominance of C_{27} or C_{31} in the different families of plants and their underlying soils. These authors also analyzed the values of soils under these different vegetal landscapes and applied the OEP (odd over even predominance index, Fig. 18.60), which is an index used like the CPI to determinate the maturation of the sample (Fig. 18.51). The obtained data shows the results of the variations resulting from the bacterial degradation processes in living soils under these vegetal communities that are characterized by an increment of the even alkanes and a reduction in the predominance of one of the odd alkanes over the others.

As we can see in Fig. 18.61 the alkanes distributions from Crvena Stijena samples that have an OEP index above 5 give results that allow us to infer that the origin of our alkanes distributions

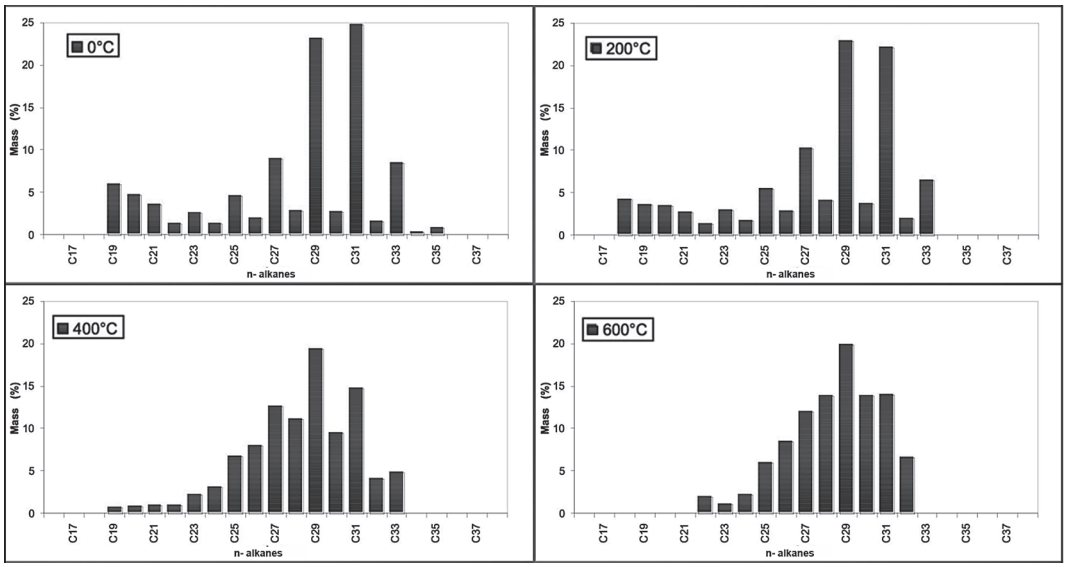

Fig. 18.58. Decay of n-alkanes in natural soil following exposure to heat.

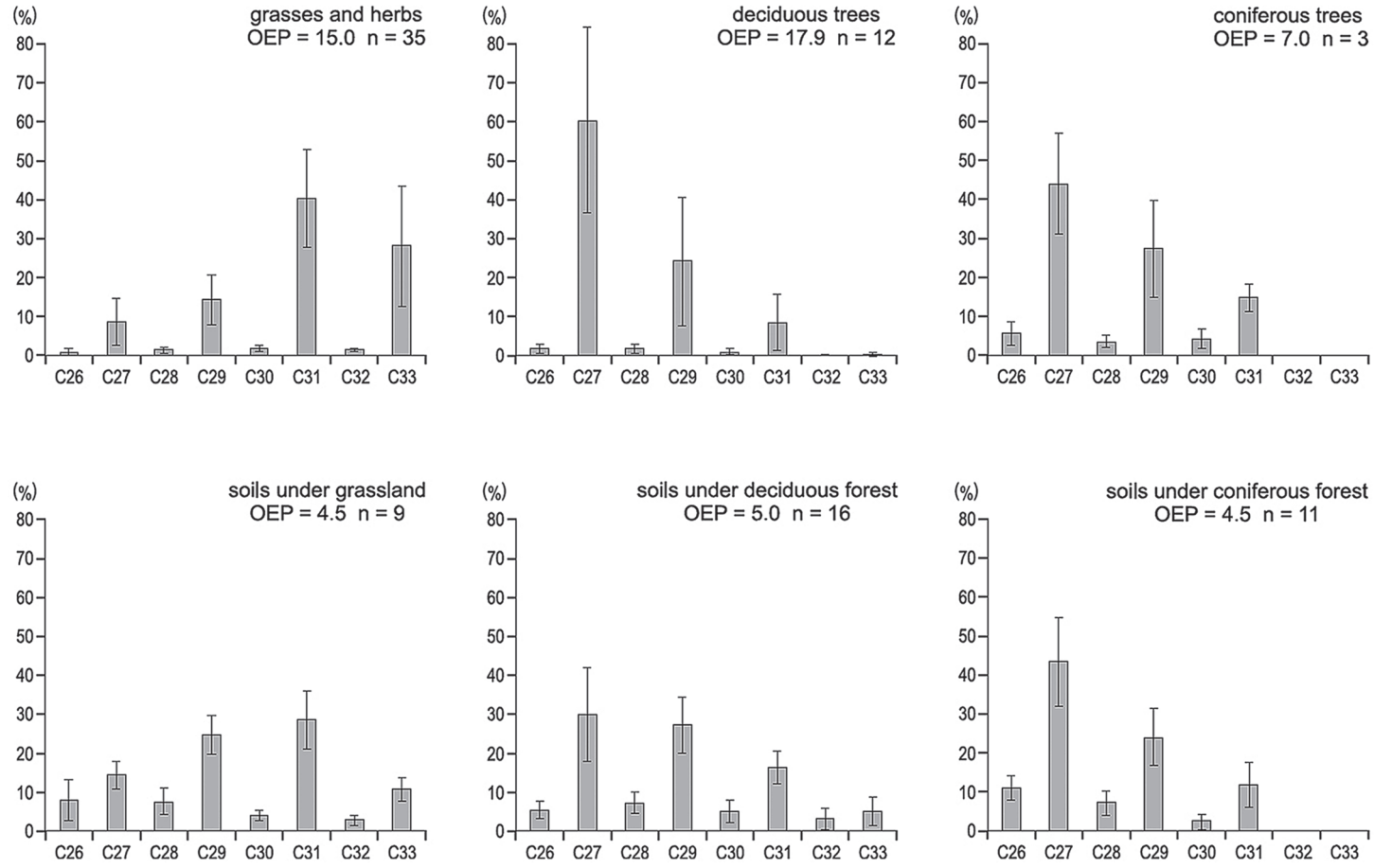

Fig. 18.59. Mean n-alkane distribution patterns from grasslands, deciduous, and coniferous forests (Zech et al. 2009). OEP=odd over even predominance. Error bars indicate standard deviation. Based on data from Zech et al. (2008a), Marseille et al. (1999), Prügel (1994), Rommerskirchen (2006), and Rumpel & Wiesenberg (unpublished).

strongly corresponds to grasses and herbs. At the same time, the analysis of all the data, including the degraded samples, upholds this inference and is very similar to the data from soils under grassland. Further isotopic analysis by CG-C-IRMS of these alkanes allows us to confirm the isotopic values of these alkanes. In the whole sequence, only one sample, coming from the white transition of the big structure 3 from layer XX, shows a distribution of alkanes that could be related to deciduous or coniferous trees, but at the same time this sample seems to be degraded, with an OEP of 1.78.

The geological, archaeozoological, and archaeobotanical data all agree in general that the environment around Crvena Stijena during the times of layers XX-XXIV was only occasionally very cold and that the area was largely forested with a predominantly coniferous and only slightly deciduous forest (Morley, Chapter 7; Morin and Soulier, Chapter 14; Shaw, Chapter 17, all this volume). If this was so, then the signature of these alkanes could reflect specific conditions near the site of Crvena Stijena where grasses and herbs dominated the environment, or they could be the product of anthropic intake. The grasses could be transported to the shelter for living activities—to make beds or rend the ground of the habitat more comfortable, or are related to Neanderthal nutrition, as was proposed by Henry, Brooks and Piperno (2011, 2014) and Fiorenza et al. (2015) for plant families of Triticeae (relatives of wheat and barley) and in the Andropogoneae or Paniceae tribes.

OEP=(C27+C29+C31+C33)/C26+C28+C30+C32)

Fig. 18.60. OEP Index (Zech et al. 2009).

Fatty Acids

As we have seen above, the fatty acids which are the principal component of the lipid families found in the samples from Crvena Stijena have characteristics that indicate a different origin than the alkanes. For example, their distribution between the different kinds of layers, concentrations, and degree of conservation are not the same as n-alkanes. Like the long alkanes, we know that the long chain saturated fatty acids ($\geq C_{21}$) are biomarkers of continental high plants (trees and leaves). The short fatty acids ($\leq C_{20}$) could represent both animal and vegetal lipids. The short chain SFA are predominant in nearly all the samples from Crvena Stijena. Their minimum proportion is 49.11% and their maximum proportion is 99.16%, with a mean of 83.88%. Only the black layer of structure 6 shows a predominance of long chain SFA in its composition. The long chain SFA have a minimum proportion of 0.83 % and a maximum proportion of 50.88%, with a mean of 16.10% (Fig. 18.62).

If we analyze the mean mass concentration of short and long chain SFA in the different kinds of layers, we observe that the concentration of long chain SFA is greatest in the soil layers, and diminishes through the black layers, the ash layers, and the reddish soils. The short SFA show a

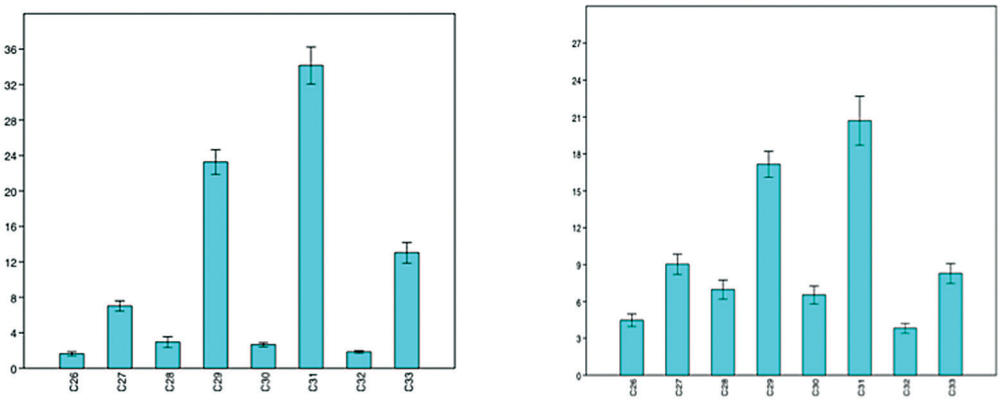

A B

Fig. 18.61. Mean n-alkane distribution patterns of alkanes between C26 and C33 from Crvena Stijena samples. A - having and OEP index superior to 5 (OEP mean 9.75, n=9). and B - all the samples of the site including degraded samples (OEP mean 4.31, n=29).

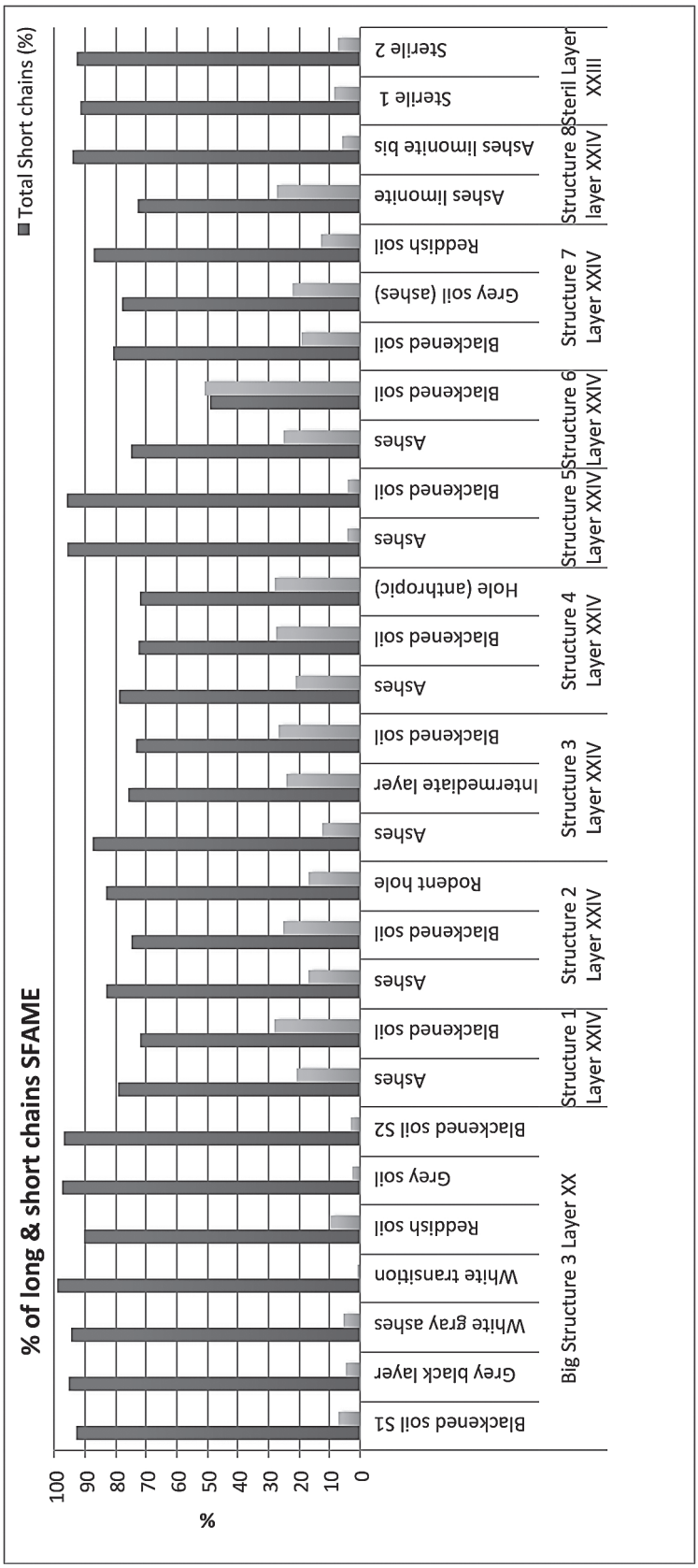

Fig. 18.62. Percentage distributions of long (≥C21) and short chain (≤ C20) saturated fatty acids for different structures sampled at Crvena Stijena.

different behavior. They are more concentrated in the blackened soils, and the soil layers, and they diminish through the reddish soils to the ash layers where the short SFA are present at their lowest concentrations (Fig. 18.63).

This differential distribution between the long and short SFA could be also related to their respective origins. As we can note, the long fatty acids diminished in concentration in agreement with the thermal alteration hypothesis presented above. Thus, the vegetal part of the SFA spectra diminishes as a function of the thermal alteration of the sample. The short SFA do not follow exactly the same pattern of decrease in their concentration, but are also more concentrated in the blackened layers and the soils than the ashes or the reddish soils. We must remember here that the sterile soil has very low concentrations of SFA, as mentioned above.

The distribution of SFA by structure and by sample shows certain differences between the studied samples. The concentration of SFA varied between the different layers and structures. As seen in Fig. 18.64, 20 of the 29 samples contain low quantities, under 0.5 mg/g, of short chain SFA. The other 9 samples are present in different structures—structure 3 of layer XX, structures 2, 3, 4, 5, and 7 in layer XXIV—and belong to different kinds of layers but mostly to blackened soils (n = 4), then Ashes (n = 2), soils (n = 1), or taphonomic disturbances (n = 1). Only one sample has more than 0.5 mg/g of long chain SFA, the intermediate grey soil of structure 3 of layer XX.

The individual distribution of fatty acids in each structure has a pattern for the short fatty acids characterized by the predominance of C_{16} followed by C_{18} and C_{14} in nearly all the structures and in the natural soil from layer XXIII (Fig. 18.65). Only one sample—the blackened soil of structure 6—has a predominance of C_{18} over C_{16}. Within this great homogeneity of the distribution of short fatty acids, the differences observed are essentially variations in the amounts C_{18} and C_{14}, with C_{16} still dominant.

For example, in the stratigraphic sequence of structure 3 of layer XX we can observe that the blackened soils have lower amounts of C_{18} than the other samples of the structure. At the same time, the blackened soils have higher amounts of C_{14} than the other layers. The proportion of C_{18} increases from the grey black layer and the white grey ashes that constitute the upper part of the ashes, and is most important in the reddish soil, followed by the white transition that underlies this soil, and decreases again in the grey soil, ending with the low amounts observed in the underlying black layer. The long chain SFA are more concentrated here in the reddish soils. The long chain SFA have a distribution centered on C_{22} or on C_{24}. The grey black layer, the blackened soil 2, and the grey soil are dominated by C_{24}, and the rest of the samples are dominated by C_{22}.

Turning to layer XXIV, in structure 1 we again observe differences between the blackened soil and the ash layer, but here the situation is inverted and it is the ash layer that shows lower concentrations of C_{18} and higher amounts of C_{14}. Here the blackened soil was better preserved and had a larger concentration of long chain SFA than the ashes. These long chain SFA show a bimod-

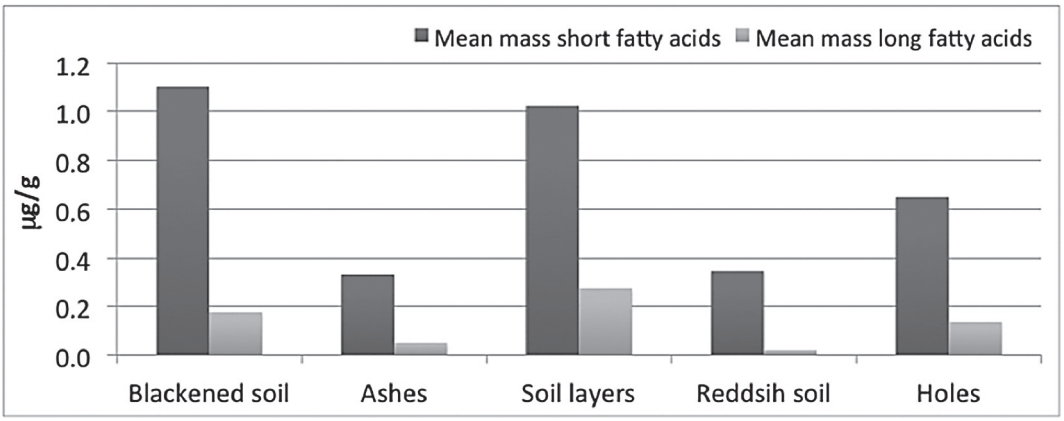

Fig. 18.63. Concentration of short and long chain SFA of the 29 samples (long chain: $>C_{20}$ and short chain: $\leq C_{20}$) in mg/m by kind of layer.

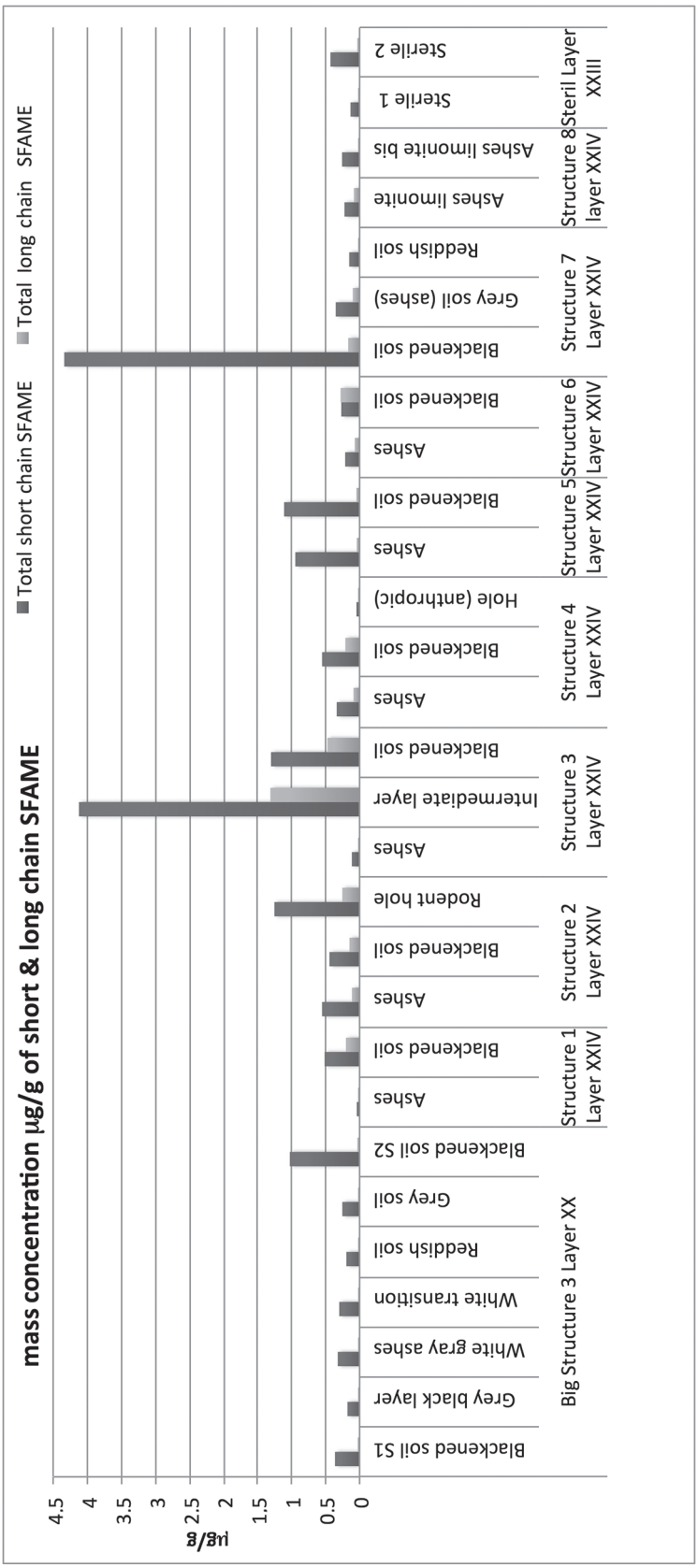

Fig. 18.64. Concentration of short and long chain SFA of the 29 samples (long chain: $>C_{20,}$ and short chain: $\leq C_{20}$) in mg/m by structure and layer.

al distribution centered on C_{20} and C_{30} for the blackened soil that has a different signature than the ashes which are more degraded and contain a concentration of C_{25}.

For structure 2, here again the blackened soil shows larger amounts of C_{18}, but in this case lower amounts of C_{14} than the ash layer. The long chain SFA are centered on C_{26} for the blackened soil and for the ash layer which is more degraded. The rodent hole is centered on C_{22} and exhibits a different distribution for this part of the layer.

Structure 3 has a very similar distribution of C_{14}, C_{16}, and C_{18} for all three samples. The only difference is the presence of C_{12} in the blackened

Fig. 18.65. Saturated fatty acids distribution for archaeological samples from different structures studied at Crvena Stijena.

soil which is absent from the other samples. For the long chain SFA, the ashes are centered on C_{22} while the blackened layer has a bimodal distribution centered on C_{24} and C_{28}, and the intermediate layer has a bimodal distribution centered on C_{22} and C_{30}.

The profile of the blackened soil of structure 4 shows proportions between C_{14}, C_{16}, and C_{18} similar to those of the blackened soil of structure 2. This similarity is observed also for the ashes, which present a smaller proportion of C_{18} than the blackened soil. The ashes of these two layers also show very low quantities of C_{12}. The anthropic hole has a profile of short SFA that is similar to the profile of the ashes, thus these two samples have similar profiles of short SFA and alkanes. As we saw in the previous samples, the long chain SFA have different distributions. The blackened soil has a bimodal distribution centered on C_{22} and C_{28}, while for the ashes this bimodal distribution is centered on C_{24} and C_{30}, and finally the anthropic hole has a bimodal distribution centered on C_{22} and C_{30}.

For structure 5, the ashes and the blackened soil have a very similar distribution for the short SFA, but the ashes and the blackened soil again have very low quantities of C_{12}. The long chain SFA of the blackened soil are centered on C_{22}, while the ashes have very low quantities of long chain SFA, with similar concentrations among them and no long chain acid has a marked predominance.

Structure 6 shows a different distribution of the short chain SFA. The blackened soil has a profile where C_{18} is greater than C_{16} and the quantity of C_{14} is very low. The ashes show greater concentrations of C_{16} than C_{18}, similar to the profiles observed for structures 2 and 4. Here C_{12} is absent. The long chain SFA of the blackened soil of structure 6 has a bimodal distribution centered on C_{22} and C_{30}. The ashes have a distribution similar to that of the ashes of structure 5 where no particular long chain SFA is predominant.

Structure 7 shows similar distributions of short SFA for the blackened layer that covers the structure and for the reddish soil, where C_{16} is predominant over C_{18}. The intermediate grey ashes soil has a little larger quantity of C_{18} and a lower quantity of C_{14}. C_{12} is absent. The long chain SFA have bimodal distributions in all three samples. They are centered on C_{22} and C_{28} in the ashes and the reddish soil, and in C_{22} and C_{30} for the blackened soil.

Finally, in structure 8 both ash layers have similar distributions for the short SFA, but for the long chain SFA they show certain differences. The first sample has a bimodal distribution with peaks at C_{22} and C_{26}, while the second one shows a unimodal distribution centered on C_{24}. A concentration of C_{26} was also observed for the blackened soil of structure 6.

A first and interesting observation is that these samples can be grouped into two main groups based on their concentrations and distributions of long chain SFA, one consisting of the samples from layer XX and the samples of the sterile layer, and a second that contains the fire structures of layer XXIV. In layer XXIV we have two further groups, one dominated by C_{22} and C_{26} and a second one where C_{30} and C_{32} can be noted in the results. These differences could be related to changes in the vegetal part of the fats that are contained in layer XX and layer XXIV, and even changes between the two groups of samples from layer XXIV.

An FCA-PCA analysis of the distribution of alkanes and SFA in Crvena Stijena allows us to understand better the groupings of our samples on the basis of the distributions of these SFA and alkane molecules (Fig. 18.66). In this analysis, SFA C_{16} and C_{18} are in opposite positions, and the alkane C_{27} is in opposition with C_{29} and C_{31} on component 2. This organization of predominant molecules groups samples of blackened soils coming from the structures 2, 3, 5, and 7 in one group (characterized by the presence of alkanes C_{29}, C_{31}, and C_{33}), the blackened soils of samples 4 and 6 in a second group characterized by the presence of C_{18} and the even long chain SFA, and finally in a third group the blackened soils of layer XX that are characterized by a strong predominance of SFA C_{16} and important amounts of SFA C_{14}.

Most of the ashes and degraded soils are related to the presence of even alkanes which denotes their thermal alteration. It is interesting to see that the sterile samples which have bacterial degradation are associated with these samples, while the sterile sample 2 that has a good preservation is in the opposite position on component 1. Finally, we can see that samples of ashes or grey layers are separated by the proportions of the SFA C_{18}, for example the ashes from structures 1 and 6 or the ashes of structure 7 that is positioned with the group showing good preservation of odd long chain alkanes.

From these results we can infer that we have differences in the composition of organic matter between black layers, thermo-altered layers such as reddish soils, and ash layers. The relations between anthropic samples and natural samples of layer XXIII show a mimetic process where naturally degraded organic matter can be confused with the organic matter present in the thermo-altered layers and the well preserved samples could be similar to the contents of some black layers. Of course, this could imply also a global contamination of the whole site with the same kind of organic matter, but this hypothesis could not explain all the differences observed here. The separation observed for the long chain SFA between the samples of layer XX and layer XXIV could be based on differential thermal degradation of the samples where the samples of structure 3b are more degraded, having a predominance of C_{27} and even alkanes.

Taking into account the difference demonstrated between the thermo-altered layers and the black layers when we compare the distribution of alkanes and the saturated fatty acids, we can compare the distribution of the unsaturated fatty acids and the branched fatty acids in our samples. As we know the unsaturated fatty acids could be an indicator of contamination of the samples with young organic matter while the branched fatty acids are an indicator of bacterial transformation and the consequent degradation of organic matter. If we analyze the relation between these two classes of lipids according to the different kinds of layers, we see that the natural layers and holes have a correlation of 0.85, the black layers 0.61 and the ash layers −0.13. Thus we can conclude that the correlation of fatty acids is positive for the natural layers and decreases for black layers and ash layers. These relationships can be seen in Fig. 18.67. This observation indicates that the samples are not contaminated by the natural composition of soil, the unsaturated fatty acids being less concentrated or directly absent in most of the thermo-altered layers. The branched fatty acids present indicate in these layers the traces of ancient bacterial activity. From this, we can deduce that the black layers conserve ancient organic matter that continues today its maturation process. The unsaturated fatty acids could disappear during the thermal alteration of these layers under the action of fires.

If the organic matter of these samples was altered, the relation between saturated fatty acids and their isotopic values could be also modified. As we have demonstrated the amount of C_{18} increases in the thermal alteration process, at the same time recent experiments show that the isotopic values of thermo-altered soils are depleted under the action of heat. Here the lower values for the C_{16}/C_{18} index correspond with the reddish soils while the ash layers and the black layers has nearly equal values, the natural soils and the holes have higher values (Fig. 18.68).

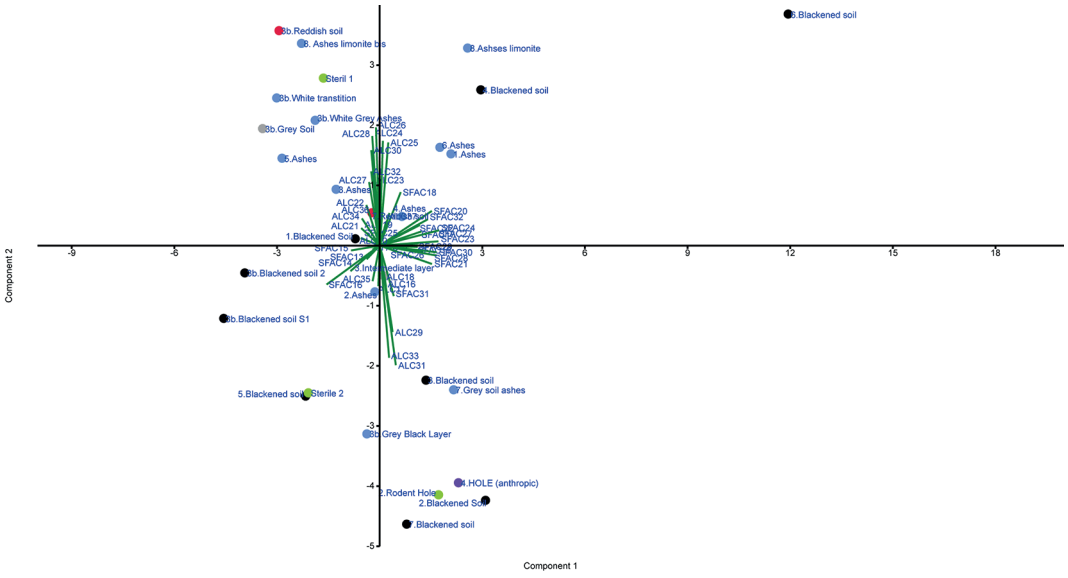

Fig. 18.66. FCA-PCA (correlation) analysis of Crvena Stijena samples (SFA and Alkanes).

Thus the SFA present in thermo-altered layers seem not to have been altered by heat action for the ash layers and the grey layers, but are a little more degraded in the reddish ones. We can conclude that the SFA present in the ash layers could be deposited in it after the thermal processes, a phenomenon that is regularly observed in cooking procedures with embers in flat structures. On the contrary, the alkanes reflect here the action of fire and derive partially from thermal cracking.

Relations to Fauna in Crvena Stijena

But what could the Neanderthals have cooked in their fire structures? As we have seen, all the samples from Crvena Stijena show a dominance of short chain fatty acids, mainly as palmitic acid (C_{16}). This predominance of short chain fatty acids suggests that the fire structures contain organic matter of animal origin. As we checked by the C_{16}/C_{18} index, these short chain fatty acids are not changed by the action of heat in the majority of the layers present at the site. Therefore, we can explore and analyze the fatty acids distributions in relation to their possible animal origin as another hypothesis for the origin of fats at this site.

Working at Crvena Stijena we must be extremely cautious. The first problem here is that the list of faunal remains from Crvena Stijena, compiled by Malez (1975) (Fig. 18.69) represents a faunal record where some species are today extinct, and consequently their biology, behavior, and adaptation cannot be exactly determined. This is true even if biologists have projected the present-day ethology of their families into the

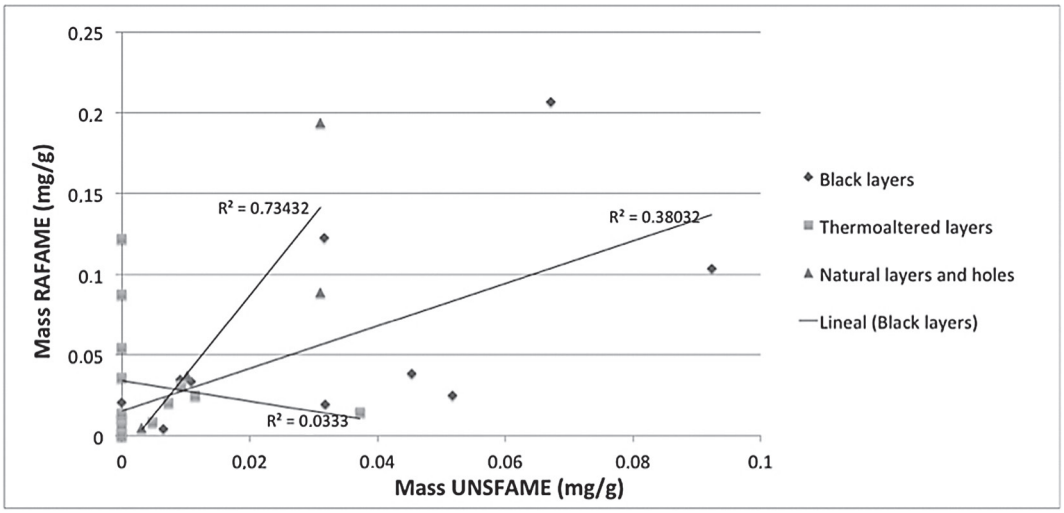

Fig. 18.67. Relation of concentration values of unsaturated fatty acids and branched fatty acids according to the different kind of layers founded at Crvena Stijena.

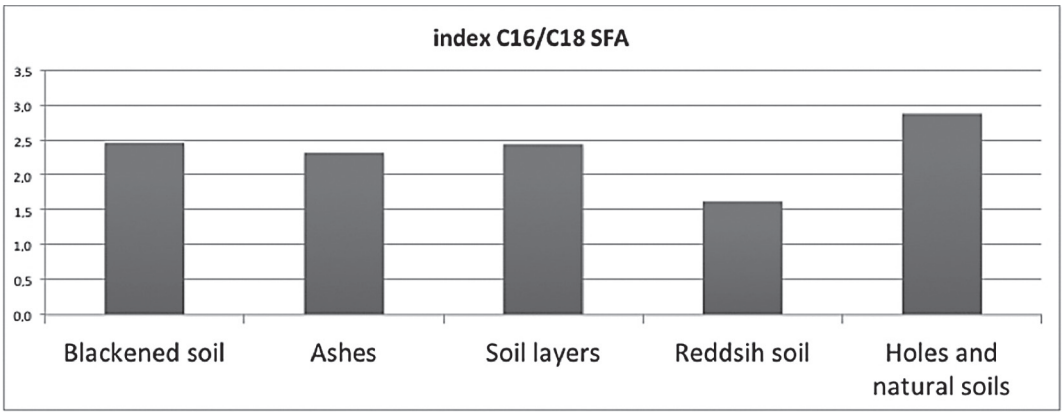

Fig. 18.68. C16/C18 SFA index for the different kinds of layers present at Crvena Stijena.

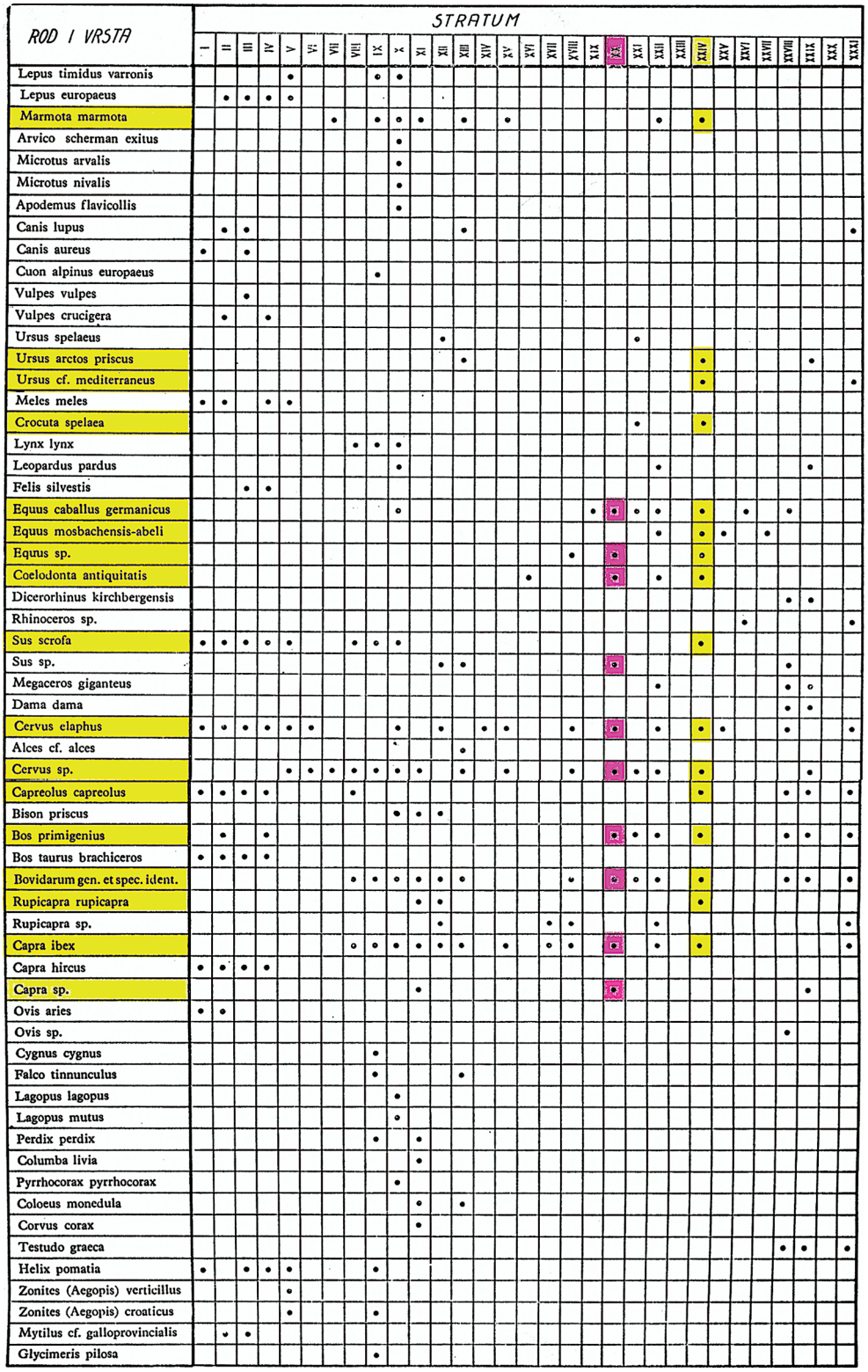

Fig. 18.69. Pleistocene faunal species list found in earlier excavations at Crvena Stijena of layers I to XXXI. Colors indicate layers XX and XXIV studied here. Layer XXIII is considered to be sterile. (after Malez 1975, with modifications)

past and if recent work is beginning to explore the paleoecology of Neanderthals and animals living in the Pleistocene and early Holocene by isotopic analysis (Wißing et al. 2015; Krajcarz et al. 2014; Richards et al. 2008; Jürgensen et al. 2017). The second problem is the difficulty of projecting the actual behavior of living species onto the past landscape around Crvena Stijena. Finally, a third problem is that some of the ancient species still extant today are at risk of extinction, and it is therefore very difficult to find or collect lipid data related to some of the animals present in the fauna from the site.

The analysis of the fauna indicates a varying spectrum of species for layers XXIV and XX. The following taxa are listed by Malez (1975) as present in layer XX: *Equus caballus germanicus, Equus* sp.*, Coelodonta antiquitatis; Sus* sp.*, Cervus elaphus, Cervus* sp.*, Bos primigenius, Bovids, Capra ibex, and Capra* sp. For layer XXIV, Malez lists as present: *Marmota marmota*, *Ursus arctos priscus*, *Ursus* cf. *mediterraneus*, *Crocuta spelaea*, *Equus caballus germanicus*, *Equus mosbachensis-abeli*, *Equus* sp., *Coelodonta antiquitatis*, *Sus scrofa*, *Cervus elaphus*, *Cervus* sp., *Capreolus capreolus*, *Bos primigenius*, Bovids, *Rupicapra rupicapra*, *Capra ibex*, and *Capra* sp. No quantitative data is given by Malez on the relative abundances of these species. Recent excavations have not recovered enough fauna for accurate assessment of relative frequencies in layer XX, but for layer XXIV by far the most common species is *Cervus elaphus*, followed in descending order of frequency by *Equus caballus ferus*, *Bos*/*Bison, Testudo* sp., *Capra ibex/caucasica*, and *Dama dama* (Morin, Chapter 14, this volume).

For many of these species still living today, fatty acids composition has not been studied or has been studied only partially—to understand specific subjects, as for *Capra ibex* or *Rupicapra rupicapra*, (Valencak and Gamsjäger 2014; Spangenberg 2010; Carrer et al. 2016), or for *Crocuta spelaea* concerning other parts of their body than their adipose tissue (Crawford et al. 1976). For example, we know the lipids of the skin of *Rupicapra rupicapra* which were studied following the discovery of an ancient piece of leather in the Swiss alps (Spangenberg 2010), or we know the isotopic values of their adipose tissue (Carrer et al. 2016) but not the exact proportions of their adipose fatty acids. In the same sense the anal fatty acids of the hyena (*Crocuta spelaea*) were studied because they play a role in their communication and social organization (Marchlewska- Kog et al. 2001), but again the distribution of SFA in the rest of the body was not detailed.

For endangered species such as the rhinoceros or the Przewalski horse that could be used for comparison with the extinct species woolly rhinoceros (*Coelodonta antiquitatis*) or *Equus caballus germanicus*, we have only a partial description of the saturated fatty acids of their plasma, detailed for C_{16} and C_{18} (Leat et al. 1979), or the total composition of their milk (for rhinoceros) (Osthoff et al. 2007).

Another point that we must take into account is the position of some animals identified at Crvena Stijena in the trophic chain. Some of the carnivores listed by Malez as present at Crvena Stijena could be there either by anthropic action or from natural circumstances. The bears and hyenas are known to us as recurrent users of shelters and caves as habitats for living, hibernating, or for scavenging. Thus, some animals may not make an important contribution to Neanderthal diet if they are not really consumed at the site. Bears are in special position because even if they are considered as omnivores and in some way competitors or dangerous for men, they are frequently included as eventual prey in the food chain of Neanderthals. Although Neanderthal diet is still being actively debated (see, for example Morin, Speth and Lee-Thorp 2017), some recent studies of isotopic composition of Neanderthal bones seem to indicate that Neanderthals were mostly carnivorous, and that their favorite prey varied by region, being large herbivores including bovids and horses in our region, and mammoth, woolly rhinoceros, and reindeer in northern European sites (Wißing et al. 2015; Richards et al. 2008; Bocherens et al. 2005a, 2005b). Other authors suggest the necessity of considering also their consumption of vegetal foods (Fiorenza 2015; Fiorenza et al. 2015), which includes natural grasses as we mentioned in the analysis of the alkanes fraction.

Working with these limitations we can still explore whether the samples of Crvena Stijena correspond to some of the families of animals listed above. As we and others have published previously (March 2013), the analysis of the distribution of the three principal saturated fatty acids, C_{14}, C_{16}, and C_{18}, can help us to investigate the possible origin

of four samples (March, Baldessari and Gross 1989; March et al. 1989, 1995, 1999; March and Soler 1999; Malainey et al. 1999b, 1999a; Eerkens 2005; Buonasera 2005; Koirala and Rosentreter 2009). A ternary plot of C_{14}, C_{16}, and C18 in the Crvena Stijena samples (Fig. 18.70) shows a unique group of thermo-altered samples of ashes and reddish soils surrounded or sometimes superposed by the better preserved samples coming from the black layers, holes, and natural sterile soils. Only one sample from structure 6 was situated outside of this group because of its high proportion of C_{18}. If we compare this distribution with data from different families of animals observed at Crvena Stijena, we observe a number of correspondences.

The distribution of the Crvena Stijena samples agrees with the distribution of values belonging to bones and marrow, and partially with values for fat and muscle, of the Bovinae, which are rich in C_{16}, with the exception of milk and butter (Badiani et al. 2002; Banskalieva et al. 2000; Baublits et al. 2006; Belitz and Grosch 1999; Cifuni et al. 2004; Crawford et al. 1970; Dalle Zotte 2002; Elias Calles et al. 2000; Enser et al. 2000; Frediksson, Eriksson and Pickova 2007; Guerrero et al. 2015; Gunstone et al. 1995; Haenlein 2004; Hilditch and Williams 1964; Hubbard and Pocklington 1968; Jandal 1996; Kagawa et al. 1996; Lucquin 2007; Malainey et al. 1999b, 1999a; Marchbanks 1989; Morgan et al. 1973; Paleari et al. 2003; Rottländer 1991; Rule et al. 2002; Warren et al. 2008; Yang et al. 2002) (Fig. 18.71).

For the Cervidae (Gunstone et al. 1995; Hilditch and Williams 1964; Hoffman and Wiklund 2006; Lucquin 2007; Malainey et al. 1999b, 1999a; Marchbanks 1989; Paleari *et al*. 2003; Petkov 1986; Phillip *et al.* 2007; Polak et al. 2008; Rottländer 1991; Sampels 2005; Volpelli *et al.* 2003; Wiklund *et al.* 2003; Zomborszky and Husvéth 2000) the samples of Crvena Stijena correspond more closely to samples of muscle lipids, enriched in C_{16}, than to fats and liver which have higher proportions of C_{18}. However, these fats and liver could explain the sample of structure 6 (Fig. 18.71).

The Suidae family (Banskalieva et al. 2000; Belitz and Grosch 1999; Dalle Zotte 2002; Enser et al. 1996, 2000; Garcìa-Olmo et al. 2002; Gunstone et al. 1995; Hilditch and Williams 1964; Hubbard and Pocklington 1968; Högberg et al. 2004; Kagawa et al. 1996; Lucquin 2007; Maw et al. 2003; Paleari et al. 2003; Pathak et al. 1959; Paredes Sabja 2002; Skewes et al. 2009; Wood et al. 2008) corresponds better with the Crvena Stijena samples than the Cervidae, showing a superposition of Suidae samples from fat, muscle, bone, and adipose tissue with most of the samples. Among the samples from Suidae, only the liver samples could explain the distribution of the sample coming from structure 6 (Fig. 18.71).

The Caprinae samples (Banskalieva et al. 2000; Gunstone et al. 1995; Haenlein 2004; Jandal 1996; Soryal *et al.* 2005; Paleari et al. 2003; Raynal-Ljutovaca *et al.* 2008; Rhee *et al.* 2000) fall mostly outside of the distribution of the Crvena Stijena samples, but again some are near the sample of structure 6. This is because of the distribution of C_{14} and C_{18} in this family (Fig. 18.71).

The Ursidae family (Käkela and Hyvärinen 1996; Cattet et al. 2001; Iverson and Oftedal 1992; Iverson et al. 2001) shows samples that are more enriched in C_{16} than most of the samples from Crvena Stijena, but the two samples found of *Ursus arctos*, which must be the species actually at the site rather than *Ursus americanus*, show some coincidence with the archeological ones (Fig. 18.71).

We can conclude this review of the big game with the Equidae family (Hilditch and Williams 1964; Gunstone et al. 1995; Paleari et al. 2003; Lee *et al.* 2007; Tonia et al. 2009; Mamani and Linares 2013) which shows only a low correspondence with the Crvena Stijena samples (Fig. 18.71).

We must mention here that the values of triglycerides, phospholipids, and cholesterol esters studied in blood samples of rhinoceros show a very significant proportion of C_{18} (C_{16}/C_{18} index 1.66), and their milk has an index of 1.77 (which is comparable only to the reddish soils, but other parts of the body should have different values that could be more comparable to Crvena Stijena samples (Leat et al. 1979; Osthoff et al. 2007).

Thus it appears that the distribution of C_{14}, C_{16}, and C_{18} fatty acids at the site coincides relatively well with the composition of Bovidae, Suidae, and Cervidae. The Caprinae, Equidae and Ursidae show only partial coincidence. The big structure 3 of layer XX, which is more enriched in C_{16}, could coincide more with Bovidae, Ursidae, and Equidae values. This could imply a different source for fatty acids in these two different layers, or some changes in behavior between layer XX and XXIV. Finally, we could find only four samples of white adipose fat (Cochet et al. 1999) of

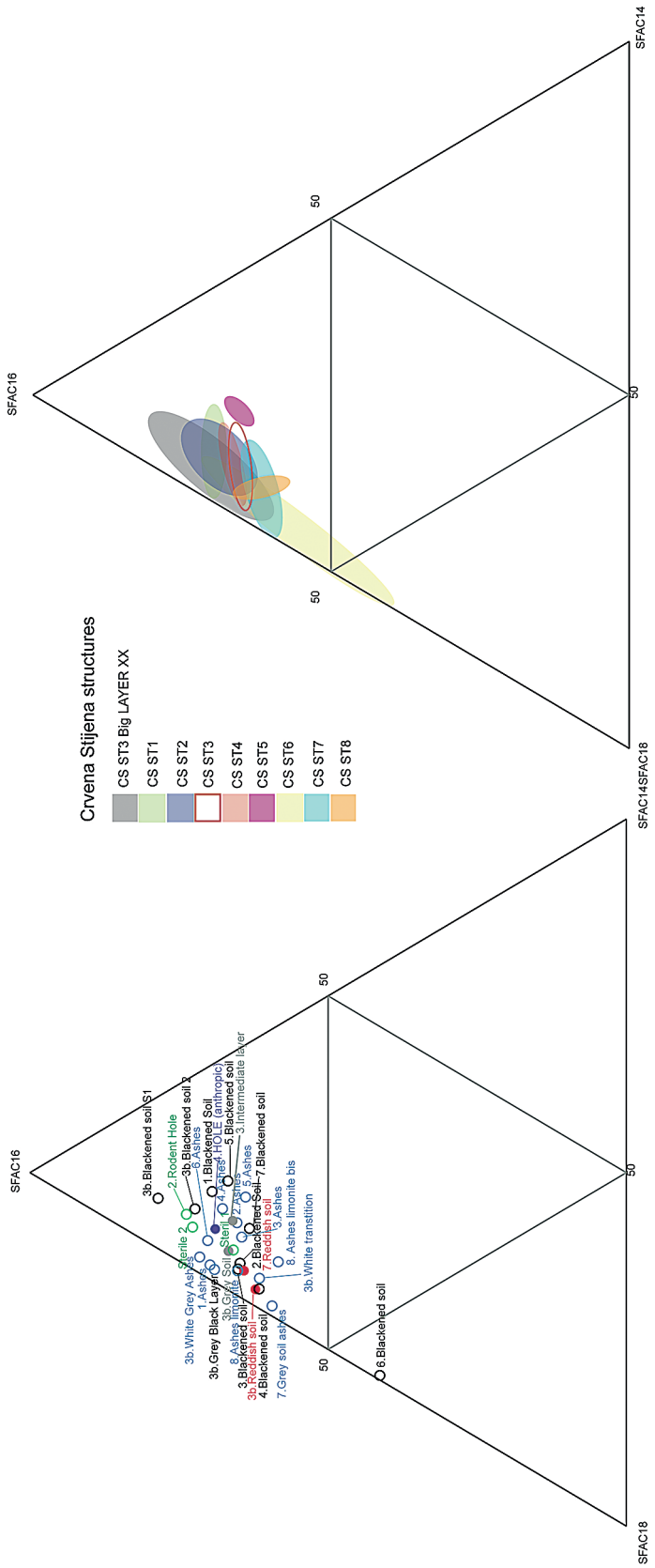

Fig. 18.70. Ternary representation of saturated fatty acids (C_{14} C_{16} & C_{18}) distribution from Crvena Stijena.

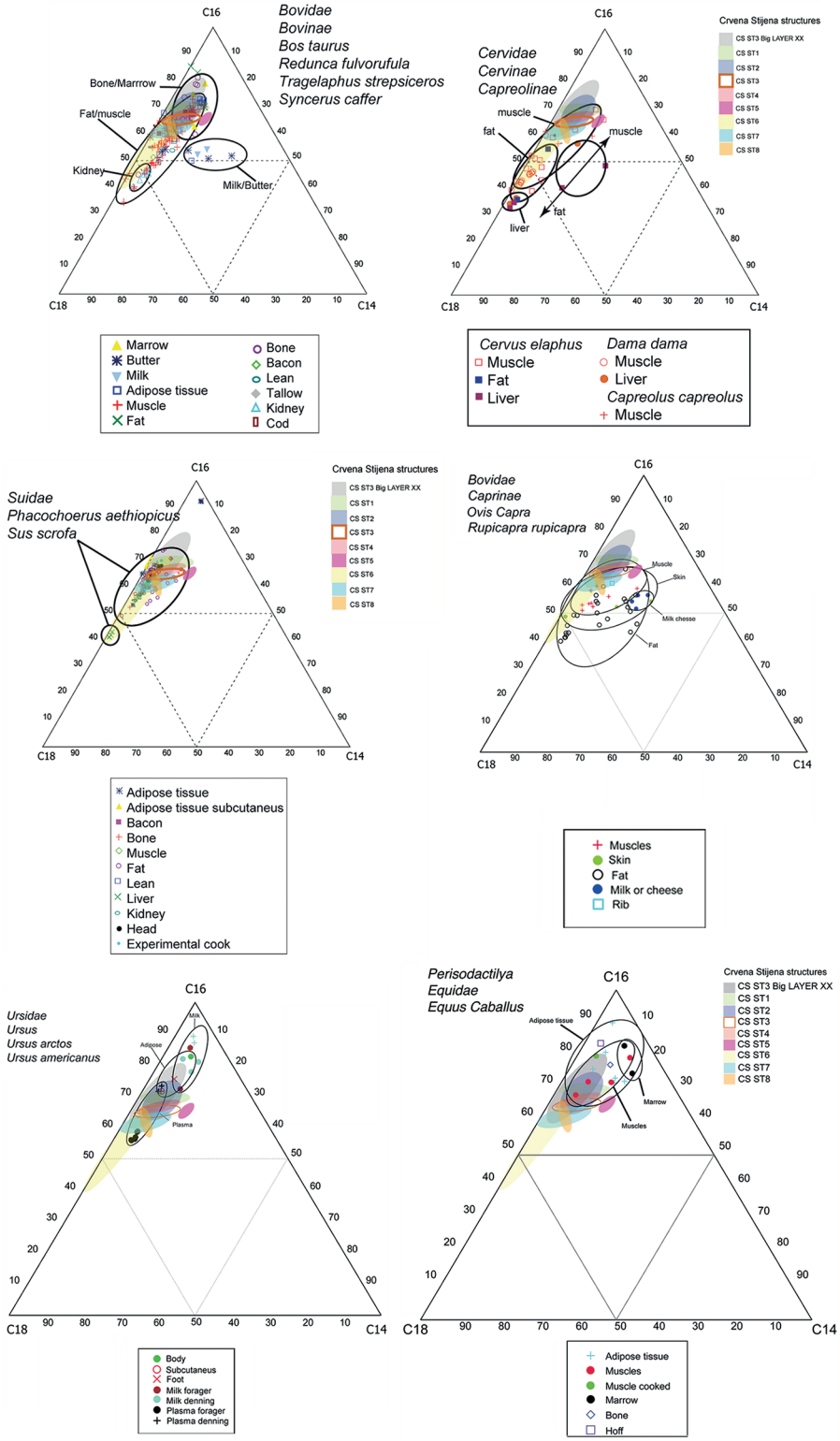

Fig. 18.71. Ternary representation of saturated fatty acids (C_{14} C_{16} & C_{18}) distribution of Bovinae, Cervinae, Suidae, Caprinae, Ursidae, and Equidae reference samples in comparison with archeological samples from Crvena Stijena.

Marmota marmota for comparison, and this does not correspond to the fatty acid distributions of the Crvena Stijena structures (Fig. 18.72). These results fit moderately well with the faunal data, which indicates a primary reliance on Cervidae, followed by Equidae and Bovidae (Morin, Chapter 14, this volume), but we need to investigate further the possible sources of organic compounds in our Crvena Stijena samples.

The Triterpenes

The triterpenes are an important family to determinate the origin of organic matter. They are recognized as biomarkers reflecting the animal or vegetal origin of a sample but are also an indicator of degradation processes and specialized activities (Charrié- Duhaut et al. 2009; Evershed 1993; Evershed et al. 1992; Evershed et al. 1997; Evershed and Connolly 1994; Heron et al. 1991; March 1995a, 1996, 1999, 2013; March et al. 1989; March et al. 2003a; March et al. 2014, March and Soler Mayor 1999; Pepe et al. 1989; Pepe and Dizabo 1990; Regert et al. 2003a; Regert and Rolando 2002; Regert et al. 2003b).

Unfortunately, the majority of the Crvena Stijena samples do not conserve this family of

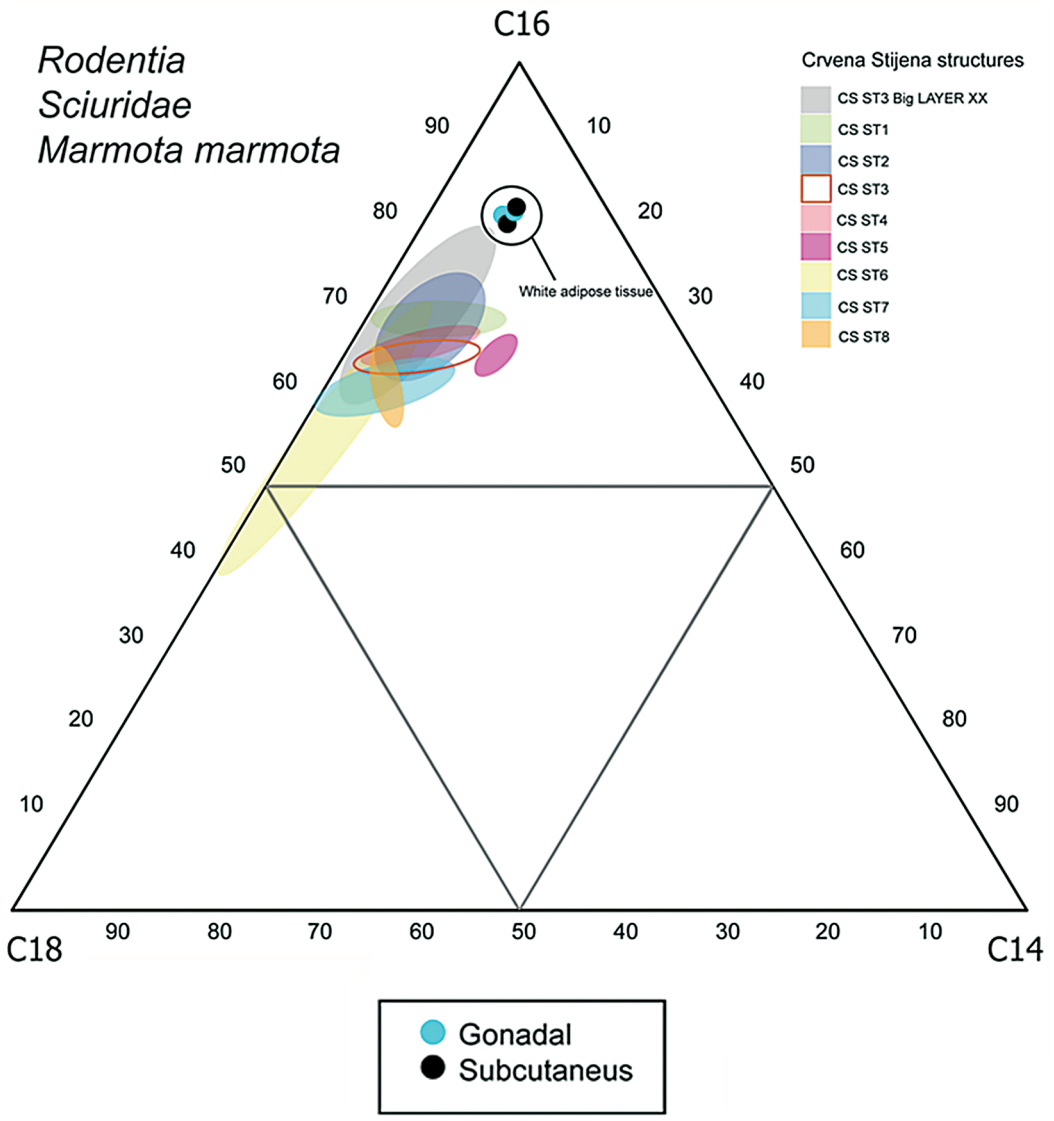

Fig. 18.72. Ternary representation of saturated fatty acids (C_{14} C_{16} & C_{18}) distribution of *Marmota marmota* SFA reference samples in comparison with archeological samples from Crvena Stijena.

molecules because of their degradation. Only five samples conserve some sterols: the rodent hole near structure 2, the ashes and the blackened soil of structure 5, one sample of ashes from structure 8 in layer XXIV, and the sterile sample 1 from layer XXIII. No sample from layer XX has conserved sterols in it (Fig. 18.73).

The sample from the rodent hole is the richest in sterol mass (3.85 μg/g) and variety, having different proportions of cholesterol (12.87%), cholestanol (2.67%), ergosta-7.22-dien-3β-ol (2.87 %), stigmasterol (13.35%), sitosterol (53.18%), and stigmastanol (7.79%). This composition indicates a mixed origin for the sterols of this sample, dominated by a vegetal composition but having also animal signatures. Both samples of structure 5 have very low concentrations, and only traces of cholesterol. The ashes sample has more cholesterol (0.02 μg/g) than the blackened one (0.004 μg/g). The ashes limonite sample from structure 8 shows very low quantities of cholesterol (0.01 mg/g) and sitosterol (0.03 mg/g), thus sitosterol is predominant in this sample (66.48%) in comparison to the 33.51% of cholesterol. Finally the sterile sample 1 has only traces of animal sterols in the form of cholesterol (89.87%), with (0.06 mg/g), and cholestanol 10.12% (0.007 mg/g).

As we see, the samples of ashes that have preserved sterols show either animal origins or a mixture of animal and vegetal origin of the sterols. The one black layer has an animal origin, as does the sterile layer. The difference between the anthropic layers and the rodent hole and the sterile 1 samples is that cholesterol is the unique animal sterol in anthropic samples, while it is accompanied by cholestanol in the rodent hole and the sterile sample. The rodent hole has a predominance of vegetal sterols that show a great diversity. This confirms the recent formation of the organic matter of these samples that could serve in future work as an indicator of rodent contamination. The low preservation of sterols at Crvena Stijena could be related to the thermal alteration of the samples, but also to a general degradation of the profile samples studied here related to the formation process of the shelter. But this absence of sterols does assure us that there has been no, or undetectable, contamination of the majority of the samples studied here by contemporary agents. Finally, and compared to the discovery of traces of fecal matter at other Neanderthal sites as El Salt or Mallaha, there are no data indicating the conservation of fecal matter in these profile samples.

Therefore, the poor preservation and the low amounts of sterols observed in the anthropic samples does not let us definitively establish the general origin of the organic matter present

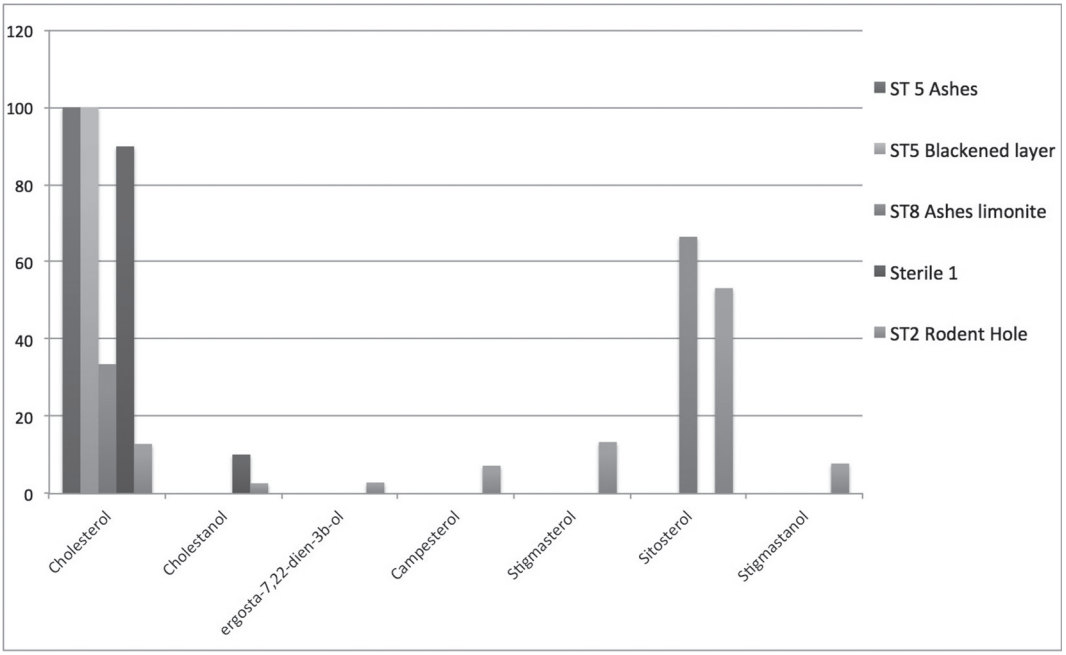

Fig. 18.73. Percentage of sterols present at Crvena Stijena.

and leaves open the possibility of either or both animal and vegetal origin of the other lipids in these samples.

Exploring the Possible Origins of Organic matter by the Analysis of Isotopic FAMEs

As we have shown at the site of Mallaha (March 2013), molecular isotopic analysis can help us better understand the origin of the organic matter of fire structures and soil samples. The CG-C-IRMS technique can be applied to FAMEs (fatty acid methyl esters) and alkanes alike to determinate their origin. We begin our exploration with the study of FAMEs, leaving the study of alkanes for future investigation. Our objective in this work is to try to define the origin of fatty acids in the different kinds of samples studied here: ash layers, black layers, and reddish soil layers. This work faces all the difficulties mentioned above for the analysis of the distributions of fatty acids, including obviously the fact that the animal species which lived in the Pleistocene can show differences with their living relatives in biology, behavior, and in adaptation. This implies that we could perhaps observe changes in nutrition that can difficult to understand by extrapolation from the examples of living animals.

First at all, we must note that not all the samples from Crvena Stijena contain sufficient material to apply this method. The reddish soil of layer XX, the ashes and the blackened soil of structure 1, the blackened soil of structure 5, and the ashes and the blackened soil of structure 6 do not give viable results and must be removed from this study. The problem lies essentially in the C_{18} concentration for the first five samples and in the C_{16} concentration for the blackened soil of structure 6.

The other samples contain enough organic matter and give reliable results of $\delta^{13}C$ isotopic values. The samples studied from Crvena Stijena have values between −34.37‰ and −25.52‰ for C_{16} and −29.40‰ and −25.76‰ for C_{18}. The mean value for C_{16} is of −29.38‰ and −27.54‰ for C_{18}. Thus, at Crvena Stijena we see that the C_{18} values are enriched in comparison to C_{16} values (Fig. 18.74).

It is interesting to note that the isotopic values of the samples form two groups, one with more enriched values and the second with more depleted ones. These two groups separate samples that we had differentiated before on the basis of some of the characteristics of the more depleted group which contains samples that show good preservation: the rodent hole, the sterile sample 2, and the two blackened layers that frame the big combustion structure 3 of layer XX. Close to these two samples we find the samples of the upper ashes and the grey soil situated under the white transition of the big structure 3 of layer XX. Other samples from the same structure are associated with the other group, in which are found all the samples from layer XXIV. In this group is found also one the best conserved samples from structure 8, while the degraded samples are also near the degraded sample of the sterile layer. The samples of structures 2, 3, 4, and 7 of layer XXIV form the enriched group and conserve a certain organization in this group, where they are close together but arrayed along an axis from less to more enriched values of C_{16} and C_{18} (Figs. 18.74-18.75).

There is no regularity in the internal position of the samples, sometimes the ashes are more enriched and sometimes the blackened layers have the more enriched values within each structure. These results indicate that each succession of layers in the fire structures has similar values that are differentiated only by a small enrichment or depletion of one of the samples in the sequence. At the same time, these results indicate that most of the fatty acids of the Crvena Stijena fire structures have the same composition even if they are not situated at the same layer. The fatty acids of the rodent hole and of the sterile layer sample 2 are situated here near some black and ash layers of layer XX, while the fatty acids of the walls of the anthropic hole are grouped with all the other samples (Fig. 18.75).

An interesting point is that the differences between samples seem to be a function of the relative proportions of C_{16} and C_{18}. In fact, if we compare the index C_{16}/C_{18} and the mean isotopic values for each sample we obtain a negative correlation value of −0.72 with an $r^2 = 0.52$ which indicates a significant trend in the proportional relation of these two acids. Where this index has higher values, in most cases the samples are more depleted, i.e., at Crvena Stijena the more the fatty acid C_{16} is concentrated in the samples, the more depleted they are. In general, given some nutriments such as deer meat, bacterial transformation enriches the values of samples in

periods of time as short as 18 months of burial, as we have demonstrated in recent experiments. A similar but lower enrichment phenomenon was observed in some kinds of cooking, such as boiling. On the contrary, heat action (above 300°C) on soil lipids provokes depletion in the isotopic signatures, as has also been shown in recent experimental work (March 2017; March et al. 2017). Consequently, the fatty acids at Crvena Stijena seem not to be depleted by the action of fire. The closeness observed between the different samples of the same structure implies a similar composition of the different stratigraphic layers, and even if we see some differences within each structure, the possibility exists that the fats deposited after combustion or coming from the waste present in black layers could spread through the whole structure considering their thinness.

If we compare the results at Crvena Stijena with other examples from different parts of the world, we can develop a hypothesis about the animal or vegetal origin of the Crvena Stijena fatty acid samples. First, if we compare the samples with lipids from C3 and C4 plants (our data and Spangenberg and Ogrinc 2001; Spangenberg and Dionisi 2001; Dungait et al. 2008, 2010), we can conclude that the fatty acids of the Crvena Stijena samples do not fit a vegetal origin (Fig. 18.76). They are more enriched than C3 plants and more depleted than C4 ones. Only three samples, of cabbage, pumpkin, and nettle, have values that match certain depleted samples of Crvena Stijena and the ash sample of structure 4. Of course, it is obvious that only nettle or some ancient species of *Brassica* could have been present in a prehistoric European context. Our purpose is only to show that some samples could have a possible vegetal origin. As shown by the alkane analysis, it is possible that these fatty acids could have come from grasses and herbs of grasslands which could have been transported to the shelter by natural or human agents. The values observed here for the

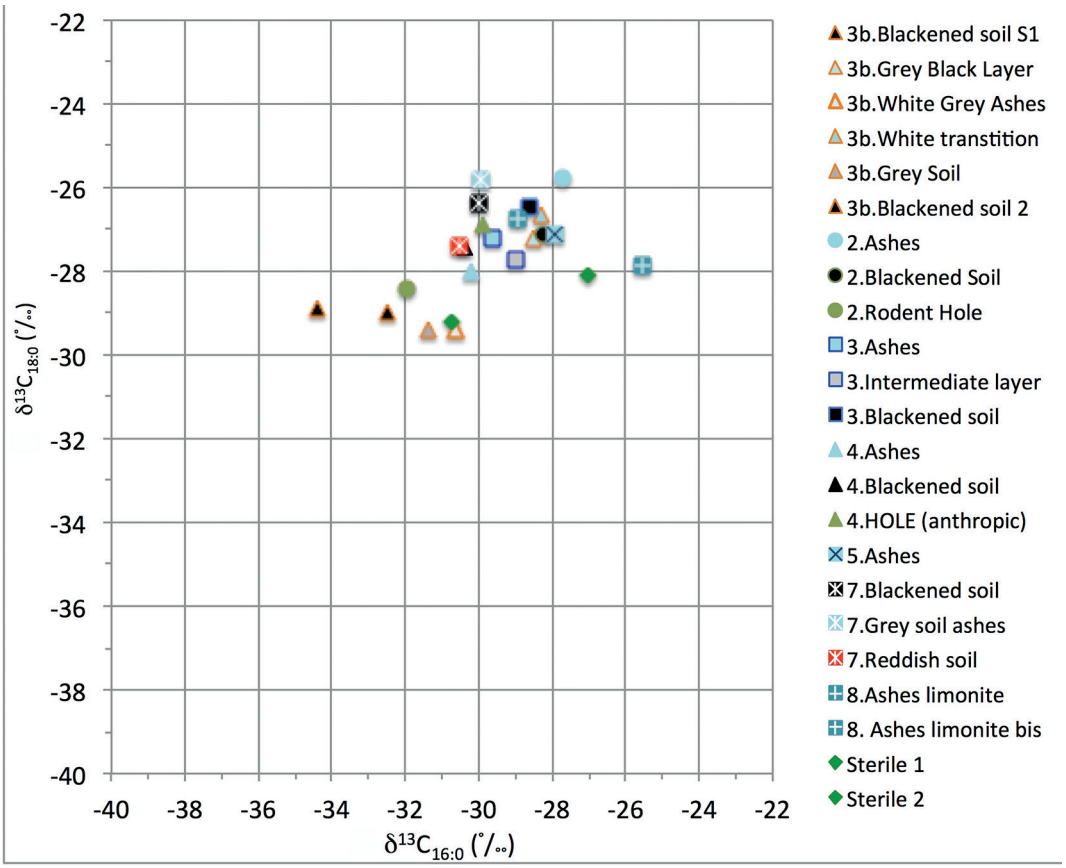

Fig. 18.74. Carbon isotope composition of stearic acid ($d^{13}C_{18:0}$) versus palmitic acid ($d^{13}C_{16:0}$) from Crvena Stijena samples.

fatty acids do not coincide with the values observed for a mesotropic grassland C3 plant community, which shows more depleted values than those observed at Crvena Stijena (mean values = −39.0 from herbs, −36.9 for shrubs, and −36.2 for trees [Dungait et al. 2008] or −37.26 from herbs, −37.66 for shrubs, and −39.02 for trees [Dungait et al. 2010]).

If we compare the mean values of these vegetal samples with animal samples obtained by our and other studies (Evershed et al. 2002; Spangenberg et al.2006; Gregg et al. 2009; Outram et al. 2009; Gregg and Slater 2010; Lucquin et al. 2016; Oras et al. 2017), we can see that Crvena Stijena has $\delta^{13}C$ values of C_{16} and C_{18} more closer to the animal samples although at Crvena Stijena the mean of C_{18} is higher than the mean value of C_{16} (Fig. 18.77). This difference could be explain by the particular animal origin of our samples. As we know, ruminants incorporate specific saturated compounds such as C18:0 directly from their diet into their tissues, following biohydrogenation of the unsaturated precursors in the rumen (Harrison and Leat 1975; Krogdahl 1985; Colonese et al. 2017). This process causes a depletion in $\delta^{13}C$ compared to the synthesized fatty acids such as C_{16}. This differential process is absent in monogastric species such as the omnivorous ones.

When we compare the samples of Crvena Stijena with the data compiled by Evershed (2008) for the British Isles (Fig. 18.78), we can see that some samples coincide with the distribution of horse, goose, or chicken, but most of the samples are situated in a diagonal between horse and pig. The ashes of structure 3 of layer XX fall with the horse samples, and the sterile sample 1 of layer XX is also found near these samples. The samples of ash from structure 4 are situated in the group of adipose samples from goose, and the intermediate layer of structure 3 gives results that coincide with values of the adipose tissue of chicken. No sample can be related to deer, cow,

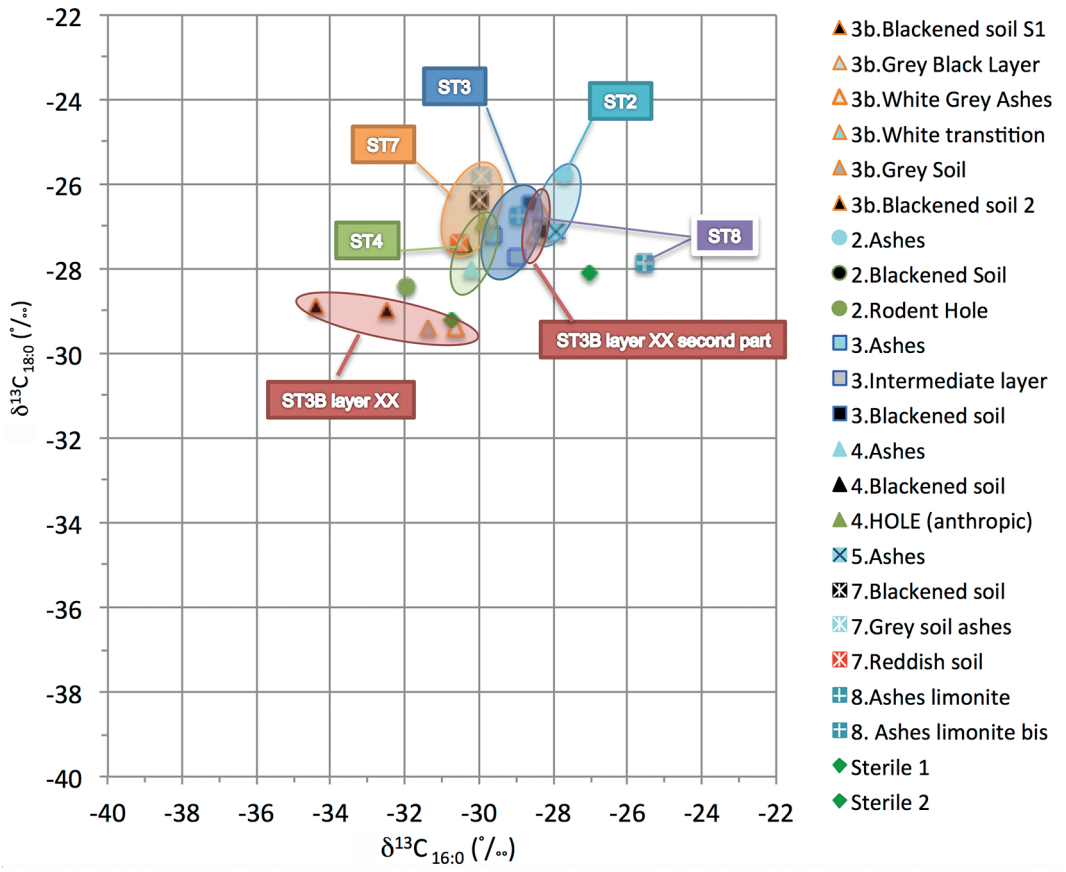

Fig. 18.75. Grouped values by structure of carbon isotope composition of stearic acid ($d^{13}C_{18:0}$) versus palmitic acid ($d^{13}C_{16:0}$) from Crvena Stijena .

or sheep fats. The comparison with the samples coming from Kazakhstan (Outram 2009) shows again a displacement of the Crvena Stijena samples away from the equine adipose area or the ruminant adipose area. Only two samples, the samples of ash limonite of layer XXIV and the sample from the sterile layer XXIII, fall in the confidence intervals presented by Outram from adipose tissues of ruminant or equine.

A comparison with the alpine region using the data of Sangenberg et al. (2006, 2010) and Carrer et al. (2016) shows different relations (Fig. 18.79). Here the enriched samples of Crvena Stijena correspond partially to pig (*Sus scrofa* domesticus) adipose tissue or with young herbivores like calf (*Bos taurus*) and lamb (*Ovis aries*). It is interesting to see that here the adipose tissues of the pig overlap both with the samples of the fire structures and also with the sample of the sterile soil. The range of the isotopic values of this species in the alpine region reflects the present heterogeneity in the alimentation of this omnivore. The samples of leather of wild boar (*Sus scrofa*), chamois (*Rupicapra rupicapra*), red deer (*Cervus elaphus*), and cattle (*Bos taurus*) are positioned near to the adipose tissue of the pig, calf, and lamb and are also near the samples coming from the fire structures of Crvena Stijena. The well-preserved samples, which present more depleted values, are close to the C3 plants of this region. But here the adipose tissue of deer and cattle seem to move away from the Crvena Stijena samples.

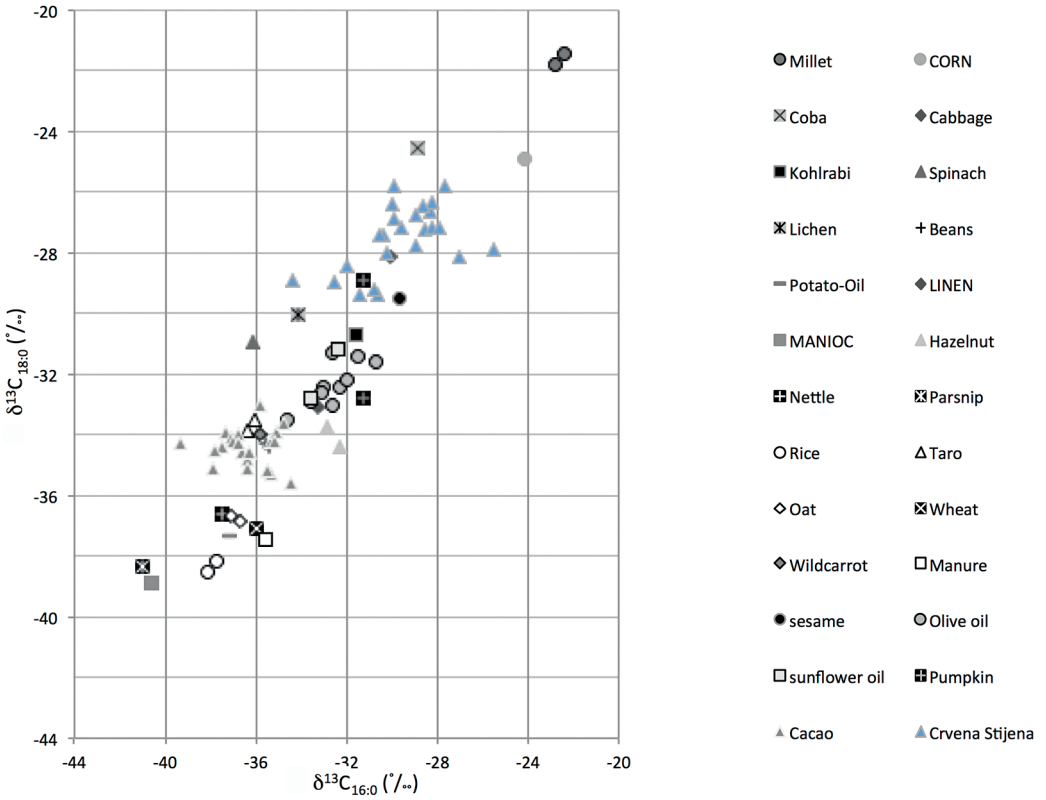

Fig. 18.76. Carbon isotope composition of stearic acid ($d^{13}C_{18:0}$) versus palmitic acid ($d^{13}C_{16:0}$) from Crvena Stijena and modern vegetal samples: millet, *Panicum miliaceum* (leaves-seeds); corn, *Zea mays* (seed); *Cola* sp. (wood); cabbage, *Brassica oleracea*; kohlrabi, *Brassica oleracea* convar; spinach, *Spinacia oleracea* (leaves); lichen (complete); beans, *Phaseolus vulgaris* (seed); taro, *Colocasia esculenta esculenta* (root); wild carrot, *Daucus carota* (root); flax, *Linum usitatissimum* (leaves); hazelnut, *Corylus avellana* (seed); rice, *Oryza sativa* (seed); manioc (cassava), *Manihot esculenta* (root); nettle, *Urtica sp.* (leaves); parsnip, *Pastinaca sativa* (root); potato. *Solanum tuberosum* (root-oil); oat, *Avena sativa* (seed); wheat, *Triticum aestivum* (seed); and cacao (butter). (Our data and Spangerberg and Ogrinc 2001; Spangerberg and Dionisi, 2001) .

The work of Carrer et al. (2016) is most interesting because he has studied the adipose tissue of the chamois (*Rupicapra rupicapra*), the alpine ibex (*Capra ibex*), the roe deer (*Capreolus capreolus*), and the alpine marmot (*Marmota marmota*) four species that are present at Crvena Stijena in a Neanderthal context. As we can see, the value for present-day *Marmota marmota*, a rodent, is situated close to the Crvena Stijena samples. The samples of *Rupicapra rupicapra* and *Capra ibex* are a little further away and more depleted. The samples of cattle (*Bos taurus*) and sheep (*Ovis aries*) are still more depleted and the most distant from the Crvena Stijena samples, as are the samples of red deer (*Cervus elaphus*) which are positioned near the milk and cheese samples.

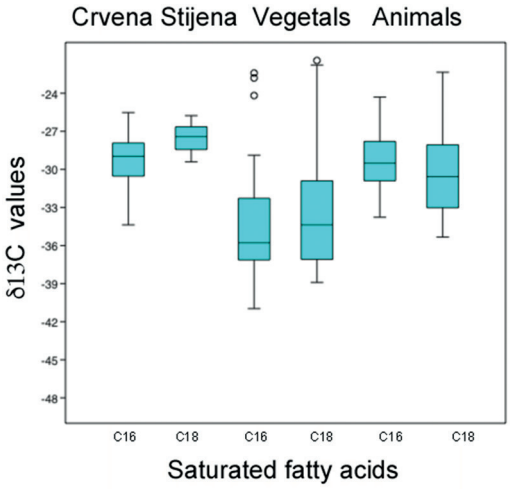

Fig. 18.77. Box chart for d^{13}C values of C16 and C18 fatty acids from our and bibliographic data used in this article.

If we compare our samples with samples coming from some distant areas like Japan (Heron et al. 2016; Lucquin et al. 2016) or North America (Graig et al. 2011, 2012, 2013; Taché and Craig 2015) we can also see some interesting relations (Fig. 18.80). When we compare our samples with the Japan reference samples we see that again the Crvena Stijena samples are situated near the samples of wild boar (*Sus scrofa*) and are distant from the samples of the wild Japanese ruminants. At the same time it interesting to observe that here the samples of Crvena Stijena are near those of freshwater fish and Salmonidae samples. This was not the case for the freshwater fish of Kazakhstan collected by Outram. Certainly, in the faunal list of Crvena Stijena fish are absent, but this could

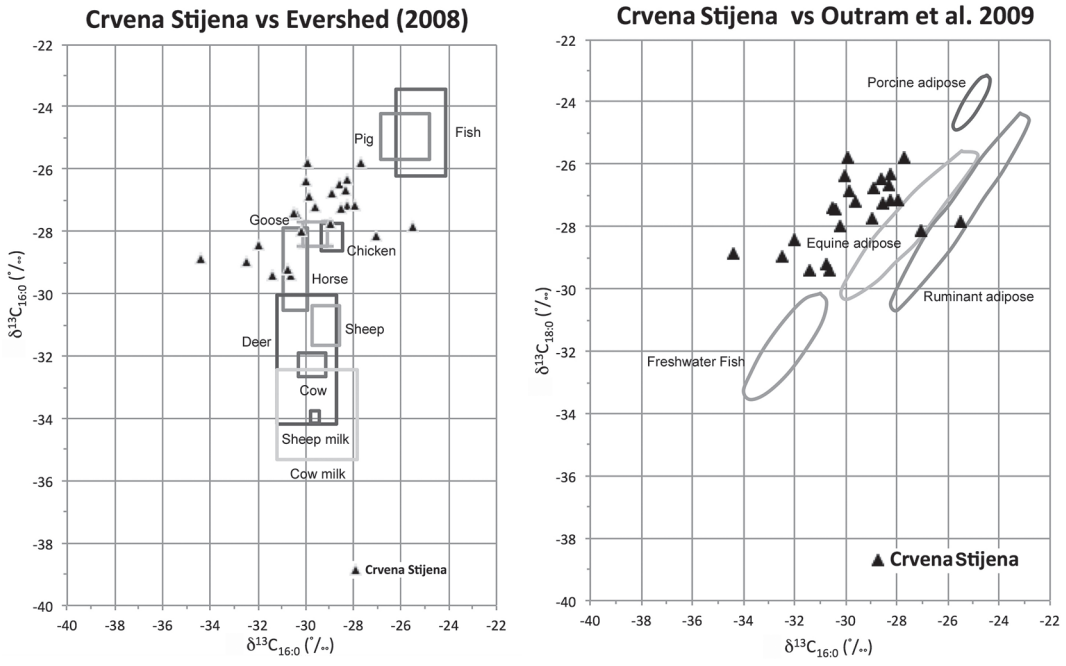

Fig. 18.78. Carbon isotope composition of stearic acid (d^{13}C $C_{18:0}$) versus palmitic acid (d^{13}C $C_{16:0}$) from Mallaha and modern animal samples: pig, fish, chicken, goose, horse, deer sheep cow, and sheep and cow milk from the British Isles (Evershed 2008) and porcine, equine and ruminant adipose and freshwater fishes from Kazakhstan (Outram et al. 2009).

be related to a conservation problem which could be envisaged as a possible explanation. More concrete is the association with the wild boar. The association with omnivore samples is repeated in the comparison with different samples, and this species is present in the layer XXIV list produced by Malez (1975). In the comparison with the North American faunal lipid references, we see first of all that there is a larger number of species situated at enriched positions similar to the position of Crvena Stijena samples. We can observe the proximity of *Ursus americanus* (an omnivore) and the *Procyon lotor* (raccoon, also an omnivore), but we also see samples of *Rangifer tarandus*. Samples coming from Crvena Stijena are always more depleted in C_{16} than the reference ones. It is interesting to see, if we consider the role that Ursidae seem to have occasionally in Neanderthal nutrition, that the only sample of the Ursidae family is situated near the samples of Crvena Stijena, which are far away from the red deer, moose, beaver, hare, muskrat, and otter. Only the white tailed deer are situated close to the Crvena Stijena samples.

Using these results we can compare in a single figure the different values from wild boar and pig (*Sus scrofa* and *Sus scrofa* domesticus) with the data obtained for the Crvena Stijena samples (Fig. 18.81). The comparison has some interesting results. The more depleted samples of Crvena Stijena fall together with the samples collected by Gregg (Gregg et al. 2009) in the Middle East, while other Crvena Stijena samples coincide with the samples of wild boar from France (March 2013) or from the alpine region (Spangenberg 2006). The samples of bones and adipose tissue coming from the work published by Colonese et al. (2017), have also show some coincidence with our Crvena Stijena samples. These results reinforce the hypothesis of the presence of lipids of *Sus scrofa* in Crvena Stijena fire structures, but it must be considered with caution because other omnivores could also have been consumed at the site. The eating of bears by Neanderthals is attested by bone isotopic studies, and the values of the only sample of *Ursus* that we have has values near the samples of Crvena Stijena. If we take into account that omnivorous animals consume a large spectrum of food sources and vary their alimentation frequently compared to herbivores, the carbon present in their fatty acids is going to represent a wide range of nutrients from both animals and plants (Budge et al. 2011; Deniro and Epstein 1978; Howland et al. 2003;

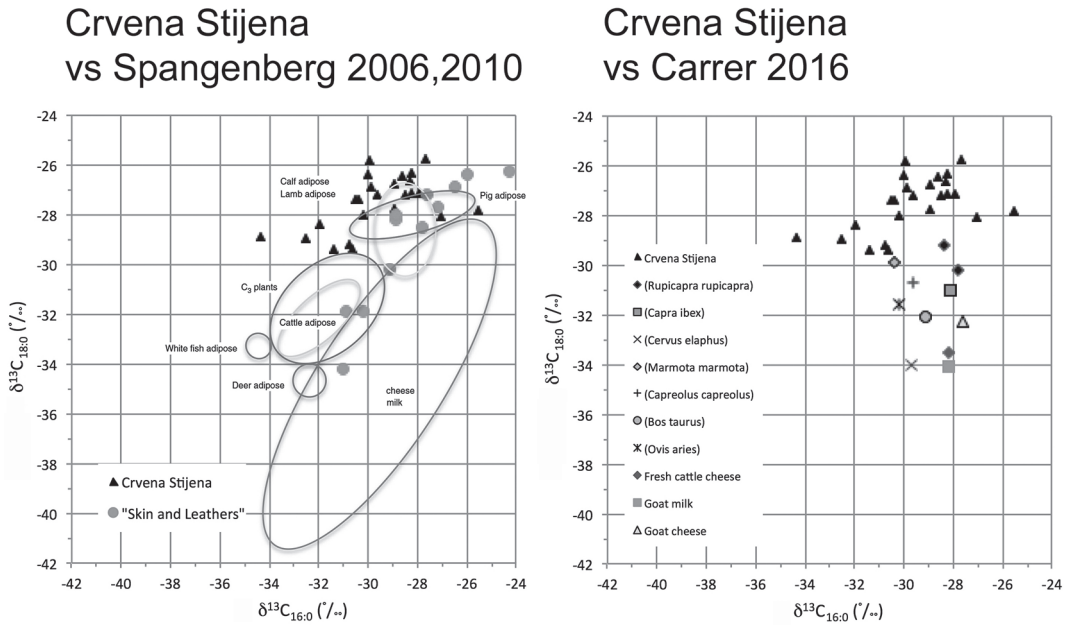

Fig. 18.79. Carbon isotope composition of stearic acid ($d^{13}C\ C_{18:0}$) versus palmitic acid ($d^{13}C\ C_{16:0}$) from Crvena Stijena (Spangerberg et al. 2006, 2010, Carrer 2016) - calf, cattle deer pig and whitefish adipose samples from different places in central Europe (from organic farms and markets) and finally cooked meat from cattle, lamb, and horse.

Rues et Chamberlain 2010; Stott et al. 1997; Trust Hammer et al. 1998), but it is difficult to believe that all the variation observed at Crvena Stijena corresponds to the variation within only one species.

As we see the problem here, it is always the more depleted (in C_{16} or C_{18}) samples of Crvena Stijena that fall in the zones of possible identification, and it remains a fact that the samples of Crvena Stijena are more enriched in C_{18} and more depleted in C_{16} in all the samples that we have analyzed here. Therefore, even if a "fat of omnivores" hypothesis can be supported by these lipid analyses, and even though the samples definitively do not reflect the more common values of ruminants, we must remember that some "cold" cases like the young cattle and sheep of the alpine region are close to samples of caribou coming from cold regions of North America, and we must be cautious and also consider other possibilities. The future study of samples of *Ursus arctos* could help us to better elucidate the omnivore hypothesis. The other problem is that even if we suppose that in the Mediterranean forest landscape there is going to be a lower proportion of C4 plants, we do not know exactly the different photosynthetic pathways of plants that could be consumed by animals in MIS 4 and 5. This could pose some problems because the Crvena Stijena samples show values that could imply the ingestion of certain proportions of C4 plants, or even CAM plants coming from ancient lakes that could have existed in the past, and could create some enrichment of C_{18} signatures (Deniro and Epstein 1978; Stott et al.1997; Morton and Schwartz 2004; Pearson et al. 2007; Rues and Chamberlain 2010; Gregg and Slater 2010). On the other hand, this hypothesis could be rejected considering the depleted values of C_{16}.

Following this discussion, if we determine their $D^{13}C$ values ($= d^{13}C_{18:0} - d^{13}C_{16:0}$) (Copley et al.2003; Copley 2005a, 2005b; Outram et al. 2009; Gregg and Slater 2010; March 2013), we observe that the Crvena Stijena samples nearly all coincide with the porcine (omnivorous) family and are in the region attributed to C3 diets, and only two samples—the degraded sterile sample 1 of layer XXIII and one of the two samples of the ash limonite layer of layer XXIV—are distributed with herbivores and could also correspond to diets more enriched in C4 (Fig. 18.82).

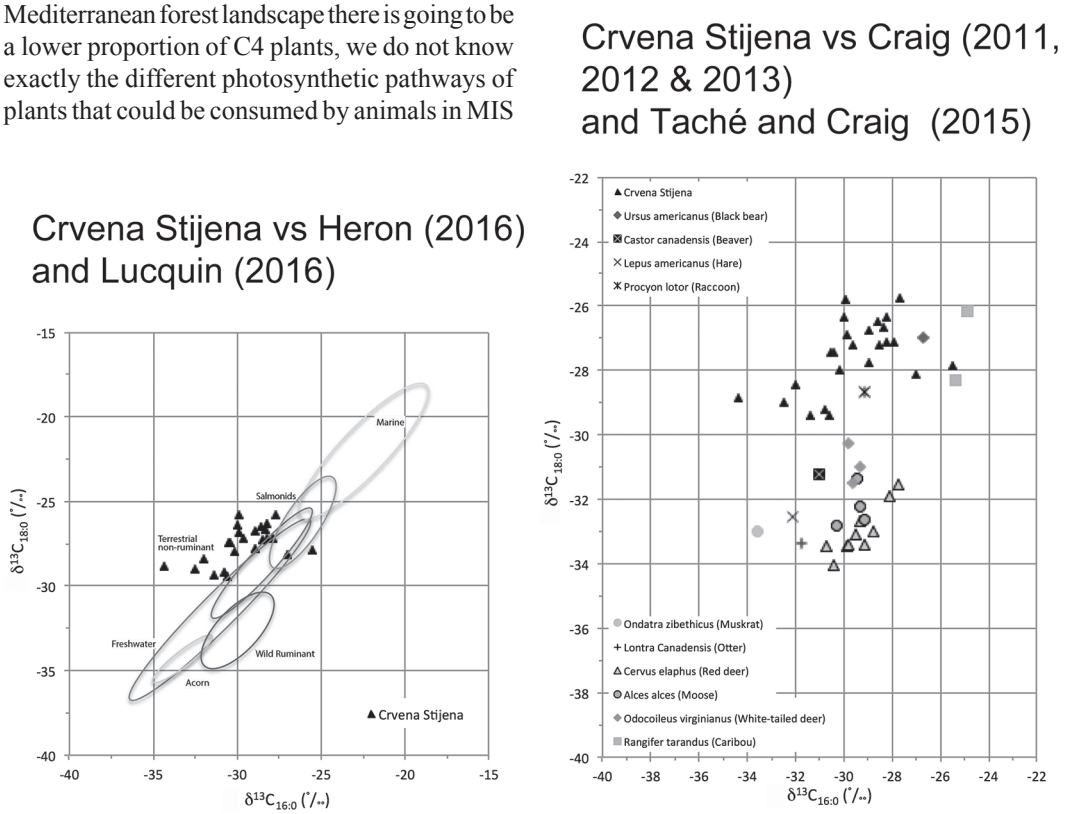

Fig. 18.80. Carbon isotope composition of stearic acid ($d^{13}C\ C_{18:0}$) versus palmitic acid ($d^{13}C\ C_{16:0}$) from Crvena Stijena and modern animal samples from Japan and north America (Japan: Heron et al. 2016, Lucquin et al. 2016; North America: Graig et al. 2011, 2012, 2013, Taché and Craig 2015).

If we link the fatty acids distributions and the isotopic results, we can conclude that the only real matches found in our results are with the Suidae and some young specimens of alpine Bovidae reported by Spangenberg. *Capra ibex* and *Rupicapra* could be also good candidates to complete the list if we think that they had a enriched diet in the past. The fats of *Ursus arctos* can also be

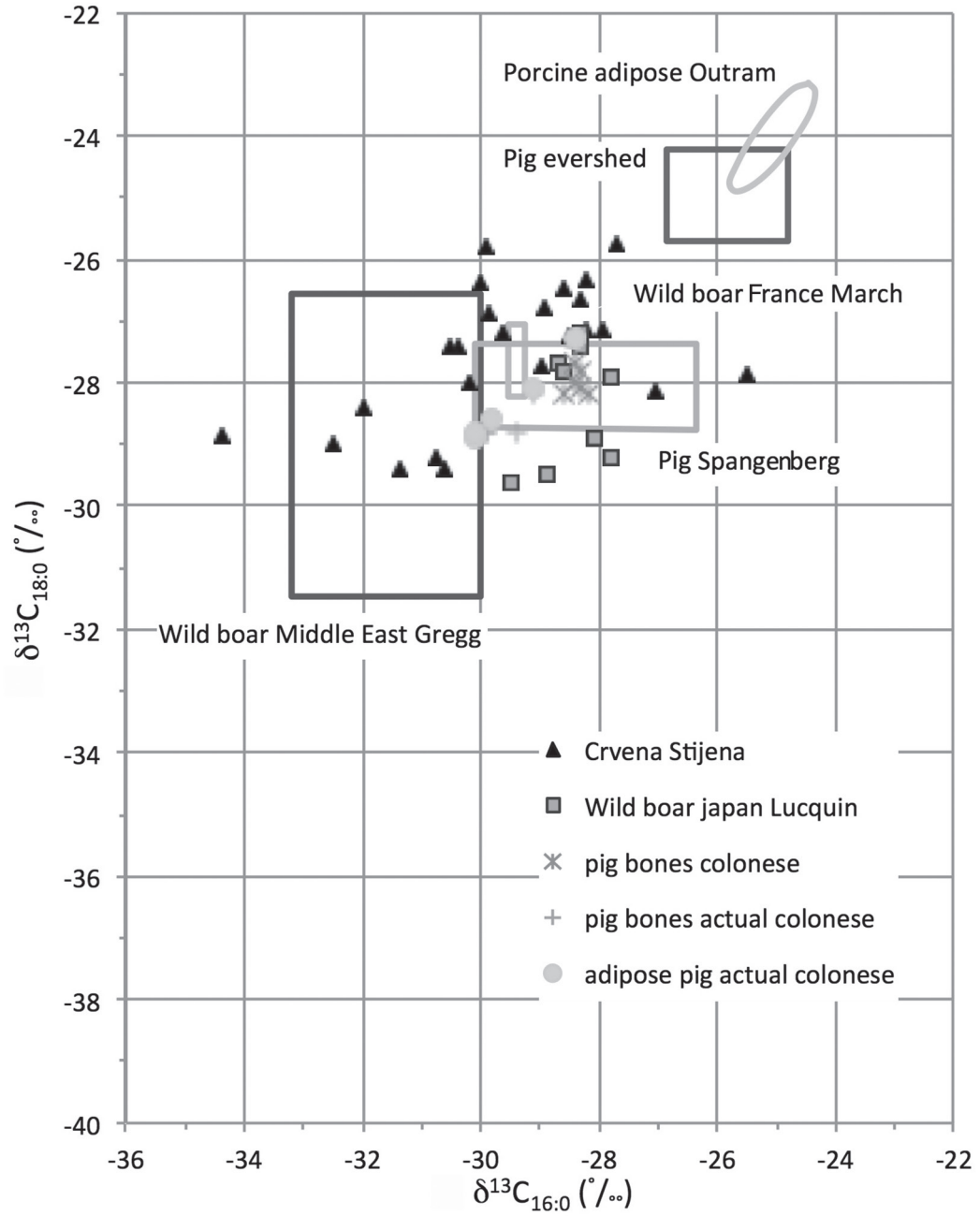

Fig. 18.81. Carbon isotope composition of stearic acid ($d^{13}C\ C_{18:0}$) versus palmitic acid ($d^{13}C\ C_{16:0}$) from Crvena Stijena and modern animal samples: wild boar adipose from Middle East samples (Gregg et al. 2009), pig adipose tissue (Spangenberg 2006), wild boar from Japan (Lucquin et al. 2016), pig from the British Isles (Evershed 2008), and pig from Kazakhstan (Outran et al. 2009); pig bones (archeological and modern C3 diet) and adipose tissue from modern samples from York, England (Colonese et al. 2017), and pig samples and wild boar hunted in France (March 2013).

taken into account, with the advantage that it is also an omnivore and that bears have depleted isotopic values of $\delta^{13}C$ in bone collagen isotopic analysis, but with the disadvantage that bear must have been consumed less than larger herbivores or suids.

Finally, there is another possibility that could support the omnivore hypothesis. Could some samples of fire structures at Crvena Stijena be contaminated with fecal matter? The presence of fecal matter at the comparable Neanderthal site of El Salt was discovered first by the presence of the sterols coprostanol, cholesterol, and cholestanol in the natural soil layers from profile samples, and then, later, of different sterols like coprostanol, cholesterol, cholestanol, and 5β-stigmastanol and coprostanone in new samples and analyses associated with extensive excavation and sampling of fire structures and soils (March et al. 2008). Drawing on my unpublished data from El Salt, a plot of $d^{13}C_{18}$ against $d^{13}C_{16}$ (Fig. 18.83) shows that samples from a blackened layer from one

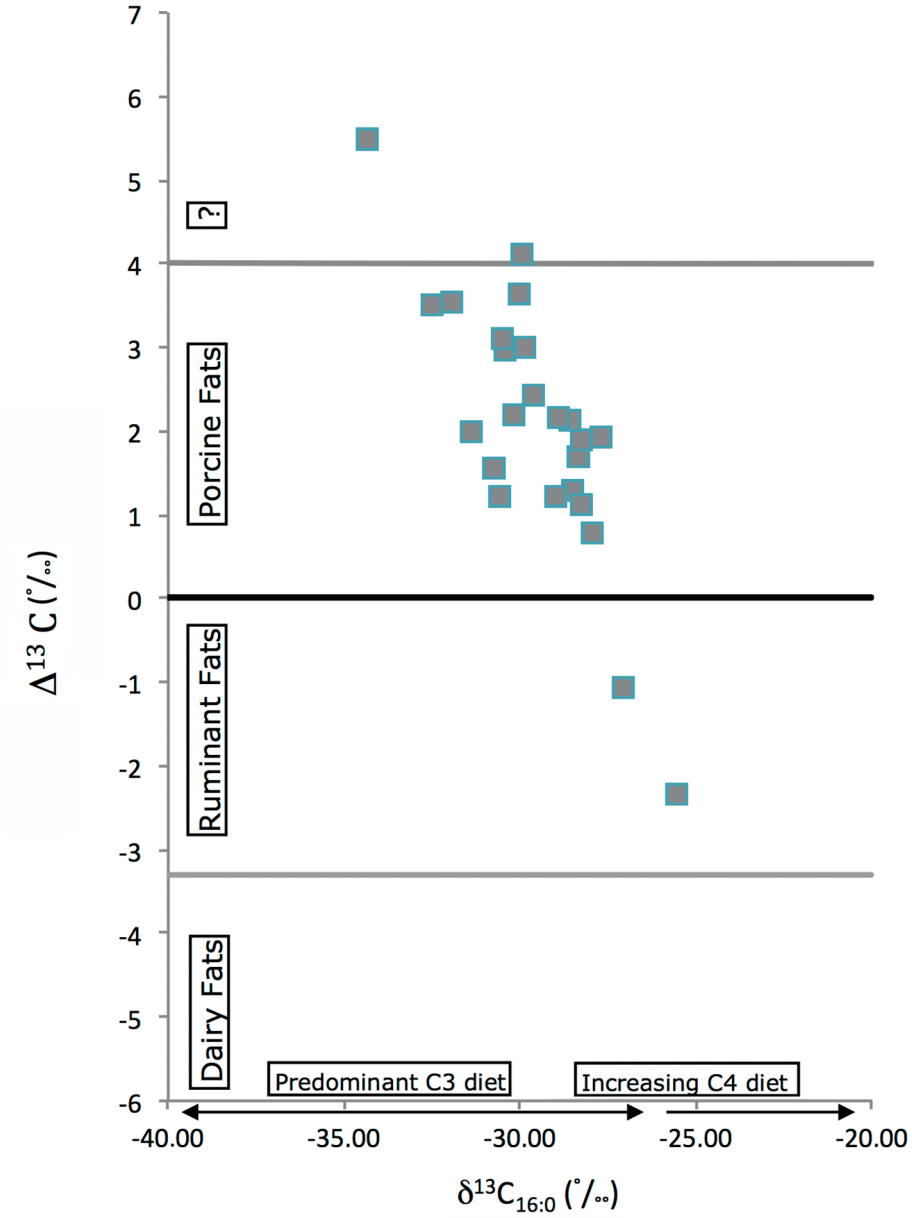

Fig. 18.82. $D^{13}C=(d^{13}C_{18:0} - d^{13}C\ C_{16:0})$, versus palmitic acid ($d^{13}C\ C_{16:0}$) from Crvena Stijena samples.

fire structure and from a white zone and a thermo-altered soil from a second structure coincide exactly with the samples coming from the ash layers of layer XXIV in Crvena Stijena, while a lichen sample coincides with the blackened layer of the big structure 3 of Crvena Stijena layer XX and is near the sterile samples from layer XXIII and the rodent hole. A sample from a bird pellet from El Salt does not coincide with any sample from Crvena Stijena.

We must mention that at El Salt, contrary to the data obtained at Crvena Stijena, the distribution of fatty acids more strongly indicates a Cervidae signature than an omnivore one. These surprising results could reinforce the "omnivore" hypothesis of the origin of the organic matter at Crvena Stijena—the Suidae family also produces fecal matter containing coprostanol. It also may open the door to one species that we so far have not considered, humans. However, other omnivorous or carnivorous species that have not yet been studied could produce coprostanol and some of their derivatives, like the hyena, whose coprolites contain calcium associated with phosphorus, which could also explain some elemental signatures observed at this site. A third hypothesis is the systematic destruction by fire of excrement and other natural remains in the living area. This could explain the association of fire with organic matter having the same isotopic signatures as we have observed. It also could be an alternative explanation for the association of fecal matter and fire structures at El Salt. Unfortunately the samples from Crvena Stijena not preserve the sterol fraction, and we cannot confirm the presence of coprostanol at the site. The rodent hole sample, the only one having well and diverse preserved sterols does not contain traces of coprostanol.

A final possibility is that an unexpected taphonomic factor, for example the ancient presence of worms, could have transformed cholesterol into coprostanol and other derivatives, producing the isotopic signatures that we have found at both sites (fatty acids distribution, sterols, and isotopic values for El Salt and only fatty acids and isotopic values for Crvena Stijena) (Bethell et al. 1994). In this case, the taphonomic processes could explain both situations, the presence of some sterol molecules at El Salt and the isotopic composition observed at both sites. Regrettably the isotopic chemical signature of worms has not yet been studied, but this could be part of a

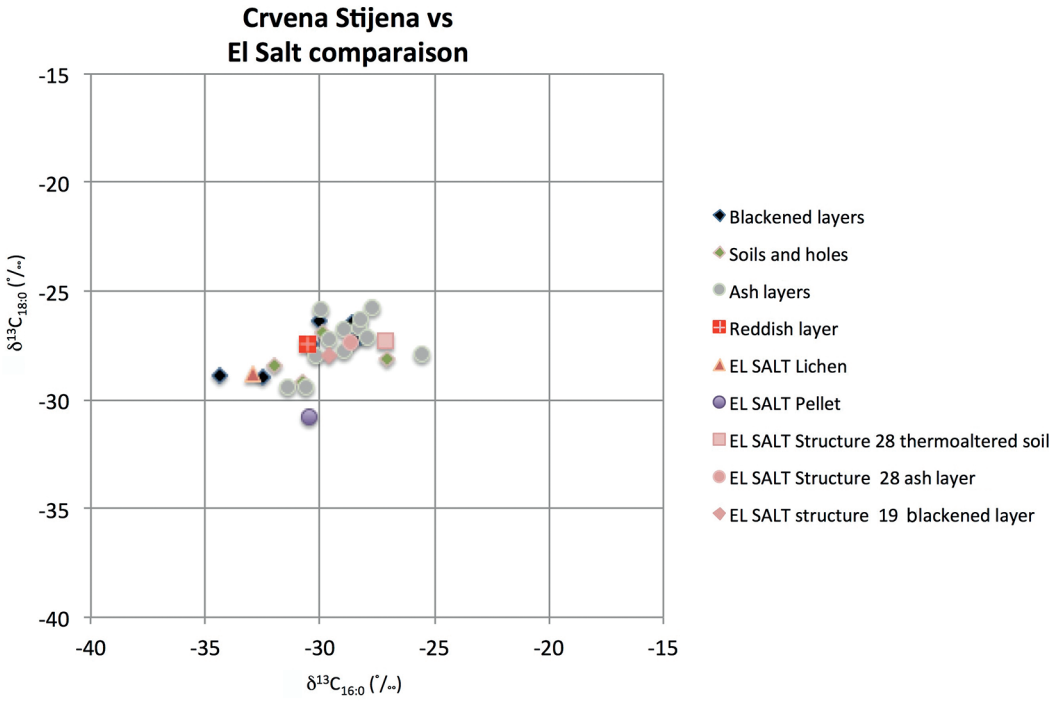

Fig. 18.83. Carbon isotope composition of stearic acid ($d^{13}C\ C_{18:0}$) versus palmitic acid ($d^{13}C\ C_{16:0}$) from Crvena Stijena and from El Salt fire structures and natural samples.

future project that should include also the study of the bones of the extinct fauna found at Crvena Stijena to complete this study.

Final Discussion and Conclusions

This extensive first study of Crvena Stijena samples has tried to obtain the maximum possible information from two sampled profiles in which fire structures are markedly present. This study contributes first at all to the understanding of formation processes of the organic matter in the site. However, it contributes also to the understanding of the formation processes of the different kinds of layers and their archaeological meaning, and to the reconstruction of the formation processes of the site. The difficulties faced here in reconstructing Neanderthal behavior related to fire required, first, the construction of a framework to interpret the organization, form, and rhythm of fire structures and, second, the application of different methods to analyze these structures, their formation processes, and their possible functions.

Proceeding in this manner, we managed to observe some regularities in Neanderthal behavior related to fire, and the formation of different series of fire structures, recognized at the field as ashes that could be the result of fire action in the anthropic soils and that could contain residues from the activities related to fire that Neanderthals had practiced. The elemental and mineralogical analyses and the organic matter approaches reveal a great homogeneity in the constitution of these fire structures and bring to the fore some aspects of their anthropic and natural formation processes. If we exclude the taphonomic hypothesis, anthropic or natural, the fire structures of Crvena Stijena were all related to cooking activities as demonstrated by the animal values of the lipid isotopic signatures and also their possible assignation to omnivores. The isotopic signatures vary within a limited range and all the samples could reflect the consumption of only one species, or a mixture of two or more that must have very similar signatures, close to those that can be found in samples of present-day fauna from the alpine region, or on the plains of North America.

If this is true, the Neanderthal inhabitants of both Crvena Stijena and El Salt could have had very much the same diet, even if the faunal lists of these two sites do not match exactly. If we take into account taphonomic explanations, both sites must have followed the same processes and patterns of organic matter degradation. Even if the this first proposition is itself extraordinary, the second one is not minor because it implies that the transformation of organic matter in these contexts was the same in these two sites although they are separated by thousands of kilometers. In either case, the recurrent forms and dispositions of Neanderthal fire structures reflect regularities in spatial behavior that imply a social construction of these spaces.

These challenging questions open the door to future projects that must include the continuation of experimental work and the resampling of these fire structures when the site will be excavated over broader, horizontal exposures in the future. New projects must also include the study of other living animal species, and also, the analysis of the bones of extinct species which could reveal their isotopic fatty acid composition. Finally, it will be necessary to compare the distribution of these fire structures in different Neanderthal sites in an effort to discover possible regularities. Meanwhile, this first analysis has tried to lay a basis for such future projects and has opened many unsolved questions for in this exciting area of research.

References Cited

Badiani, A., Stipa, S., Bitossi, F., Gatta, P. P., Vignola, G., Chizzolini, R. 2002. Lipid composition, retention and oxidation in fresh and completely trimmed beef muscles as affected by common culinary practices. *Meat Science* 60, 169-186.

Baković, M., Mihailović, B., Mihailović, D., Morley, M., Vušović-Lučić, Z., Whallon, R., Woodward, J. 2009. Crvena Stijena Excavations 2004–2006. *Journal of Eurasian Prehistory* 6(1-2), 3-31.

Banskalieva, V., Sahlu, T., Goetsch, A. L. 2000 Fatty acid composition of goat muscles and fat depots: a review. *Small Ruminant Research* 37, 255-268.

Bar Yosef, O., Cavalli-Sforza, L., March, R. J., Piperno, M. (eds.) 1996. Colloquia Vol. 5, The Lower and Middle Paleolithic: Colloquium IX, *The Study of Human Behavior in Relation to Fire in Archaeology: New Data and Methodologies for Understanding Prehistoric Fire Structures; Colloquium X, The Origin of Modern Man*. XIII International Congress of

prehistoric and protohistoric sciences Forli, Italia-8/14 September 1996. A.B.A.C.O. Edizioni, Forlì, Italy.

Baublits, R. T., Brown, A. H. Jr., Pohlman, F. W., Rule, D. C., Johnson, Z., Onks, D. O., Murrieta, C. M., Richards, C. J., Loveday, H. D., Sandelin, B. A., Pugh, R. B. 2006. Fatty acid and sensory characteristics of beef from three biological types of cattle grazing cool-season forages supplemented with soyhulls. *Meat Science* 72, 100-107.

Belitz, H.-D., Grosch W. 1999. Food chemistry. (translated by P. Hesser, C. Sprinz, S. Jordan, M. Burghagen) (2nd ed.). Springer Verlag, Berlin, Heidelberg.

Bellomo, R.V. 1994. Methods of determining early hominid behavioural activities associated with the controlled use of fire at FxJj 20 Main, Koobi Fora, Kenya. *Journal of Human Evolution* 27, 173-195.

Bèrgadà, M., Poch, R. M., Cervell, J. M. 2015. On the presence of gypsum in the archaeological burial site of Cova des Pas (Menorca, western Mediterranean). *Journal of Archaeological Science* 53, 472-481.

Bethell, P. H., Ottaway, J., Goad, L. J., Evershed, R. P. 1994. The study of molecular markers of human activity: the use of coprostanol in the soil as an indicator of human faecal material. *Journal of Archaeological Science* 21, 619-632.

Binford, L.R. 1983. *In pursuit of the Past*. Thames and Hudson, London.

Binford, L.R. 1978. *Nunamiut Ethnoarchaeology*. Academic Press, New York.

Binford, L.R. 1996. Hearth and home, the spatial analysis of ethnographically documented rock shelter occupations as a template for distinguishing between human and hominid use of sheltered space. In N. Conard and F. Wendorf (eds.), *Middle Paleolithic and Middle Stone Age Settlement Systems*. A.B.A.C.O, Edizioni, Forlì, Italy, 229-239.

Bocherens, H., Drucker, D., Billiou, D., Moussa, I. 2005a. Une nouvelle aproche pour évaluer l'etat de conservation de l'os et du collagène pour les mesures isotopiques (datation au radiocarbon, isotopes stables du carbone et de l'azote). *L'Anthropologie* 109, 557-567.

Bocherens, H., Drucker, D. G., Billiou, D., Patou-Mathis, M., Vandermeersch, B. 2005b. Isotopic evidence for diet and subsistence pattern of the Saint-Césaire I Neanderthal: review and use of a multi-source mixing model. *Journal of Human Evolution* 49, 71-87.

Buonasera, T. 2005. Fatty acid analysis of prehistoric burned rocks: a case study from central California. *Journal of Archaeological Science* 32, 957-965.

Carrer, F., Colonese, A. C., Lucquin, A., Petersen Guedes, E., Thompson, A., Walsh, K., Reitmaier, Th., Craig, O. E. 2016. Chemical Analysis of Pottery Demonstrates Prehistoric Origin for High-Altitude Alpine Dairying in PLoS ONE 11(4), e0151442. doi:10.1371/journal.pone.0151442 April 21, 2016 1-11.

Cattet, M. R. L., Watts, P. D., Sim J. S. 2001. Variation in the chemical composition of adipose tissue of three species of ursids. Canadian Journal of Zoology 79, 1512-1517.

Charrié-Duhaut, A., Burger, P., Maurer, J., Connan, J., Albrecht, P. 2009. Molecular and isotopic archaeology: Top grade tools to investigate organic archaeological materials. *Comptes Rendus Chimie*, Volume 12, Issues 10-11, October-November 2009, 1140-1153.

Cifuni, G. F., Napolitano, F., Riviezzi, A. M., Braghieri, A., Girolami, A. 2004 Fatty acid profile, cholesterol content and tenderness of meat from Podolian young bulls. *Meat Science* 67, 289-297.

Clark J. D., Harris, J. W. K. 1985. Fire and its roles in early hominid lifeways. *The African Archaeological Review* 3, 3-27.

Cochet, N., Georges, B., Meister, R., Florant, G. L., Barré, H. 1999. White adipose tissue fatty acids of Alpine marmots during their yearly cycle. *Lipids* Vol. 34(3), 275-281.

Colonese, A. C., Lucquin, A., Guedes, E. P., Thomas, R., Best, J., Fothergill, B. T., Sykes, N., Foster, A., Miller, H., Poole, K., Maltby, M., Von Tersch, M., Craig, O. E. 2017. The identification of poultry processing in archaeological ceramic vessels using in-situ isotope references for organic residue analysis. *Journal of Archaeological Science* 78, 179-192.

Cooper, J. E., Bray E. E. 1963. A postulated role of fatty acids in petroleum formation. *Geochimica et Cosmochimica Acta* 27, 1113-1127.

Copley, M. S., Berstan, R., Dudd S. N., Docherty, G., Mukherjee, A. J. Straker, V. Payne, S., Evershed, R. P. 2003. Direct chemical evidence for widespread dairying in prehistoric Britain. *Proceedings of the National Academy*

of Sciences of the USA 100, 1524-1529.

Copley, M. S., Berstan, R., Dudd, S. N., Straker, V., Payne, S., Evershed, R. P. 2005a. Dairying in antiquity. I. Evidence from absorbed lipid residues dating to the British Iron Age*, Journal of Archaeological Science* 32 4, 485-503.

Copley, M.S., Berstan, R., Straker, V., Payne, S., Evershed, R.P. 2005b. Dairying in antiquity. II. Evidence from absorbed lipid residues dating to the British Bronze Age, *Journal of Archaeological Science* 32 4, 505-521.

Costamagno, S., Thèry-Parisot, I., Brugal, J.-P., Guibert, R. 2005. Taphonomic consequences of the use of bones as fuel. Experimental data and archaeological application. In *9th ICAZ Conference, Durham, 2002*, Vol. 7. Oxford Books, Oxford, 52-62.

Courty, M. A., Carbonell, E., Vallverdú-Poch, J., Banerjee, R. 2012. Microstratigraphic and multi-analytical evidence for advanced Neanderthal pyrotechnology at Abric Romani (Capellades, Spain). Quaternary International 247, 294-312.

Craig, O. E., Steeleb, V. J., Fischer, A., Hartz, S., Andersen, S. H., Donohoe, P., Glykou, A., Saul, H., Jones, D. M., Koch, E., Heron, C. P. 2011. Ancient lipids reveal continuity in culinary practices across the transition to agriculture in northern Europe. *Proceedings of the National Academy of Sciences of the USA* 108, 17910-15.

Craig, O. E., Allen, R. B., Thompson, A., Stevens, R. E., Steele, V. J., Heron, C. P. 2012. Distinguishing wild ruminant lipids by gas chromatography/combustion/isotope ratio mass spectrometry. *Rapid Communications in Mass Spectrometry* 26, 2359-64.

Craig, O. E., Saul, H., Lucquin, A., Nishida, Y.,Taché, K., Clarkes, L., Thompson, A., Altoft, D.T., Uchiyama, J., Ajimoto, M., Gibbs, K., Isaksson, S., Heron, C. P., Jordan, P. 2013. Earliest evidence for pottery use. *Nature* 496, 351-54.

Crawford, M. A., Gale, M. M., Woodford, M. H., Casperd, N. M. 1970. Comparative studies on fatty acid composition of wild and domestic meats. *International Journal of Biochemistry,* 1(3), 295-305.

Crawford, M. A., Casperd, N. M., Sinclair, A. J. 1970. The long chain metabolites of linoleic and linolenic acids in liver and brain in herbivores and carnivores. *Comparative Biochemistry and Physiology - Part B: Biochemistry and Molecular Biology* 54B, 395-401.

Dalle Zotte, A. 2002. Perception of rabbit meat quality and major factors influencing the rabbit carcass and meat quality. *Livestock Production Science* 75, 11-32.

Deniro M. J., Epstein S. 1978. Influence of diet on the distribution of carbon isotopes in animals *Geochimica et Cosmochimica Acta* 42, 495-506.

Dungait J. A. J., Docherty, G., Straker, V., Evershed R. P. 2008. Interspecific variation in bulk tissue, fatty acid and monosaccharide d13C values of leaves from a mesotrophic grassland plant community. *Phytochemistry* 69, 2041-2051.

Dungait J. A. J., Docherty, G., Straker, V., Evershed, R. P. 2010 Seasonal variations in bulk tissue, fatty acid and monosaccharide d13C values of leaves from mesotrophic grassland plant communities under different grazing managements *Phytochemistry* 71, 415-428.

Eglinn, G., Hamilton, R. J., 1963. The distribution of alkanes. In T. Swain (ed.), *Chemical Plant Taxonomy*. Academic Press, 187-217.

Eglinn, G., Pancost, R. 2004. Immortal molecules. *Geoscientist* 14, 4-16.

Eglinn, T. I., Eglinn, G. 2008. Molecular proxies for paleoclimatology. *Earth and Planetary Science Letters* 275, 1-16.

Eerkens, J. W. 2005. GC-MS Aanalysis and fatty acid ratios of archaeological potsherds from the western Great Basin of north America. *Archaeometry* 47, 83-102.

Elias Calles, J. A., Gaskins, C. T., Busboom, J. R., Duckett, S. K., Cronrath, J. D., Reeves, J. J. 2000. Sire variation in fatty acid composition of crossbred Wagyu steers and heifers. *Meat Science* 56, 23-29.

Emsley, J., 1998. *The Elements*, 3rd ed. Clarendon Press, Oxford.

Enser, M., Hallett, K., Hewett, B., Fursey, G. A., Wood, J. D. 1996. Fatty acid content and composition of English beef, lamb and pork at retail. *Meat Science* 42, 443-458.

Enser, M., Richardson, R. I., Wood, J. D., Gill, B. P., Sheard, P. R. 2000. Feeding linseed to increase the n-3 PUFA of pork: fatty acid composition of muscle, adipose tissue, liver and sausages. *Meat Science* 55, 201-212.

Evershed, R. P. 1993. Biomolecular archaeology and lipids. *World Archaeology* 25(1), 74-93.

Evershed, R. P., Bethell, P. H., Reynolds P. J., Walsh, N. J. 1997. 5β-Stigmastanol and Related 5β-Stanols as Biomarkers of Manuring: Analysis of Modern Experimental Material and Assessment of the Archaeological Potential. *Journal of Archaeological Science* 24, 485-495.

Evershed, R. P., Dudd, S. N., Coppley, M. S., Mutherjee, A. 2002. Identification of animals fats via compound specific d ^{13}C values of individual fatty acids: assessments of results for reference fats and lipid extracts of archaeological pottery vessels. *Documenta Praehistorica* XXIX, 73-96.

Evershed, R. P. Heron, C., Charters, S., Goad, L. J. 1992. The survival of food residues: new methods of analysis, interpretation and application. In A. M. Pollard (ed.), *New Developments in Archaeological Science. A Joint Symposium of the Royal Society and the British Academy, February 1991*. Oxford University Press, 187-208.

Evershed, R. P., Connolly, R. C. 1994 Post-mortem transformations of sterols in bog body tissues. *Journal of Archaeological Science* 21, 577-583.

Ferreri J. C., March R. J. 1996. Using numerical models to analyze archaeological simple fire structures. In O. Bar-Yosef, L. L. Cavalli-Sforza, R. J. March and M. Piperno (eds.), *The Lower and Middle Palaeolithic. The Origin of Modern Man*. XIII International Congress of the IUPPS. Forlì-Italia 1996. Section 5, Colloquium X. A.B.A.C.O. Edizioni, Forlì, Italy, 57-63.

Ficken K. J., Li, B., Swain, D. L., Eglinn, G. 2000. An n-alkane proxy for the sedimentary input of submerged/ floating freshwater aquatic macrophytes. *Organic Geochemistry* 31, 745-749.

Fiorenza, L. 2015. Reconstructing diet and behaviour of Neanderthals from Central Italy through dental macrowear analysis. *Journal of Anthropological Sciences* 93, 1-15.

Fiorenza, L., Benazzi, S., Henry, A. G., Salazar-Garcia, D. C., Blasco, R., Picin, A., Wroe, S., Kullmer, O. 2015. To meat or not to meat? New perspectives on Neanderthal ecology. *American Journal of Physical Anthropology* 156, 43-71.

Forsten, A., Dimitrijevic, V. 2004 Pleistocene horses (genus *Equus*) in the central Balkans. *Annales Géologiques de la Péninsule Balkanique* 65(2002-2003), 55-75 Belgrade.

Frausto Da Silva, J. J. R., Williams, R. J. P. 2001. *The Biological Chemistry of the Elements: the Inorganic Chemistry of Life*. Oxford University Press, Oxford.

Fredriksson Eriksson, S., Pickova, J. 2007. Fatty acids and tocopherol levels in M. Longissimus dorsi of beef cattle in Sweden - A comparison between seasonal diets *Meat Science* 76, 746-754.

Friedli, H., Lötscher, H., Oeschger, H., Siegenthaler, U., Stauffer, B. 1986. Icecore record of the $^{13}C/^{12}C$ ratio of atmospheric CO2 in the past two centuries. *Nature* 324, 237-38.

García-Olmo, J., De Pedro, E., Garrido, A., Paredes, A., Sanabria, C., Santolalla, M., Salas, J., García-Hierro, J. R., Gonzalez, I., García-Cachang, M. D., Guirao, J. 2002. Determination of the precision of the fatty acid analysis of Iberian pig fat by gas chromatography. Results of a mini collaborative study. *Meat Science* 60, 103-109.

Goldberg, P., Dibble, H., Berna, F., Sandgathe, D., McPherron, S. J. P., Turq, A. 2012. New evidence on Neandertal use of fire: examples from Roc de Marsal and Pech de l'Aze IV. *Quaternary International* 247, 325-340.

Goudsblom, J. 1992. *Fire and Civilization*. Viking, London.

Gregg, M. W., Banning, E. B., Gibbs, K., Slater, G. F. 2009. Subsistence practices and pottery use in Neolithic Jordan: molecular and isotopic evidence. *Journal of Archaeological Science* 36, 937-946.

Gregg, M. W., Slater, G. F. 2010. A new method for extraction, isolation and transesterification of free fatty acids from archaeological pottery. *Archaeometry* 52, 833-854.

Guil-Guerrero, J. L., Rodríguez-García, I., Kirillova, I. Shidlovskiy, F., Ramos-Bueno, R. P., Savvinov, G., Tikhonov, A. 2015. The PUFA-Enriched Fatty Acid Profiles of some Frozen Bison from the Early Holocene found in the Siberian Permafrost *Nature Scientific Reports* 5, 7926.

Gunstone, F. D., Harwood, J. L., Padley, F. B. 1995. *The lipid handbook*. Chapman and Hall, London & New York.

Haenlein, G.F.W. 2004. Goat milk in human nutrition. *Small Ruminant Research* 51, 155-163.

Henry, A. G., Brooks, A. S., Piperno, D. R. 2011. Microfossils in calculus demonstrate

consumption of plants and cooked foods in Neanderthal diets (Shanidar III, Iraq; Spy I and II, Belgium). *Proceedings of the National Academy of Sciences of the USA* 108, 486-491.

Henry, A. G., Brooks, A. S., Piperno, D. R. 2014. Plant foods and the dietary ecology of Neanderthals and early modern humans. *Journal of Human Evolution* 69, 44-54.

Henry, D. O., Hietala, H. J., Rosen, A. M., Demidenko, Y. E., VitaliyI, U., Armagan, T. L. 2004. Human Behavioral Organization in the Middle Paleolithic: Were Neanderthals Different? *American Anthropologist* 106, 17-31.

Henry, D. O. 2012. The palimpsest problem, hearth pattern analysis, and Middle Paleolithic site structure. *Quaternary International* 247, 246-266.

Harrison, F. A., Leat, M. F. 1975. Digestion and absorption of lipids in non-ruminant and ruminant animals: a comparison. *Proceedings of the Nutrition Society* 34, 203-210.

Heron, C., Evershed, R. P., Goad, L. J., Denham, V. 1991. New approaches to the analysis of organic residues from archaeological ceramics. in P. Budd, B. Chapman, C. Jackson, R. Janaway and B. Ottaway (eds.), *Archaeological Sciences 1989. Proceedings of a Conference on Archaeological Sciences*. Oxbow Monographs 9, Oxbow Publications, Oxford, 332-339.

Heron, C., Habu J., Katayama Owens, M., Ito Y., Eley, Y., Lucquin, A., Radini, A., Saul, H., Debono Spiteri, C., Craig, O. E. 2016. Molecular and isotopic investigations of pottery and 'charred remains' from Sannai Maruyama and Sannai Maruyama No. 9, Aomori Prefecture, Japan. *Japanese Journal of Archaeology* 4, 29-52.

Hilditch, T. P., Williams, P. N. 1964. *The Chemical Constitution of Natural Fats.* Chapman-Hall, London.

Hoffman, L.C., Wiklund E. 2006. Game and venison - meat for the modern consumer *Meat Science* 74, 197-208.

Högberg, A., Pickova, J., Stern, S., Lundström, K., Bylund, A.-C. 2004. Fatty acid composition and tocopherol concentrations in muscle of entire male, castrated male and female pigs, reared in an indoor or outdoor housing system. *Meat Science* 68, 659-665.

Hubbard, A. W., Pocklington W. D. 1968. Distribution of fatty acids in lipids as an aid to the identification of animal tissues. I. - Bovine, porcine, ovine and some avian species. *Journal of the Science of Food and Agriculture* 19, 571-577.

Hough, W. 1926. *Fire as an Agent in Human Culture*. Bulletin of the United States National Museum 139.

Hough, W. 1928. The Story of Fire. Doubleday, Doran & Company, Garden City, N. Y.

Ivanova S., Gurova, M., Spassov, N., Hristova, L., Tzankov, N., Popov, V., Marinova, E., Makedonska, J., Smith, V., Ottoni, C., Lewis, M. 2016. Magura Cave, Bulgaria: A multidisciplinary study of Late Pleistocene human palaeoenvironment in the Balkans *Quaternary International* 415, 86-108.

Iverson, S. J., Oftedal, O. T. 1992. Fatty Acid composition of Black Bear (*Ursus americanus*) milk during and after the period of winter dormancy. *Lipids* 27, 940-943.

Iverson, S. J., McDonald, Jr., J. E., Smith, L. K. 2001, Changes in the diet of free-ranging black bears in years of contrasting food availability revealed through milk fatty acids. *Canadian Journal of Zoology* 79, 2268-2279.

Jandal, J. M. 1996. Comparative aspects of goat and sheep milk. *Small Ruminant Research* 22, 177-185.

James. S. R. 1989. Hominid use of fire in the Lower and Middle Pleistocene: A review of the evidence. *Current Anthropology* 30, 1-26.

James, S. R. 1996. Early Hominid use of fire: Recent approaches and methods for evaluation of the evidence. In O. Bar-Yosef, L. L. Cavalli-Sforza, R. J. March and M. Piperno (eds.), *The Lower and Middle Palaeolithic. The Origin of Modern Man*. XIII International Congress of the IUPPS. Forlì-Italia 1996. Section 5, Colloquium X. A.B.A.C.O. Edizioni, Forlì, Italy, 65-75.

Joly, D., March, R. J. 2003. Étude des ossements brûlés: nouvelles méthodes pour la détermination des temperatures. In Frère Sautôt et al. (eds.) Le Feu Domestique et ses Structures au Néolithique et aux Âges des Métaux. Actes du colloque Bourg-en-bresse 7 et 8 Octobre 2000 Beaune (France) Préhistoires (Vol. 9). Editions Monique Mergoil, Montagnac, 299-311.

Kagawa, M., Matsubara, K., Kimura, K., Shiono, H., Fukui, Y. 1996. Species identification by the positional analysis of fatty acid composition in triacylglyceride of adipose and bone tissues. *Forensic Science International* 79, 215-226.

Käkela, R., Hyvärinen, H. 1996. Site-specific fatty acid composition adipose tissues of several northern aquatic and terrestrial mammals. *Comparative Biochemistry and Physiology - Part B: Biochemistry and Molecular Biology* 115, 501-514.

Karavanić, I. 2007. Le Moustérien en Croatie. *L'Anthropologie* 111, 321-345.

Karkanas, P., Shahack-Gross, R., Ayalon, A., Bar-Matthews, M., Barkai, R., Frumkin, A., Gopher, A., Stiner, M. C. 2007. Evidence for habitual use of fire at the end of the Lower Paleolithic: Site-formation processes at Qesem Cave, Israel. *Journal of Human Evolution* 53, 197-212.

Krajcarz, M. T., Krajcarz, M., Marciszak, A. 2014. Paleoecology of bears from MIS 8 and MIS 3 deposits of Bisnik Cave based on stable isotopes ($d^{13}C$, $d^{18}O$) and dental cementum analyses. *Quaternary International* 326-327, 114-124.

Koirala, B., Rosentreter, J. 2009. Examination of prehistoric artifacts via fatty acid methyl ester (FAME) techniques using modern environmental stewardship. *Journal of Archaeological Science* 36, 1229-1242.

Krogdahl, A., 1985. Digestion and absorption of lipids in poultry. *Journal of Nutrition* 115, 675-685.

Lee, Ch.-E., Seong, P.-N., Oh, W.-Y., Ko, M.-S., Kim, K.-I., Jeong, J.-H. 2007. Nutritional characteristics of horsemeat in comparison with those of beef and pork. *Nutrition Research and Practice* 1, 70-73.

Leat, W. M. F., Northrop, Ch. A., Buttress, N., Jones, D. M. 1979. Plasma lipids and lipoproteins of some members of the order perissodactyla. *Comparative Biochemistry and Physiology - Part B: Biochemistry and Molecular Biology* 63, 275-281.

Leroi-Gourhan, A., Brézillon, M. (eds.). 1972. *Fouilles de Pincevent - Essai d'Analyze Ethnographique d'un Habitat Magdalénien (la Section 36)*. VII° supplément à *Gallia Préhistoire*, CNRS, Paris.

Lucquin, A. 2007. Étude Physico chimique des méthodes de cuisson pré et proto historiques. Ph.D. dissertation, Université de Rennes.

Lucquin, A., Gibbs, K., Uchiyama, J., Saul, H., Ajimoto, M., Eley, Y., Radini, A., Heron, C. P., Shoda, S., Nishida, Y., Lundy, J., Jordan, P., Isaksson, S., Craig, O. E. 2016. Ancient lipids document continuity in the use of early hunter-gatherer pottery through 9,000 years of Japanese prehistory. *Proceedings of the National Academy of Sciences of the USA* 113, 3991-3996.

McCarthy, R. D., Duthie, A. H. 1962. A rapid quantitative method for the separation of free fatty acids from other lipids. *The Journal of Lipid Research* 3, 117-119.

Malainey, M. E., Przybylski, R., Sherriff, B. L. 1999a. The fatty acid composition of native food plants and animals of Western Canada. *Journal of Archaeological Science* 26, 83-94.

Malainey, M. E., Przybylski, R., Sherriff, B. L. 1999b. The effects of thermal and oxidative degradation on the fatty acid composition of food plants and animals of Western Canada: implications for the iIdentification of archaeological vessel residues. *Journal of Archaeological Science* 26, 95-103.

Malez, M. 1975. Kvartarna fauna Crvene Stijene. In Đ. Basler (ed.), *Crvena stijena - zbornik radova*. Zajednica kulturnih ustanova, Posebno izdanje 3-4, Nikšić, 147-169.

Mallol, C., Hernández, C. M., Cabanes, D., Sistiaga A., Machado, J., Rodríguez, Á., Pérez, L., Galván, B. 2013. The black layer of Middle Paleolithic combustion structures. Interpretation and archaeostratigraphic implications *Journal of Archaeological Science* 40, 2515-2537.

Mamani-Linares, L. W., Gallo, C. 2013. Perfil de ácidos grasos de carne de ovino y caballo criados bajo un sistema de producción extensiva. *Revista de Investigaciones Veterinarias del Perú* 24(3), 257-263.

March, R. J., Baldessari, A., Gross, E. G. 1989. Determinacion de compuestos orgánicos en estructuras de combustion arqueológicas. In M. Olive and Y. Taborin (eds.), *Nature et Function des Foyers Préhistoriques*, Actes du Colloque International de Nemours (1987), Mémoires du Musée de Préhistoire d'Ile-de-France 2. APRAIF, Nemours, 47-58.

March, R. J., Baldessari, A., Gros, E. G., Ferreri, J. C., Morello, O., Rodano, R. 1989. Étude des structures de combustion archéologiques d›Argentine. *Bulletin de la Société Préhistorique Française*, 10-12, 384-392.

March, R. J. 1995. *Méthodes physiques et chimiques appliquées à l'étude des structures de combustion préhistoriques: l'approche par*

la chimie organique Thèse de Doctorat, 3 vol., Université de Paris I, Panthéon Sorbonne.

March R. J. 1996. L'étude des structures de combustion préhistoriques: une approche interdisciplinaire. In O. Bar-Yosef, L. L. Cavalli-Sforza, R. J. March and M. Piperno (eds.), *The Study of Human Behavior in Relation to Fire in Archaeology: New Data and Methodologies for Understanding Prehistoric Fire Structures*. XIII International Congress of the IUPPS. Forlì-Italia 1996. Section 5, Colloquium IX. A.B.A.C.O. Edizioni, Forlì, Italy, 251-275.

March, R.J. 1999. Chimie organique appliquée à l'étude des structures de combustion du site de Túnel I. *Revue d'Archéometrie* 23, 127-156.

March R. J. 2002. Il controllo del fuoco. In *Il Mondo dell'Archeologia*, vol. II. Enciclopedia Italiana Treccani, 807-812.

March R. J. 2013. Searching for the Functions of Fire Structures in Eynan (Mallaha) and their Formation Processes: a Geochemical Approach, In O. Bar Yosef and F. Valla (eds.), *Natufian Foragers in the Levant: Terminal Pleistocene Social Changes in Western Asia*. International Monographs in Prehistory, Archaeological Series 19, Ann Arbor, Michigan, 227-283.

March, R. J. 2017. Finding, Analyzing, and Interpreting Organic Matter in Archaeology: A Complex Subject. Paper presented at the symposium, "The science of organic residue analysis and the art of cultural interpretation," 82nd Annual Meeting, Society for American Archaeology.

March, R. J., Ferreri, J. C. 1989. Sobre el estudio de estructuras de combustión arquelógicas mediante replicaciones y modelos numéricos, In M. Olive and Y. Taborin (eds.), *Nature et Function des Foyers Préhistoriques*. Actes du colloque international de Nemours (1987), Mémoires du Musée de Préhistoire d'Ile-de-France 2. APRAIF, Nemours, 59-69.

March, R. J., Ferreri, J. C. 1991. Aplicación de modelos numéricos para la inferencia del tiempo de quemado en estructuras de combustión arqueológicas: Influencia de parámetros, In *Actas del IX Congreso Nacional de Arqueologia Chilena*. Museo Nacional de Historia Natural, Santiago de Chile, Chile, 157-168.

March, R. J., Muhieddine, M., Canot, E. 2010. Simulation 3D des structures de combustión préhistoriques. In R. Vergnieux and C. Delevoie C. (eds.), *Actes du Colloque Virtual Retrospect 2009*, Archéovision 4. Editions Ausonius, Bordeaux, 29-39.

March, R. J., Joly, D., Lucquin, A., Dumarçay, G. 2006. Les activités liées à l'utilisation du feu. In P. Bodu, M. Julien, B. Valentin, G. Debout (eds.), *Un dernier hiver à Pincevent: les magdaléniens du Niveau IV-0 (Pincevent, La Grande-Paroisse, Seine-et-Marne), Gallia Préhistoire* 48, 89-108.

March, R. J., Dumarçay, G., Lucquin, A. 2006. De la gestion des déchets de combustion à l'organization de l'espace. In P. Bodu, M. Julien, B. Valentin, G. Debout (eds.), *Un dernier hiver à Pincevent: les magdaléniens du Niveau IV-0 (Pincevent, La Grande-Paroisse, Seine-et-Marne), Gallia Préhistoire* 48, 109-116.

March, R. J., Dorta, R., Sistiaga, A., Galván, B., Hernández, C. 2008. Tras el fuego de los neandertales. Química Orgánica aplicada al estudio de los fogones de El Salt. In *Actas del VI Congreso Ibérico de Arqueometria, 7-9 Octobre 2007*. Museo Nacional de Arqueología, Madrid, 28-41.

March, R. J., Guillou, C., Cordero., J. A., Thiebault, J.-N., Ganier, P. H. 2017. Processus de formation des signatures lipidiques dans les sols: une approche expérimentale. Paper presented at the 40th Colloquium of GMPCA. Rennes, France April 2017.

March, R. J., Largeau, C., Guenot, P. 2003. Les structures de combustion du bronze final du gisement Le Closeau (IFP et Parcelle Mairie) 2: Leur function. In M.-C. Frère-Sautot (ed.), *Le feu domestique et ses structures au néolithique et aux âges des métaux,* (Actes du colloque Bourg-en-Bresse 7 octobre 2000 Beaune 8 Octobre 2000) Préhistoires (Vol. 9). Ed. Monique Mergoil, Montagnac, 177-198.

March, R. J., Lucquin, A., Joly, D., Muhieddine, M., Ferreri, J. C., 2014. Processes of formation and alteration of archaeological fire structures: complexity viewed in the light of experimental approaches. *Journal of Archaeological Method and Theory* 21:1-45.

March, R. J., Monnier, J. L, Largeau, C. 2006. L'homo erectus et le feu: la géochimie sur la trace des plus anciens foyers européens. In *Actes du Colloque de Carqueiranne, Les Matières Organiques en France: Etat de l'Art et Prospectives*. 22-24 Janvier 2006 Carqueiranne, France, 1-21.

March, R. J., Soler Mayor, B. 1999. Etude de cas: analyze functionnelle de la structure 1. In M. Julien and J.-L. Rieu (eds.), *Occupations du Paléolithique Supérieur dans le Sud-Est du Bassin Parisien*, D.A.F. 78. Maison de Sciences de l'Homme, Paris, 102-129.

Marchbanks, M. L. 1989. Lipid analysis in archaeology: an initial study of ceramics and subsistence at the George C. Davis site. Master of Arts dissertation, The University of Texas at Austin, Austin.

Marchlewska- Kog, A., Lepri, Jh. J., Müller-Schawrze, D. 2001. *Chemical signals in Vertebrates*. Proceedings of the ninth International Symposium on chemical signals in Vertebrates held July 25-29 2000, in Krakow Poland. Springer Science.

Marseille, F., Disnar, J. R., Guilet, B., Noack, Y. 1999. n-Alkanes and free fatty acids in humus and A1 horizons of soils under beech, spruce and grass in the Massif-Central (Mont-Lozère), France. *European Journal of Soil Science* 50, 433-441.

Maw, S. J., Fowler, V. R., Hamilton, M., Petchey, A. M. 2003. Physical characteristics of pig fat and their relation to fatty acid composition. *Meat Science* 63, 185-190.

Meignen, L., Bar-Yosef, O., Goldberg, P. 1989. Les structures de combustion moustériennes de la grotte de Kébara (Mont Carmel, Israel). In M. Olive and Y. Taborin (eds.) *Nature et Function des Foyers Préhistoriques*, Actes du Colloque International de Nemours (1987). Mémoires du Musée de Préhistoire d'Ile-de-France 2. APRAIF, Nemours, 141-146.

Meignen, L., Bar-Yosef, O., Goldberg, P., Weiner, S. 2001. Le feu au Paléolithique moyen: Recherches sur les structures de combustion et le statut des foyers. L'exemple du Proche-Orient. *Paléorient* 26, 9-22.

Mentzer, S. M. 2012. Microarchaeological Approaches to the Identification and Interpretation of Combustion Features in Prehistoric Archaeological Sites. *Journal of Archaeological Method qnd Theory* 21, 616-668.

Mercier, N., Valladas, H., Joron, J. L., Schiegl, S., Bar-Yosef, O., Weiner, S. 1995. Thermoluminescence (TL) Dating and the problem of geochemical evolution of the sediments. A case study: the Mousterian levels at Hayonim. *Israel Journal of Chemistry* 35, 137-142.

Morgan, E. D., Cornford, C., Pollock, D. R. J., Isaacson, P. 1973. The transformation of fatty matérial buried in soil. *Science and Archaeology* 10, 9-10.

Morin, E., Speth, J. D., Lee-Thorp, J. 2017. Middle Paleolithic diets: A critical examination of the evidence. In J. Lee-Thorp and M.A. Katzenberg (eds.), *Oxford Handbook of the Archaeology of Diet*, in press.

Morley, M. W. 2007. Mediterranean Quaternary Rockshelter Sediment Records: A Multi-Proxy Approach to Environmental Reconstruction. Ph.D. dissertation, Department of Geography, School of Environment and Development, Faculty of Humanities, University of Manchester.

Morton, J., Schwartz, H. P. 2004. Paleodietary implications from isotopic analysis of food residues on prehistoric Ontario ceramics. *Journal of Archaeological Science* 31, 503-17.

Movius, H. I. 1975. *Excavation of the Abri Pataud, Les Eyzies (Dordogne)*. American School of Prehistoric Research, Bulletin 30. Peabody Museum Harvard University, Cambridge Massachussets.

Movius, H. I. 1977. *Excavation of the Abri Pataud, Les Eyzies (Dordogne): Stratigraphy*. American School of Prehistoric Research, Bulletin 31. Peabody Museum Harvard University, Cambridge Massachussets.

Muhieddine, M., Canot, E., March, R., Delannay, R., 2011. Coupling heat conduction and water−steam flow in a saturated porous medium. *International Journal for Numerical Methods in Engineering* 85, 1390-1414.

Nicholson, R. 1993. A morphological investigation of burnt animal bone and an evaluation of its utility in archaeology. *Journal of Archaeological Science* 20, 411-428.

Osthoff, G., Hugo, A., de Wit, M. 2008 Milk composition of a free-ranging white rhinoceros (*Ceratotherium simum*) during late lactation. *Mammalian Biology* 73, 245-248.

Otte, M. 2012. The management of space during the Paleolithic, *Quaternary International* 247, 212-229.

Outram, A. K., Stear, N. A., Bendrey, R., Olsen, S., Kasparov, A., Zaibert, V., Thorpe, N., Evershed, R. P. 2009. The earliest horse harnessing and milking, *Science* 323, 1332-1335.

Oras, E., Lucquin, A., Lõugas, L., Tõrv, M., Kriiska, A., Craig, O. E. 2017. The adoption of pottery by north-east European hunter-gatherers:

Evidence from lipid residue analysis *Journal of Archaeological Science* 78, 112-119.

Paleari, M. A., Moretti, V. M., Beretta, G., Mentasti, T., Bersani, C. 2003. Cured products from different animal species. *Meat Science* 63, 485-489.

Pathak, S. P., Roy, S. K., Trivedi, B. N. 1959. The fatty acid composition and glyceride structure of indian wild-boar fat. *The Biochemical Journal* 71, 593-596.

Paredes Sabja, D. G. 2002. Caracterización de carne de Jabalí (*Sus scrofa*) procedente de animales criados en Chile. Tesis presentada como parte de los requisitos para optar al grado de Licenciado en Ingeniería en Alimentos. Universidad Austral de Chile Facultad de Ciencias Agrarias Escuela de Ingeniería en Alimentos.

Pearson, J. A., Buitenhuis, H., Hedges, R. E. M., Martin, L., Russell, N., and Twiss, K. C., 2007. New light on early caprine herding strategies from isotope analysis: a case study from Neolithic Anatolia. *Journal of Archaeological Science* 34, 2170-2179.

Pepe, C., Dizabo, P., Scribe, P., Dagaut, J., Fillaux, J., Saillot, A., 1989. Les marqueurs biogeochimiques: application à l'archéologie. *Revue d'Archéometrie* 13, 1-12.

Pepe, C., Dizabo, P. 1990. Etude d'une fosse du 13ème siècle par les marqueurs biogéochimiques: chantier archéologique du Louvre (Paris). *Revue d'Archéométrie* 14, 23-28.

Petkov, R. 1986. Fatty acid content of the lipid fraction of the meat from deer and roe deer. *Veterinarno-Meditsinski Nauki* 23, 53-57. (in Bulgarian).

Phillip, L. E., Oresanya, T. F., St. Jacques, J. 2007. Fatty acid profile, carcass traits and growth rate of red deer fed diets varying in the ratio of concentrate:dried and pelleted roughage, and raised for venison production. *Small Ruminant Research* 71, 215-221.

Pine, S. 2001. *Fire: A Brief History*. University of Washington Press.

Polak, T., Rajar, A., Gašperlin, L., Žlender, B. 2008. Cholesterol concentration and fatty acid profile of red deer (*Cervus elaphus*) meat. *Meat Science* 80, 864-869.

Prügel, B., Loosveldt, P., Garrec, J. P. 1994. Changes in the content and constituents of the cuticular wax of *Picea abies* (L.) Karst. in relation to needle ageing and tree decline in five European forest areas. *Trees* 9, 80-87.

Raynal-Ljutovaca, K., Lagriffoul, G., Paccard, P., Guillet, I., Chilliard, Y. 2008. Composition of goat and sheep milk products: an update. *Small Ruminant Research* 79, 57-72.

Regert, M., Garnier, N., Decavallas, O., Cren-Olivé, C., Rolando, C. 2003a. Structural characterization of lipid constituents from natural substances preserved in archaeological environments. *Measurement Science Technology* 14, 1620-1630.

Regert, M., Vacher, S. Moulherat, C., Decavallas, O. 2003b. Adhesive production and pottery function during the Iron Age at the site of Grand Aunay (Sarthe, France). *Archaeometry* 45, 101-120.

Regert, M., Rolando, C. 2002. Identification of Archaeological Adhesives Using Direct Inlet Electron Ionization Mass Spectrometry. *Analytical Chemestry* 74, 965-975.

Rhee, K. S., Waldron, D. F., Ziprin, Y. A., Rhee, K. C. 2000. Fatty acid composition of goat diets vs intramuscular fat. *Meat Science* 54, 313-318.

Richards, M. P., Taylor, G., Steele, T., McPherron, S. P., Soressi, M., Jaubert, J.,.

Orschiedt, J., Mallye, J. B., Rendu, W., Hublin, J. J. 2008. Isotopic dietary analysis of a Neanderthal and associated fauna from the site of Jonzac (Charente-Maritime), France. *Journal of Human Evolution* 55, 179-185.

Roebroeks, W., Villa, P. 2011. On the earliest evidence for habitual use of fire in Europe. *Proceedings of the National Academy of Sciences of the USA* 108, 5209-5214.

Rommerskirchen, F., Plader, A., Eglinn, G., Chikaraishi, Y., Rullkötter, J. 2006. Chemotaxonomic significance of distribution and stable carbon isotopic composition of long-chain alkanes and alkan-1-ols in C4 grass waxes. *Organic Geochemistry* 37, 1303-1332.

Rottländer, R. C. A. 1991 Die resultate der modernen Fettanalytik und ihre Anwendung auf die prähistorische Forschung. *Archaeo-Physika*, 12, 1-354.

Ruess L., Chamberlain, P. M. 2010. The fat that matters: Soil food web analysis using fatty acids and their carbon stable isotope signature. *Soil Biology and Biochemistry* 42, 1898-1910.

Rule, D. C., Broughton, K. S., Shellito, S. M., Maiorano, G. 2002. Comparison of muscle fatty acid profiles and cholesterol concentra-

tions of bison, beef cattle, elk, and chicken. *Journal of Animal Science* 80, 1202-1211.

Salazar-Garcia D. C., Power R. C., Sanchis Serra A., Villaverde, V., Walker, M.J., Henry, A. G. 2013. Neanderthal diets in central and southeastern Mediterranean Iberia. *Quaternary International* 318, 3–18.

Sampels, S. 2005. Fatty Acids and Antioxidants in Reindeer and Red Deer: Emphasis on Animal Nutrition and Consequent Meat Quality. Doctoral thesis *Faculty of Natural Resources and Agricultural Sciences Department of Food Science* Swedish University of Agricultural Sciences Uppsala.

Sandgathe, D. M., Dibble, H. L., Goldberg, P., McPherron, S. P. , Turq, A., Niven, L., Hodgkins, J., 2011. On the Role of Fire in Neandertal Adaptations in Western Europe: evidence from Pech de l'Aze and Roc de Marsal, France. *PaleoAnthropology* 2011, 216-242.

Schiegl S., Goldberg P., Bar-Yosef O., Weiner S. 1996. Ash deposits in Hayonim and Kebara Caves, Israel: Macroscopic, microscopic and mineralogical observations, and their archaeological implications. *Journal of Archaeological Science* 23, 763–781.

Schroth, A.W. Bostick, B. C. Graham, M. Kaste, J. M. Mitchell, M. J. & Friedland A. J. 2007. Sulfur species behavior in soil organic matter during decomposition *Journal of Geophysical Research,* 112, 1–10

Sistiaga Gutiérrez, A. ; March, R. ; Hernández Gómez C. & Galván Santos B. 2011. Aproximación desde la química orgánica al estudio de los hogares del yacimiento del Paleolítico medio de El Salt (Alicante, España*) Recerques del Museu D'Alcoi*, 20, 47-70

Shahack-Gross, R., Berna, F., Karkanas, P., Lemorini, C., Gopher, A., & Barkai, R., 2014. Evidence for the repeated use of a central hearth at Middle Pleistocene (300 ky ago) Qesem Cave, Israel. Journal of Archaeological Science. 44, 12-21.

Sinninghe Damste J. S., de Leeuw J. W. 1989. Analysis, structure and geochemical significance of organically-bound sulfur in the geosphere: state of the art and future research. *Organic Geochemistry* 16 , 1077–1101

Skewes, O., Morales, R., Mendoza, N., Smulders F.J.M., Paulsen P. 2009. carcass and meat quality traits of wild boar (sus scrofa s. l.) with 2n = 36 karyotype compared to those of phenotypically similar crossbreeds (2n = 37 and 2n = 38) raised under the same farming conditions fatty acid profile and cholesterol. *Meat science 83* (2009) 195–200

Sorensen, A.C. 2017. On the relationship between climate and Neandertal fire use during the Last Glacial in south-west France. *Quaternary International* 436, 114-128

Soryal, K. A., Beyene, F. A., Zeng, S., Bah, B., Tesfai, K., 2005. Effect of goat breed and milk composition on yield, sensory quality, fatty acid concentration of soft cheese during lactation. *Small Ruminant Research*. 58, 275–281.

Spangenberg J. E., Dionisi, F. 2001 Characterization of Cocoa Butter and Cocoa Butter Equivalents by Bulk and Molecular Carbon Isotope Analyses: Implications for Vegetable Fat Quantification in Chocolate. *Journal Agricultural and Food Chemistry* 49, 1534-1540

Spangenberg, J. E., Ferrer, M., Tschudin, P., Volken, M., Hafner, A. 2010 Microstructural, chemical and isotopic evidence for the origin of late neolithic leather recovered from an ice field in the Swiss Alps *Journal of Archaeological Science* 37, 1851–1865

Spangenberg, J. E., Jacomet, S., & Schibler, J., 2006. Chemical analyses of organic residues in archaeological pottery from Arbon Bleiche 3, Switzerland—evidence for dairying in the late Neolithic, *Journal of Archaeological Science, 33,* 1–13.

Spangenberg, J. E., Ogrinc, N. 2001. Authentication of vegetable oils by bulk and molecular carbon isotope analyses e with emphasis on olive oil and pumpkin seed oil, *Journal of Agricultural and Food Chemistry 49*; 1534-1540.

Speth, J. D., 2006. Housekeeping, Neandertal-Style. Hearth Placement and Midden Formation in Kebara cave (Israel). In: Hovers, E.L., Kuhn, S.L. (Eds.), Transitions before the Transition. Evolution and Stability in the Middle Paleolithic and Middle Stone Age. Springer, New York, 171-188.

Stiner M. C., Kuhn S. L., Weiner S., Bar-Yosef, O. 1995. Differential burning, recrystallisation, and fragmentation of archaeological bone. *Journal of Archaeological Science* 22, 223–237.

Stott, A. W., Davies, E., Evershed, R. P., 1997. Monitoring the routing of dietary and biosynthesised lipids through compound specific isotope ($\delta^{13}C$) measurements at natural abundance. *Naturwissenschaften* 84, 82-86.

Taché, K., Craig, O. E. 2015. Cooperative harvesting of aquatic resources triggered the beginning of pottery production in north-eastern North America. *Antiquity*, 89, Issue 343, 177-190.

Théry-Parisot, I., 2001. Economie des combustibles au Paleolithique. CNRS, Paris.

Théry-Parisot, I., 2002. Fuel Management (Bone and Wood) During the Lower

Aurignacian in the Pataud Rock Shelter (Lower Palaeolithic, Les Eyzies de Tayac,Dordogne, France). Contribution of Experimentation. *Journal of. Archaeological Science* 29, 1415-1421.

Thompson, T. J. U., Gauthier, M., Islam, M. 2009. The application of a new method of Fourier transform infrared spectroscopy to the analysis of burned bone. *Journal of Archaeological Science,* 36, 910–914.

Tinoco, P., Almendros G., Sanz J., González-Vázquez R. González –Vila, F.J. 2006: Molecular descriptors of the effect of fire on soils under pine forest in two continental Mediterranean soils. *Organic Geochemistr*y 37, 1995–2018

Tonial, I. B., Aguiar, A. C., Oliveira, C. C., Bonnafé, E. G., Visentainer, J. V., de Souza, N. E., 2009 Fatty acid and cholesterol content, chemical composition and sensory evaluation of horsemeat *South African Journal of Animal Science* 39 328-332

Van Andel T.H. & Tzedakis P.C., 1996. Paleolithic landscapes of Europe and environs, 150,000-25,000 years ago: an overview. *Quaternary Science Reviews* 15, 481–500.

Vandenbroucke M., Largeau C. 2007. Kerogen origin, evolution and structure *Organic Geochemistry* 38, 719–833.

Vaquero, M., Pastó, I., 2001: The definition of spatial units in Middle Palaeolithic sites: the hearth-related assemblages. *Journal of Archaeological Science* 28, 1209-1220.

Vidal-Matutano, P. 2016. Firewood and hearths: Middle Palaeolithic woody taxa distribution from El Salt, stratigraphic unit Xb (Eastern Iberia) *Quaternary International* in press. https://doi.org/10.1016/j.quaint.2016.07.040

Volpelli, L. A., Valusso, R., Morgante, M., Pittia, P., & Piasentier, E. 2003: Meat quality in male fallow deer (Dama dama): Effects of age and supplementary feeding. *Meat Science*, 65, 555–562.

Warren, H. E. Scollan, N. D. Enser, M. Hughes, S. I. Richardson, R. I., Wood, J. D. 2008. Effects of breed and a concentrate or grass silage diet on beef quality in cattle of 3 ages. I: Animal performance, carcass quality and muscle fatty acid composition *Meat Science 78*, 256–269

Weiner, S., Goldbergb P., Bar-Yosef, O. 1993: Bone Preservation in Kebara Cave, Israel using On-Site Fourier Transform Infrared Spectrometry *Journal oj Archaeological Science*, 20, 613-627

Weiner, S., Xu, Q., Goldberg, P., Liu, J, Bar-Yosef O. 1998: Evidence for the use of fire at Zhoukoudian, China. *Science* 28, 251–253.

Wiesenberg, G. L. B., Lehndorff, E., Schwark L. 2009. Thermal degradation of rye and maize straw: Lipid pattern changes as a function of temperature *Organic Geochemistry* 40, 167–174

Whallon, R. 2007. Social territories around the Adriatic in the late Pleistocene. In: R. Whallon (ed.) *Late Paleolithic Environments and Cultural Relations around the Adriatic* BAR International Series 1716, Archaeopress Oxford 61 - 65.

Wißing, Ch., Rougier, H., Crevecoeur, I., Germonpré, M., Naito, Y. I., Semal, P., Bocherens, H. 2015 Isotopic evidence for dietary ecology of late Neandertals in North-Western Europe. *Quaternary International* 411, 327-345

Wiklund, E., Manley, T. R. Littlejohn, R. P. & Stevenson-Barry, J. M. 2003 Fatty acid composition and sensory quality of Musculus longissimus and carcass parameters in red deer (Cervus elaphus) grazed on natural pasture or fed a commercial feed mixture. *Journal of the Science of Food and Agriculture,* 83, 419–424.

Wood, J. D. 2008 Effects of breed and a concentrate or grass silage diet on beef quality in cattle of 3 ages. I: Animal performance, carcass quality and muscle fatty acid composition *Meat Science 78* (2008) 256–269

Wrangham, R. 2009: Catching Fire: How Cooking Made Us Human Basic Books, New York.

Yang, A., M. C. Lanari, Brewster, M. & Tume, R. K. 2002: Lipid stability and meat colour of beef from pasture - and grain-fed cattle with or without vitamin E supplement. *Meat Science, 60*: 41-50.

Yellen, J. E. 1977: Archaeological Approaches to the Present: Models for Reconstructing the Past (Studies in archeology) Academic Press New York, 275 p.

Zech, M., Buggle, B., Leiber, K., Marković, S., Glaser, B., Hambach, U., Huwe, B., Stevens, Th., Süegi, P., Wiesenberg, G., & Zöller, L. 2009 Reconstructing Quaternary vegetation history in the Carpathian Basin, SE Europe, using n-alkane biomarkers as molecular fossils : Problems and possible solutions, potential and limitations Quaternary Science Journal 58, 148–155

Zech, M., Buggle, M., Markovic, S., Lucic, T., Stevens, T., Gaudenyo, T., Jovanovic, M., Huwe, B. & Zöller, L. 2008: First Alkane Biomarker Results for the Reconstruction of the Vegetation History of the Carpathian Basin (SE Europe). – In: Reitner, et al. (eds.): Veränderter Lebensraum – Gestern, Heute und Morgen, DEUQUA Symposium 2008. *Abhandlungen der Geologischen Bundesanstalt* 62, 123-127.

Zomborszky, Z. & Husvéth, F. 2000: Liver total lipids and fatty acid composition of shot red and fallow deer males in various reproduction periods. *Comparative Biochemistry and Physiology* Part A, 126, 107-114.

Appendix

Layer XX										
Name of layer	**X Center**	**Y Center**	**Displacement in Y (Z)**	**Displacement in X**	**Width**	**Thickness**	**Perim.**	**Area**	**Length**	**Height**
Ashes 20-1	-66.00	7.60			19.06	1.40	40.36	18.81	40.36	3.20
Ashes 20 -2b	-45.60	7.40	-0.20	20.40	17.50	1.40	36.56	17.48	36.56	2.30
Ashes 20-2	-73.00	3.60	-3.80	-27.40	20.40	1.80	42.83	20.13	42.83	3.09
Ashes 20-3	-28.20	4.20	0.60	44.80	20.00	0.70	42.20	10.99	42.20	2.95
Ashes 20-3b	-3.40	4.20	0.00	24.80	30.64	4.40	72.44	62.43	72.44	9.13
Ashes 20-4	28.40	-1.20	-5.40	31.80	15.50	1.50	32.06	13.89	32.06	2.15
Ashes 20-5	33.20	-2.00	-0.80	4.80	8.10	1.30	17.77	5.96	17.77	1.75
Ashes 20-6	59.40	-4.00	-2.00	26.20	17.30	1.00	35.17	9.06	35.17	1.00
Structure 3 Upper part of white grey ashes	79.40	-8.40	-4.40	20.00	40.40	2.90	87.13	60.59	87.13	13.40
Structure 3 White transition ashes	52.80	-7.60	0.80	-26.60	183.55	6.40	383.27	534.13	383.27	24.75
Ashes 20 -7	44.60	-13.40	-5.80	-8.20	31.40	4.40	65.56	71.03	65.56	5.25
Ashes 20 - 8	80.20	-19.00	-5.60	35.60	21.51	2.70	45.58	33.99	45.58	3.88
Ashes 20 - 9	-4.80	-13.80	5.20	-85.00	33.73	1.40	70.03	22.84	70.03	2.55
Ashes 20 -10	29.00	-14.60	-0.80	33.80	24.55	1.90	51.57	22.13	51.57	2.42
Ashes 20-11	50.00	-19.40	-4.80	21.00	13.85	1.00	29.88	10.19	29.88	4.58
Ashes 20 -11b	70.40	-22.60	-3.20	20.40	31.80	3.00	69.03	63.66	69.03	5.30
Layer XX										
Name of layer	**X Center**	**Y Center**	**Displacement in Y (Z)**	**Displacement in X**	**Width**	**Thickness**	**Perim.**	**Area**	**Length**	**Height**
Reddish layer 1	33.625	-4.025			14.85	0.8	30.883	7.883	30.883	2.05
Structure 3 reddish soil	97.938	-18.475	-14.45	64.31	57.975	1.9	122.555	80.819	122.555	14.65
Reddish layer 2	75.115	-19.25	-0.77	-22.82	13.67	0.8	28.599	7.419	28.599	2.9
Reddish layer 3	115.72	-26.45	-7.20	40.61	4.2	1	9.672	2.909	9.672	1.62

Appendix - *Continued on next page…*

Appendix - *Continued*

Layer XXIV										
Name of layer	**X Center**	**Y Center**	**Displacement in Y (Z)**	**Displacement in X**	**Width**	**Thickness**	**Perim.**	**Area**	**Length**	**Height**
Ashes 24-3	17.05	-9.95			12.60	2.50	32.02	26.31	32.02	7.30
Ashes 24-4	28.90	-14.39	4.44	11.85	32.80	3.10	73.58	70.53	73.58	6.29
Ashes 24-5	20.37	-21.45	7.06	-8.53	15.63	1.90	34.96	17.40	34.96	5.58
Ashes 24-1	-1.44	-16.29	-5.17	-21.82	14.18	1.30	32.91	13.75	32.91	7.49
Ashes 24-2	-3.01	-19.03	2.74	-1.57	16.04	1.90	38.12	25.56	38.12	8.78
Ashes 24-10	52.00	-21.63	2.60	55.01	11.90	1.50	29.02	20.92	29.02	5.85
Ashes 24-39	93.77	-29.75	8.13	41.77	11.91	0.90	24.67	3.82	24.67	1.32
Ashes 24-6	25.11	-30.28	0.53	-68.66	18.41	2.10	38.79	31.11	38.79	3.45
Ashes 24-12	87.78	-30.90	0.62	62.67	16.96	1.30	35.85	13.47	35.85	1.71
Ashes 24-7	34.16	-31.91	1.01	-53.62	23.21	2.40	50.70	27.99	50.70	3.52
Ashes 24-13	89.11	-33.59	1.68	54.95	10.92	0.50	25.28	4.44	25.28	2.13
Ashes 24-8	42.22	-34.40	0.81	-46.89	8.68	1.90	19.06	7.13	19.06	1.93
ashes 24-14	91.90	-34.75	0.35	49.68	17.35	0.50	36.12	5.06	36.12	2.16
Ashes 24-15	86.73	-35.49	1.10	44.50	30.05	2.10	64.10	32.00	64.10	2.92
Ashes 24-9	36.25	-36.42	0.92	-50.48	8.82	1.90	19.57	11.90	19.57	2.79
Ashes 24-11	73.00	-36.76	0.34	36.75	78.30	3.10	167.55	111.44	167.55	6.52
Ashes 24-17	0.45	-40.20	3.44	-72.56	19.41	2.70	48.18	37.15	48.18	9.31
Ashes 24-18	39.01	-43.79	3.59	38.57	12.88	1.30	27.51	12.13	27.51	2.70
Ashes 24-16	102.27	-41.06	-2.72	63.25	19.91	2.10	45.45	19.68	45.45	5.93
Ashes 24-26	60.06	-44.17	3.10	-42.21	27.92	4.20	62.76	61.33	62.76	7.37
Ashes 24-19	36.99	-46.64	2.48	-23.07	28.36	1.70	58.63	33.42	58.63	4.08
Ashes 24-29	69.71	-44.15	-2.49	32.71	9.83	0.60	21.47	4.23	21.47	2.15
ashes 24-20	41.90	-48.53	4.37	-27.81	8.60	0.70	18.53	4.84	18.53	1.35
Ashes 24-30	76.45	-44.78	-3.74	34.55	14.16	2.10	31.86	16.39	31.86	2.72
Ashes 24-27	55.84	-48.27	3.49	-20.61	25.88	2.40	55.05	30.69	55.05	5.96
Ashes 24-21	18.52	-49.29	1.01	-37.32	44.68	2.10	93.79	73.42	93.79	3.95
Ashes 24-31 b	83.63	-47.13	-2.16	65.11	14.55	2.40	33.93	20.95	33.93	4.35

Appendix - *Continued on next page…*

Appendix - *Continued*

Name of layer	X Center	Y Center	Displacement in Y (Z)	Displacement in X	Width	Thickness	Perim.	Area	Length	Height
Ashes 24-31	67.50	-48.09	0.96	-16.12	18.76	1.40	42.36	17.13	42.36	3.08
Ashes 24-36	82.38	-48.39	0.30	14.88	6.61	1.10	14.72	5.66	14.72	1.59
Ashes 24-37	93.35	-49.78	1.39	10.97	14.57	0.90	31.97	8.08	31.97	3.53
Ashes 24-40	94.82	-49.91	0.13	1.47	4.68	0.40	10.13	1.20	10.13	0.86
Ashes 24-38	88.55	-51.84	1.93	-6.27	24.96	2.80	57.74	55.50	57.74	5.00
Ashes 24-32	58.95	-52.51	0.66	-29.60	34.49	3.00	74.58	59.03	74.58	6.69
Ashes 24-22	-0.10	-53.97	1.46	-59.05	12.59	1.60	27.47	9.94	27.47	1.95
Ashes 24-23	19.04	-54.08	0.11	19.15	6.73	1.20	13.97	5.14	13.97	1.65
Ashes 24-24	22.21	-55.74	1.67	3.17	7.78	1.30	16.59	5.90	16.59	1.99
Ashes 24-25	31.22	-56.11	0.37	9.01	14.48	1.80	32.79	18.27	32.79	5.24
Ashes 24-33	42.65	-58.28	2.16	11.43	7.69	1.60	16.90	8.14	16.90	1.75
Ashes 24-35	55.61	-57.94	-0.34	12.96	13.12	3.90	29.68	42.01	29.68	4.49
Ashes 24-34	42.45	-62.40	4.46	-13.16	6.25	1.30	14.66	5.56	14.66	2.06
Ashes 24-41	2.98	-61.93	0.47	-39.48	14.25	1.80	32.43	18.69	32.43	4.75
LAYER XXIV										
Name	**X Center**	**Y Center**	**Displacement in Y (Z)**	**Displacement in X**	**Width**	**Thickness**	**Perim.**	**Area**	**Length**	**Height**
Reddish layer 24-4	89.575	-29.975			23.45	2.2	50.225	19.429	50.225	2.15
Reddish layer 24-1	72.16	-37.45	-7.475	-17.415	84.08	4	177.665	109.673	177.665	8.1
Reddish Layer 24-5	103.34	-44.88	-14.905	31.18	5.48	0.3	12.115	1.614	12.115	0.72
Reddish layer 24-2	18.975	-54.775	-17.325	-1.7	5.65	0.9	12.019	3.51	12.019	1.55
Reddish layer 24- 3	20.675	-56.9	-12.02	-82.665	9.25	1	20.107	7.093	20.107	1.9

Appendix - *Continued on next page…*

Appendix - *Continued*

Layer XX	Combustion Areas layer XX					
Name of layer	Width of area	X Center of Area	Displacement into X Area	Y(Z) Center of area	Displacement in Y (Z area)	Internal distance between structures
Ashes 20-1	19.60	-66.00	4.70	7.60	2.10	0.00
Ashes 20 -2b	48.00	-61.30	-46.50	5.50	-0.20	10.00
Ashes 20-2						
Ashes 20-3	50.00	-14.80	-43.20	5.70	6.80	0.00
Ashes 20-3b						
Ashes 20-4	15.50	28.40	-20.60	-1.10	1.70	0.00
Ashes 20-5	39.00	49.00	3.80	-2.80	12.70	14.00
Ashes 20-6						
Structure 3 Upper part of white grey ashes	40.40	52.80	-5.00	-15.50	0.50	0.00
Structure 3 White transition ashes	183.55					0.00
Ashes 20 -7	65.00	57.80	50.40	-16.00	-1.50	11.00
Ashes 20 - 8						
Ashes 20 - 9	60.00	7.40	-58.50	-14.50	5.90	2.00
Ashes 20 -10						
Ashes 20-11	46.00	65.90		-20.40		0.00
Ashes 20 -11b						
Layer XXIV	Combustion Areas layer XXIV					
Name of layer	Width of area	X Center of Area	Displacement into X Area	Y(Z) Center of area	Displacement in Y (Z area)	Internal distance between structures
Ashes 24-3	12.60	17.05	-11.85	-9.95	4.44	0.00
Ashes 24-4	32.80	28.90	8.53	-14.39	7.06	0.00
Ashes 24-5	15.63	20.37	21.82	-21.45	-5.17	0.00

Appendix - *Continued on next page…*

Appendix - *Continued*

Name of layer	Width of area	X Center of Area	Displacement into X Area	Y(Z) Center of area	Displacement in Y (Z area)	Internal distance between structures
Ashes 24-1	14.18	-1.44	1.57	-16.29	2.74	0.00
Ashes 24-2	16.04	-3.01	-55.01	-19.03	2.60	0.00
Ashes 24-10	11.90	52.00	-41.77	-21.63	8.13	0.00
Ashes 24-39	11.91	93.77	37.67	-29.75	0.65	0.00
Ashes 24-6	80.50	56.10	-2.50	-30.40	2.00	33.90
Ashes 24-12						
Ashes 24-7	72.10	58.60	-10.20	-32.40	2.30	37.80
Ashes 24-13						
Ashes 24-8	62.80	68.80	1.80	-34.70	1.20	36.70
ashes 24-14						
Ashes 24-15	70.00	67.00	-6.00	-35.90	0.86	31.50
Ashes 24-9						
Ashes 24-11	78.30	73.00	55.00	-36.76	3.64	0.00
Ashes 24-17	54.70	18.00	-84.27	-40.40	0.66	25.40
Ashes 24-18						
Ashes 24-16	19.91	102.27	53.77	-41.06	3.64	0.00
Ashes 24-26	51.50	48.50	-7.70	-44.70	1.50	0.00
Ashes 24-19						
Ashes 24-29	39.60	56.20	16.40	-46.20	1.10	21.10
ashes 24-20						
Ashes 24-30	87.00	39.80	-34.90	-47.30	0.20	1.80
Ashes 24-27						
Ashes 24-21						

Appendix - *Continued on next page…*

Appendix - *Continued*

Name of layer	Width of area	X Center of Area	Displacement into X Area	Y(Z) Center of area	Displacement in Y (Z area)	Internal distance between structures
Ashes 24-31 b	33.00	74.70	-15.40	-47.50	2.30	0.00
Ashes 24-31						
Ashes 24-36	21.70	90.10	-4.72	-49.80	0.11	0.40
Ashes 24-37						
Ashes 24-40	4.68	94.82	23.32	-49.91	2.59	0.00
Ashes 24-38	52.30	71.50	63.40	-52.50	1.60	0.00
Ashes 24-32						
Ashes 24-22	28.80	8.10	-31.90	-54.10	2.70	9.50
Ashes 24-23						
Ashes 24-24	43.90	40.00	-37.03	-56.80	-5.13	2.50
Ashes 24-25						
Ashes 24-33						
Ashes 24-35						
Ashes 24-34	6.25	42.45	-39.48	-62.40	-0.47	0.00
Ashes 24-41	14.25	2.98		-61.93		